VIRAL INTERFERON REGULATORY FACTORS INHIBIT THE IMMUNE RESPONSE FOLLOWING RHESUS RHADINOVIRUS INFECTION

By

Bridget A Robinson

A DISSERTATION

Presented to the Department of Molecular Microbiology and Immunology
and the Oregon Health & Science University
School of Medicine
in partial fulfillment of the requirements for the degree of

Doctor of Philosophy

June 2011

School of Medicine

Oregon Health & Science University

CERTIFICATE OF APPROVAL

_____

This is to certify that the PhD dissertation of

Bridget A Robinson

has been approved

_____
Advisor / Scott Wong

_____
Member / Klaus Früh

_____
Member / Mihail Iordanov

_____
Member / Ilhem Messaoudi

_____
Member / Mark Slifka

TABLE OF CONTENTS

FIGURES and TABLES

Page #

ACKNOWLEDGEMENTS

I would like to acknowledge all of those within the OHSU community who have helped to shape me into a better scientist and offered guidance, wisdom and support during my journey through graduate school at OSHU. In particular, I'd like to thank my mentor, **Dr. Scott Wong**, for taking me into his lab and giving me the opportunity to work in a model system not often available to graduate students. I'd also like to thank Dr. Wong for his mentorship, friendship, and his willingness to let me develop independently as a scientist. I'd also like to extend a special thank you to **Dr. Ilhem Messaoudi** for her mentorship and guidance in my scientific endeavors, as well as for her patience and constant support, especially during the mania of the last two years. And the rest of my committee, **Dr. Mark Slifka**, **Dr. Klaus Früh**, and **Dr. Mihail Iordanov**: adequate training is critical for graduate students, and I appreciate the time and effort they have extended on my behalf.

The past and present members of the **Wong Lab** have also been an essential part of my success, as well as my sanity. I appreciate their scientific contributions and their friendship; daily life in the lab would not be as enjoyable without such great people. A special thank you to my fellow lab-mate, **Dr. Ryan Estep**, whose mentorship, support, and patience have been invaluable to my training. Ryan is also a trusted friend and a great snowboarding companion, and it will be difficult not seeing him in the lab every day.

My greatest thanks is reserved for my friends and family, because they are the people who keep me afloat no matter what life throws my way. My parents, **Cheryl and Randy Robinson**, have always offered unconditional support in life and in my pursuit of a higher degree. The **PMCB class of 2004** is an amazing group of people, and I've appreciated being a part of such an intelligent and entertaining bunch of scientists. I look forward to maintaining those friendships as we all push forward in our scientific careers. I have been lucky to become friends with so many lovely people while in Portland, and a few deserve specific recognition: **Dr. Christina Lorentz**, **Dr. Dustin Johnsen**, **Dr. Joshua Walker**, and **Dr. Deanne Tibbitts**. I appreciate and love these people more than I can express, and am forever thankful for their love, friendship, entertaining wit, and support. Completing this journey without the above named people would've been unnecessarily difficult, and certainly not as much fun – the countless memories will remain with me always.

ABSTRACT

Kaposi's Sarcoma-associated herpesvirus (KSHV) and rhesus macaque rhadinovirus (RRV), two closely related γ-herpesviruses, are unique in their acquisition and expression of a cluster of genes with significant homology to cellular interferon (IFN) regulatory factors (IRFs). Initial studies of KSHV vIRFs demonstrated their varied function in immune evasion and tumorigenesis. However, inadequate models for studying *de novo* KSHV infection, as well as KSHV-associated diseases, makes RRV the most acceptable alternative for evaluating the role(s) of vIRFs during *de novo* infection, and in the development of disease. We have generated and characterized a vIRF deletion virus, vIRF-ko RRV, with all eight vIRFs deleted (ORFs R6-R13), using the bacterial artificial chromosome (BAC) clone of $RRV_{17577.}$ *In vitro* analyses demonstrated that vIRF-ko RRV infection resulted in increased induction of type I and type II IFN during *de novo* RRV infection, which correlated with a significant increase in the nuclear accumulation of cellular IRF-3, necessary for driving transcription of type I IFN. Furthermore, vIRF-ko RRV infection of rhesus macaques results in undetectable viral loads, increased Th1 cytokine production and earlier T cell responses, as well as diminished B cell hyperplasia, a defining characteristic of RRV infection. Further *in vitro* analyses of individual RRV vIRF clones demonstrated that expression of R6 vIRF significantly inhibited transcription mediated by cellular IRF-3, as well as type I IFN. Moreover, R6 vIRF specifically binds to cellular IRF-3, which may explain the IRF-3 dysregulation and inhibition of type I IFN observed during RRV infection. Additionally, three other vIRFs (ORFs R7, R8, and R9) demonstrated transforming capacity *in vitro*, suggesting each

vIRF has a potentially unique and varied role in immune evasion and pathogenesis. Overall, our findings demonstrate the significant inhibitory role vIRFs have on the IFN response, as well as their wide-ranging impact during RRV infection in the rhesus macaque. If these data can be extrapolated to KSHV-associated disease, our findings would suggest that targeting vIRFs could be a potential therapeutic option to enhance immune responses and inhibit B cell proliferation before malignancies develop.

CHAPTER 1

INTRODUCTION

I. Human Herpesviruses

A. Classification

Herpesviruses are ubiquitous in nature, with most animal species harboring at least one herpesvirus. There are eight viruses that naturally infect humans as their primary target, and these are designated Human Herpesvirus 1(HHV-1) through HHV-8. Viruses were initially categorized within the *Herpesviridae* family based on virion architecture, including a single linear dsDNA genome, an amorphous, proteinacious material (tegument) surrounding the icosahedral capsid, and an envelope containing glycoprotein spikes on the surface (199, 200). Additional biological properties of herpesviruses include nuclear replication of the DNA genome, destruction of the infected cell during lytic replication, and development of latency within the infected host (199).

Herpesviruses are further divided into 3 subfamilies, *Alphaherpesvirinae*, *Betaherpesvirnae*, and *Gammaherpesvirinae,* dependent mostly on cellular tropism during latency, growth properties, host range, sequence and genomic organization (199). Alphaherpesviruses have a short life cycle; these viruses grow rapidly with efficient cellular destruction in culture, and can establish latency within the sensory ganglia of the infected host. Members of the alphaherpesvirus subfamily include Herpes Simplex Virus 1 (HSV 1) and HSV 2, also referred to as HHV-1 and HHV-2, as well as HHV-3, also known as Varicella-Zoster Virus (VZV) (199). HSV-1 and HSV-2

have a broader host range than VZV, which replicates almost exclusively within specific human cell types (49).

Viruses within the *Betaherpesvirinae* subfamily are characterized by a long viral life cycle, and a host range restricted to a specific species. Members of the *Betaherpesvirinae* subfamily include HHV-5, also known as Human Cytomegalovirus (HCMV) (199), HHV-6A, HHV-6B, and HHV-7 (258). These viruses have slow growth properties in cell culture, and infected cells often become enlarged (cytomegalia). Latency is established within secretory glands, lymphoreticular cells, T cells and monocytes (199, 258).

The *Gammaherpesvirinae* subfamily includes viruses with a narrow host range that is confined to the taxonomic order in which the natural host belongs. These viruses are specific for B and T cells, and also establish latency within the lymphoid population (81). *In vitro*, gammaherpesviruses infect a variety of cellular populations in the peripheral blood, as well as epithelial cells and fibroblasts. This subfamily includes the γ1-lymphocryptovirus HHV-4, also known as Epstein-Barr Virus (EBV) (199), and the γ2-rhadinovirus HHV-8, also known as Kaposi's Sarcoma-associated Herpesvirus (KSHV) (163).

B. Virion Structure and Genomic Organization

Herpesviridae consist of a large (~120-230kb), linear, dsDNA genome, encoding an estimated 70-200 open reading frames (ORFs). The dsDNA genome of all mammalian

herpesviruses includes about 40 core genes, which encode capsid proteins, envelope glycoproteins, DNA replication proteins and DNA packaging/cleavage proteins (167). The remaining ORFs encode for accessory proteins, and are not essential for growth of the virus *in vitro*. However, the accessory proteins are often necessary for viral replication in the host animal, as they play a variety of necessary roles in immune evasion, and development and maintenance of latency (200). All the mammalian herpesvirus genomes contain terminal and/or internal repeated regions that either flank or interrupt the long unique segment of the genome. These repeated regions contain cis signals for packaging and cleavage of new genomes during infection (158), and the terminal repeats flanking the KSHV genome are also required for the maintenance of the genome during latency (13). Additionally, each virus contains at least one origin of replication (*ori*Lyt), which is at least ~100bp in length and necessary for initiating DNA replication during the lytic infection cycle (12, 24, 266).

The viral nucleic acid is encapsidated in an icosahedral capsid measuring ~100nm in diameter (200). Surrounding the capsid, and extending to the envelope, is the amorphous, proteinacious material that makes up the tegument. The variability in the amount of tegument differs among herpesviruses and is also relative to where the virion is within the cell; a thicker tegument is seen in virions within cytoplasmic vacuoles as compared to virions accumulating in the perinuclear space. Additionally, herpes virions have a lipid envelope which includes 7-20 viral glycoproteins protruding from the surface (200) (Fig. 1.1A).

Mature herpes virions vary in size from 120-260nm, due to both differences in the amount of tegument and the condition of the viral envelope (200). The exact number of protein species present within the virion is unknown and is variable between viruses. Proteomic analyses have identified between 24 and 71 viral proteins present within the envelope, the tegument, the capsid, and some proteins with unknown location (155, 168, 264). Likewise, a number of host proteins are also included within herpesvirus virions (155, 264), but their role and necessity during infection have not been determined. Additionally, viral mRNAs are also packaged within the KSHV virion, posing them for immediate translation during infection (14).

C. Herpesvirus Life Cycle

A generic schematic of the herpesvirus life cycle is included in Figure 1.1B, and each step will also be explained in the following text. The initial step in the herpesvirus life cycle is binding of the virion, via glycoproteins, to host receptors on the cell surface; heparan sulfate is a common binding receptor utilized by herpesviruses. A fusion event follows the initial binding interaction and involves different host and viral receptors than the initial binding event. Interactions between glycoproteins on the viral envelope and host proteins on either the plasma membrane or endosomal membrane result in fusion and release of the viral capsid and tegument proteins into the cytosol. The capsid is then shuttled to the nuclear envelope where the linear viral genome is delivered into the nucleus through the nuclear pore. The genome circularizes and becomes associated with histones, making it a suitable template for RNA polymerase II (200). Transcription of viral genes subsequently occurs in a temporally ordered fashion (97).

The initial genes are transcribed within hours after the virus enters the cell, and are termed immediate early (IE) genes, categorized as such due to their insensitivity to cycloheximide (CHX). Insensitivity to CHX means these viral genes do not require newly synthesized viral proteins before they are expressed, and the IE proteins generally function to inhibit the host's innate antiviral defenses (237). The second group of viral genes expressed are termed early genes, and are expressed between 12-48 hours post-infection (hpi). The early genes are sensitive to CHX, but are insensitive to chemicals that inhibit viral replication, such as phosphonoacetic acid (PAA), and thus, many of the early genes function to promote viral replication. The third and final group of viral genes transcribed are termed late genes. The late genes encode for the structural proteins that are necessary for virion assembly (97).

Replication of the herpesvirus genome initiates at one or more of the *ori*Lyt sites and results in at least one round of θ replication. After this, replication occurs via a rolling circle mechanism, generating concatamers of herpesvirus genomes that are cleaved and packaged into preformed capsids in the nucleus (24). The filled capsids undergo nuclear egress, associate with tegument proteins and don a viral glycoprotein-studded envelope as they exit the cell. There is still some debate about the assembly steps following encapsidation in the nucleus, but a widely accepted model is that filled capsids undergo an envelopment-development-re-envelopment process as they move through the nuclear membrane, then through the golgi, and are finally released from the cell (81, 155, 217) (Fig. 1.1B).

In addition to the distinct lytic replication cycle described above, herpesviruses also establish a latent infection in the host. During latency, only a small subset of the viral genes are transcribed and no viral progeny are produced (81, 200). Latent virus is maintained in the nucleus as an episome, and in the case of HSV-1 and HSV-2, which latently infect neurons, the only viral product that can be detected are the latency-associated transcripts (LATs) (200). KSHV establishes latency within B cells and the viral genome is also maintained in the nucleus as an episome, tethered to host chromosomes via a viral protein, latency-associated nuclear antigen 1 (LANA-1/ORF73) (13). Cells latently infected with KSHV limit their viral gene expression to a few key proteins, including LANA-1 (81). KSHV has also ensured its genome is efficiently replicated and distributed to daughter cells at each cell division (81). Because herpesviruses have developed methods to maintain their genome latently within non-dividing cells or developed ways to replicate their genome without inducing lytic infection, they have ensured their lifetime persistence within the infected host.

FIGURE 1.1. Herpesvirus structure and replication cycle. (A) A generic schematic of the organization and components of a herpes virion. **(B)** A diagram of the replication cycle is shown together with electron micrographs of the respective stages. After attachment (1) and penetration (2), capsids are transported to the nucleus (N) (3) via interaction with microtubules (MT) (4), docking at the nuclear pore (NP) (5) where the viral genome is released into the nucleus. Here, transcription of viral genes and genome replication occur (6). Concatemeric replicated viral genomes are cleaved to unit-length during encapsidation (8) into preformed capsids (7), which then leave the nucleus by budding at the INM (9) followed by fusion of the envelope of these primary virions located in the perinuclear space (10) with the outer nuclear membrane (11). Final maturation then occurs in the cytoplasm by secondary envelopment of intracytosolic capsids via budding into vesicles of the trans-Golgi network TGN (12) containing viral glycoproteins (black spikes), resulting in an enveloped virion within a cellular vesicle. After transport to the cell surface (13), vesicle and plasma membranes fuse, releasing a mature, enveloped virion from the cell (14). RER, rough endoplasmic reticulum; M, mitochondrion; G, Golgi apparatus. *Figure and legend for (B) adapted from* (155) *and reprinted with permission.*

A

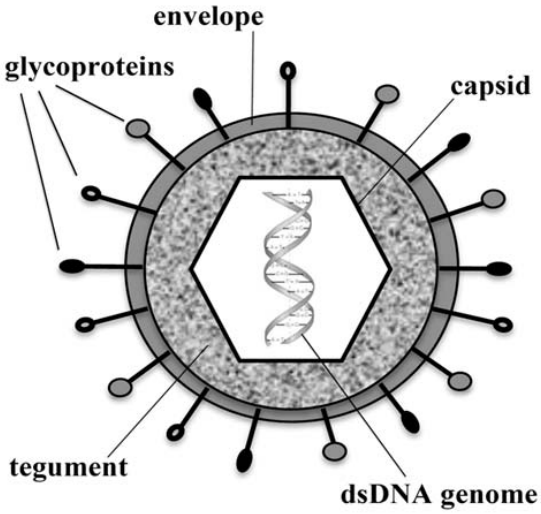
envelope
glycoproteins
capsid
tegument
dsDNA genome

B

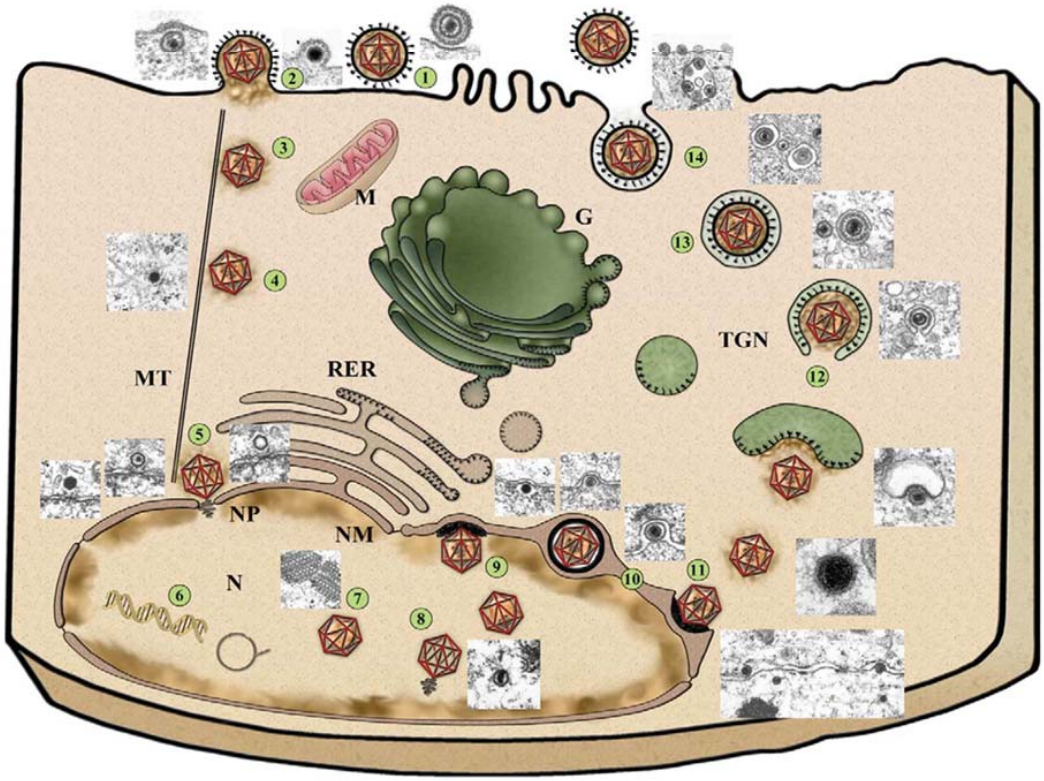
1
2
3
4
5
6
7
8
9
10
11
12
13
14
M
G
TGN
MT
RER
NP
NM
N

D. Diseases Associated with Human Herpesviruses

Primary herpesvirus infections can often be asymptomatic, but this section will highlight common clinical outcomes of symptomatic herpesvirus infections. HSV-1 and HSV-2, two alphaherpesviruses, target mucosal epithelium during primary infection, and result in ulcerative and vesicular lesions of the mouth and genitals, respectively (252). HSV-1 and HSV-2 are neurotropic, and thus, remain latent within the trigeminal ganglia following primary infection, and lytic reactivation results in similar symptoms as those during primary infection, but the frequency of reactivation varies greatly among individuals. In rare cases, HSV infection is also associated with encephalitis, which is often fatal if left untreated (252).

Primary infection with VZV, also an alphaherpesvirus, usually occurs during childhood and results in varicella (chicken pox), a vesicularized rash that appears all over the body due to infection of T cells and the systemic nature of primary infection (49). Similar to HSV-1 and -2, VZV is also neurotropic and develops latency in the trigeminal and dorsal root ganglia. Reactivation of VZV results in herpes zoster, often referred to as shingles, a painful, vesicular rash confined to specific regions of the skin, usually on one side of the body served by a single spinal nerve (116). Unlike chicken pox, herpes zoster can result in severe, prolonged pain, known as post-herpetic neuralgia (116). Development of a live, attenuated vaccine for VZV has dramatically reduced rates of chicken pox in the US, and halved the cases of herpes zoster in elderly individuals (174).

CMV, a well-studied betaherpesvirus, is mostly associated with opportunistic disease, as primary infection of immune-competent individuals is usually asymptomatic. However, primary CMV infection of pregnant women can lead to serious congenital diseases including CNS damage, hearing loss, and mental retardation of the fetus. Reactivation of latent CMV can cause complications when the immune system is compromised, such as after organ transplantation or during an advanced stage of AIDS (158). HHV-6 and HHV-7 are also betaherpesviruses, and belong to the roseola genus. Primary infection with HHV-6 or HHV-7 can result in exanthem subitum, a common disease in infants characterized by sudden fever and subsequent development of a rash on the trunk and face. Exanthem subitum is sometimes accompanied by seizure, and also rarely associated with meningitis and encephalitis (258). HHV-6A, and to a lesser extent HHV-6B, have also been associated with multiple sclerosis. However, HHV-6, like many other suspected viruses, has never been directly demonstrated as a causative pathogen in development of multiple sclerosis (243).

Gammaherpesviruses, EBV and KSHV, are both lymphotropic, and are both directly associated with a variety of T cell and B cell malignancies (33). Accordingly, EBV and KSHV also establish latency within B cells (196). About 90% of the population is infected with EBV, and primary infection is associated with infectious mononucleosis in about 25% of individuals (196). Moreover, latent EBV infections can also potentiate the development of a number of lymphomas, including non-Hodgkin's lymphoma, Burkitt's lymphoma, nasopharyngeal carcinoma, T cell and NK cell lymphomas, and post-transplant lymphoma (33, 196). Whether the virus directly drives development of

the malignancy, or whether EBV infection assists in the progression via tumorigenic or anti-apoptotic mechanisms, is still uncertain (196). KSHV, also known as HHV-8, is the most recently identified human herpesvirus (41). KSHV is recognized as the etiological agent of Kaposi's Sarcoma (41), an endothelial neoplasm, and is also implicated in the development of two distinct B cell disorders, primary effusion lymphoma (PEL) (37) and multicentric Castleman's disease (MCD) (220). These KSHV-associated diseases will be discussed in more detail in the following section.

II. Kaposi's Sacroma-associated Herpesvirus

A. Identification and General Characteristics

Kaposi's Sarcoma-associated Herpesvirus (KSHV), or Human Herpesvirus 8 (HHV-8), was first identified in 1994 by Yaun Chang and Patrick Moore, who used representational differential analysis to identify this previously unknown herpesvirus in a KS lesion from an AIDS patient (41). KSHV is encoded by a 120kb dsDNA genome and is included in the γ2-herpesvirinae, or rhadinovirus, genus in which Herpesvirus Saimiri (HSV) is the prototypic member (81). Unlike other human herpesviruses, seroprevalence in the general population is fairly low (1-3%) in the US. However, KSHV seroprevalence is higher within specific groups, such as HIV-positive, homosexual/bisexual males (30%), children (20-30%) and adults (50-70%) living within specific regions in Africa, and within elderly men of Mediterranean descent (<10%) (83, 181). The virus is associated with Kaposi's Sarcoma, a neoplasm of endothelial origin, as well as 2 B cell lymphomas, pleural effusion lymphoma (PEL) (37) and multicentric Castleman's disease (MCD) (220).

KSHV appears to be transmitted in a variety of ways, but the exact routes are not entirely clear (181). Saliva seems to play a pivotal role in the transmission of this virus, as suggested by the high salivary viral loads. Likewise, high seroprevalence in children in endemic areas eliminates sexual contact as a main route of transmission (34, 65, 181). However, within areas of low seroprevalence, such as the US, sexual transmission is likely the main route of transmission, as KSHV infection in adolescents is rare (65). Additionally, men who engage in homosexual activities have a much higher rate of seroprevalance versus heterosexual men (30% vs 1%), and this increases with occurrence of other sexually transmitted infections, suggesting the presence of inflammatory cells or a weakened immune status may increase the likelihood of sexual transmission (181). There are few reports of blood transmission of KSHV, and accounts of vertical transmission have not reported virus within breast milk, so shedding via saliva is also the likely route in cases of vertical transmission, as well (65, 181).

KSHV DNA and viral transcripts have been identified in a variety of cell types in infected humans, including endothelial cells (25), epithelial cells, keratinocytes, monocytes (22, 159), and B cells, which are an important reservoir of KSHV latency (8, 159). Likewise, *in vitro* studies have confirmed that KSHV can infect endothelial cells, epithelial cells, fibroblasts, B cells (191), keratinocytes (208), macrophages (189) and dendritic cells (DCs) (250) (189), but infection results in a predominantly latent

infection (81). However, latently infected B cells and endothelial cells can be treated with phorbol esters to induce lytic replication in a small percentage of cells (191, 241).

KSHV binding and entry into cells appears to require different receptors and entry mechanisms based on cell type. Initial binding of KSHV to endothelial cells is mediated through interactions between viral glycoproteins, K8.1 and gB, with heparin sulfate on the cell surface (5, 19, 245). There also appears to be a second binding interaction between gB and $\alpha 3\beta 1$ integrins on endothelial cells, as well (6). Differentially, KSHV binds to DC-specific intracellular adhesion molecule-3 grabbing non-integrin (DC-SIGN) to gain entry into B cells (188), DCs and macrophages (189), but the viral protein(s) that mediates this binding has yet to be identified. KSHV gains entry into endothelial cells (88), fibroblasts (4), and B cells (188) via clathrin-mediated endoctyosis, but it's also been demonstrated that KSHV utilizes macropinocytosis for entry into endothelial cells (187). Although there is not a complete understanding of KSHV binding and entry, the wide cellular distribution of heparin sulfate and multiple mechanisms of viral entry could explain how KSHV is able to infect so many different cell types.

B. KSHV-associated Pathologies

1. Kaposi's Sarcoma

The most recognized pathology associated with KSHV infection is Kaposi's Sarcoma (KS). KS was first described in 1872 by Moritz Kaposi, who defined it as 'an idiopathic multiple pigmented sarcoma' (114, 151). At that time, KS was considered a

rare, slowly progressing disease, and was most commonly seen in elderly men of Mediterranean and Eastern European descent. However, when previously healthy, young, homosexual men started presenting with an aggressive, fatal form of KS in 1981 (79), it quickly redefined KS as a more significant health concern. Early studies showed that, within the US, persons with AIDS were 20,000 times more likely to have KS than persons within the general population (15). Likewise, throughout the 1980s and into the 1990s, the incidence of KS among AIDS patients was between 15-30%, and KS was often the presenting disease in these individuals (15, 104). Fortunately, the advent of highly active antiretroviral therapy (HAART) for treatment of HIV in the mid-1990s has considerably decreased the incidence of KS and KS-associated death (65, 104). However, KS still remains the most prevalent HIV-associated malignancy (223), and is a significant health concern for those who do not have access to HIV treatments, cannot afford treatment, or are non-compliant. Moreover, recent studies have documented an increase in KS in HIV-infected individuals receiving long-term HAART and maintaining low HIV viral loads and stable CD4 T cell numbers (152). These recent data suggest that, in addition to KSHV infection and immune-suppression, other unidentified factors are important for development of KS.

KS is described as a multi-focal angioproliferative disease. KS lesions are present on the dermis, oral cavity, and visceral organs, and are composed of proliferating spindle cells of endothelial origin, as well as a high number of infiltrating immune cells (89). KSHV can be detected in circulating B cells (8), and in the characteristic spindle cells (25) and monocytes (22) within KS lesions of infected individuals. Most cells within

KS lesions are latently infected, with only ~3% demonstrating lytic antigen production (89). The lesions are also highly vascularized, but the new blood vessels are abnormal and leaky, giving the lesions their characteristic purplish color (89).

Kaposi's Sarcoma can be categorized into 4 distinct forms: 1) classic KS, 2) epidemic or AIDS-associated KS, 3) endemic or African KS, and 4) transplant-associated KS (65). Classic KS is seen in elderly men of Mediterranean descent and is not associated with HIV infection. Classic KS was the variant initially described by Dr. Kaposi (114), and is usually a less aggressive form of the disease, resulting in dermal lesions restricted to the lower extremities. AIDS-associated KS is a more aggressive form of the disease and as its name implies, is associated with an advanced stage of HIV infection. These individuals often have lesions appearing on the lower and upper extremities, the face, the oral cavity and the visceral organs, and disease often results in a poor outcome (11). Endemic KS was prevalent in Africa long before the HIV epidemic, and compared to other parts of the world, there's a higher incidence among women and children. In some endemic regions in Africa, KS incidence is >50% (83, 90). Transplant-associated KS results in patients undergoing immunosuppressive therapy following an organ transplant, and will often regress when patients stop taking immune suppressing drugs (65).

Treatment options for KS depend on the severity of disease and the immune status of the individual. Surgical excision of lesions, laser or cryo-therapy and topical chemotheraputics are choice treatments in mild cases, but do not prevent development

of new lesions (223). In aggressive KS cases, low dose systemic chemotheraputics are usually employed. More recently, less traditional treatment options have shown promise in clinical studies, including the tyrosine kinase inhibitor, imatinib (60, 223). In HIV-positive individuals, HAART is the recommended treatment, and can reduce the extent of disease and reduce the incidence of new cases of KS (60, 104). The increased angiogenesis seen in KS can also be targeted in a number of ways to limit tumor growth. Rapamycin blocks the mammalian target of rapamycin (mTor) directly, leading to a decrease in growth signals. Likewise, targeting vascular endothelial growth factor (VEGF), which can signal through the mTor pathway and is also a product of mTor signaling, also inhibits transformation (222). None of these treatments are solely directed against the virus, but antivirals on their own are not that effective at treating KS, as the majority of tumor cells within the lesions are latently infected and these drugs specifically target lytic replication (139). However, a combination of these therapies is often employed for the most benefit.

2. B cell disorders

a. Primary Effusion Lymphoma (PEL)

Soon after identifying KSHV as the etiological agent of Kaposi's Sarcoma (41), KSHV infection was also identified in AIDS patients with body-cavity based lymphomas (37). This type of lymphoma is characterized by pleural, pericardial, or peritoneal effusions, and is now referred to as primary effusion lymphoma (PEL) (36). PEL is a rare disease and only accounts for about 2% of AIDS–associated lymphomas (223), but

unfortunately, patients with PEL also have a poor prognosis, with an average survival time of 2-5 months (36).

Further analysis of this particular lymphoma characterized PEL cells as differentiated, hyperblastic plasma cells due to their surface expression of CD138, lack of surface immunoglobulin, as well as clonal immunoglobulin gene rearrangements (36). Other defining traits of PEL cells include expression of CD45, but a lack of characteristic B cell markers (e.g., CD19). Also, PEL cells generally do not have rearrangements in the c-myc gene, nor do they have alterations in Bcl-2, Ras, or p53 genes (36). Therefore, because dysregulation of these oncogenes is often a factor in the development of malignancies, it's apparent that KSHV infection is able to drive transformation via other unique mechanisms. Latent KSHV (50-150 genome copies/cell) is detected within PEL, with the majority of cells expressing the latency proteins, LANA-1 (ORF73), vCyclin (ORF72) and vFLIP (ORF71), as well as kaposin (ORF K12) and LANA-2/vIRF-3 (ORF K10.5). Additionally, a small percentage of these cells are also expressing vIL-6 (ORF K2) (89). Moreover, there are also a marked expression cellular IL-6 within PEL tumors (223); and the fact that IL-6 and vIL-6 are both capable of driving proliferation of B cells (99) makes these cytokines potentially crucial factors in the development of PEL (162, 166).

There is not a standard protocol for treating PEL, and because of the rarity of this type of lymphoma, it's not feasible to test therapies via clinical trials. However, because PEL usually develops in cases of advanced AIDS, HAART is already being

administered and combining HAART with antiviral drugs can promote survival (223). In another study patients with PEL were treated with antiviral drugs and valproate, a histone-deacetylase inhibitor, which increased KSHV lytic replication and increased apoptosis of PEL cells in these patients (35). Likewise, rapamycin and NFκB inhibitors both lead to apoptosis of PEL cell lines *in vitro*, providing two other potential treatments (216).

b. Multicentric Castleman's Disease (MCD)

MCD is an aggressive lymphoproliferative disorder involving multiple lymph nodes and extranodal sites. KSHV is associated with nearly all cases of MCD in HIV-positive individuals, and is characterized by enlarged germinal centers within the affected lymph nodes. MCD tumor cells are characterized as plasmablastic cells that are less differentiated than PEL cells due to their expression of IgM and pre-plasma B cell markers, IRF4 and Blimp1, as well as their lack of CD138 expression (38). The expansion of B cells in patients with MCD is accompanied by an increase in IL-6 levels, which is likely enhanced by vIL-6, as well (179). Approximately 10-50% of the B cells within the affected lymph nodes are positive for KSHV LANA-1 (latent antigen), and 5-25% of these cells also express vIRF-1 (ORF K9) and vIL-6 (lytic antigens) (179), suggesting both latent and lytic transcriptional programs of KSHV-infected cells in MCD, differing from a predominantly latent KSHV infection in KS and PEL.

Therapies for MCD are often in the context of HAART for simultaneous treatment of HIV, and usually include steroids and chemotherapy (11). Similar to PEL, it's thought

that cellular IL-6 and vIL-6 are also potential growth factors driving development of MCD (11). Accordingly, monoclonal antibodies against IL-6, as well as CD20, have proven efficacious in treating MCD (223). Antiviral therapy has also proven useful in inducing regression of MCD due to the higher incidence of lytic KSHV replication in MCD (35).

C. Novel KSHV Genes and Proposed Roles in Pathogenesis

KSHV encodes a number of genes that have suggested roles in pathogenesis (Table 1.1), including several viral homologues of cellular genes likely pirated from the host throughout the evolution of the virus (10, 89). These viral genes include homologues to IL-6 (vIL-6/ORF K2), CC chemokine ligands (vCCL-1, -2, -3/ORFs K6, K4, K4.1), Bcl-2 (vBcl-2/ORF 16), cyclinD (vCyc/ORF 72), CD200 (vCD200/ORF K14), a G-protein coupled receptor (GPCR) with homology to the IL-8 receptor (vGPCR/ORF 74), a complement control protein (vKCP/ORF 4), caspase 8 (FLICE)-like inhibitory protein (vFLIP/ORF K13), and viral interferon regulatory factors (vIRF-1, -2, -3, -4/ORFs K9, K11/11.1, K10.5/10.6, K10/10.1) (10). The cellular homologues of these genes have roles in inflammation, the interferon (IFN) response, and apoptosis. Moreover, *in vitro* studies have demonstrated these viral proteins also function within the same pathways, sharing functions with their cellular homologues, as well as possessing distinct functions of their own (Table 1.1) (10, 89). For example, the vIRFs have inhibitory roles in the induction of IFN and IFN-signaling, specifically antagonizing cellular IRFs, and KSHV vIRF-1 can also promote cellular transformation

[reviewed in (170)]. A separate section will further detail the functions of vIRFs and their potential role in KSHV pathogenesis.

The viral cytokine/chemokine proteins, vIL-6 and vCCLs, possess similar functions as their cellular counterparts. For example, cellular IL-6 and vIL-6 both bind to the same receptor, function to promote cellular proliferation (42, 110, 166), and also promote angiogenesis by inducing production of vascular endothelial growth factor (VEGF) (9). Differentially, vIL-6, but not cellular IL-6, also functions to antagonize IFN-α-mediated cell cycle arrest by inhibiting the IFN-stimulated gene factor 3 (ISGF3) complex from driving transcription (42). Moreover, because vIL-6 is one of the few viral proteins readily detectable in PEL and MCD tumors (11, 223), it is potentially a crucial player in development of these B cell disorders. The vCCL proteins show homology to macrophage inflammatory proteins (MIPs), and they function to initiate similar signaling cascades, regulate chemotaxis, and drive a Th2-polarized response that provides a potential immune evasion strategy (194). Additionally, KSHV vCCLs (45), along with vBcl-2 and vFLIP (89), can all inhibit apoptotic signaling, potentially functioning in an oncogenic capacity during disease development.

KSHV also encodes viral homologues that are expressed on the surface of the infected cell. KSHV vCD200 shares sequence and functional homology with cellular CD200, a cell surface molecule with a broad expression profile (78). Both the viral and cellular CD200 proteins bind to the CD200 receptor, present mostly on T cells and myeloid cells, and inhibit Th1 cytokine production and neutrophil function (78, 195). KSHV

vGPCR is also expressed on the cell surface, and shares homology with cellular IL-8 receptor. Binding of IL-8 to cellular IL-8R or the viral homologue (vGPCR) induces a signaling cascade that promotes neutrophil migration and inflammatory signaling (218). KSHV vGPCR, however, encodes a mutation in a highly conserved sequence that renders the vGPCR constitutively active, removing the need for IL-8 binding. Expression of vGPCR on the cell surface results in an upregulation of mitogenic pathways and increased production of cytokines and chemokines in theose cells (218), and can independently promote cellular transformation (160, 218).

The current collection of data establishes a multitude of functions for the KSHV immunomodulatory proteins (Table 1.1), including manipulation of innate and adaptive immune responses, as well as potentiating transformation (10). Many of these findings, however, have yet to be validated during disease progression *in vivo* due to constraints within the current systems available for studying KSHV pathogenesis (169).

Table 1.1 Immunomodulatory proteins encoded within KSHV

ORF	Gene product	Function
Intercellular Communication		
K2	vIL-6	IL-6 homologue
K4	vCCL2	CCR3 and CCR8 agonist; CCR1, CCR2, CCR5, CCR10, CXCR4, CX_3CR1 and XCR1 antagonist
K4.1	vCCL3	CCR4 agonist
K6	vCCL1	CCR8 agonist
K13	vFLIP	Prevents apoptosis in some cells
Intracellular Defenses		
Type I IFN		
ORF45	ORF45	Prevents IRF7 activation
ORF50	RTA	Promotes IRF7 ubiquitylation and degradation
K9	vIRF1	Prevents IRF3-mediated transcription
K10.5–K10.6	vIRF3	Enhances IRF3- and IRF7-mediated transcription?
K11.1–K11	vIRF2	Prevents IRF1- and IRF3-mediated transcription; binds and inhibits PKR
Apoptosis		
K1	K1	Activates AKT signalling
K2	vIL-6	Inhibits IFN-mediated apoptosis in cells
K7	vIAP	Links BCL-2 to effector caspases
ORF16	vBCL-2	BCL-2 homologue
ORF45	ORF45	Prevents IRF7 activation
ORF50	RTA	Inhibits p53 transcriptional activity
K9	vIRF1	Binds p53, ATM kinase and GRIM19
K10.5–K10.6	vIRF3	Binds and inhibits p53
K13	vFLIP	Blocks recruitment and/or activation of caspases
ORF73	LANA	Binds p53
Intercellular Interactions		
K1	K1	Downregulates BCR surface expression
K3	MIR1	Downregulates HLA-A, HLA-B, HLA-C and HLA-E molecules, as well as CD1d
K5	MIR2	Downregulates HLA-A, HLA-B, CD86, ICAM1 and PECAM1 molecules, as well as CD1d
K14	vCD200	CD200 homologue, inhibits myeloid functions
K15	K15	Inhibits B-cell signalling
Others		
ORF4	KCP	Inhibitor of complement activation
ORF37	SOX	Induces host shut-off by promoting messenger RNA degradation

Abbreviations: CCL, chemokine ligand; CCR, CC chemokine receptor; FLIP, FLICE-like inhibitory protein; RTA, replication and transcription activator; IAP, inhibitor of apoptosis; LANA, latency-associated antigen; MIR, modulator of immune recognition; KCP, KSHV complement protein; SOX, shutoff and exonuclease protein. Table reprinted with permission (51).

D. Models of KSHV Pathogenesis

Studying KSHV pathogenesis has proved difficult for two main reasons. First, there is inefficient KSHV lytic replication within cultured cells. In cultured B cells and endothelial cells, KSHV infection predominantly results in a latent infection. Use of phorbol esters can induce lytic replication within latently infected PEL cells, but only in ~25% of these cells (39), and only a quarter of those cells actually complete the lytic cycle (193). Since the majority of viral genes are expressed during lytic replication, examination of specific viral genes has been mostly outside the context of infection. Secondly, it has been difficult to develop an animal model due to the species specificity of KSHV. Efforts to develop an animal model to study KSHV pathogenesis will be discussed further.

Initial attempts to develop an *in vivo* model of KSHV focused on utilizing an immuno-compromised mouse (61, 180, 182). An early study transferred KSHV-infected PEL cells into a SCID-hu mouse, resulting in development of a B cell tumor, but the tumor consisted solely of the grafted PEL cells (182). Moreover, KSHV did not spread to murine tissues, or even to human PBMCs when they were grafted at the same time as the PEL cells (182). Another study utilized SCID-hu Thy/Liv mice that were infected via direct inoculation of purified KSHV into the grafted human thymus and liver tissue under the kidney capsule (61). Lytic and latent antigens were detected via RT-PCR within the transplanted B cell population, but no human cells were detected outside of the transplant, nor were KSHV antigens detected within any murine tissues/cells (61). A subsequent study utilized NOD/SCID mice, which were infected with purified KSHV

(180). This potential model demonstrated KSHV infection of murine cells via lytic and latent transcript detection, as well as LANA protein expression during latency. Additionally, productive KSHV infection was also determined via detection of virus via electron microscopy, and KSHV maintained latency for >4 months PI within the B cell population, a major site of latency in KSHV-infected humans. However, the total cell population infected with KSHV was less than 1% in these mice, and these animals did not develop any KSHV-associated diseases (180). Overall, the use of small animal models does not allow for study of pathogenesis, as the development of KSHV-associated diseases is limited and usually confined to transplanted human tissues (77, 180). Likewise, these animals have an impaired immune system, so it is not possible to study immune evasion or the immune response unless human PBMCs are also transplanted within these mice (61, 180, 182). The utilization of small animal models is limited in its utility with a focus on latency, but not on disease, lytic replication, or immune response.

Due to the troubles developing a small animal model, it was hypothesized that KSHV infection of non-human primates may yield better results due to the higher order of similarity between primate species (192). However, KSHV infection of Simian Immunodeficiency Virus (SIV)+ and SIV- rhesus macaques (RM) did not result in detectable levels of lytic or latent KSHV transcripts or the development of anti-KSHV antibodies. Viral DNA was detected in the first 6 months and at necropsy within the bone marrow and spleen, demonstrating persistence within the RMs. Collectively, the low level of infection, lack of anti-KSHV humoral response, and lack of KSHV-

associated diseases also makes KSHV infection of RMs an ineffective model (192). KSHV infection of common marmosets, a more recently developed primate model, has also been explored as a potential system for studying KSHV pathogenesis (40). The infected marmosets did not demonstrate any B cell hyperplasia, but KSHV established a persistent infection within B cells. Additionally, KSHV infection of marmosets induced a robust humoral response, and one of the marmosets even developed a KS-like lesion (40). However, similar to KSHV infection of RMs, this group was also unable to detect viral transcripts or recover virus from the infected animals (40). Common marmosets are new world monkeys, taxonomically distinct from the more closely related old world monkeys and humans. Moreover, common marmosets also have fewer MHC-I alleles, which could make them susceptible to a broader range of pathogens, and likely why these animals were susceptible to KSHV infection and development of KS-like disease (40). Therefore, it's important to consider that the interaction between the host immune system and the virus will be different in the context of a polymorphic MHC locus, and could account for differences in KSHV pathogenesis in humans, old world monkeys (RM), and new world monkeys (marmoset).

Another approach to study KSHV pathogenesis is to utilize a virus similar to KSHV and study infection in its natural host. There are two γ-herpesviruses with homology to KSHV that are being utilized as models, murine herpesvirus 68 (MHV-68) and rhesus macaque rhadinovirus (RRV). MHV-68 is a natural pathogen within mice and also maintains homology and co-linear genomic organization with KSHV (242). Utilization of a species-specific model of virus infection facilitates study of more precise virus-host

interactions, the immune response, and direct development of disease. Indeed, MHV-68 infection of mice results in development of lymphoproliferative disorders and clonal B cell lymphoma in ~9% of mice following MHV-68 infection (224). Lymphomas are associated with lymph nodes and extranodal sites, similar to MCD, and viral DNA could be detected within the tumor, demonstrating latency. However, lytic MHV-68 antigens were not detected in these animals (224). Another drawback, in addition to the lack of detectable lytic replication, is that MHV-68 does not encode a number of the unique, cellular homologues that are potentially novel and essential players in KSHV-associated disease. These genes include vMIP, vIL-6, vFLIP, vCD200, and vIRF (242), which have each been demonstrated to have specific tumorigenic and immune evasion functions (249). Moreover, KSHV infection results in more dramatic pathologies in immune-compromised individuals, as during HIV co-infection, and specifically addressing KSHV-associated disease in the context of an underlying HIV infection cannot be adequately modeled within a mouse, due to the absence of a murine homologue of HIV.

The other γ-herpesvirus being used as a model of KSHV pathogenesis is RRV, a natural pathogen in RMs. RRV shares a higher degree of co-linearity with KSHV, and can be analyzed in the context of SIV co-infection in RMs. This model system will be discussed in detail in the subsequent section.

III. Rhesus Rhadinovirus

A. Identification and General Characteristics

Rhesus macaque rhadinovirus (RRV) was independently isolated from RMs at two different primate centers in the late 1990s (58, 207), and sequence analysis demonstrated considerable homology to the most recently identified human herpesvirus, KSHV (7, 41, 207). The first strain, $RRV_{26\text{-}85}$, was isolated from a healthy RM at the New England Primate Research Center, and ELISA analyses proved that RRV was pervasive throughout that colony, as well as two additional colonies that were sampled (58). Shortly thereafter, a highly homologous strain of RRV (RRV_{17577}) was isolated from a RM at the Oregon National Primate Research Center that was infected with SIV and presenting with a lymphoproliferative disorder (256). Sequence characterization of RRV placed it within the γ2-herpesvirinae subfamily, in which KSHV and Herpesvirus saimiri (HVS) are also members, and it's now known that RRV naturally infects >95% of the RMs in primate centers around the US (251). However, experimental RRV infection of RMs has only associated strain 17577 with development of specific pathologies (69, 147, 172, 256).

RRV has a 131kb dsDNA genome with an essentially co-linear organization with KSHV (7, 207), and is considered to be the RM homologue of KSHV (Figure 1.2). RRV encodes 79 ORFs, 68 of which align with those encoded in KSHV, including a collection of ORFs with homology to cellular genes (207). Novel RRV ORFs and their homology with KSHV ORFs will be discussed further in a subsequent section.

RRV infection of fibroblasts in culture results in predominantly lytic replication, allowing for easy study of the lytic replication cycle and for analysis of specific viral genes. In general, propagation of RRV is also easier in comparison to the limited amount of lytic replication that can be induced in KSHV culture systems (59). B cells can also be infected by RRV in culture (18) (personal observation), but propagation of latently infected B cells has been difficult, and is achieved only in the presence of EBV co-infection (18).

B. RRV-associated Pathologies

Since the initial isolation of RRV, experimental infection of RMs with RRV_{17577} validated the role of RRV in development of B cell disorders and lymphomas in SIV/RRV co-infected RMs (69, 171, 172). *De novo* RRV infection of RMs results in acute viremia during the first 4 weeks following infection which subsides to undetectable levels within the following weeks, with intermittent spikes in viral loads often coinciding with immune-suppression due to SIV infection or development of RRV-associated diseases (172, 256). Initially, RRV infection results in development of a characteristic B cell hyperplasia within 4-6 weeks post-infection. Subsequently, within the context of SIV infection, RRV infection is also associated with non-Hodgkin's lymphoma and other B cell lymphomas in about 25% of cases (69, 172, 256). Development of RRV-associated lymphoproliferative disorder includes an increase in total B cells in peripheral blood and lymph nodes, persistent lymphadenopathy, splenomegaly, and hypergammaglobulinemia, closely resembling the pathology of MCD in patients co-infected with KSHV/HIV (172, 256). Also similar

to KSHV infection in humans, an important site of latency in RRV-infected RMs is within B cells (16).

Additionally, one RM that was experimentally co-infected with SIV and RRV_{17577} developed retroperitoneal fibromatosis (RF) (85, 172), which closely resembles KS in humans. However, other documented cases of RF have not been associated solely with RRV, so the direct link to RF is uncertain (29, 85).

C. Novel RRV Genes and Differences/Similarities with KSHV

All identified ORFs encoded within KSHV have at least one homologous ORF within RRV, save ORFs K3 and K5 [modulator of immune recognition 1 (MIR1) and MIR2], K7 [viral inhibitor of apoptosis (vIAP)], and K12 (kaposin) (Fig. 1.2). Therefore, similar to KSHV, RRV also encodes a number of ORFs with homology to cellular genes, and overall, RRV dedicates a large percentage of its genome to ORFs that code for proteins involved in immune evasion and pathogenesis (10) (Table 1.1). *In vitro* examination of some of these RRV ORFs has verified they possess similar functions as those demonstrated for the related ORFs within KSHV. For example, RRV vGPCR (ORF 74), which shares homology with cellular IL-8 receptor, induces secretion of VEGF and possesses transforming potential *in vitro* and *in vivo,* similar to KSHV GPCR (68). RRV also encodes a viral homologue to CD200 (vCD200/ORF R15), which is expressed on the surface of infected cells and inhibits monocyte function similar to cellular CD200 and KSHV vCD200, but RRV vCD200 is also secreted, a characteristic specific to the RRV protein (129). KSHV and RRV also encode

complement control proteins (ORF 4 in both) that are each expressed on the surface of the virion, and function to inhibit the classical complement cascade (149, 221). RRV vIL-6 also functions similarly to KSHV vIL-6, as well as cellular IL-6 (i.e., driving proliferation of B cells) (99, 113), and of particular significance is that vIL-6 is expressed within tumors in RRV-infected RMs (171), similar to KSHV-infected individuals with PEL and MCD (11, 179). These findings suggest that vIL-6, along with cellular IL-6, are likely important factors for driving B cell proliferation in KSHV-associated malignancies (11, 179, 223). Further study of these RRV proteins in disease development and immune evasion in infected RMs will hopefully provide unique insight into the impact of their KSHV homologues in KSHV-infected individuals.

Additionally, RRV encodes 8 vIRFs, similar to the 4 vIRFs encoded within KSHV, and thus, are hypothesized to similarly function to inhibit IFN signaling and promote tumorigenesis (7, 170, 207). This thesis focuses on the role of vIRFs during RRV infection, and further analyzes key mechanisms involved in vIRF function in hopes of better understanding the role of vIRFs in KSHV-associated disease.

FIGURE 1.2. Alignment of KSHV and RRV genomes. ORFs are colored according to their inclusion within specific herpesvirus subfamilies, and are oriented with the pointed end at the 3' end of each ORF. ORF, open reading frame. TR, terminal repeats. *Figure and legend adapted from (7) and reprinted with permission.*

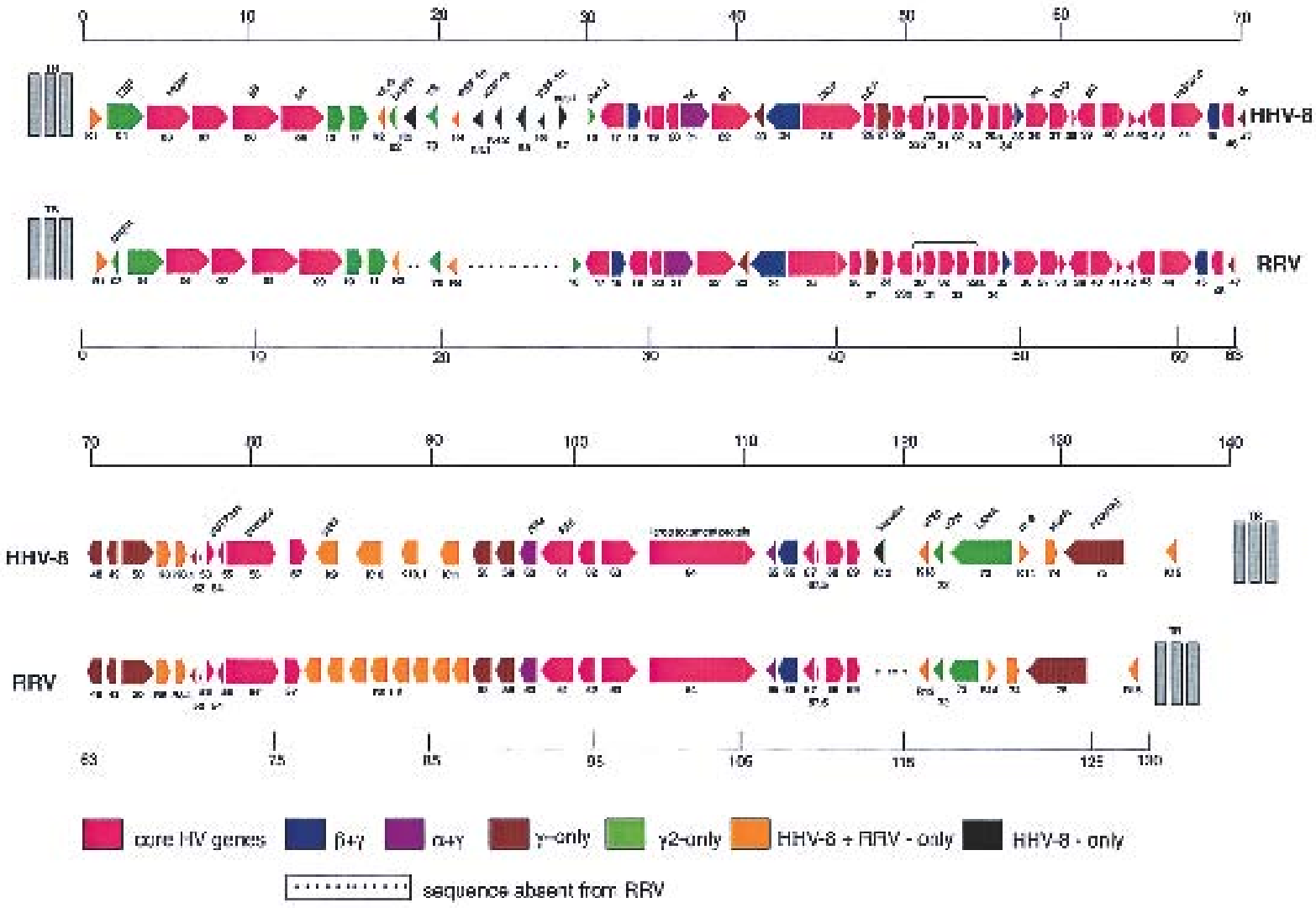
HHV-8
RRV
HHV-8
RRV
core HV genes
β+γ
α+γ
γ-only
γ2-only
HHV-8 + RRV - only
HHV-8 - only
sequence absent from RRV

D. RRV Infection of RMs as a Model for Studying KSHV Pathogenesis

RRV has been demonstrated to be a great model for studying KSHV pathogenesis for a number of reasons. First, RRV and KSHV have co-linear genomes, and almost all of the unique genes encoded within KSHV are present within RRV (7, 207). Additionally, KSHV encodes several genes unique to itself and RRV, providing an exclusive opportunity for direct analysis of the functions of these viral proteins during disease in the natural host. Secondly, RRV infection in culture results in a predominantly lytic infection, allowing for easy study of viral genes during the context of *de novo* infection. Of significant importance is that RRV and KSHV infection of their respective hosts results in similar pathologies (69, 172, 256), and we can recapitulate complications and disease associated with KSHV and HIV co-infection through RRV and SIV co-infection in the RM. Specifically, the ability to co-infect RMs with SIV, and the inclusion of many of the unique KSHV genes in the RRV genome, promote RRV as a more ideal model when compared to the MHV-68 infection in mice. RRV infection of RMs provides a more comparable system for studying the roles of specific viral proteins in KSHV pathogenesis, the specific immune response and latency. Moreover, recent development of a bacterial artificial chromosome (BAC) clone of RRV has provided a tool to target viral genes for deletion to specifically analyze their molecular function *in vitro*, as well as their impact during RRV infection and disease in the RM (69).

IV. The Immune Response to Primary Herpesvirus Infection

A. General Aspects of Innate immunity

The innate immune response is the initial line of defense against invading pathogens, and is separated from the adaptive response due to its immediate and non-specific recognition of pathogens, and lack of memory. The innate response includes mechanical (e.g., epithelial barrier), chemical (e.g., lysozyme in tears/sweat) and microbiological (e.g., normal flora) barriers, activation of complement within the plasma, and cellular components including phagocytic cells, Natural Killer (NK) cells, and antigen-presenting cells (APCs) (105). Phagocytic cells and APCs will engulf and destroy pathogens, and their indiscriminate recognition of pathogens initiates production of IFN and other cytokines and chemokines that comprise an immediate inflammatory response, which will help shape the adaptive immune response. Aspects of pathogen recognition, induction of the IFN response, and initiation of an adaptive response will be discussed in the following sections.

B. Pathogen Recognition - (PRRs and PAMPs)

Incoming pathogens are immediately sensed via innate immune recognition molecules present on host cell membranes and within the cytoplasm. These innate recognition molecules are collectively referred to as pattern-recognition receptors (PRRs), aptly named for their capacity to recognize pathogen-associated molecular patterns (PAMPs), unique to invading pathogens (115, 176, 255). PAMPs can be lipids, sugars, proteins, or nucleic acids, distinct from that found within the host based on their structure and composition, as well as their localization within the cell (176). Following recognition

of their cognate PAMPs, PRRs initiate signaling cascades through specific adaptor molecules that result in activation of IκB kinase (IKK)-related kinases, Tank-binding kinase (TBK) and IKK-ε, and subsequently converges on the activation of NFκB and cellular IRFs which promote transcription of type I IFNs and other pro-inflammatory cytokines (94) (Figure 1.3). Specifically, activation of NFκB leads to induction of pro-inflammatory cytokines including IL-1, IL-6, TNF-α and IL-15 (3, 175). Induction of NFκB alongside activation of IRF-3 leads to induction of IFN-β, and activation of IRF-7 and/or IRF-3 leads to induction of multiple subtypes of IFN-α (115) (Figure 1.3). These type I IFNs are a vital part of the innate immune response, and also important for initiating an effective adaptive immune response (93, 146).

The most well-studied PRRs are the Toll-like receptors (TLRs). TLRs are a family of membrane-associated glycoproteins (9 defined receptors in humans), whose expression on APCs, including B cells, monocytes, macrophages, and DCs, is crucial for innate antigen detection (115). TLRs 1, 2, 4, 5, and 6 are expressed on the plasma membrane and can recognize an array of PAMPs found on bacteria, fungi, and viruses. TLRs 3, 7, 8, and 9 are expressed within endosomal and lysosomal membranes; each recognizes a specific type of nucleic acid, and are thought to have evolved to primarily recognize viruses (115). TLR9 specifically recognizes unmethylated CpG-containing motifs present in bacterial and viral DNA, making herpervirus genomic DNA a potential ligand within an infected cell. Indeed, TLR9 plays a role in recognizing alpha-, beta-, and gamma-herpesviruses, including KSHV (176, 250) (Table 1.2). Studies have demonstrated that viral entry is necessary for TLR9 recognition and induced signaling

(74, 144, 226, 238), but there may be variations on the exact ligand for TLR9 between herpesviruses. Infection of murine plasmacytoid DCs (pDCs) with UV-inactivated HSV-1 still resulted in stimulation of the TLR9 pathway, which demonstrates viral replication is not necessary for TLR9-induced signaling (124) and suggests genomic DNA is the TLR9 ligand for HSV-1. However, UV-inactivated KSHV did not stimulate IFN-α production in pDC cultures (250), suggesting the TLR9 ligand may be a replication intermediate or that UV-inactivation of the virus disrupted the TLR9 ligand.

TLRs 2, 3, and 4 also recognize other components found on the herpes virion, as well as products of herpesvirus replication in the infected cell (176) (Table 1.2, Figure 1.3). TLR2, which recognizes lipopeptides, was the first TLR demonstrated to recognize herpesviruses (50). Specifically, TLR2 is thought to recognize glycoproteins on the virion envelope, as demonstrated for HCMV (23), and TLR2 mediates innate signaling following recognition of HSV-1 (126), HSV-2 (219), HCMV (23, 50), and VZV (246) at the cell surface. Of interest, KSHV is the only human herpesvirus recognized by TLR4 (128), whose most notable ligand is lipopolysaccharide (LPS) found on Gram-negative bacteria. The TLR4 ligand on KSHV has not been identified, but is hypothesized to be an envelope glycoprotein or other virion component as UV-inactivated virus is also able to trigger TLR4 signaling (128).

Cytosolic PRRs include the RNA-helicase domain-containing proteins, RIG-I and MDA5, which recognize and bind to specific species of RNA (255) and have been

demonstrated to play a role in innate signaling via recognition of replication intermediates during HSV and EBV infection (1, 44, 153). A number of cytosolic PRRs that recognize dsDNA have also been demonstrated to recognize human herpesviruses, including the DNA-dependent activator of IFN-regulatory factors (DAI) (56, 227), IFN-γ-inducible protein 16 (IFI16) (117, 235), and DEAH box protein 9 (DHX9) and DHX36 (119) (Table 1.2, Fig. 1.3).

Although recognition of herpesviruses by multiple PRRs induces similar signaling cascades all resulting in the induction of type I IFNs and other cytokines, it does not mean the multiple PPR interactions are necessarily redundant. Cell-specific expression of PRRs elevates the necessity of certain receptors. For example, TLR7 and TLR9 are the sole TLRs expressed in pDCs, the main IFN-α producing cell type in the body (47, 215), making TLR9 recognition of herepsviruses a potentially crucial step in the innate response to herpesvirus infection (91, 145).

C. The Interferon Response during Virus Infection

1. Type I and Type II IFN

Interferons are a family of secreted proteins with a variety of roles in innate immunity, cell growth regulation, and immune activation. IFNs can be divided into three groups (Type I-III), based on biological activities and receptor use (73). Type I IFNs were initially identified in the 1950s due to their potent antiviral properties (101). Type I IFNs include multiple subtypes of IFN-α (13 in humans), as well as a single type each of IFN-β, IFN-ω, IFN-κ, and IFN-ε (146). IFN-α and IFN-β are the most extensively

studied type I IFNs and have the most biological impact due to expression in a variety of cell types, and will be the focus of further discussion. IFN-α is produced primarily by pDCs, the main producers of type I IFN in the blood (75). Differentially, IFN-β is produced by a variety of cell types, including fibroblasts and epithelial cells (146). There are two waves of type I IFN production. The first wave is driven by PRR recognition of virus and results in activation of IRF-3, IRF-7, and NFκB, which drive transcription of IFN-β (112, 138, 260) and IFN-α_1 (84, 136) (Fig. 1.3).

The initial wave of type I IFN potentiates transcription of more type I IFN, consisting mostly of different subtypes of IFN-α (146). The potentiated induction of type I IFN constitutes the second wave of IFN production. The second wave of type I IFN production relies heavily on IRF-7, which, itself, is also IFN-inducible. Type I IFN subsequently binds to its cognate receptor, which consists of 2 distinct chains, IFNaR1 and IFNaR2, on the cell surface. Binding of IFN to its receptor activates specific receptor-associated kinases, Tyk1 and Jak2, which then phosphorylate signal transducer and activator of transcription 1 (STAT1) and STAT2. The heterodimer of phosphorylated STAT1 and STAT2 associates with IRF-9 to form the IFN-stimulated gene factor 3 (ISGF3) complex, which, through IRF9 binding to the IFN-stimulated response element (ISRE), drives transcription of 100s of IFN-stimulated genes (ISGs) that orchestrate the antiviral state (101, 244) (Fig. 1.3).

FIGURE 1.3. Schematic representation of PRRs and IFN signaling. During viral infection, a two-wave antiviral response takes place. In the first wave, PRRs recognize viral PAMPs such as dsDNA, dsRNA, ssRNA, and 5'-PPP ssRNA. PRRs that recognize nucleic acids in human herpesviruses include TLR3, TLR9, DAI, RIG-I, and MDA5, and are shaded in blue. These PRRs initiate a signaling cascade that includes TBK1 and IKK kinases, and converges on the activation of c-Jun, IRF-3, IRF-7, and NFκB (p65/p50). These transcription factors cooperate to induce transcription of IFN-β that is then secreted. In response to TLR7 and TLR9 stimulation, IRF-7 is specifically activated which leads to expression and secretion of various subtypes of IFN-α. IFN-α/β signals through its cognate receptor composed of two subunits, IFNAR1 and IFNAR2. Following binding, the signal is transduced to the associated-receptor kinases, Jak1 and Tyk2, which respectively phosphorylate STAT1 and STAT2. Phosphorylated STAT1 and STAT2 heterodimerize and associate with IRF-9 (also known as p48) to form a complex called ISGF3. This complex translocates into the nucleus to induce the expression of ISGs encoding antiviral effectors which amplify the antiviral state. Type II IFN, IFN-γ, is not induced following PRR signaling, but is a crucial cytokine in development of an adaptive antiviral immune response. IFN-γ signals through a similar pathway as IFN-α/β, but it uses a specific receptor, adapters and STATs, and drives transcription of a different set of genes. ISGF3, IFN-stimulated gene factor 3; ISRE, IFN-stimulated response element; GAS, IFN-γ activated sequence. *Figure and legend adapted and reprinted from (237).*

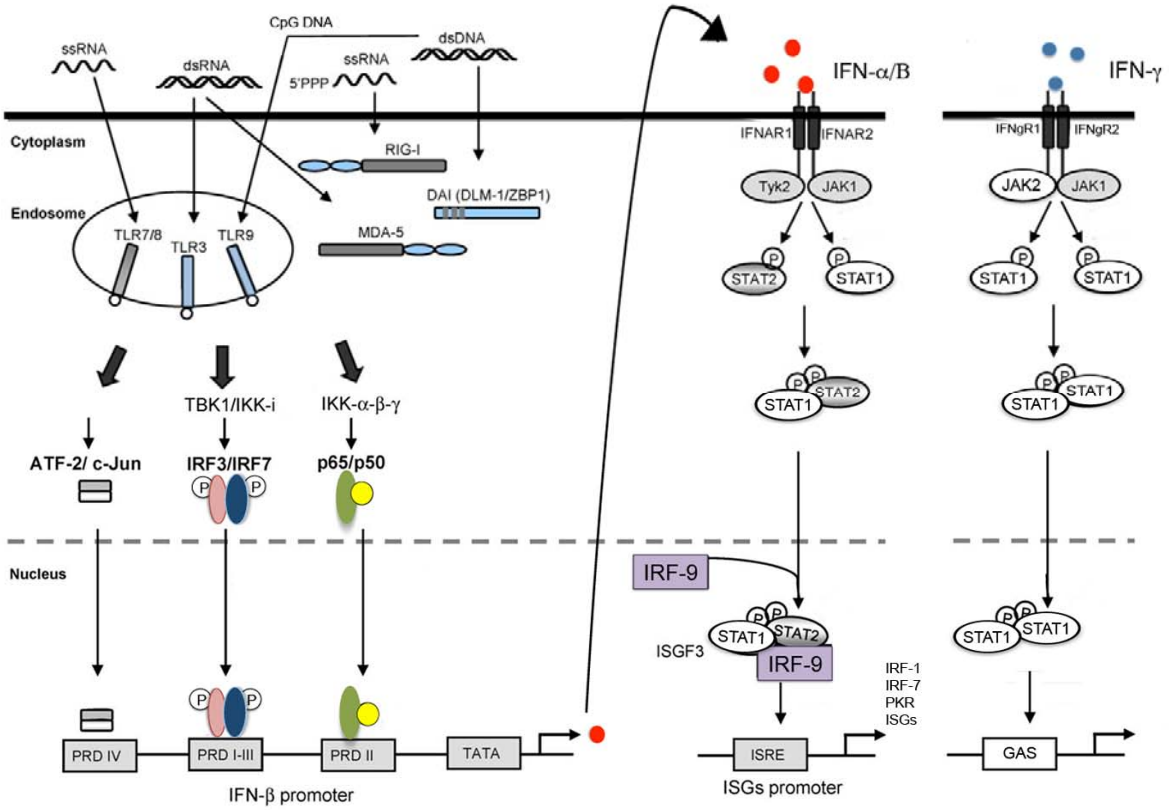
ssRNA
dsRNA
CpG DNA
ssRNA
5'PPP
dsDNA
Cytoplasm
RIG-I
DAI (DLM-1/ZBP1)
Endosome
TLR7/8
TLR3
TLR9
MDA-5
TBK1/IKK-i
IKK-α-β-γ
ATF-2/ c-Jun
IRF3/IRF7
p65/p50
Nucleus
PRD IV
PRD I-III
PRD II
TATA
IFN-β promoter
IFN-α/B
IFNAR1
IFNAR2
Tyk2
JAK1
STAT2
STAT1
IRF-9
ISGF3
IRF-1
IRF-7
PKR
ISGs
ISRE
ISGs promoter
IFN-γ
IFNgR1
IFNgR2
JAK2
JAK1
STAT1
GAS

Table 1.2: PRRs and PAMPs in human herpesvirus infection

PRR	Virus	Proposed PAMP
TLR2	HSV-1	virion component
	HSV-2	virion component
	VZV	virion component
	HCMV	gB and/or gH
	EBV	virion component/dUTPase
TLR3	HSV-1	dsRNA
	EBV	EBERs
TLR4	KSHV	envelope glycoprotein
TLR9	HSV-1	genomic DNA
	HSV-2	genomic DNA
	HCMV	genomic DNA
	EBV	genomic DNA
	KSHV	genomic DNA
DAI	HSV-1	genomic DNA
	HCMV	genomic DNA
MDA5	HSV-1	replication intermediate
pol III and RIG-I	HSV-1	genomic DNA
	EBV	genomic DNA
IFI16	HSV-1	genomic DNA
	KSHV	genomic DNA
DHX and DHX36	HSV	genomic DNA

Abbreviations: PRR, pattern recognition receptor; PAMP, pathogen-associated molecular pattern; TLR, toll-like receptor; DAI, DNA-dependent activator of interferon regulatory factors; MDA, melanoma differentiation-associated gene 5; DHX, DEAH box protein; HSV, herpes simplex virus; VZV, varicella-zoster virus; HCMV, human cytomegalovirus; EBV, Epstein-Barr virus; KSHV, Kaposi's sarcoma-associated herpesvirus; EBER, EBV-encoded small RNA; gB, glycoprotein B. Table data collected from (117, 128, 176, 250).

Type II IFN includes a single member, IFN-γ, and is critical for an effective adaptive immune response during a virus infection. IFN-γ induction is mediated via T-cell receptor engagement and cytokine signaling, including type I IFNs, IL-12, and IL-18. The expression of IFN-γ is generally restricted to NK cells and activated T-cells, and is mediated by the collective cooperation of numerous transcription factors, including NFκB, T-bet, STATs and others (146). IFN-γ is distinct from type I IFNs, and thus, signals through a unique receptor. However, the type II IFN receptor is similar to the type I IFN receptor in that it is composed of two distinct chains and induces a similar signaling pathway. Following engagement of the receptor, Jak1 and Jak2 kinases phosphorylate STAT1, which then dimerizes, translocates to the nucleus, and drives transcription via binding to IFN-γ activated sequences (GAS) in the promoter of target genes (184) (Fig 1.3).

It should be noted that there is a third classification of IFN, type III IFN (-λ1, -λ2, and -λ3), which has similar antiviral effects as type I IFN (64). However, type III IFNs signal through a different receptor than type I IFN, suggesting additional, disparate effects that have yet to be fully characterized and will not be discussed here.

2. Interferon Regulatory Factors

Interferon regulatory factors (IRFs) are a family of transcription factors that direct transcription of IFN, as well as other cytokines and chemokines (94). There are nine characterized IRFs in human cells, each with specific roles and expression patterns (94) (Table 1.3). IRFs have a DNA binding domain within the N-terminus that includes a

pentad tryptophan motif, required for binding to ISRE within promoters of IFN-responsive genes (94). The C-terminus of IRFs includes protein-interaction domains that mediate interactions between other IRFs and transcriptional cofactors, and may also serve as a regulatory domain (66, 94).

The first IRF identified as a positive regulator of type I IFN transcription was IRF-1 (157). Since these initial studies, it's been demonstrated that IRF-3 and IRF-7 are the critical IRFs involved in virus-induced production of type I IFN (115, 203). IRF-3 is constitutively expressed in most cell types, but constitutive expression of IRF-7 is restricted to some lymphoid cells and pDCs and is IFN-inducible in other cell types (94). Under normal conditions, IRF-3 and IRF-7 are maintained mostly in the cytoplasm in an inactive state. Following virus infection, PRR-induced signaling activates IKK-related kinases, TBK-1 and IKKε, which phosphorylate IRF-3 and IRF-7 at the C-terminus. Phosphorylated IRF-3 and IRF-7 form homo- or hetero-dimers that subsequently accumulate in the nucleus to direct transcription of type I IFN (94) (Fig 1.3).

Due to the constitutive expression of IRF-3 in most cell types, it is a crucial player in driving transcription of IFN-β in direct response to virus infection (112, 138, 260). The IFN-β promoter contains four distinct positive regulatory domains (PRD I-IV), two of which have sequence similar to the ISRE (PRD I/III), and are binding sites for IRF-3 (2) (Fig. 1.3). Additionally, IRF-3 must also bind p300/CBP (138, 248, 260), a transcriptional cofactor and histone acetyltransferase, and associate with other cellular

factors, including NFκB and c-Jun, which collectively form the 'enhancesome' required to induce transcription of IFN-β (Fig. 1.3) (94, 231). Therefore, induction of IFN-β is possible in most cell types and occurs quickly following virus infection, but requires the cooperation of several distinct transcription factors.

IRF-7 is only constitutively expressed in some lymphoid cells and pDCs, but is IFN-inducible in most cell types. IRF-7 does not require NFκB or p300/CBP for its transcriptional activities, and is crucial for driving transcription of most subtypes of IFN-α (95, 148, 202) (Table 1.3). Specifically, IRF-7 can drive transcription of IFN-β and IFN-α_1 directly following virus infection (84), and because of its expression pattern, IRF-7 plays a special role in IFN-α production in pDCs (53). Moreover, because expression of IRF-7 is induced upon IFN signaling in most cell types, IRF-7 plays a significant role in amplification of the IFN response, which involves transcription of the various subtypes of IFN-α (95, 202).

In addition to IRF-3 and IRF-7, IRF-5 is also an important factor in virus-induced innate signaling. However, IRF-5 doesn't seem to play a role in induction of type I IFNs, but is vital for induction of other pro-inflammatory cytokines, including IL-6, TNF-α, and IL-12 (94, 123, 228). Specifically, IRF-5 is a critical downstream regulator of TLR9 mediated signaling, and is necessary for transcription of IL-12p40 via binding the ISRE in the promoter (228). The necessity of IRF-5 induction of other pro-inflammatory cytokines is not fully understood, but IRF-5 likely cooperates with NFκB for induction of IL-6 and TNF-α (123).

Another essential IRF involved in type I IFN signaling is IRF-9, also known as ISGF3γ (94) (Table 1.3). Following type I IFN binding to the IFNα/β receptor, JAK-STAT signaling culminates in formation of ISGF3, which includes STAT1, STAT2 and IRF9, which drives transcription of 100s of ISGs (57, 244) (Fig. 1.3). Thus, IRF-9 is a key player in the amplification phase of IFN-signaling.

The remaining IRFs have various roles in enhancing or inhibiting transcription of other cytokines/chemokines in response to specific stimuli and within specific cell subsets. Overall, the IRFs are crucial players in orchestrating immune signaling spanning from virus-induced induction of IFN to Th1-promoting cytokines during the adaptive immune response (94) (Table 1.3).

TABLE 1.3: IRFs and their functions in the immune response

IRF	Role in Immune Response	Expression	Examples of Target Genes
IRF1	Stimulates expression of IFN-inducible genes	Constitutive and IFN-inducible in various cell types	iNOS, Caspase-1, TAP1, CIITA
	Enhances TLR-dependent gene induction in IFN-γ		IFN-β, IL-12p35, IL-12p40
IRF2	Antagonizes IRF-1 and IRF-9; attenuates type I IFN responses	Constitutive and IFN-inducible in various cell types	represses IFN-inducible genes, IL-12p40
IRF3	Induces Type I IFNs and chemokines following virus infection	Constitutive in various cell types	IFN-α1, IFN-β
IRF4	Binds to MyD88 and negatively regulates TLR-dependent induction of pro-inflammatory cytokines	Constitutive in B cells, MΦs, mDCs and pDCs	Indirectly represses IL-12p40, IL-6, TNF-α
IRF5	Binds to MyD88, and induces TLR-dependent induciton of pro-inflammatory cytokines	Constitutive in B cells and DCs	Type I IFNs, IL-6, TNF-a
IRF6	Unknown	Constitutive in skin	
IRF7	Binds to MyD88 and induces Type I IFNs upon TLR signaling	Constitutive in B cells, pDCs and monocytes.	Type I IFNs
		Inducible by Type I IFN in various cell types	
IRF8	Required for TLR-9 signaling in DCs (binds to adapter, TRAF6)	Constitutive in B cells, MΦs, CD8+ DCs, and pDCs	
	Stimulates IFNγ-inducible genes		IL-12p40, iNOS, PML
	Promotes Type I IFN in DCs		Type I IFNs
IRF9	Binds STAT1 and STAT2 to form ISGF3, stimulates transcription of type I IFN-inducible genes		IRF-1, IRF-7, PKR, OAS

iNOS, inducible nitric oxide synthase; CTIIA, class II major histocompatibility complex transactivator; TAP, transporter associated with antigen processing; TRAF, Tumor Necrosis Factor Recepter-associated factor; PML, promyelocytic leukemia protein; PKR, dsRNA-dependent Protein Kinase; OAS, 2'5' oligodenylate synthetase.

3. The Role of IFN in the Adaptive Immune Response

An adaptive immune response is distinguished from innate responses due to antigen specificity and memory (105). The adaptive response develops more slowly than innate immune responses, involves antigen processing and presentation, as well as development of T cell and antibody responses that are specific to each pathogen (105). However, development of an effective adaptive immune response also relies on the innate immune response, including Type I IFN (Fig. 1.4). Type I IFNs are important for maturation and activation of DCs (102, 143, 161), which promote antigen presentation necessary for driving a specific T cell response. Additionally, type I IFNs can also directly affect T cell development, function, proliferation and survival (100, 150, 232). Moreover, type I IFNs, along with IL-12, IL-18 and type II IFN, have a role in specifically driving a Th1 T cell response, important in antiviral immunity. In addition to directly inducing cytokines for development of a Th1 response, type I IFNs further promote the Th1 response by simultaneously blocking the development of an IL-4 mediated Th2 response (100). These findings collectively show the importance of type I IFNs, not only for orchestrating an antiviral state, but also for driving an effective adaptive immune response during virus infection.

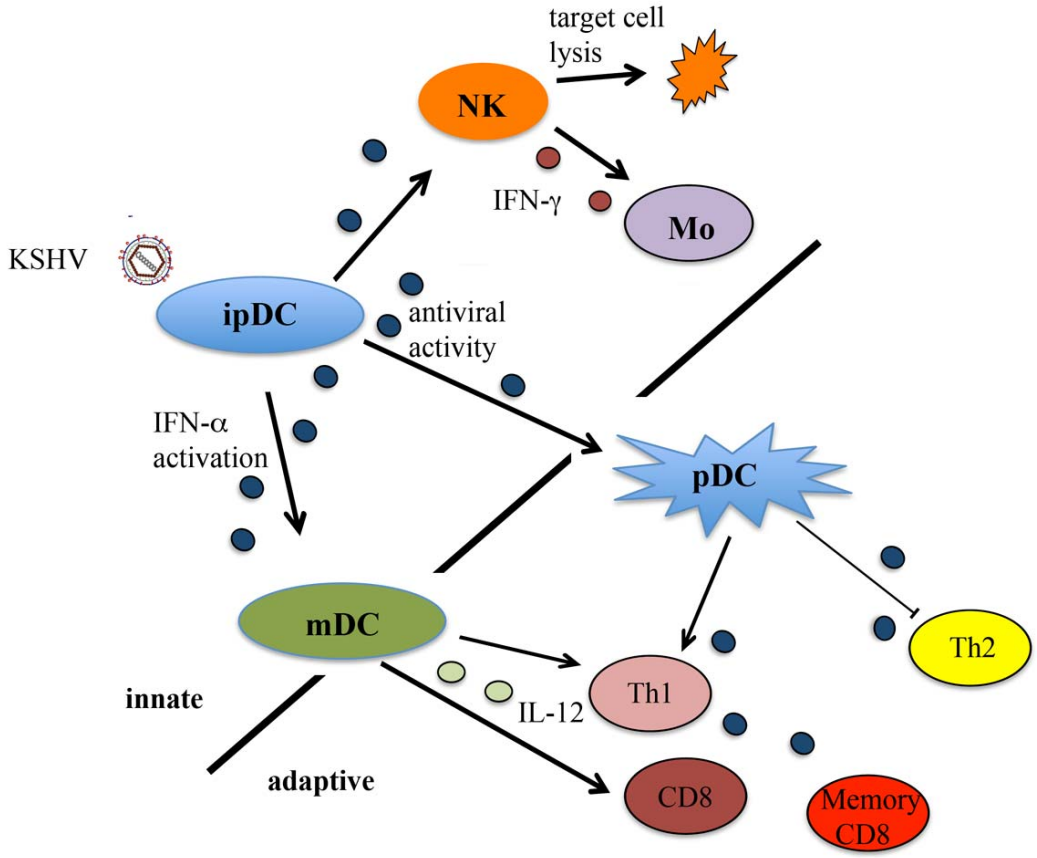

FIGURE 1.4. Schematic representation of the role of type I IFN on the innate and adaptive immune response. Plasmacytoid dendritic cells (pDCs) respond to KSHV stimulation with the production of IFN-α and pro-inflammatory cytokines. IFN-α then functions to activate other components of the innate immune response, including natural killer (NK) cells, which respond by targeting infected cells for lysis and by making IFN-γ, which can further activate monocytes (Mo) and macrophages. IFN-α can also promote activation of myeloid DCs (mDCs), which help promote the Th1 response. Activated pDCs can move into the lymph node, upregulate co-stimulatory molecules and present antigen, but also continue to make IFN-α. IFN-α has been implicated in aiding IL-12 in driving a Th1 response, as well as directly promoting immunological memory. Simultaneously, IFN-α can directly inhibit Th2 cytokine production by interfering with IL-4 signaling.

V. Mechanisms of Immune Evasion

A. General Strategies

In order to establish a persistent, lifelong infection, herpesviruses have developed a number of mechanisms to evade the host immune response (237). Viruses can target 4 main areas of the immune response: 1. inhibition of the IFN response, 2. inhibition of chemokines/cytokines and their signaling, 3. inhibition of lymphocyte (T cells, B cells, NK cells) molecules/receptors, and 4. inhibition of antigen processing and presentation (105). The subsequent sections will focus predominantly on evasion of the IFN response during herpesvirus infection, highlighting distinct mechanisms and functions of a few specific viral proteins.

B. Evasion of the IFN Response during Herpesvirus Infection

1. Inhibition of the IFN response during CMV, HSV, VZV, and EBV infection

The ability to inhibit the innate antiviral response is crucial during establishment of herpesvirus infection, as well as for persistence of the virus. Due to the virtually immediate induction of type I IFNs following virus infection, herpesviruses encode a number of immediate early (IE) proteins that have redundant functions and/or function at various steps within the IFN signaling pathway (Fig. 1.5) (237), demonstrating how crucial it is for viruses to inhibit this response. These viral proteins interfere with pathogen detection, directly inhibit a range of proteins in subsequent signaling cascades, and ultimately disrupt transcription of IFN and IFN-stimulated genes (Fig. 1.5).

During CMV infection, one of the IE proteins, IE86, can independently inhibit IFN-β transcription, as well as transcription of IL-8, MIP-1α, and RANTES by interfering with NFκB activation (229, 230) (Fig. 1.4). Similarly, HSV-1 encodes several IE proteins that inhibit the induction of IFN-β at multiple points in the pathway. HSV infected cell protein 0 (ICP0) can disrupt the induction of type I IFN by inhibiting the nuclear accumulation of IRF-3 (237). Moreover, ICP0 also functions to disrupt TLR2 mediated induction of pro-inflammatory cytokines, likely through degradation of an adaptor molecule upstream of NFκB activation (236). Additionally, HSV ICP34.5 interacts with TBK and blocks phosphorylation and activation of IRF-3 (240) (Fig. 1.5). The end result of all these disparate functions is inhibition of type I IFN transcription.

Similarly, VZV also inhibits induction of type I IFN via multiple mechanisms. VZV infection results in stabilization of IκB which retains NFκB in the cytoplasm (237), and VZV IE62 specifically inhibits IRF-3 phosphorylation (209), blocking two critical factors needed for IFN-β transcription.

EBV expresses an IE protein, BGLF4, that doesn't inhibit phosphorylation or activation of IRF-3, but blocks its binding at the IFN-β promoter (247). Additionally, EBV encodes two other proteins, BZLF1 and LF2, that interfere with the dimerization and activation of IRF-7, which also leads to inhibition of type I IFN (92, 257). Furthermore, because pCDs constitutively express IRF-7 and are the main IFN-α producing cells in the body, these 2 EBV proteins have an important role in inhibiting the majority of IFN-α production during EBV infection.

There are also viral proteins that inhibit subsequent IFN-induced signaling and transcription (Fig. 1.5). For example, EBV encodes two latent proteins, LMP2A and LMP2B, that induce the degradation of IFN receptors, reducing IFN signaling at the initiation point (214). Likewise, HCMV infection leads to decreased expression of several components in the type I IFN signaling pathways, including Jak1 and IRF-9, which results in decreased expression of IFN-regulated genes, such as MHC-I (156). HSV-1 encodes another IE protein, ICP27, that blocks IFN-induced signaling cascade either directly by inhibiting STAT1 phosphorylation (109), or indirectly by inducing secretion of another protein that acts upstream of Jak1 (108); both mechanisms would ultimately block IFN-stimulated gene transcription.

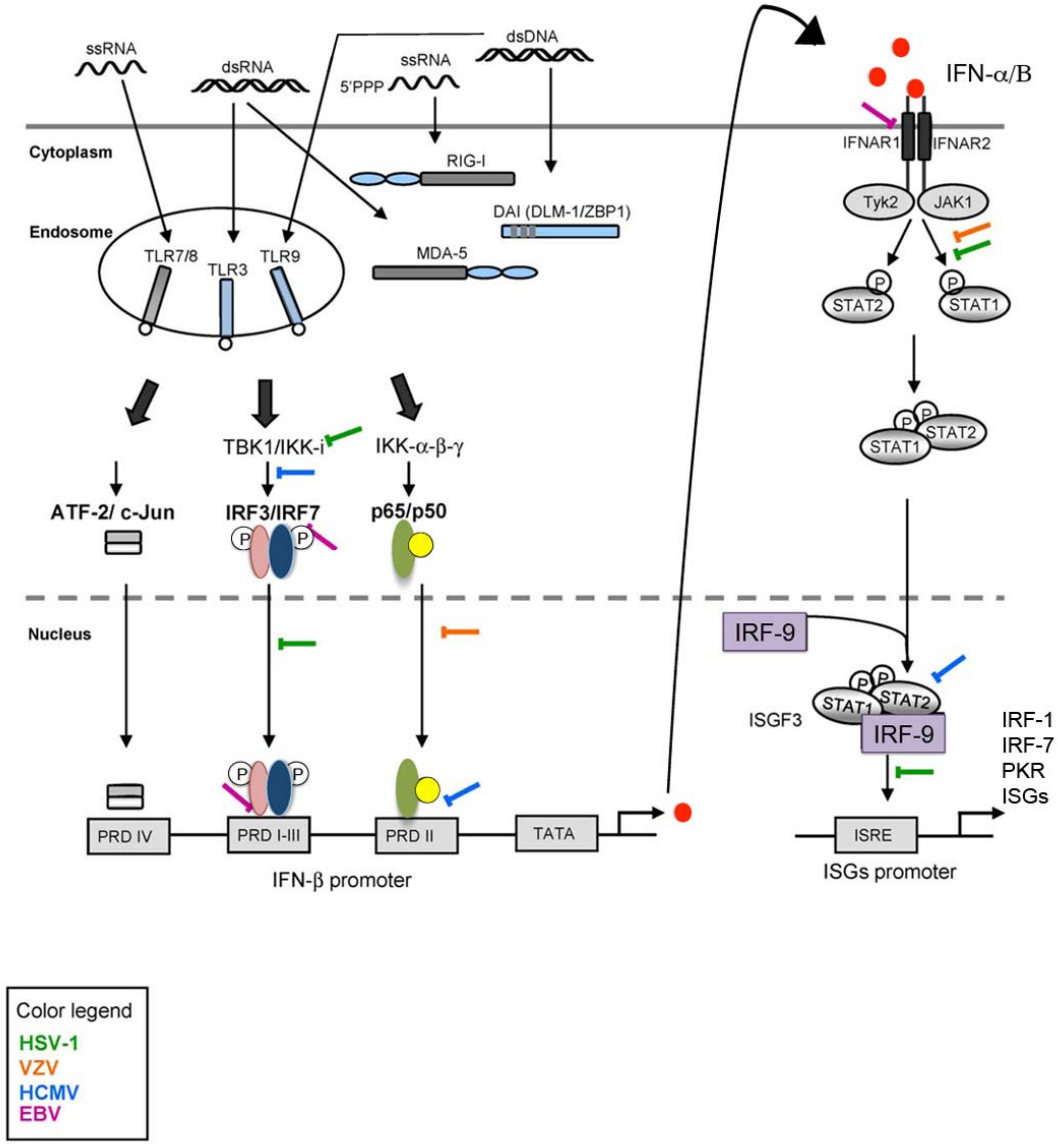

FIGURE 1.5. Herpesvirus Inhibition of PRR-induced and IFN-induced signaling. Schematic overview of herpesvirus interference with the IFN response. Herpesviruses enocode proteins that interfere with PRR-induced signaling, as well was IFN-induced signaling pathways. The cellular targets are depicted with colored bars for each of the 4 herpesviruses listed. HSV-1, herpes simplex virus 1; VZV, varicella-zoster virus; HCMV, human cytomegalovirus; EBV, Epstein-Barr virus. *Figure and legend adapted and reprinted with permission (237).*

2. Inhibition of the IFN Response during KSHV Infection

KSHV infection is detected by at least 2 different PRRs, TLR4 on the cell membrane (128), and TLR9 in the endosome (250), which initiate innate signaling cascades. Therefore, similar to other human herpesviruses, KSHV also encodes multiple proteins that interfere with PRR-induced signaling and the IFN pathway (Fig. 1.6). The most notable are vIRFs because of their unique homology to cellular IRFs. KSHV vIRFs have been extensively studied, and will be detailed in a later section.

KSHV encodes several proteins that have inhibitory functions in the IFN pathway. KSHV replication and transcription activator (RTA/ORF 50), which is necessary for initiating lytic replication and is the master regulator of viral gene transcription, can inhibit induction of IFN-α by promoting IRF-7 degradation (261). Likewise, virion-associated IRF-7 binding protein (IRF-7 BP/ORF 45) binds IRF-7 and prohibits IRF-7 phosphorylation, and thus, inhibits IRF-7 mediated transcription of IFN-α (265). Both of these KSHV proteins are present early during lytic infection, RTA because it's the necessary driving factor for lytic replication and IRF-7 BP because it's carried in with the virion. Additionally, KSHV basic-region leucine zipper protein (KbZIP/ORF K8) also interferes with the induction of type I IFN by binding to the PRD I/III regions of the IFN-β promoter and blocking IRF-3 binding and transcription (132). Moreover, KbZIP also binds to p53, inhibiting p53-induced transcription and blocking apoptosis (178). Inhibiting apoptosis is a significant aspect of driving transformation; thus, KbZIP has potential functions in both tumorigenesis and immune evasion.

Subsequent to the initial PRR-induced signaling, KSHV also functions to inhibit type I and type II IFN-induced signaling. KSHV regulator of IFN function (RIF/ORF 10) functions by binding to Jak1 and Tyk2, inhibiting their activation and the phosphorylation and activation of STAT1 and STAT2, ultimately blocking type I IFN-induced signaling (21). KSHV vIL-6, in addition to its potential role in driving B cell malignancies (99), is also capable of inhibiting type I IFN activity (42). The capacity of vIL-6 to inhibit the IFN response and promote cellular proliferation are at least partially linked in that vIL-6 specifically inhibits IFN-α induced transcription of p21, the cyclin-dependent kinase inhibitor, resulting in unrestrained proliferation of PEL cells (42). Two additional viral proteins, MIR1 and MIR2 (ORFs K3 and K5), inhibit type II IFN signaling via targeting the IFN-γ receptor for degradation (135) (Fig. 1.6).

VI. Viral Interferon Regulatory Factors

A. KSHV vIRFs

1. vIRF-1

KSHV vIRF-1 is a 449 AA protein encoded by ORF K9, and was the first vIRF identified based on its sequence similarity (~13% AA identity) to cellular IRFs, specifically cellular IRF-8 (ICSBP) and IRF-9 (ISGF3γ) (162). Despite the similarities with cellular IRFs, vIRF-1 lacks the typical tryptophan cluster within the N-terminal DNA-binding domain that is necessary for cellular IRFs to bind to DNA and drive transcription (162).

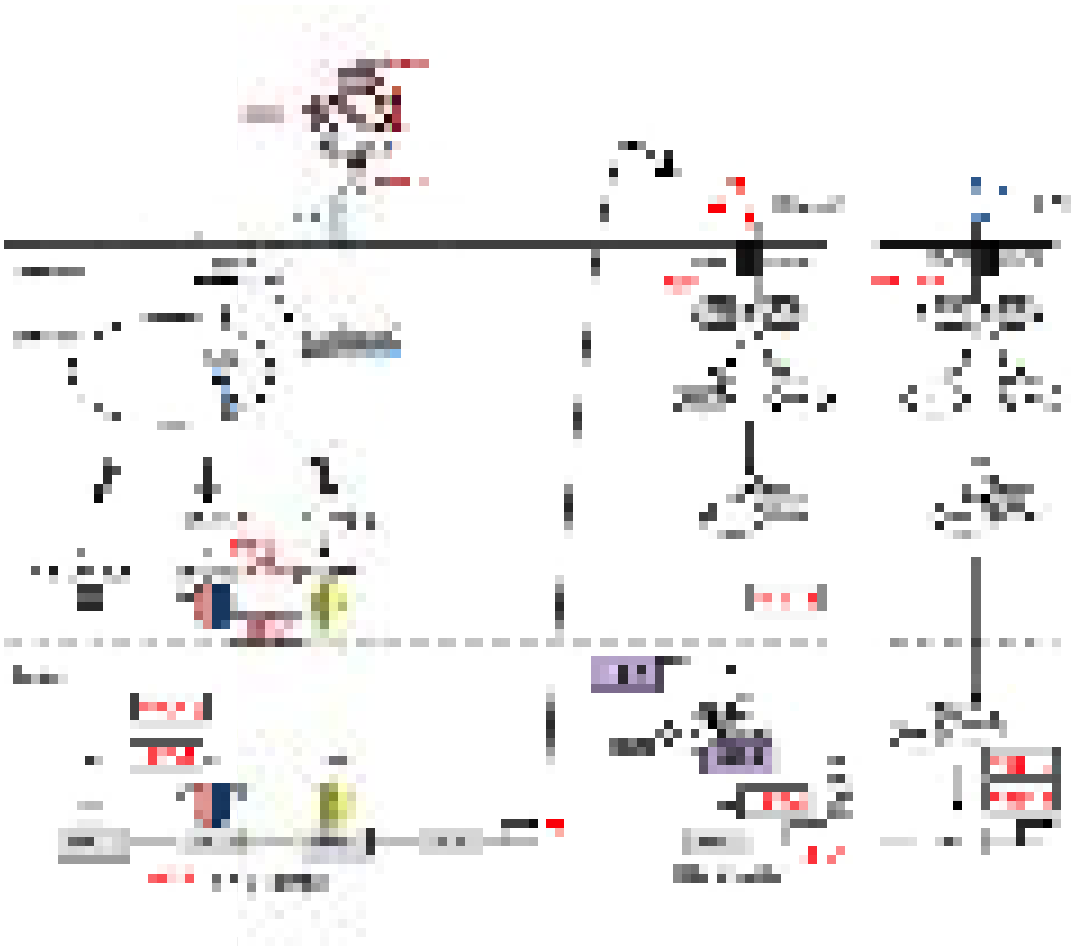

FIGURE 1.6. KSHV inhibition of PRR-induced and IFN-induced signaling. KSHV stimulates TLR4 and TLR9 leading to activation of IRF-3 and IRF-7, and induction of type I IFNs. KSHV encodes viral proteins (shown in red) that inhibit PRR signaling and IFN-induced signaling at various steps within these pathways. vIRF, viral IFN regulatory factor; RTA, replication and transcription activator; K-bZIP, KSHV basic leucine zipper protein; RIF, regulator of IFN function; MIR, modulator of immune recognition.

Transcription of vIRFs was analyzed in KSHV-infected PEL cells via northern blot analysis. The data demonstrated vIRF-1, as well as vIRF-2, -3, and -4, is expressed on its own transcript with an independent promoter and polyadenylation signal (52). KSHV vIRF-1 is expressed at low levels in latently infected PEL cells (52) and within KS lesions, which are comprised of mostly latently infected cells (62), but vIRF-1 expression is induced to much higher levels during lytic KSHV replication in PEL cell lines (52, 162, 185) and expression is mostly nuclear (185, Inagi, 1999 #70). During lytic expression of vIRF-1, transactivation is at least partially reliant on the viral transactivator, Rta, encoded by ORF 50 (43). These expression analyses suggest vIRF-1 functions both in latency and during lytic replication, and its association with all forms of KSHV-associated malignancies further suggests vIRF-1 fulfills a variety of crucial functions during KSHV infection.

Due to the sequence similarity with cellular IRFs, KSHV vIRF-1 was initially hypothesized to interfere with cellular IRFs and their role in transcriptional regulation. Indeed, vIRF-1 inhibits virus-induced transcription of IFN (31, 137), type I and type II IFN-induced transcription (76, 82, 134, 267), and specifically inhibits IRF-1 (31, 76, 267) and IRF-3 (31, 137) mediated transcription in transient expression assays. Inhibition of transcription is not mediated via vIRF-1 directly binding to the ISRE (76, 137, 267) or the similar PRD elements in the IFN-β promoter (31, 137); nor does vIRF-1 inhibit transcription via blocking cellular IRFs from binding to DNA. And despite studies demonstrating that vIRF-1 can bind to cellular IRF-1 (31), IRF-2 (31), IRF-3 (31, 137), IRF-7 (137), and IRF-8 (31), these interactions are generally weak and do not

block activation of the cellular IRFs or inhibit them from binding DNA (31, 137). Rather, KSHV vIRF-1 binds to the transcriptional co-activators, p300 and CBP, and inhibits the crucial binding of p300/CBP to IRF-3 (31, 133, 137, 210), as well as inhibits p300 histone acetyltransferase activity (133). Therefore, vIRF-1 mediated inhibition of cellular IRFs is via competition for binding to co-activators, p300/CBP. This mechanism of inhibition supports the failure of vIRF-1 to inhibit IRF-7 mediated transcription (137), as IRF-7 does not require p300/CBP to induce transcription (136). Additional studies have demonstrated that through interactions with p300/CBP, vIRF-1 can also inhibit transcription of MHC-1 (127). KSHV vIRF-1 likely functions to inhibit the interaction between p300 and STAT proteins (17, 98, 262) resulting in vIRF-1 mediated inhibition of IFN-induced transcription. More recently, vIRF-1 has been demonstrated to independently downregulate TLR-4 transcript and protein, and downregulation of TLR-4 results in increased rates of KSHV infection (128). These findings are significant, because HIV-infected individuals with an inhibitory mutation in their TLR-4 allele demonstrated higher incidence of MCD and higher KSHV viral loads (128), demonstrating another potential role for vIRF-1 in the promotion of KSHV pathogenesis.

Although the majority of the data suggests vIRF-1 inhibits transcription, one study has demonstrated that vIRF-1 can activate transcription of genes if it's directed to the DNA through interactions with a DNA binding protein (198). Likewise, vIRF-1 may also serve to activate transcription of viral genes, as well (177). Testing a pool of random oligonucleotides, Park et al identified a consensus sequence that is bound by vIRF-1, which closely aligned with sequence in the promoter region of three viral genes, vIL-6

(ORF K2), vDHFR (ORF 2) and MIR1 (ORF K3) (177). Accordingly, siRNA knock down of vIRF-1 in latently infected PEL cells resulted in a decrease in vIL-6 (134), suggesting vIRF-1 is critical for vIL-6 expression which potentiates B cell proliferation.

KSHV vIRF-1 also has oncogenic potential and functions to inhibit apoptosis by a variety of mechanisms (170). Initial studies of vIRF-1 demonstrated expression in NIH3T3 cells led to increased cellular proliferation, loss of contact inhibition, and these cells induced tumor formation when introduced into nude mice (82, 134). Specifically, vIRF-1 can stimulate expression of the oncogene, c-myc (106), as well as bind to p53 and inhibit p53-induced transcription, resulting in decreased apoptosis and unrestrained growth potential (164, 212). Likewise vIRF-1 also reduces control of cellular proliferation induced by TGF-β via binding to SMAD3 and SMAD4 and inhibiting their binding to DNA in TGF-β-responsive promoters (211). KSHV vIRF-1 also inhibits apoptosis through another unique mechanism, binding and sequestering Bim in the nucleus. Bim is a pro-apoptotic protein that would normally act with other Bcl-2 family proteins at the mitochondrial membrane (46). These data demonstrate the emphasis KSHV has on interfering with cell cycle controls, as vIRF-1 alone utilizes at least 4 distinct mechanisms to promote cellular proliferation and inhibit cell death.

Most of these studies have been performed in latently infected PEL cells, and in transient expression assays, and little is known about the role of vIRF-1 during *de novo* KSHV infection. A BAC clone of KSHV was generated to easily target viral genes for deletion (263), and vIRF-1 (ORF K9) was deleted to validate the utility of this system

for generating recombinant KSHV clones. However, additional analyses of the vIRF-1 deletion mutant were not performed, and we do not know whether deletion of vIRF-1 alters KSHV viral replication, virion production, or changes the IFN response during *de novo* KSHV infection (263). Regardless, the wildtype BAC clone of KSHV is still predisposed to go latent after infection in cell culture, so addressing the role of vIRF-1 during *de novo* lytic infection is still problematic in this system.

2. vIRF-2

KSHV vIRF-2 is a 2.4kb spliced transcript, encoded by ORF K11/K11.1 (52). KSHV vIRF-2 is constitutively expressed in latently infected PEL cells, and is induced further following induction of lytic replication (52). Similar to vIRF-1, vIRF-2 is capable of inhibiting type I IFN-induced transcription, as well as type III IFN-induced transcription (80), and can specifically inhibit IRF-1 and IRF-3 mediated transcription when either is co-expressed with vIRF-2 in transient reporter assays (80). KSHV vIRF-2 was also unable to inhibit IRF-7 mediated transcription (80), but unlike vIRF-1, however, vIRF-2 was also unable to inhibit IFN-γ induced transcription (80).

Prior to the aforementioned studies, there were also functional studies on exon 1 of vIRF-2 (vIRF-2x1), encoded by ORF K11.1 (30, 32, 120). vIRF-2x1 encodes a 20kDa protein that inhibits transcription mediated by NFκB, IRF-1 and IRF-3 (32). One study demonstrated that vIRF-2x1-mediated inhibition of IRF-1 specifically abolished transcription of CD95L (FasL), a potent pro-apoptotic protein, and thus, vIRF-2x1 has an anti-apoptotic function, as well (120). Transcriptional inhibition may be attributed to direct binding of vIRF-2x1 to the NFκB binding sequence (32); however, vIRF-2x1 can

also bind to IRF-1, IRF-2, IRF-8, NFκB p65, and CBP/p300, and any of these interactions could also play a role in inhibiting transcription (32). And yet, another study demonstrated vIRF-2x1 can also bind PKR and release the PKR-mediated block of protein translation during viral infection (30). However, northern analysis on RNA collected from stimulated (to induce lytic replication) and unstimulated PEL cells failed to demonstrate the predicted 0.6kb transcript for vIRF-2x1; instead, a 2.2 kb transcript was detected in three separate analyses, which corresponds to full-length vIRF-2 (32, 52, 107). It should be noted, however, that vIRF-2x1 was detected within KSHV-infected PEL cells via western analysis in one study (30). Therefore, whether expression of vIRF-2x1 occurs naturally during KSHV infection is still under debate. Thus, the functions attributed to vIRF-2x1 may be insignificant in a natural setting.

3. vIRF-3

KSHV vIRF-3 is a 73kDa protein generated from a 1.9kb spliced transcript encoded by ORF K10.5 (52, 142). vIRF-3 shares the most sequence similarity with cellular IRF-4, a lymphoid-specific IRF (142, 197). vIRF-3 is constitutively expressed in latently infected B cells, and in almost all KSHV-infected cells in MCD tumors (197). Due to its expression during latency, as well as its nuclear localization, vIRF-3 has also been named latency-associated nuclear antigen 2 (LANA-2) (197).

Similar to vIRF-1, vIRF-3 can inhibit IFN-γ mediated gene transcription, which was shown to result in a decrease in MHC-II expression in infected PEL cells (206). Likewise, KSHV vIRF-3 also interferes with the type I IFN pathway via blocking

cellular IRF-3 (142), IRF-5 (253), IRF-7 (111, 142) and NFκB mediated transcription (213), as well as by inhibiting PKR (67). The ability to interfere with IRF-7 mediated transcription would give vIRF-3 a specific role in inhibiting induction of IFN-α. This appears to be unique to vIRF-3, as neither vIRF-1 nor vIRF-2 demonstrated this function, but also seems appropriate given that vIRF-3 expression is restricted to hematopoietic cells, the main site of IRF-7 expression (94). In contrast to these findings, another study demonstrated that vIRF-3 expression enhances IRF-3 and IRF-7 mediated transcription following Sendai Virus infection (140). These studies were done in two different cell culture systems, which could explain the disparity, but the latter results may also indicate that vIRF-3 could have a stimulatory function in certain cell types. Moreover, since these studies were done outside of the context of KSHV infection, the intended stimulatory activity of vIRF-3 may be directed toward a viral gene, rather than toward induction of IFNs. Indeed, the promoter of vIL-6 contains two ISRE that are responsive to IFN-induced signaling (42), and vIL-6 plays an important role in driving proliferation in KSHV-associated B cell disorders. Therefore, vIRF-3 may play a role in driving transcription of vIL-6 to promote B cell proliferation during KSHV infection.

Moreover, inhibition of IRF-5 (253), p53 (197), and stimulation of c-myc-dependent transcription (141) also demonstrate vIRF-3 has a role in enhancing cellular proliferation and limiting apoptosis. Indeed, one study has demonstrated that vIRF-3 is required for continuous proliferation of PEL cells in culture, demonstrating its true oncogenic capacity (254).

4. vIRF-4

KSHV vIRF-4 is a 2.9kb spliced transcript, encoded by ORFs K10 and K10.1, and is strongly induced during lytic replication (52). There have been fewer functional studies on this vIRF, and it has not been demonstrated to be important for inhibition of IFN signaling. However, one study demonstrated that vIRF-4 functions to downregulate p53-induced apoptosis (131). KSHV vIRF-4 binds to murine double minute 2 (MDM2), a protein that negatively regulates p53 via two proposed mechanisms: ubiquitination and degradation of p53 (71), and/or blocking the transactivation domain of p53 (96). Binding of vIRF-4 to MDM2 stabilizes MDM2, increases ubiquitination of p53, and results in decreased levels of apoptosis (131). These findings implicate a role for vIRF-4, along with other vIRFs, in promoting tumorigenesis during KSHV infection.

B. RRV vIRFs

1. Identification and Comparison with KSHV vIRFs

RRV encodes eight vIRFs (ORFs R6-R13) in a cluster between ORFs 57 and 58, and all 8 vIRFs are predicted to be unspliced transcripts (7, 207) (Fig. 1.2). The RRV vIRFs share sequence similarity with KSHV vIRF-1, which was identified and named due to its sequence similarity to cellular IRFs, specifically IRF-8 (ICSBP) and IRF-9 (ISGF3) (162). Therefore, the 8 RRV vIRFs were also compared to human (207) and rhesus (data not shown) cellular IRF-8 and IRF-9. Of the 8 RRV vIRFs, R10 vIRF shares the highest similarity with rhesus cellular IRF-8 and IRF-9, about 16% and 18% identity, respectively. The other 7 RRV vIRFs share between 11-15% identity with cellular

IRF-8 and IRF-9 (data not shown). Also similar to KSHV vIRF-1, the 8 RRV vIRFs do not have the 5 characteristic tryptophans that are required for DNA binding (207) (Fig. 1.7). Therefore, it is hypothesized that the RRV vIRFs do not function via directly binding to promoter elements of target genes. Additionally, 5 of the RRV vIRFs (R6, R7, R8, R10, R11) share about 25% AA identity with KSHV vIRF-1, but there does not appear to be significant sequence similarities between the RRV vIRFs and KSHV vIRF-2, -3, or -4 (207) (Fig. 1.7, Table 1.4). Further sequence analysis amongst the 8 RRV vIRFs suggests the first 4 vIRFs (ORF R6-R9) were likely acquired initially, and these 4 later underwent a duplication event, resulting in a total of 8 vIRFs (207). The amino acid identities between the RRV vIRFs are listed in Table 1.4, and sequence alignments are shown in Fig. 1.7. Whether this equates to functional redundancy between the first 4 vIRFs and each of their respective duplicate vIRFs is a question of interest. Additionally, RRV vIRFs R6 and R10, which represent one pair of potential duplicated genes, share the most similarity with KSHV vIRF-1 (Table 1.4), which leads one to posit that R6 and R10 vIRFs may show the most functional overlap with KSHV vIRF-1.

B. Project Summary and Rationale

Although there has been considerable characterization of the molecular functions of the 4 KSHV vIRFs, there has been difficulty studying their role during infection due to poor lytic replication in culture and inadequate animal models (169). Due to the unique nature of these viral proteins, it's hypothesized that they play novel roles in pathogenesis and immune evasion. To our knowledge, RRV is the only other virus that encodes vIRFs, in addition to several other genes that are specific to KSHV and RRV

(7, 207). Moreover, the genomic organization of KSHV and RRV is very similar (Fig. 1.2), and RRV infection results in mostly lytic replication in culture and results in KSHV-like diseases in its natural host, collectively making RRV infection an ideal system for further study of vIRFs. Recent development of a BAC clone of RRV allows for targeted deletion of specific viral ORFs to assess their role during *de novo* infection *in vitro* and *in vivo* (69). Studying the role(s) of vIRFs, and other novel viral genes, within the context of RRV infection is the most relevant way to assess their impact on the immune response and pathogenesis, with the ultimate objective to relate these findings to KSHV-associated pathologies.

C. Author's Contributions

All the work in Chapter 2 was performed by the author with the exception of Figure 2.1 A (S.W.W.). In Chapter 3, the author performed all experiments except Figure 3.1A, 3.1B (H.L.), and Figure 3.5 (F.E), and the author contributed 50% to Figures 3.2A and 3.2B, Figure 3.3, and Figure 3.4 (M.A.O.). The author performed all experiments in Chapter 4.

FIGURE 1.7. Alignment of RRV vIRFs and KSHV vIRF-1. The ClustalW alignment of the 8 RRV vIRFs (ORFs R6-R13) and KSHV vIRF-1 (ORF K9). Amino acids are colored according to the following classifications: basic residues in blue (H,K,R), acidic residues in green (D,E), polar residues in red (C, N, S, T, Q, Y), and non-polar residues in black (A, F, G, I, L, M, P, V, W). The five tryptophan residues (W) conserved within the N-terminal DNA-binding domain of cellular IRFs are labeled 1-5. There is a conserved cysteine at the position of the fourth tryptophan in all the RRV vIRFs, and a conserved change to an arginine in 6 of the RRV vIRFs at the position of the fifth tryptophan. Positions with homologous residues in more than half of the vIRFs are labeled with an asterisk (*****), and positions with conserved residue classification are marked with a period (**.**).

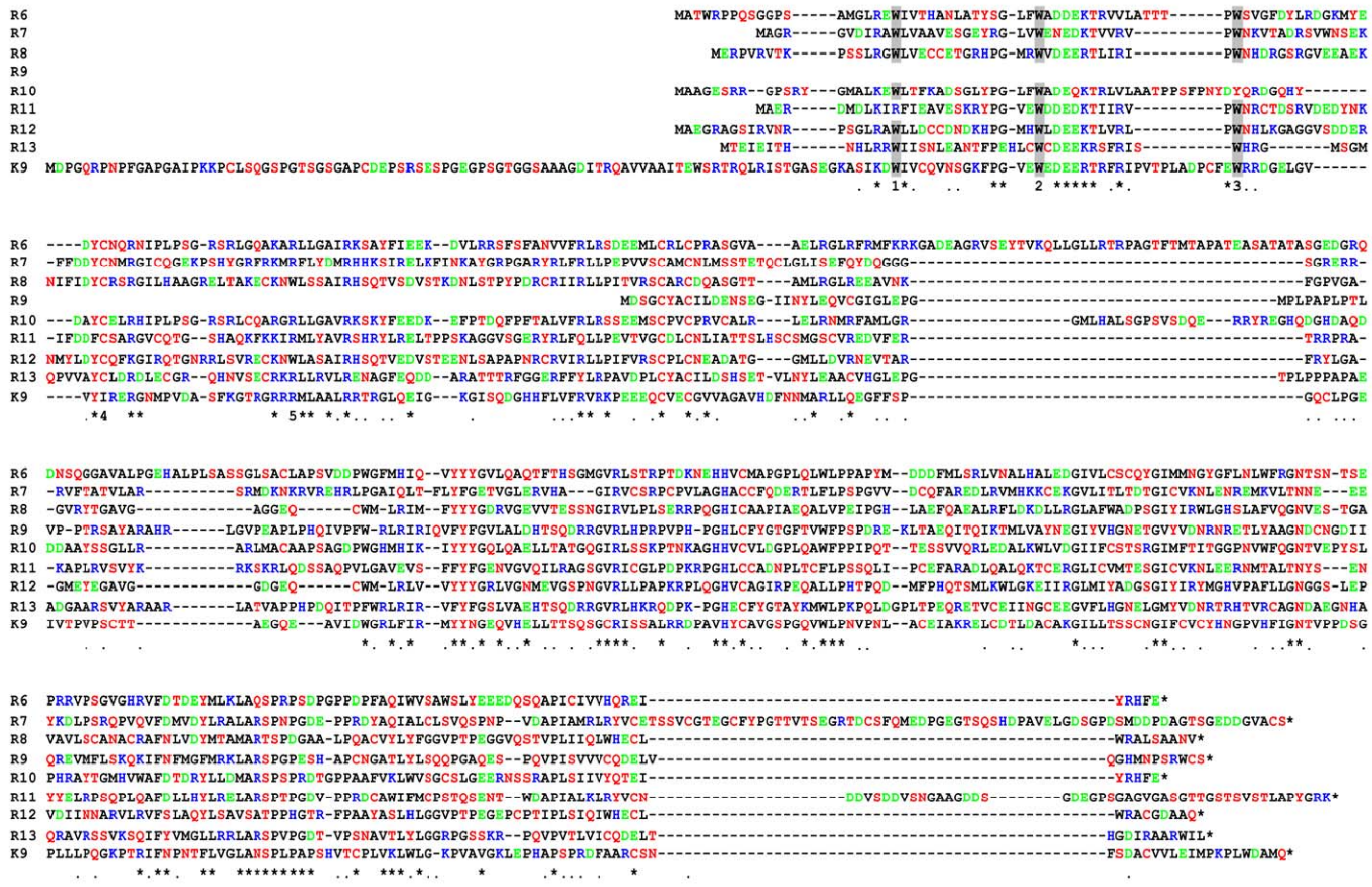
R6 MATWRPPQSGGPS-----AMGLREWIVTHANLATYSG-LFWADDEKTRVVLATTT------PWSVGFDYLRDGKMYE
R7 MAGR-----GVDIRAWLVAAVESGEYRG-LVWENEDKTVVRV----------PWNKVTADRSVWNSEK
R8 MERPVRVTK-----PSSLRGWLVECCETGRHPG-MRWVDEERTLIRI----------PWNHDRGSRGVEEAEK
R9
R10 MAAGESRR--GPSRY---GMALKEWLTFKADSGLYPG-LFWADEQKTRLVLAATPPSFPNYDYQRDGQHY-------
R11 MAER-----DMDLKIRFIEAVESKRYPG-VEWDDEDKTIIRV----------PWNRCTDSRVDEDYNK
R12 MAEGRAGSIRVNR-----PSGLRAWLLDCCDNDKHPG-MHWLDEEKTLVRL----------PWNHLKGAGGVSDDER
R13 MTEIEITH------NHLRRWIISNLEANTFPEHLCWCDEEKRSFRIS----------WHRG-------MSGM
K9 MDPGQRPNPFGAPGAIPKKPCLSQGSPGTSGSGAPCDEPSRSESPGEGPSGTGGSAAAGDITRQAVVAAITEWSRTRQLRISTGASEGKASIKDWIVCQVNSGKFPG-VEWEDEERTRFRIPVTPLADPCFEWRRDGELGV------
. * 1*. .. ** 2 ***** .*. *3..
R6 ----DYCNQRNIPLPSG-RSRLGQAKARLLGAIRKSAYFIEEK--DVLRRSFSFANVVFRLRSDEEMLCRLCPRASGVA----AELRGLRFRMFKRKGADEAGRVSEYTVKQLLGLLRTRPAGTFTMTAPATEASATATASGEDGRQ
R7 -FFDDYCNMRGICQGEKPSHYGRFRKMRFLYDMRHHKSIRELKFINKAYGRPGARYRLFRLLPEPVVSCAMCNLMSSTETQCLGLISEFQYDQGGG----------SGRERR-
R8 NIFIDYCRSRGILHAAGRELTAKECKNWLSSAIRHSQTVSDVSTKDNLSTPYPDRCRIIRLLPITVRSCARCDQASGTT----AMLRGLREEAVNK----------FGPVGA-
R9 MDSGCYACILDENSEG-IINYLEQVCGIGLEPG----------MPLPAPLPTL
R10 ---DAYCELRHIPLPSG-RSRLCQARGRLLGAVRKSKYFEEDK--EFPTDQFPFTALVFRLRSSEEMSCPVCPRVCALR----LELRNMRFAMLGR----------GMLHALSGPSVSDQE---RRYREGHQDGHDAQD
R11 -IFDDFCSARGVCQTG--SHAQKFKKIRMLYAVRSHRYLRELTPPSKAGGVSGERYRLFQLLPEVTVGCDLCNLIATTSLHSCSMGSCVREDVFER----------TRRPRA-
R12 NMYLDYCQFKGIRQTGNRRLSVRECKNWLASAIRHSQTVEDVSTEENLSAPAPNRCRVIRLLPIFVRSCPLCNEADATG----GMLLDVRNEVTAR----------FRYLGA-
R13 QPVVAYCLDRDLECGR--QHNVSECRKRLLRVLRENAGFEQDD--ARATTTRFGGERFFYLRPAVDPLCYACILDSHSET-VLNYLEAACVHGLEPG----------TPLPPPAPAE
K9 ----VYIRERGNMPVDA-SFKGTRGRRRMLAALRRTRGLQEIG---KGISQDGHHFLVFRVRKPEEEQCVECGVVAGAVHDFNNMARLLQEGFFSP----------GQCLPGE
.*4 ** * 5** *.*.. .. * . ...** * . .* *.*. ..* .* .. . .
R6 DNSQGGAVALPGEHALPLSASSGLSACLAPSVDDPWGFMHIQ--VYYYGVLQAQTFTHSGMGVRLSTRPTDKNEHHVCMAPGPLQLWLPPAPYM--DDDFMLSRLVNALHALEDGIVLCSCQYGIMMNGYGFLNLWFRGNTSN-TSE
R7 -RVFTATVLAR----------SRMDKNKRVRERHRLPGAIQLT-FLYFGETVGLERVHA---GIRVCSRPCPVLAGHACCFQDERTLFLPSPGVV--DCQFARERDLRVMHKKCEKGVLITLTDTGICVKNLENREMKVLTNNE---EE
R8 -GVRYTGAVG----------AGGEQ------CWM-LRIM--FYYYGDRVGEVVTESSNGIRVLPLSERRPQGHICAAPIAEQALVPEIPGH--LAEFQAEALRFLDKDLLRGLAFWADPSGIYIRWLGHSLAFVQGNVES-TGA
R9 VP-PTRSAYARAHR------LGVPEAPLPHQIVPFW-RLRIRIQVFYFGVLALDHTSQDRRGVRLHPRPVPH-PGHLCFYGTGFTVWFPSPDRE-KLTAEQITQIKTMLVAYNEGIYVHGNETGVYVDNRNRETLYAAGNDCNGDII
R10 DDAAYSSGLLR----------ARLMACAAPSAGDPWGHMHIK--IYYYGQLQAELLTATGQGIRLSSKPTNKAGHHVCVLDGPLQAWFPPIPQT--TESSVVQRLEDALKWLVDGIIFCSTSRGIMFTITGGPNVWFQGNTVEPYSL
R11 -KAPLRVSVYK----------RKSKRLQDSSAQPVLGAVEVS--FFYFGENVGVQILRAGSGVRICGLPDPKRPGHLCCADNPLTCFLPSSQLI--PCEFARADLQALQKTCERGLICVMTESGICVKNLEERNMTALTNYS---EN
R12 -GMEYEGAVG----------GDGEQ------CWM-LRLV--VYYYGRLVGNMEVGSPNGVRLLPAPKRPLQGHVCAGIRPEQALLPHTPQD--MFPHQTSMLKWLGKEIIRGLMIYADGSGIYIRYMGHVPAFLLGNGGS-LEP
R13 ADGAARSVYARAAR-------LATVAPPHPDQITPFWRLRIR--VFYFGSLVAEHTSQDRRGVRLHKRQDPK-PGHECFYGTAYKMWLPKPQLDGPLTPEQRETVCEIINGCEEGVFLHGNELGMYVDNRTRHTVRCAGNDAEGNHA
K9 IVTPVPSCTT----------AEGQE---AVIDWGRLFIR--MYYNGEQVHELLTTSQSGCRISSALRRDPAVHYCAVGSPGQVWLPNVPNL--ACEIAKRELCDTLDACAKGILLTSSCNGIFCVCYHNGPVHFIGNTVPPDSG
. . . *. *.* .**.* *..* .. . .****. * . **.*.. . *.*** .. . .. *... .**. . . . . **. .
R6 PRRVPSGVGHRVFDTDEYMLKLAQSPRPSDPGPPDPFAQIWVSAWSLYEEEDQSQAPICIVVHQREI----------YRHFE*
R7 YKDLPSRQPVQVFDMVDYLRALARSPNPGDE-PPRDYAQIALCLSVQSPNP--VDAPIAMRLRYVCETSSVCGTEGCFYPGTTVTSEGRTDCSFQMEDPGEGTSQSHDPAVELGDSGPDSMDDPDAGTSGEDDGVACS*
R8 VAVLSCANACRAFNLVDYMTAMARTSPDGAA-LPQACVYLYFGGVPTPEGGVQSTVPLIIQLWHECL----------WRALSAANV*
R9 QREVMFLSKQKIFNFMGFMRKLARSPGPESH-APCNGATLYLSQQPGAQES--PQVPISVVVCQDELV----------QGHMNPSRWCS*
R10 PHRAYTGMHVWAFDTDRYLLDMARSPSPRDTGPPAAFVKLWVSGCSLGEERNSSRAPLSIIVYQTEI----------YRHFE*
R11 YYELRPSQPLQAFDLLHYLRELARSPTPGDV-PPRDCAWIFMCPSTQSENT--WDAPIALKLRYVCN----------DDVSDDVSNGAAGDDS--------GDEGPSGAGVGASGTTGSTSVSTLAPYGRK*
R12 VDIINNARVLRVFSLAQYLSAVSATPPHGTR-FPAAYASLHLGGVPTPEGEPCPTIPLSIQIWHECL----------WRACGDAAQ*
R13 QRAVRSSVKSQIFYVMGLLRRLARSPVPGDT-VPSNAVTLYLGGRPGSSKR--PQVPVTLVICQDELT----------HGDIRAARWIL*
K9 PLLLPQGKPTRIFNPNTFLVGLANSPLPAPSHVTCPLVKLWLG-KPVAVGKLEPHAPSPRDFAARCSN----------FSDACVVLEIMPKPLWDAMQ*
. . *.**. ** ********* ..* ***.*.. * .*... . * . .

TABLE 1.4: Similarities between vIRFs (% Identity / % Homology)

vIRF	K9	R6	R7	R8	R9	R10	R11	R12	R13
K9	100 / 100	28 / 21	28 / 19	29 / 19	NS	34 / 26	30 / 25	NS	NS
R6		100 / 100	31 / NS	26 / 19	30 / 32	54 / 48	NS	NS	NS
R7			100 / 100	35 / 26	NS	NS	51 / 41	33 / 25	NS
R8				100 / 100	NS	31 / 24	36 / 24	61 / 51	29 / 21
R9					100 / 100	29 / 19	24 / 22	30 / 19	58 / 53
R10						100 / 100	23 / 23	34 / 26	NS
R11							100 / 100	34 / 26	31 / 25
R12								100 / 100	NS
R13									100 / 100

NS, No significant homology
Reprinted with permission (Searles, et al 1999)

CHAPTER 2

Viral Interferon Regulatory Factors Inhibit Induction of Type I and Type II IFN during Rhesus Macaque Rhadinovirus Infection

Bridget A Robinson[1,2], Ryan D Estep[2], Ilhem Messaoudi[1,2,3], Scott W Wong*[1,2,3]

[1] Department of Molecular Microbiology and Immunology, Oregon Health & Science University, Portland, OR 97239
[2] Vaccine and Gene Therapy Institute, Beaverton, OR 97006
[3] Division of Pathobiology and Immunology, Oregon National Primate Research Center,
Beaverton, OR 97006

* Corresponding author
Vaccine and Gene Therapy Institute
505 NW 185th Ave
Beaverton, OR 97006
Phone: 503.690.5285
Fax: 503.418.2719
wongs@ohsu.edu

Running Title: vIRFs inhibit IFN production during RRV infection

* This manuscript was submitted for publication to the *Journal of Virology* in May 2011

ABSTRACT

Kaposi's sarcoma-associated herpesvirus and rhesus macaque rhadinovirus (RRV), two closely related γ-herpesviruses, are unique in their expression of viral homologs of cellular interferon regulatory factors (IRFs), termed viral IRFs (vIRFs). To assess the role of the vIRFs during *de novo* infection, we have utilized the bacterial artificial chromosome clone of RRV_{17577} (WT_{BAC} RRV) to generate a recombinant virus with all 8 of the vIRFs deleted (vIRF-ko RRV). Infection of primary rhesus fibroblasts and peripheral blood mononuclear cells (PBMCs) with vIRF-ko RRV results in earlier and increased induction of type I (-α/β) and type II (-γ) interferon (IFN). Additionally, plasmacytoid dendritic cells maintained higher levels of IFN-α production in PBMC cultures infected with vIRF-ko RRV, as compared to WT_{BAC} RRV infection. Moreover, nuclear accumulation of IRF-3, which is necessary for induction of type I IFN, was also inhibited following WT_{BAC} RRV infection. These findings demonstrate that during *de novo* RRV infection, the vIRFs are inhibiting induction of IFN at the transcriptional level, and one potential mechanism is via disruption of cellular IRF-3 localization.

INTRODUCTION

The interferon (IFN) response is integral to a host's antiviral defenses. IFNs are divided into three distinct types (Type I-III), characterized by sequence, receptor usage and biological activity (146). There are two well-studied type I IFNs (IFN-α and -β). IFN-α, which is expressed as multiple subtypes (13 in humans), is primarily produced by plasmacytoid dendritic cells (pDCs) (75). IFN-β, on the other hand, is produced by a wide variety of cell types, including fibroblasts and epithelial cells (146). One of the most important and earliest studied functions of type I IFNs is the promotion of an antiviral state within a virus-infected cell, as well as surrounding cells (101). Moreover, type I IFN signaling also stimulates the adaptive immune response through promotion of T cell survival, function, and proliferation (100, 150, 232), activation of natural killer (NK) cells (165), and maturation and activation of dendritic cells (DCs) (102, 143, 161). Type II IFN (IFN-γ) is produced by activated T cells and NK cells, promotes activation of monocytes and macrophages (244), and is crucial for an effective Th1 adaptive response. Type III IFNs (IFN-λ1, λ2, and λ3) are the most recently identified. They exhibit innate and antiviral properties similar to type I IFNs, but they signal through a different receptor, so their biological impact is likely distinct (64).

The expression of IFN is governed by a family of transcription factors known as interferon regulatory factors (IRFs) (94). In particular, transcription of type I IFN (IFN-α/β) relies on the activation of IRF-3 and IRF-7, highly homologous proteins that become activated via C-terminal phosphorylation (203). IRF-3 is constitutively

expressed in most cell types and becomes phosphorylated following recognition of a variety of pathogen-associated molecular patterns (PAMPs) (122), including viral nucleic acids (259). Following C-terminal phosphorylation of IRF-3, homodimeric complexes accumulate in the nucleus where interaction with the transcriptional cofactor p300/CBP potentiates transcription of IFN-β (112, 138, 260), human IFNα_1 (84, 136), and murine IFN-α_4 (203). Activation of IRF-7 occurs in a similar manner, except it has a more restricted expression profile; IRF-7 is constitutively expressed in some lymphoid cells and pDCs, and is transcriptionally up-regulated following type I IFN signaling in a variety of cell types (148, 202). Because of the specific cell-type expression and regulation, IRF-7 plays a vital role in the induction of IFN-α in pDCs (53), and is crucial for induction of most IFN-α subtypes that constitute the second wave of type I IFN production (148, 202, 203). To efficiently withstand IRF-dependent antiviral responses and establish an infection within the host, viruses have evolved a number of mechanisms to interfere with cellular IRFs, the induction of IFN, and subsequent IFN-induced signaling (10, 26).

Kaposi's sarcoma-associated herpesvirus (KSHV) and rhesus macaque rhadinovirus (RRV), two highly-related γ-herpesviruses, are unique in that they are the only viruses known to encode genes with significant homology to cellular IRFs, aptly named viral interferon regulatory factors (vIRFs) (7, 194, 201, 207). Because of their unique homology to cellular IRFs, it has been hypothesized that the vIRFs employ novel mechanisms of immune evasion. Indeed, 3 of the 4 vIRFs encoded within KSHV can individually inhibit induction of IFN and IFN-induced signaling by disrupting the

functions of cellular IRF-1, IRF-3, IRF-5, and IRF-7 (31, 32, 76, 80, 82, 111, 142, 253, 267). The inhibitory mechanisms employed by each of the vIRFs are varied, suggesting each vIRF plays a unique and significant role. For example, KSHV vIRF-1 binds to the transcriptional co-activator p300/CBP and blocks the necessary interaction between p300/CBP and cellular IRF-3, effectively inhibiting transcription of type I IFNs and other p300-dependent cytokines (31, 133, 137, 210). KSHV vIRF-3 can directly interact with cellular IRF-7 to block IRF-7 binding at promoter regions, thus, inhibiting subsequent transcription of several subtypes of IFN-α (111). Moreover, KSHV vIRFs also interfere with cell cycle control proteins and apoptosis [reviewed in (170)]. The aforementioned studies have provided insight into the molecular strategies employed by the KSHV vIRFs to inhibit IFN induction and signaling, but have not thoroughly defined their roles in the context of *de novo* KSHV infection due to inefficient lytic replication *in vitro* [reviewed in (169)]. In contrast, RRV displays robust lytic replication *in vitro* and encodes 8 vIRFs (ORFs R6-R13) with similarity to KSHV vIRF-1 (207), providing a unique opportunity to study the roles of the vIRFs during the early phase of *de novo* infection. Sequence analysis suggests that RRV likely acquired the first 4 vIRFs (ORFs R6-R9) initially, and that these genes later underwent a duplication event to result in a total of 8 vIRFs within the RRV genome (207). Therefore, it is plausible that the duplicated vIRFs (R10-R13) share redundant functions with their respective antecedents. Even despite the duplication of these genes, the vIRFs potentially have overlapping functions on the pathways they impact, as is the case for the KSHV vIRFs. For example, KSHV vIRFs 1-3 have disparate molecular functions, but they collectively interfere with IFN induction and signaling (170).

In this study, we tested the hypothesis that the RRV vIRFs have antagonistic effects on cellular IRFs, and IRF-dependent induction of interferon (IFN). To do so, we have generated a recombinant RRV clone lacking all 8 vIRF genes (vIRF-ko RRV) using the WT_{BAC} RRV_{17577} (69). Results presented herein demonstrate that vIRF-ko RRV can infect rhesus fibroblasts (RFs) and peripheral blood mononuclear cells (PBMCs) with similar efficiency as WT_{BAC} RRV. Moreover, deletion of the vIRFs resulted in increased induction of type I and type II IFN in RRV-infected RFs and rhesus PBMCs, along with increased production of IFN-α within pDCs. The increased induction of type I IFN was preceded by an increase in IRF-3 nuclear accumulation, which is significantly inhibited during WT_{BAC} RRV infection. These data suggest the vIRFs play a critical role in dampening antiviral responses early during RRV infection, which may be necessary for subsequent evasion of the adaptive immune response, development of latency, and/or pathogenesis.

MATERIALS AND METHODS

Cells, Virus, Drugs, and Cytokines. Primary rhesus fibroblasts (RFs) and telomerized RFs (tRFs) (121) were grown in DMEM (Mediatech, Herndon, VA) supplemented with 10% fetal bovine serum (FBS) (HyClone, Ogden, UT). Peripheral blood mononuclear cells (PBMCs) were isolated from whole blood of Expanded Specific Pathogen-Free (ESPF) rhesus macaques (RMs) using Histopaque (Sigma Aldrich, St. Louis, MO), per the manufacturer's guidelines, and cultured in RPMI (Mediatech). ESPF RMs are serologically negative for Rhesus Rhadinovirus (RRV), Simian Immunodeficiency Virus (SIV), Type D Simian Retrovirus (SRV), Herpesvirus Simiae (B virus), Simian T-lymphotropic Virus (STLV-1), Rhesus Cytomegalovirus (RCMV) and Simian Foamy Virus (SFV).

A plaque purified isolate of wildtype RRV, WT RRV_{17577} (256), was used exclusively for the microarray analyses. The remainder of the studies utilized a plaque-purified isolate of bacterial artificial chromosome (BAC)-derived RRV_{17577} (WT_{BAC} RRV_{17577}) (69). All RRV stocks were purified through a 30% sorbitol cushion and re-suspended in PBS, and viral titers were determined using serial dilution plaque assay in RFs. The Cantell strain of Sendai Virus (SeV) was purchased from Charles River (Wilmington, MA), and Herpes Simplex Virus 1 (HSV-1), strain F, was a generous gift from Dr. David Johnson (Oregon Health & Science University).

Cycloheximide (CHX) (Sigma) was re-suspended in EtOH and used at a final concentration of 50μg/ml to inhibit protein synthesis during RRV infection. Phosphonoacetic acid (PAA) (Sigma) was re-suspended in PBS and used at a final

concentration of 300μM to inhibit viral replication. Poly(I:C) (Sigma) was re-suspended in PBS and transfected into cells using TransIT LT1 transfection reagent (Mirus, Madison, WI). Recombinant human IFN-α2 (PBL, Piscataway, NJ) was re-suspended in PBS with 0.1% BSA and used at a final concentration of 10 U/ml.

Construction of a vIRF-ko RRV clone using the WT RRV_{17577} Bacterial Artificial Chromosome (BAC). Construction of vIRF-ko RRV was performed using the WT_{BAC} RRV_{17577} DNA as a template (69). First, an FRT-flanked kanamycin-resistance cassette (Kan^R) was engineered with 40bp arms of homologous RRV sequence to target the 10.9kb region (nucleotides 78436-89386) encoding the 8 vIRFs (ORF R6 – ORF R13) within RRV. The Kan^R cassette with RRV homology arms was then cloned into pSP73 and sequenced before the linearized cassette was electroporated into the recombinogenic *E. coli* strain, EL250 (130), which contains WT RRV_{17577} BAC. Recombinant EL250 clones were selected for kanamycin resistance, and BAC-DNA was subsequently isolated using a standard alkaline lysis method to identify potential clones containing the Kan^R cassette in place of the vIRFs. EL250 clones with successful recombination of the vIRF region were then treated with arabinose to induce Flp recombination within the EL250 system for removal of the Kan^R cassette within the BAC.

For Southern blot analysis, BAC-derived DNA was isolated from EL250 clones, digested with Hind III overnight at 37°C, visualized on a 0.7% agarose gel, and subsequently transferred to Duralon-UV membrane (Stratagene, La Jolla, CA). Probes were DIG-labeled using the DIG-High Prime kit (Roche, Indianapolis, IN), and

hybridization, washing, and detection were done per kit protocol. Probes were made for the vIRF deleted region (Kan^R cassette), the intact vIRF region (ORF R9), and an additional RRV gene (ORF 4), as a control.

Generation of infectious virus using the vIRF-ko RRV BAC DNA. Infectious virus was isolated from RRV_{17577} BAC DNA as previously described (69). Briefly, vIRF-ko RRV_{17577} BAC DNA from EL250 clones was transfected into RFs using TransIT LT1 reagent (Mirus Bio, Madison, WI). After the development of RRV-associated cytopathic effect (256), supernatant and cells were collected, freeze-thawed once, and sonicated to release any cell-associated virus. The virus collected after this transfection underwent two rounds of infection in RFs transiently transfected with Cre-recombinase, to remove the floxed BAC cassette. To confirm removal of the BAC cassette, the BAC cassette insertion site between ORF57 and R6 was amplified and sequenced using purified viral DNA as a template. The recombinant virus subsequently went through two rounds of plaque purification in RFs to obtain a purified clone of vIRF-ko RRV.

Viral DNA Isolation and Complete Genome Hybridization. As previously described (69), RFs were infected with BAC-derived WT or vIRF-ko RRV (MOI=.01) and allowed to progress to complete CPE before supernatant and cells were collected and digested overnight with proteinase K. Viral DNA was then isolated via cesium chloride centrifugation (77,400xg for 72h). Fractions containing viral DNA were pooled and dialyzed against Tris-EDTA. Viral DNA from vIRF-ko RRV-infected cells was subsequently analyzed via Complete Genome Hybridization (CGH) at NimbleGen

Systems, Inc. (Madison, WI), as described (69). WT_{BAC} RRV_{17577} DNA was used as a reference genome, and data was analyzed using SignalMap software (NimbleGen Systems, Inc.) to identify potential nucleotide changes in vIRF-ko RRV.

***In vitro* growth curves.** Single-step (MOI=2.5) and multistep (MOI=0.1) growth curve analyses were carried out in rhesus fibroblasts (RFs). Cells were seeded in culture tubes (Corning, Aston, MA) at a density of $2x10^5$ cells per tube, and infected in duplicate the following day. After a 2h adsorption period, tubes were washed twice with phosphate-buffered saline to remove any unbound virus, and fresh media was added. Cells and supernatants were collected at 2, 12, 24, 48, 72, and 96h post-infection. Samples were freeze-thawed once, then sonicated to release any remaining cell-associated virus before titers were determined via plaque assay in RFs.

RNA Isolation, RT-PCR and Real Time PCR. RNA was isolated from tRFs and rhesus PBMCs using the RNeasy kit (Qiagen, Valencia, CA) and DNased with RQ1 DNase (Promega, Madison, WI) per kit protocols. To assess RRV transcripts and IFN-β expression in WT_{BAC} RRV-infected tRFs and rhesus PBMCs, RT-PCR was performed using the Superscript III One-step RT-PCR with Platinum Taq (Invitrogen, Carlsbad, CA). Transcripts were detected with specific oligo pairs for each of the eight RRV vIRFs (ORF R6-R13), RRV vMIP (ORF R3), rhesus IFN-β, and glyceraldehyde 3-phosphate dehydrogenase (GAPDH) (Table 2.1).

For expression analyses of type I and type II IFNs, first strand cDNA synthesis was carried out using the High Capacity cDNA RT kit (ABI, Foster City, CA), and cDNA

was subsequently amplified using the TaqMan PreAmp master mix (ABI) and TaqMan gene expression assays specific for the following transcripts: IFN-β (Rh_03648734), IFN-$\alpha_{1/13}$ (Rh_03456606), IFN-γ (Rh-02621721), and GAPDH (Rh_02621745) (ABI). All data was normalized to the levels of GAPDH in each sample, and normalized levels of IFN transcripts were made relative to a standard sample included on each plate; either poly:IC-treated tRFs (10ug, 6h), or rhesus PBMCs treated with recombinant human IFN-α (10U, 6h).

3' RACE. Primary rhesus fibroblasts were infected (MOI=2) for 72h, followed by RNA extraction and first-strand cDNA synthesis (described above). Rapid amplification of 3' cDNA ends (3' RACE) was performed using the GeneRacer Kit (Invitrogen) with gene-specific primers upstream of the stop codon of ORF 57 (**ORF-57gsp** 5' ACG CGC AAA AAC ACG CTA GCG 3') or ORF 58 (**ORF-58gsp** 5' GCT CCT CGG ACT TGT ACA CTA TT 3'). 3' RACE products were analyzed on a 1% agarose gel, purified, and cloned into pCR4-TOPO (Invitrogen), and at least 3 clones of each product were subsequently sequenced.

Microarray analyses. RFs were infected with WT RRV_{17577} (MOI=5) for 24, 48, and 72 hours post-infection (hpi), in the presence of cycloheximide (CHX), phosphonoacetic acid (PAA), or EtOH for each time point, respectively. CHX, PAA, or EtOH (control) was added 2h prior to infection and maintained throughout infection. RNA extraction was performed with an RNA isolation kit, per kit protocol (Ambion, Austin, TX). Further RNA processing, Cy3/Cy5 labeling, hybridizations, washes and

scans were performed by the Spotted Microarray Core (SMC). Samples were analyzed using an RRV-specific DNA-spotted microarray, as detailed previously (172). Each of the 84 RRV ORFs were represented by three 70mers, 2 of which detected each transcript, and a 3rd 70mer that detected a hypothetical transcript in the antisense direction. Sequences for the 70mers used for the RRV-specific microarray were also published previously (172). Duplicate experimental samples were analyzed with a comparative based method, using uninfected RFs as the common reference sample.

Native PAGE and Immunoblotting. Protocols for native PAGE analysis of dimeric forms of cellular IRF-3 was originally described (103). Briefly, 7.5% Ready Gels (Bio-Rad, Hercules, CA) were pre-run (30 min at 40 mA, 4C) with 25 mM Tris (pH8.4) and 192 mM glycine with and without 1% sodium deoxycholate (Sigma) in the cathode and anode chamber, respectively. Lysates were re-suspended in native sample buffer and electrophoresed for 60 min at 25 mA. Proteins were then transferred to PVDF membrane (Bio-Rad) via semi-dry transfer (60min at 100mA, R.T.), and probed with anti-human IRF-3 pAb (FL-423) (Santa Cruz, Santa Cruz, CA). Data was analyzed using densitometry to quantify the intensity of IRF-3 within the dimerized band compared to the intensity of total IRF-3 (total intensity of IRF-3 within the dimeric and monomeric bands).

Immunofluorescence. Telomerized RFs (tRFs) were grown on glass coverslips in 12-well plates, and fixed with 4% paraformaldehyde in PBS (20min, R.T.). Cells were then permeabilized and blocked in 5% normal goat serum (ngs)/0.1% Triton X in PBS

(PBST) (1h, R.T.) prior to staining, and all subsequent steps were performed in 1% ngs/PBST. Cells on coverslips were stained with anti-human IRF-3 mAb (clone SL012.1) (BD Pharmingen, San Diego, CA) overnight at 4C, and subsequently stained with anti-mouse IgG-Texas Red (Vector Labs, Burlingame, CA). Nuclei/DNA were detected using Hoechst 33258 dye. Cells on coverslips were mounted onto slides using Vectashield mounting medium (Vector Labs) and examined on a Zeiss Axio Imager.M1 microscope (Zeiss Imaging Solutions, Thornwood, NY). Images were acquired using a Zeiss Axiocam camera (MRm) with Axiovision software (version 4.6), and subsequently processed using Adobe Photoshop (Adobe Systems, San Jose, CA).

Intracellular Cytokine Staining. Peripheral blood mononuclear cells (PBMCs) were freshly isolated from six individual ESPF rhesus macaques (described above), and maintained in serum-free media. Three to four million PBMCs were infected (MOI=1) and treated with Brefeldin A (0.02 μg/μl) (Sigma) during the final 6h of each experiment to block cytokine secretion. PBMCs were then surface stained with the following antibodies: CD3 (SP34), CD20 (B9E9), CD14 (M5E2), HLA-DR (L243), CD11c (3.9), and CD123 (6H6) to delineate myeloid dendritic cells (mDCs) ($CD3^-$, $CD20^-$, $CD14^-$, $HLA\text{-}DR^+$, $CD11c^+$, $CD123^-$) and plasmacytoid DCs ($CD3^-$, $CD20^-$, $CD14^-$, $HLA\text{-}DR^+$, $CD11c^-$, $CD123^+$). Cells were subsequently fixed in fixation buffer (BioLegend) for 20min at 4C, permeabilized and stained for intracellular IFN-α (MMHA-2). IFN-α was labeled using Zenon labeling technology, per kit protocol (Molecular Probes, Eugene, OR). Samples were acquired on an LSRII instrument (BD, San Jose, CA), and data were analyzed using FlowJo software (TreeStar, Ashland, OR).

Statistical Analysis. Data were analyzed using GraphPad Instat (GraphPad Software, La Jolla, CA), and significant differences were determined via paired *t-test*, with values of $p \leq 0.05$ considered significant.

RESULTS

RRV vIRFs are expressed early during infection. We initially examined the transcriptional expression of the 8 vIRFs during WT RRV_{17577} infection of rhesus fibroblasts (RFs). To do so, we used chemical inhibitors to inspect the ordered kinetic expression of viral genes, typical of Herpesvirus infection (97). Using a RRV-specific oligonucleotide-based microarray (172), we utilized a comparative hybridization-based approach to determine vIRF expression as immediate early [(cycloheximide (CHX)-resistant at 24 hours post-infection (hpi)], early (phosphonoacetic acid-resistant at 48 hpi), or late (accumulation at 72 hpi). Total RNA was collected from infected cells, labeled cDNA was then hybridized to the array, and data was analyzed using a common reference sample, uninfected RFs. These data clearly show immediate-early expression kinetics for R6, R8, R10, and R12 vIRFs, demonstrated by the marked increase in transcript at 24 hpi in the presence of CHX (Fig. 2.1A). Interestingly, R6, R8, and R10 vIRFs are also expressed with distinct late kinetics, demonstrated by a second increase in expression at 72 hpi, rather than a progressive accumulation of transcript over time (Fig. 2.1A).

To verify the immediate-early expression of the vIRFs, we performed reverse-transcription PCR (RT-PCR) to analyze the vIRF transcripts during the first 24h of WT_{BAC} RRV infection in the absence of drug. RT-PCR revealed early and sustained expression of all eight vIRFs during the first 24h of infection (Fig. 2.1B). Specifically, R10 already demonstrated strong expression at 3 hpi, and R6, R7, and R11 were all

present by 6 hpi (Fig. 2.1B). Four of the vIRFs (R7, R9, R11, and R13) demonstrated sensitivity to CHX (Fig. 2.1A), yet we detected transcript within the first 24 hpi in the absence of drug (Fig. 2.1B). This suggests that efficient expression of these vIRFs in RRV-infected RFs is enhanced by, or requires, additional viral proteins not included in the virion. Moreover, the expression pattern of the first four vIRFs (R6-R9) closely parallels the expression pattern of the duplicated vIRFs (R10-R13) (207), demonstrating the sequence-related vIRFs are similar in their temporal expression. Overall, these data demonstrate early expression of the vIRFs during RRV infection of RFs, and would position their respective proteins to be present during virus-stimulated induction of IFN.

Generation of vIRF-ko RRV using WT_{BAC} RRV_{17577}. To determine the collective role of the vIRFs during RRV infection, we utilized an infectious BAC-derived clone of RRV_{17577} (69) to generate a recombinant clone lacking all 8 vIRFs, designated vIRF-ko RRV. Because the vIRFs are encoded within a cluster in the RRV genome (Fig. 2.2A), we were able to delete all 8 concurrently. To achieve this, we replaced the vIRFs with a single kanamycin resistance (Kan^R) cassette via homologous recombination using the FLP/FRT recombination system within the E. coli strain, EL250 (130) (Fig. 2.2A). To verify targeted recombination of the vIRFs, BAC-derived DNA was digested and examined via Southern analysis after the initial recombination of the vIRF region, and again after FLP removal of the Kan^R cassette (Fig. 2.2B). Deletion of the vIRFs and FLP removal of the Kan^R cassette resulted in a 199bp lesion including a single FRT site (48bp) in the genomic region where the vIRFs were deleted. To verify this, BAC-DNA from the vIRF-ko RRV clone was isolated, and the genomic region containing the vIRF

deletion was amplified and sequenced to confirm targeted deletion and that there were no changes in surrounding genomic sequence (data not shown).

BAC DNA from the vIRF-ko EL250 clone was subsequently transfected into RFs, resulting in the production of infectious virus. This virus was subsequently used to infect RFs transiently expressing Cre recombinase to remove the LoxP-flanked BAC cassette (69), and then subjected to two rounds of plaque purification in RFs to obtain a purified isolate of vIRF-ko RRV. Viral DNA was then purified and analyzed via comparative genomic hybridization (CGH) to compare the complete genomic sequence of vIRF-ko RRV viral DNA to that of WT_{BAC} RRV_{17577}. Previous studies have demonstrated the utility of CGH for identification of single nucleotide changes, insertions, and deletions within different strains of RRV, as well as WT_{BAC} RRV_{17577} viral isolates (69). No other nucleotide changes were detected in the vIRF-ko RRV isolate using this method (Fig. 2.3), indicating that WT_{BAC} RRV and vIRF-ko RRV have identical sequence outside the deleted vIRF region.

WT_{BAC} and vIRF-ko RRV infect RFs and rhesus PBMCs, and have similar *in vitro* growth potential. To evaluate viral replication in the absence of the vIRFs, single-step (MOI=2.5) and multistep (MOI=0.1) growth curves were performed to assess viral growth and spread, respectively. In both the single-step (Fig. 2.4A) and multi-step (Fig. 2.4B) growth analyses, vIRF-ko RRV displayed similar growth kinetics and magnitude as WT_{BAC} RRV. We conclude that the vIRFs are not essential for RRV infection,

replication or spread during RRV infection of RFs *in vitro*. Thus, any phenotypic differences between WT_{BAC} and vIRF-ko RRV infection in RFs cannot be simply attributed to altered growth potential.

Although RRV infection of fibroblasts is easily studied, peripheral blood mononuclear cells (PBMCs), and B cells specifically, represent an important cellular target for RRV in the rhesus macaque (16). Therefore, to determine if lack of the vIRFs alters RRV infection in a more relevant cell type, we also assessed WT_{BAC} and vIRF-ko RRV infection of rhesus PBMCs. Because such a small percentage of PBMCs get infected with RRV *in vitro* (data not shown), we were unable to compare growth properties within PBMCs using standard plaque assay. Thus, we instead utilized RT-PCR to verify the presence of RRV transcripts to demonstrate RRV infection of rhesus PBMCs. We first assayed for viral Macrophage Inflammatory Protein (vMIP), encoded by ORF R3 (207), since we can readily detect vMIP sequence (DNA and RNA) in RRV-infected PBMCs, even at low levels of infection (data not shown). In fact, we were able to detect vMIP transcript in both WT_{BAC} and vIRF-ko RRV-infected PBMCs throughout the entire 48h time course (Fig. 2.4C). Additionally, we looked for the presence of one of the vIRF transcripts to verify that the vIRFs are also expressed during RRV infection of PBMCs. We chose the vIRF encoded by ORF R10, because it was transcribed early and persisted during the first 24h in RRV-infected RFs (Fig. 2.1B). As expected, vIRF R10 transcript was only present in WT_{BAC} RRV-infected PBMCs, and transcript was present at 3 hpi, and persisted through 48 hpi (Fig. 2.4C). Although we were unable to efficiently compare growth properties of WT_{BAC} and vIRF-ko RRV in PBMCs, these

data demonstrate that removal of the vIRFs did not prevent RRV infection of rhesus PBMCs, and that vIRF expression also occurs early during infection of PBMCs, represented by R10 vIRF.

Deletion of the vIRFs did not alter gene expression of adjacent ORFs. We next confirmed that gene expression of the ORFs directly upstream (ORF 57) and downstream (ORF 58) of the deleted vIRFs was still intact during vIRF-ko RRV infection. RRV ORF 57 encodes a protein with immediate early expression and shares similarity with ORF 57 of other γ-herpesviruses, which function in nuclear export of unspliced viral mRNA (27, 169, 225). RRV ORF 58 is also conserved among γ-herpesviruses (169), and encodes a protein with putative epithelial binding function, as was demonstrated for Epstein-Barr virus (234). The coding regions for ORF 57 and ORF 58 are oriented in opposing directions, both being transcribed toward the vIRF region (Fig. 2.2A), so we utilized 3' RACE with gene-specific primers within ORF 57 and ORF 58 to verify maintenance of both transcripts during vIRF-ko RRV infection. We identified two poly(A) sites that yielded full-length ORF 57 transcripts in WT_{BAC} and vIRF-ko RRV-infected tRFs (Fig. 2.5A and B). The poly(A) site further downstream of the stop codon is preferentially used during vIRF-ko RRV infection, while the poly(A) site that overlaps with the stop codon is preferentially used during WT_{BAC} RRV infection (Fig. 2.5B). There was also a third, less abundant product identified for ORF 57 in vIRF-ko RRV-infected cells (Fig. 2.5), which resulted in an abbreviated transcript. Transcription of ORF 58 also utilizes multiple poly(A) sites during WT_{BAC} and vIRF-ko RRV infection, but the dominant transcript used the same

poly(A) site (Fig. 2.5C), and resulted in a full-length transcript (Fig. 2.5D). These data suggest that removal of the vIRFs did not significantly impact transcription of adjacent ORFs during RRV infection of tRFs.

Deletion of the vIRFs results in increased induction of type I and type II IFNs during RRV infection. To examine whether the vIRFs collectively function to inhibit induction of IFNs, we measured the induction of type I (IFN-β and IFN-α) and type II (IFN-γ) IFN in WT_{BAC} and vIRF-ko RRV-infected tRFs and rhesus PBMCs. Induction of IFN-β occurs early during viral infection in a variety of cell types, including fibroblasts, so we initially assayed levels of IFN-β transcript within the first 24h of RRV infection in tRFs. Using reverse transcription (RT)-PCR, it was evident that WT RRV infection induced very little IFN-β, only faintly detectable at 12 hpi (Fig. 2.6A). Deletion of the vIRFs, however, resulted in increasing levels of IFN-β transcript between 12-24 h post-RRV infection (Fig. 2.6A), demonstrating that the vIRFs inhibit the induction of IFN-β during RRV infection of tRFs.

To quantify the induction IFNs during WT_{BAC} and vIRF-ko RRV infection in tRFs, we measured type I and type II IFN transcripts during a 72h time course via semi-quantitative real time-PCR. Each sample was normalized to GAPDH levels, and made relative to a positive control sample (IFN-α-treated PBMCs or poly(I:C)-treated tRFs). As described above, WT_{BAC} RRV is not a robust inducer of IFN-β (Fig. 2.6A), and it's especially evident when compared to a known stimulus, poly(IC), which induced 10^5

times more IFN-β (Fig 2.6B). However, deletion of the vIRFs resulted in an average 2-fold increase in IFN-β transcript at 72 hpi as compared to WT_{BAC} RRV, although these data were not statistically significant (Fig. 2.6B). In contrast to the tRFs, we were unable to detect any IFN-β message within mock or RRV-infected rhesus PBMCs in these studies (Fig. 2.6B).

To further assess type I IFN response during RRV, we also examined induction of IFN-α_1, as it is the only IFN-α subtype that is induced upon viral infection (84, 136). As measured by real time RT-PCR, the induction of IFN-α_1 in WT_{BAC} RRV-infected tRFs was unremarkable throughout the 72h time course, with levels between 0.5-1% of the magnitude of IFN-α_1 induction after poly(IC) stimulation (Fig. 2.6C). However, vIRF-ko RRV infection of tRFs resulted in a progressive increase in IFN-α_1 transcript that culminated in 3-fold higher induction at 72 hpi compared to WT_{BAC} infection (Fig. 2.6C). Within PBMCs, the levels of IFN-α_1 transcript peaked much earlier, at 12h post-RRV infection, with nearly 2-fold higher induction during vIRF-ko RRV infection compared to WT_{BAC} RRV (Fig. 2.6C). Moreover, the induction IFN-α_1 at 6 hpi in vIRF-ko RRV-infected PBMCs was 12-fold higher than during WT_{BAC} RRV infection (Fig. 2.6C). These data further demonstrate that the vIRFs are effectively inhibiting the induction of type I IFNs during RRV infection in tRFs and PBMCs.

Lastly, we assessed the impact of vIRFs on induction of type II IFN, IFN-γ, during RRV infection. Within tRFs, vIRF-ko RRV induced IFN-γ expression at 48-72 hpi,

whereas WT_{BAC} RRV infection completely inhibited induction (Fig. 2.6D). RRV infection of PBMCs induced IFN-γ with similar kinetics as IFN-α_1 induction, peaking at 12 hpi (Fig. 2.6D), and vIRF-ko RRV infection induced significantly more IFN-γ at 6 hpi (Fig. 2.6D). Collectively, these data demonstrate the vIRFs can significantly reduce and delay induction of both type I and type II IFN during RRV infection.

The vIRFs limit IFN-α production by pDCs in RRV-infected PBMCs. To determine if the vIRF-dependent inhibition of IFN transcripts correlates with reduced IFN production, we examined IFN-α production in RRV-infected PBMCs via intracellular cytokine staining (ICCS). Freshly isolated PBMCs from six expanded specific pathogen free (ESPF) rhesus macaques were infected with WT_{BAC} or vIRF-ko RRV (MOI=1) for 12, 24, and 48h. For all samples, Brefeldin A was added during the last 6h of incubation to inhibit cytokine secretion. Subsequently, PBMCs were surface stained to delineate plasmactyoid dendritic cells (pDCs) ($CD3^-$, $CD20^-$, $CD14^-$, HLA-DR^+, $CD11c^-$, $CD123^+$) (28) (outlined in Fig. 2.7A), as they are the major producers of type I IFN in PBMCs (47, 215). Subsequently, IFN-α production was measured using ICCS. HSV-1 stimulation of rhesus PBMCs, used as a positive control, resulted in marked production of IFN-α specifically within the pDC population (Fig. 2.7A), similar to previous findings (47, 215). Likewise, approximately 15% of the pDC population was producing IFN-α at 12 hpi in both WT_{BAC} and vIRF-ko RRV-infected PBMC cultures (Fig. 2.7B and C). Interestingly, IFN-α production was sustained in vIRF-ko RRV-infected cultures, with approximately 17% of the pDCs still producing IFN-α at 24 hpi (Fig. 2.7B and C). In contrast, only 6% of the pDCs still produced IFN-α at 24

hpi in WT_{BAC} RRV-infected cultures (Fig. 2.7B and C). Thus, we conclude that deletion of the vIRFs results in sustained production of IFN-α following RRV infection of PBMCs.

The vIRFs alter the localization of cellular IRF-3 during RRV infection. IRF-3 is a vital component of the transcription machinery that drives transcription of type I IFN (84, 136, 203) following viral infection. Therefore, we monitored activation of cellular IRF-3 during the initial 24h of infection with RRV. We did not detect a decrease in overall levels of IRF-3 after WT_{BAC} or vIRF-ko RRV infection, as measured by total IRF-3 present in whole cell extracts (data not shown). Moreover, both WT_{BAC} and vIRF-ko RRV induced similar levels of IRF-3 dimerization, which peaked at 6-12 hpi, as measured via native PAGE and western analysis (Fig. 2.8A and B). However, deletion of the vIRFs resulted in increased nuclear accumulation of IRF-3 at 6 hpi (Fig. 2.8C and D). Indirect immunofluorescence of total IRF-3 demonstrated that 61% of cells contained IRF-3 in the nucleus at 6 hpi in vIRF-ko RRV-infected cells, compared to only 30% in cultures infected with WT_{BAC} RRV (Fig. 2.8C and D). This observation suggests that interference with nuclear accumulation of IRF-3 is one potential mechanism utilized by vIRFs to inhibit induction of type I IFN during RRV infection.

DISCUSSION

KSHV allocates a significant portion of its genome to encoding immunomodulatory proteins (10). Of particular interest are the viral interferon regulatory factors (vIRFs), unique to KSHV and RRV, a closely related simian γ-Herpesvirus (7, 194, 201, 207). KSHV vIRF-1 was initially identified and named because of its sequence similarities with cellular IRFs; specifically, it shares 13% sequence identity with IRF-8 and IRF-9 (162). Moreover, *in vitro* studies have demonstrated that KSHV vIRF-1, -2, and -3 have various inhibitory effects on the cellular IRFs (170). Similarly, RRV encodes eight vIRFs that also share homology with cellular IRF-8 and IRF-9, as well as approximately 20% AA identity with KSHV vIRF-1 (207), and are also proposed to interfere with the transcriptional functions of cellular IRFs. Deletion of the vIRFs using WT_{BAC} RRV, presented herein, has finally enabled us to assess the impact of vIRFs during *de novo* RRV infection; something that has proved difficult with KSHV, due to poor lytic replication. These data are the first to demonstrate that deletion of the vIRFs results in increased gene expression/production of IFN and increased nuclear accumulation of IRF-3 during *de novo* RRV infection. These results suggest that the vIRFs can inhibit the innate, antiviral response, thereby providing an advantage to RRV.

The IFN response is an important component to a cell's antiviral defenses. To effectively circumvent the induction of IFN, an invading pathogen must also act quickly. Accordingly, our transcriptional analysis has demonstrated that all 8 vIRFs are detected by 12 hpi via RT-PCR, and vIRF R10 was expressed as early as 3 hpi in RRV-

infected tRFs and PBMCs (Fig. 2.1 and 2.4). Additionally, we performed a more stringent kinetic examination of vIRF expression in our microarray analysis, and identified that 4 of the vIRFs (R6, R8, R10, and R12) were expressed with true, immediate early kinetics, as demonstrated by their expression in the presence of cycloheximide (CHX). Thus, because their expression is independent of new viral protein synthesis, these four vIRFs may be the key players in inhibiting induction of IFN during RRV infection (Fig. 2.6). The remaining four vIRFs (R7, R9, R11, and R13), however, were sensitive to CHX, demonstrating their early expression is dependent on newly synthesized viral proteins not present within the virion. Moreover, our inability to detect significant expression of these 4 vIRFs at any time point in our microarray analyses suggests that efficient expression of R7, R9, R11, and R13 may also be dependent on cell-specific factors not present in RFs. Previous transcriptional studies of $RRV_{26\text{-}95}$ also demonstrated variable expression for all 8 vIRFs, but did not see the paralleled expression between the first four vIRFs (R6-R9) and their respective, duplicated vIRFs (R10-R13) as we demonstrated during RRV_{17577} infection (Fig. 2.1) (63). Nonetheless, the transcriptional analyses of $RRV_{26\text{-}95}$ did demonstrate that at least 2 vIRFs (corresponding to R6 and R10) were expressed as early as 6-12 hpi (63). Likewise, KSHV vIRF-1 is also transcriptionally up-regulated upon induction of lytic replication in KSHV-infected B cells (62). Accordingly, three of the KSHV vIRFs possess a variety of mechanisms to independently inhibit induction of IFNs and IFN-induced signaling (170). Therefore, the early expression of the vIRFs during RRV infection suggests they play a role in inhibiting the innate antiviral response, including induction of IFN.

Comparison of WT_{BAC} and vIRF-ko RRV *de novo* infection has demonstrated that deletion of the vIRFs did not significantly alter infection in RFs and PBMCs. Viral growth and spread in RFs is comparable between WT_{BAC} and vIRF-ko RRV infection, and deletion of the vIRFs resulted in minimal effects on expression of ORFs adjacent to the deleted region. We did detect an additional, truncated ORF57 transcript in vIRF-ko RRV infection, but it was not as abundant as the 2 full-length transcripts. Moreover, because viral growth appeared unaltered, it's unlikely the additional, truncated transcript interferes with efficient expression of ORF57. Our analyses of RRV-infected cultures of PBMCs, however, did not allow for quantification of viral infection and growth, but we can conclude that vIRF-ko RRV can still infect PBMC cultures, as demonstrated by the expression of viral transcripts during the first 48 hpi (Fig. 2.4). Likewise, we have yet to thoroughly analyze the specific populations infected with RRV in the peripheral blood, and whether this is altered after deletion of the vIRFs. Still, we have demonstrated that presence of the RRV vIRFs significantly decreases and delays the induction of type I and type II IFN during RRV infection of tRFs and PBMCs. The magnitude of the response was dramatically lower in tRFs, which likely explains comparable growth of vIRF-ko RRV (Fig. 2.4), despite induction of IFN. However, vIRF-ko RRV infection of PBMCs resulted in early induction of type I and type II IFN transcripts, as well as sustained production of IFN-α protein, compared to a significantly abbreviated response after WT_{BAC} RRV infection. Not surprisingly, the IFN-α produced within RRV-infected PBMCs was restricted to pDCs, which are known to produce large amounts of IFN-α in response to a number of different viruses (72, 75). These data do not directly demonstrate the pDCs producing IFN-α are infected.

However, pDCs are unique in their sole expression of toll-like receptor 7 (TLR7) and TLR9, specifically equipping them to recognize bacterial and viral nucleic acids, including genomic DNA from several herpesviruses (118, 176). Moreover, it's recently been demonstrated that KSHV infection of pDCs induces production of IFN-α in a TLR9-dependent manner (250). Therefore, the detection of RRV transcripts by 3 hpi in RRV-infected PBMC cultures, and the dramatic increase in IFN transcript at 6 hpi imply the pDCs are responding to direct infection with RRV, likely through recognition of its genomic DNA.

Induction of type I IFNs is orchestrated by IRF-3, constitutively expressed in most cell types, and IRF-7, constitutively expressed in pDCs. These IRFs are quickly activated following viral infection, and subsequently accumulate in the nucleus where they drive transcription of type I IFNs. We've demonstrated that the presence of the vIRFs inhibits IRF-3 nuclear accumulation within the first six hours of RRV infection, preceding the inhibition of type I IFN induction during RRV infection. Distinct mechanism(s) of IRF-3 dysregulation have yet to be determined, but the vIRFs likely target multiple cellular proteins as demonstrated for the KSHV vIRFs. For example, KSHV vIRF-1 can bind p300/CBP and inhibit its essential interaction with IRF-3 (31, 137), and KSHV vIRF-3 can bind to and retain NFκB in the cytoplasm (213). Thus, both vIRFs are independently interfering with two necessary factors in the induction of type I IFN. Further examination is required to determine the exact functions of the individual RRV vIRFs in the inhibition of IFN, and specifically define the mechanism(s) of IRF-3 dysregulation.

In addition to establishing an antiviral state early during viral infection, type I IFNs (α/β) also have effects on NK cells (20, 165), T cells (100, 150, 232) and DCs (102, 143, 161), directly impacting the adaptive immune response. Therefore, the inhibition of type I IFNs by vIRFs could disrupt both the innate and adaptive immune responses during *in vivo* RRV infection. Additionally, our data demonstrate the RRV vIRFs also inhibit the induction of type II IFN, IFN-γ, which is essential for promoting an efficient Th1 immune response. In fact, previous *in vitro* analyses demonstrated KSHV vIRF-1 and vIRF-3 can also interfere with type II IFN signaling. Specifically, KSHV vIRF-1 inhibits transcription induced by IFN-γ (134, 267), and results in decreased surface expression of MHC-I (127). Likewise, KSHV vIRF-3 similarly inhibits IFN-γ-responsive promoters, resulting in decreased expression of MHC-II on latently infected B cells (206). The distinct late expression of a subset of the RRV vIRFs may translate to additional roles that specifically target IFN-γ, or other IRF-dependent cytokines, to further interfere with the adaptive immune response. Our preliminary examination of IFN-γ production in RRV-infected PBMC cultures, T cells and DCs specifically, did not show any measurable production over mock-infected cultures in the first 24 hpi (data not shown), despite the significant induction at the transcript level in vIRF-ko RRV infection (Fig. 2.5). However, the vIRF-mediated inhibition of IFN-γ may be important in other cell types that weren't examined here, such as natural killer cells (20, 233), or at later times during RRV infection, potentially in response to other cytokines, such as IL-12 (165). Differentially, individual RRV vIRFs may enhance transcription of some cellular genes, as shown for KSHV vIRF-1 (198) and vIRF-3 (140, 141). Moreover, a

role for vIRFs in stimulation of IRF-mediated transcription (140) could promote cytokine-enhanced reactivation of the virus (159). Future studies will utilize vIRF-ko RRV to focus on the impact of vIRFs during *in vivo* RRV infection of the rhesus macaque to further our understanding of their role(s) in immune evasion and pathogenesis.

FIGURE. 2.1. Expression of 8 vIRFs during Rhesus Rhadinovirus infection. **(A)** To analyze immediate early, early, and late transcripts during WT RRV_{17577} infection, RFs were infected (MOI=5) for 24h in the presence of cycloheximide (CHX) (50μg/ml), 48h in the presence of phosphonoacetic acid (PAA) (300μM), or 72h without drug (EtOH only), respectively. Transcript expression was analyzed using an RRV-specific spotted microarray. The level of expression of the 8 vIRFs in RRV-infected RFs was determined using a comparative-based method (Cy3/Cy5), using mock-infected cells as the reference sample. Each vIRF transcript was detected using two separate probes (a and b), and this data is a representative of 2 biological replicates. **(B)** tRFs were infected (MOI=2) and RNA was extracted at 3, 6, 12, and 24 hpi, and analyzed via RT-PCR using 8 vIRF-specific oligo pairs (Table 2.1). As controls for RNA input and purity, levels of GAPDH were analyzed in each sample, as well as a reaction run without reverse transcriptase. hpi, hours post-infection. GAPDH, glyceraldehyde 3-phosphate dehydrogenase.

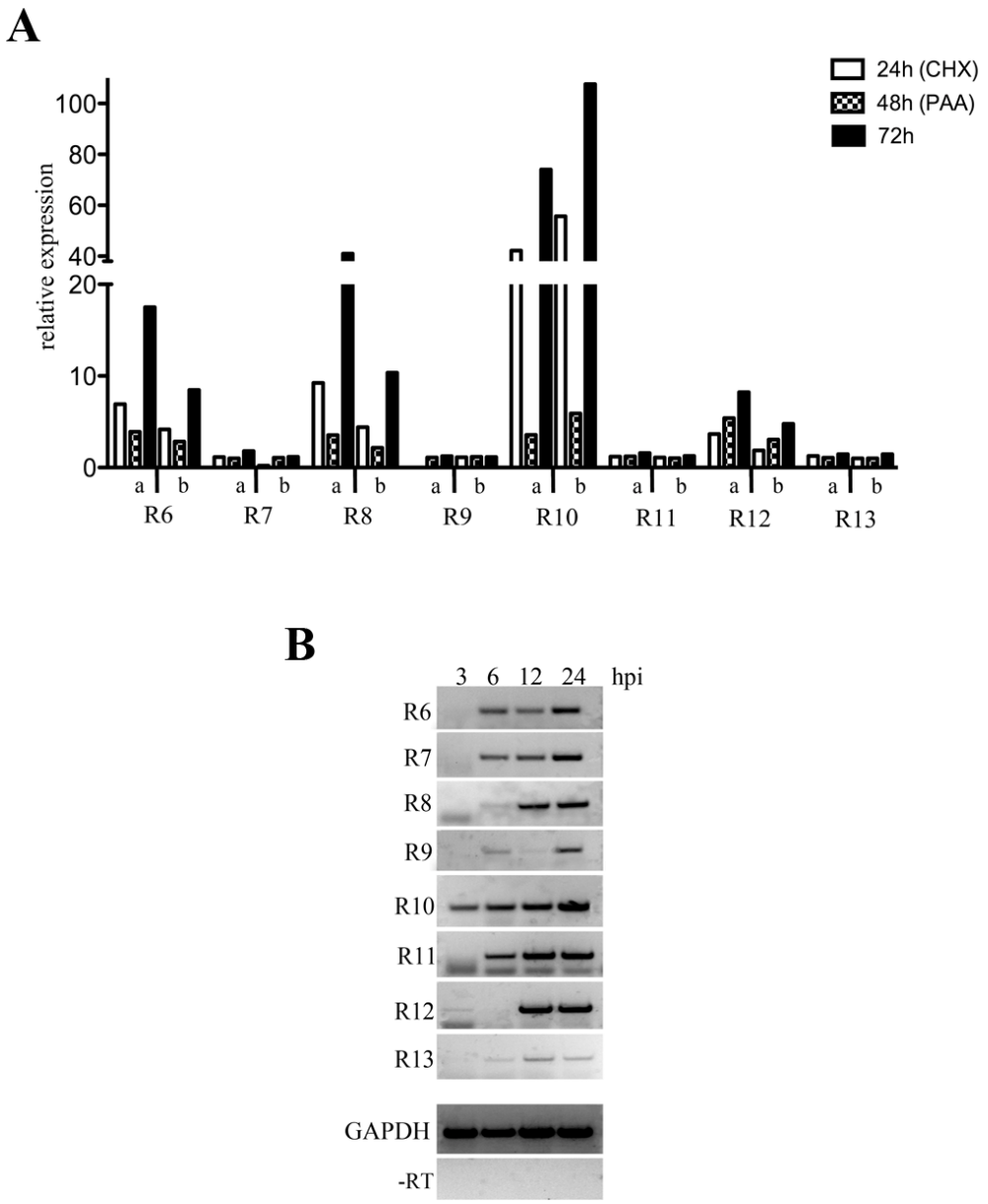
A
24h (CHX)
48h (PAA)
72h
relative expression
100
80
60
40
20
10
0
a b a b a b a b a b a b a b a b
R6 R7 R8 R9 R10 R11 R12 R13
B
3 6 12 24 hpi
R6
R7
R8
R9
R10
R11
R12
R13
GAPDH
-RT

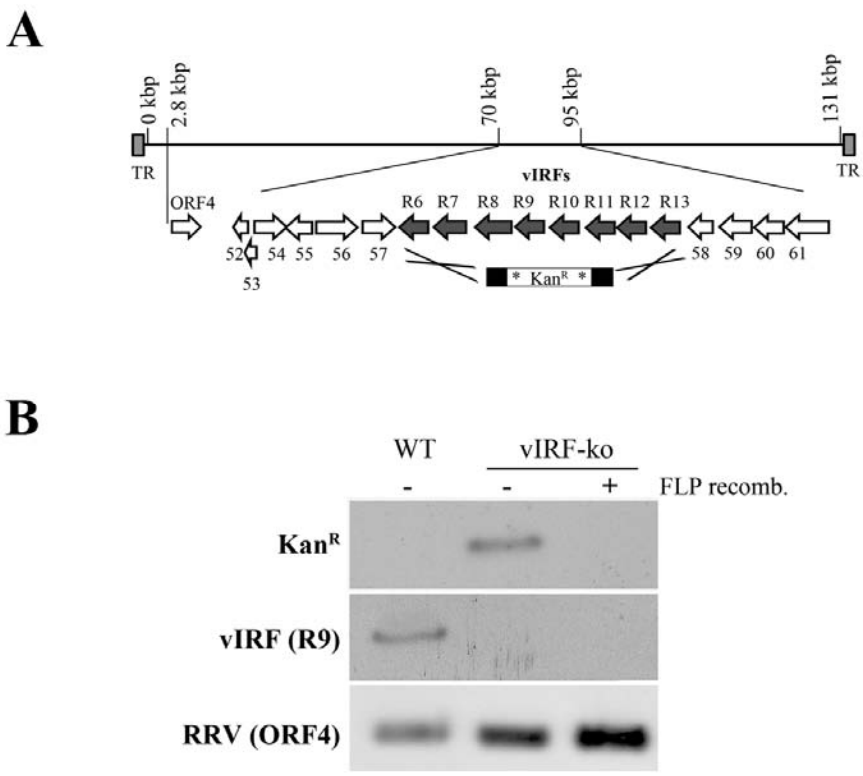

FIGURE 2.2. Construction and molecular characterization of vIRF-ko RRV using WT_{BAC} RRV_{17577}. **(A)** A schematic representation of the RRV genome illustrating the location and orientation of the eight vIRFs (ORFs R6 – R13) encoded within a 10.95kb region (nucleotides 78436-89386) between ORF57 and ORF58. The genomic region encompassing the 8 vIRFs was targeted for deletion via homologous recombination within the recombinant E. coli strain, EL250. The entire region was recombined with an FRT-flanked kanamycin resistance (Kan^R) cassette with 40bp homology arms (shaded regions) to recombine with sequence directly upstream and downstream of the vIRF region. FRT sites are illustrated with an asterisk (*). **(B)** WT_{BAC} RRV_{17577} DNA was isolated from EL250s before and after recombination of the vIRF region, and again after the Kan^R cassette was removed via Flp recombination. DNA was digested with HindIII, run on an agarose gel and Southern blot analysis was performed using DIG-labeled probes against the vIRF region, the Kan^R gene, and another RRV gene (ORF4), as a control. TR, terminal repeats. FRT, Flp recognition target. Flp, Flippase.

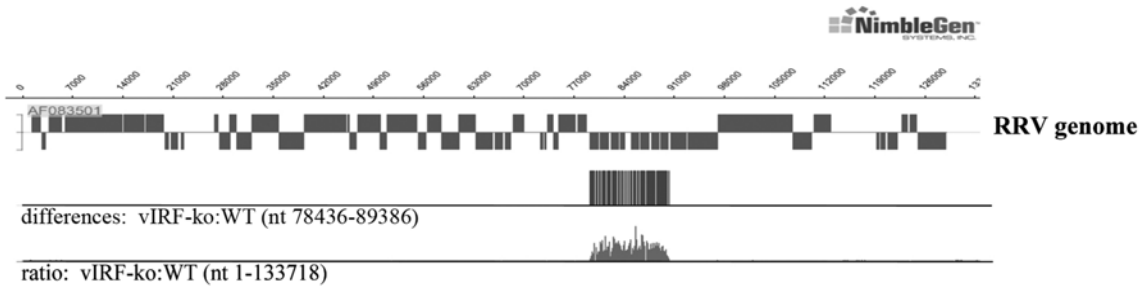

FIGURE. 2.3 Comparative Genome Hybridization. An array was designed containing oligos spanning the entire RRV_{17577} genome (forward and reverse strands). WT_{BAC} RRV_{17577} DNA was used as a reference sample, and we directly compared viral DNA from the vIRF-ko RRV recombinant clone to identify potential nucleotide changes, deletions, and insertions. Any alterations within the vIRF-ko RRV genome resulted in incomplete hybridization to the array, depicted in the ratio of vIRF-ko:WT, and signaled a potential mismatch in the identified genomic region (nt 78436-89386). This comparison identified the region of vIRF deletion as shown, but no other changes were detected within the vIRF-ko RRV genome.

FIGURE 2.4. WT_{BAC} RRV and vIRF-ko RRV infection of RFs and rhesus PBMCs. RFs were infected with WT_{BAC} RRV and vIRF-ko RRV in **(A)** single step (MOI=2.5) and **(B)** multi-step (MOI=0.1) growth curves. Infected RFs were harvested at specified time points and subjected to serial-dilution plaque assay on RFs to ascertain viral titer, displayed as plaque forming units (PFU) / ml (±SEM). **(C)** Rhesus PBMCs were isolated from ESPF rhesus macaques and infected with WT_{BAC} RRV or vIRF-ko RRV (MOI=1). RNA was harvested at indicated time points, and analyzed via RT-PCR for RRV vMIP (ORF R3), RRV vIRF (ORF R10), and GAPDH, as a loading control. Oligo pairs used for each transcript are listed in Table 2.1, and viral transcripts were detected using 300ng RNA, and GAPDH was detected using 50ng RNA per sample. Samples were simultaneously run with Taq polymerase only (-RT) to verify absence of contaminating DNA, and purified RRV DNA was used as a positive control (+). PBMCs, peripheral blood mononuclear cells; ESPF, expanded specific-pathogen free; vMIP, viral macrophage inflammatory protein; GAPDH, glyceraldehyde 3-phosphate dehydrogenase.

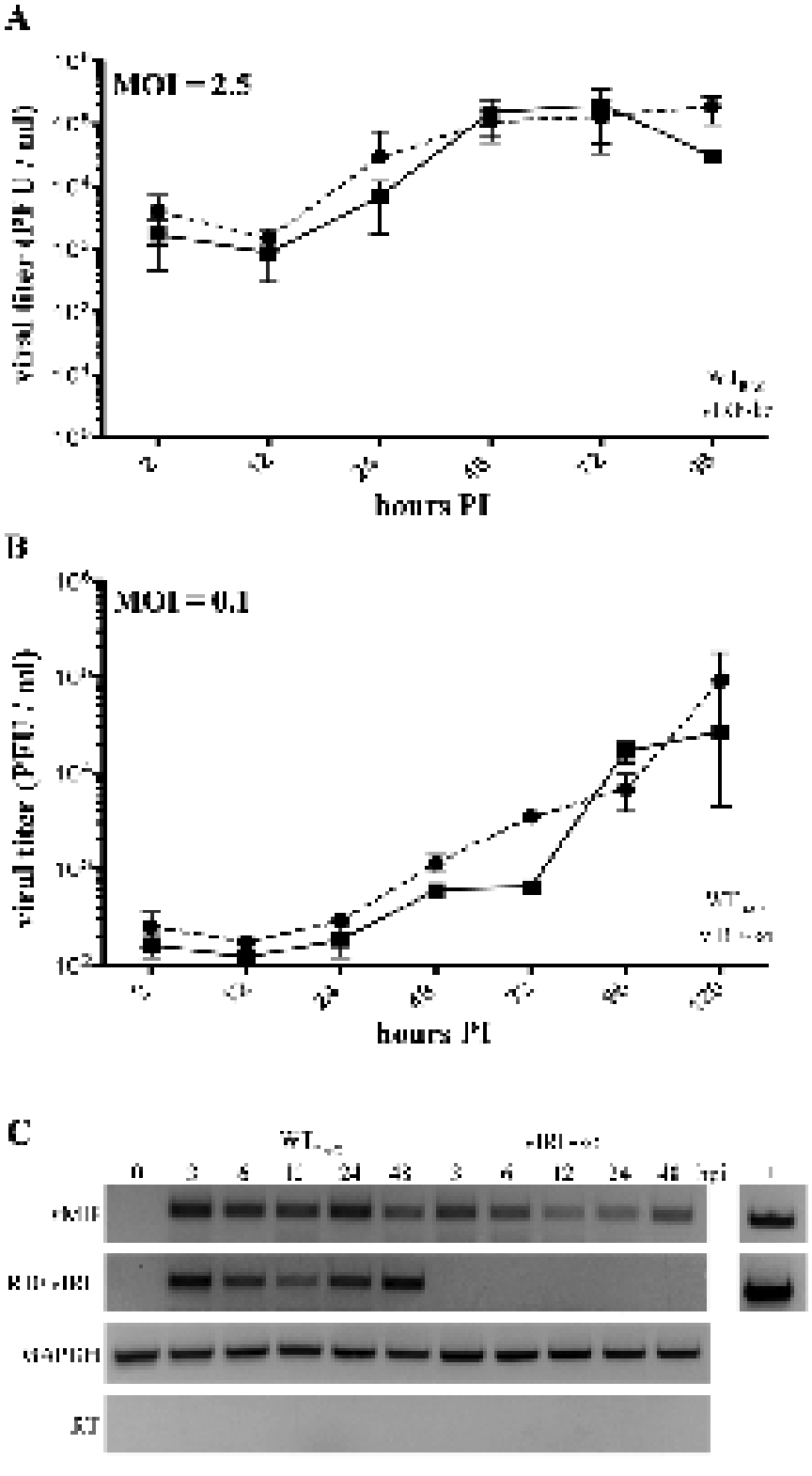
A
MOI = 2.5
hours PI
B
MOI = 0.1
hours PI
C
0
3
6
12
24
48
3
6
12
24
48
hpi
GAPDH

FIGURE 2.5. 3' RACE analysis of ORFs adjacent to deleted vIRF region. Rhesus fibroblasts were infected with WT_{BAC} RRV or vIRF-ko RRV (MOI=1), and RNA was harvested at 72 hpi and analyzed via 3' RACE to verify transcription of ORF 57 and ORF 58, the two ORFs directly upstream and downstream of the vIRF region. (A) 3' RACE analysis of ORF 57 demonstrated 2 products in WT_{BAC} and VIRF-ko RRV infection (arrows, labeled a and b). A third transcript was detected in vIRF-ko RRV infection, but resulted in a truncated transcript (#). (B) Both full-length products were cloned and sequenced, and correspond to transcripts using 2 distinct poly(A) sites (shaded in gray). The stop codon is underlined, and the addition of the poly(A) tail is noted with the symbol, >. (C) 3' RACE analysis of ORF 58 demonstrated a dominant, full-length product in WT_{BAC} and vIRF-ko RRV infection (arrow). (D) This product was subsequently cloned and sequenced to identify a single poly(A) site (shaded in gray) upstream of the stop codon (underlined), and the addition of the poly(A) tail is marked (>) downstream of the stop codon.

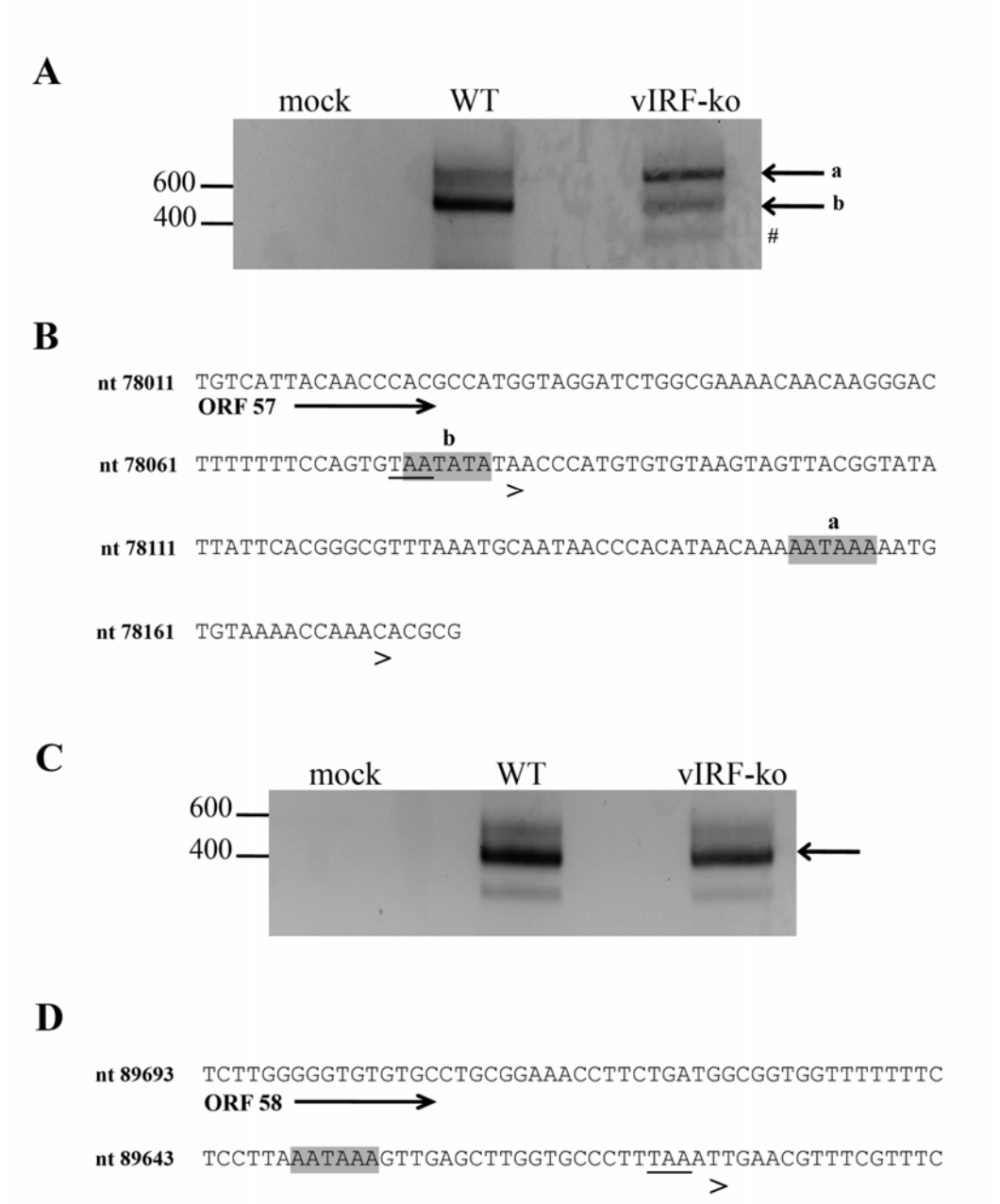
A
mock
WT
vIRF-ko
600
400
a
b
#
B
nt 78011 TGTCATTACAACCCACGCCATGGTAGGATCTGGCGAAAACAACAAGGGAC
ORF 57
b
nt 78061 TTTTTTTCCAGTGTAATATATAACCCATGTGTGTAAGTAGTTACGGTATA
a
nt 78111 TTATTCACGGGCGTTTAAATGCAATAACCCACATAACAAAAATAAAAATG
nt 78161 TGTAAAACCAAACACGCG
C
mock
WT
vIRF-ko
600
400
D
nt 89693 TCTTGGGGGTGTGTGCCTGCGGAAACCTTCTGATGGCGGTGGTTTTTTTC
ORF 58
nt 89643 TCCTTAAATAAAGTTGAGCTTGGTGCCCTTTAAATTGAACGTTTCGTTTC

FIGURE 2.6. Induction of type I and type II IFN during RRV infection. Telomerized RFs (tRFs) and ESPF rhesus PBMCs were infected with WT_{BAC} RRV or vIRF-ko RRV (MOI=1), and RNA was analyzed at indicated time points via (A) RT-PCR or (B-D) real-time PCR. (A) RT-PCR was performed using 300ng RNA per sample for detection of IFN-β in RRV-infected tRFs. Detection of GAPDH was used as a loading control, and samples were run with Taq polymerase only (-RT) to demonstrate absence of contaminating DNA. Oligos used for RT-PCR are listed in Table 2.1. (B-D) RNA from infected tRFs and infected PBMCs was also used to prepare and amplify cDNA for semi-quantitative real time PCR specific for (B) IFN-β, (C) IFN-α_1, and (D) IFN-γ using the Taqman PreAmp master mix and GeneExpression Assays (ABI) specific for rhesus transcripts. All transcripts were normalized to levels of GAPDH in each sample, and made relative to a positive control sample included on each plate. The positive control for IFN-α and IFN-β transcripts was cDNA from tRFs transfected with poly(IC) (10ug/ml, 6h), and the positive control for IFN-γ was cDNA from PBMCs treated with recombinant human IFN-α2 (10Units/ml, 6h). Data are averaged (± SEM) from at least three independent experiments each in tRFs and PBMCs. **, $p \leq 0.01$. *, $p \leq 0.05$. N.S., not significant. ND, not detected.

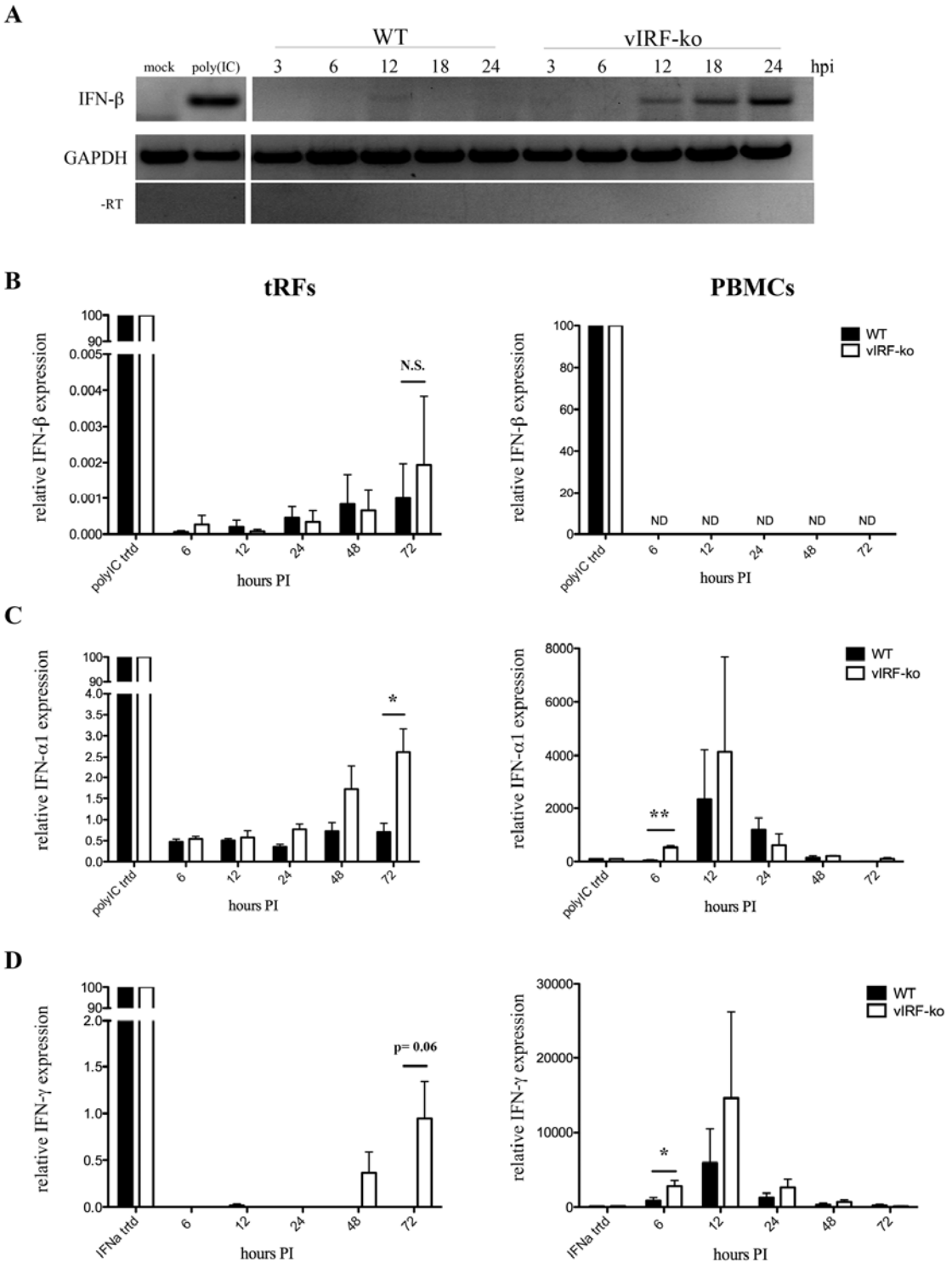
A
WT
vIRF-ko
mock
poly(IC)
3
6
12
18
24
3
6
12
18
24
hpi
IFN-β
GAPDH
-RT
B
tRFs
PBMCs
relative IFN-β expression
N.S.
ND
polyIC trtd
hours PI
WT
vIRF-ko
C
relative IFN-α1 expression
*
**
D
relative IFN-γ expression
p= 0.06
IFNa trtd

FIGURE. 2.7. Production of IFN-α by pDCs in RRV-infected PBMC cultures. Freshly collected peripheral blood mononuclear cells (PBMCs) from six ESPF rhesus macaques (RM) were used for the following experiments. Four million PBMCs were mock-infected, or infected with WT_{BAC} or vIRF-ko RRV (MOI=1) in serum-free media. During the last 6h of infection, brefeldin A (0.02 μg/μl) was added to inhibit cytokine secretion, and at 12, 24, and 48 hpi, cells were surface stained for CD3, CD20, CD14, HLA-DR (MHC-II), CD11c, and CD123. PBMCs were then subsequently fixed and IFN-α production was measured via intracellular cytokine staining, and cells were analyzed via flow cytometry. (A) Surface marker expression was utilized to delineate cellular populations within the PBMC cultures: T cells ($CD3^+$), B cells ($CD20^+$), monocytes (Lin^-, MHC II^+, $CD14^+$), and dendritic cells (DCs) (Lin^-, MHC II^+, $CD14^-$). The DC population was further delineated into myeloid DC (CD11c+, CD123dim) and plasmacytoid DC ($CD11c^-$, $CD123^+$) subsets. IFN-α production was then measured in the mDC and pDC populations, as well as the total DC population, and the percentage of cells producing IFN-α is shown in each histogram. (B) IFN-α production within the pDCs is shown from a representative experiment at 12, 24, and 48 hpi. PBMCs were stimulated with HSV-1 for 12h as a positive control for IFN-α production. (C) Comparison of the percentage of pDCs producing IFN-α at each time point in WT_{BAC} or vIRF-ko RRV-infected PBMC cultures (n = 6). PBMCs from each of the 6 RMs are represented by the same symbol at all time points. N.S., not significant.

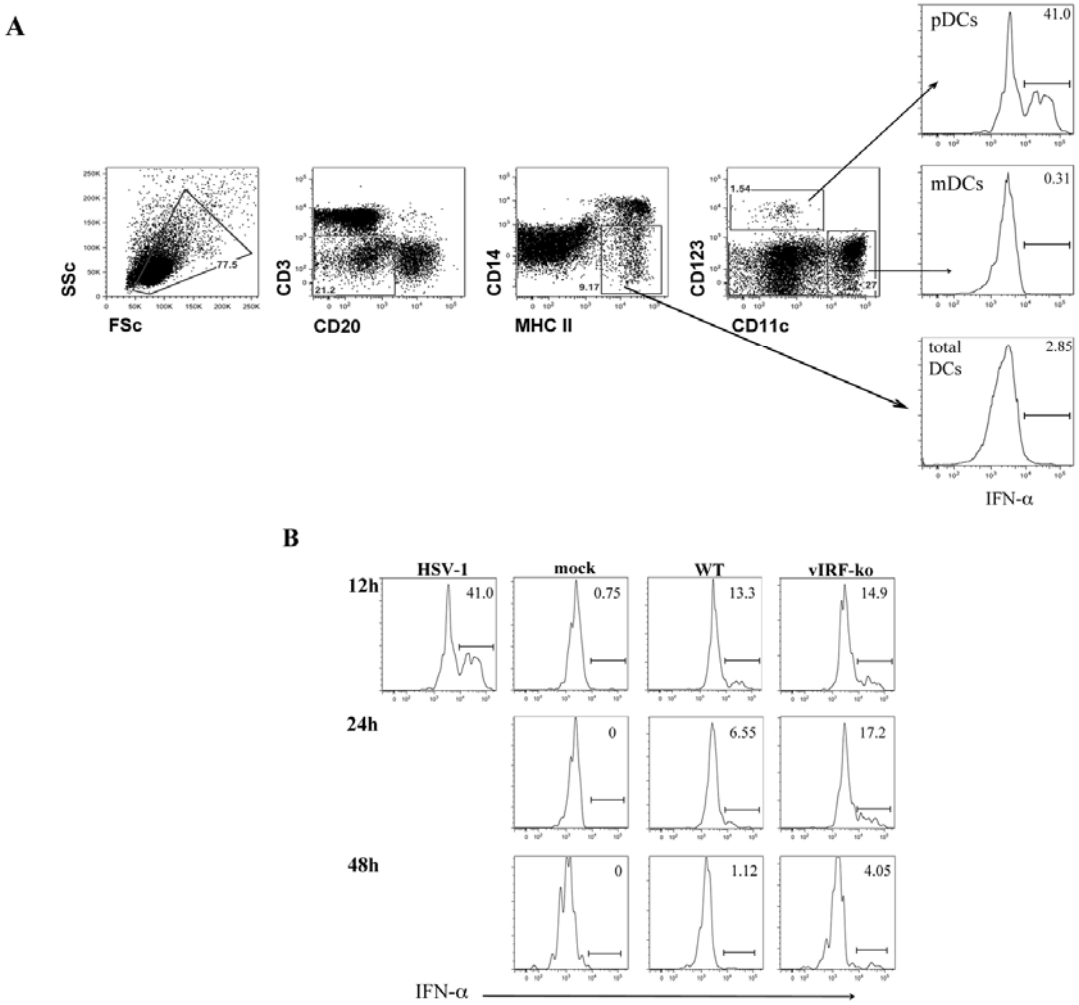
A
SSc
FSc
77.5
CD3
CD20
21.2
CD14
MHC II
9.17
CD123
CD11c
1.54
27
pDCs
41.0
mDCs
0.31
total
DCs
2.85
IFN-α
B
HSV-1
mock
WT
vIRF-ko
12h
41.0
0.75
13.3
14.9
24h
0
6.55
17.2
48h
0
1.12
4.05
IFN-α
C
% pDCs producing IFN-α
N.S.
p = 0.009
p = 0.10
RM 1
RM 2
RM 3
RM 4
RM 5
RM 6
WT
vIRF-ko
12
24
48
hours PI

FIGURE 2.8. Nuclear accumulation of IRF-3 is inhibited during RRV infection of RFs. Telomerized RFs (tRFs) were infected with WT_{BAC} RRV or vIRF-ko RRV (MOI=1). **(A)** Native cellular lysates (40ug) were run on a 7.5% polyacrylamide, non-denaturing gel, with 1% sodium deoxycholate in the cathode chamber. Proteins were transferred to a PVDF membrane, and probed for total cellular IRF-3 to distinguish monomeric and dimeric forms (α-hu IRF-3 pAb FL-423, Santa Cruz). **(B)** Data were analyzed using densitometry to quantify the amount of IRF-3 present in the dimeric form (slower migrating band), compared to the total IRF-3 within each lysate. Data is expressed as a percentage based on this ratio (% of IRF3 present in dimeric form), and presented as an average (± SEM) of 3 independent experiments. **(C)** A representative image of tRFs that were fixed and analyzed via indirect immunofluorescence for total cellular IRF-3 (α-hu IRF-3 mAb, clone SL012.1) at 6hpi (shown in red). Nuclei were detected using DAPI (blue). tRFs were transfected with Poly(IC) (10ug, 6h) as a positive control for IRF-3 activation/nuclear localization. Magnification, x400. (D) Cells were analyzed at time points indicated, and the percentage of cells expressing IRF-3 in the nucleus was calculated by counting ~200 cells in each sample. Data are represented as a mean of 5 separate experiments (± SEM). N.S., not significant. *, $p \leq 0.05$.

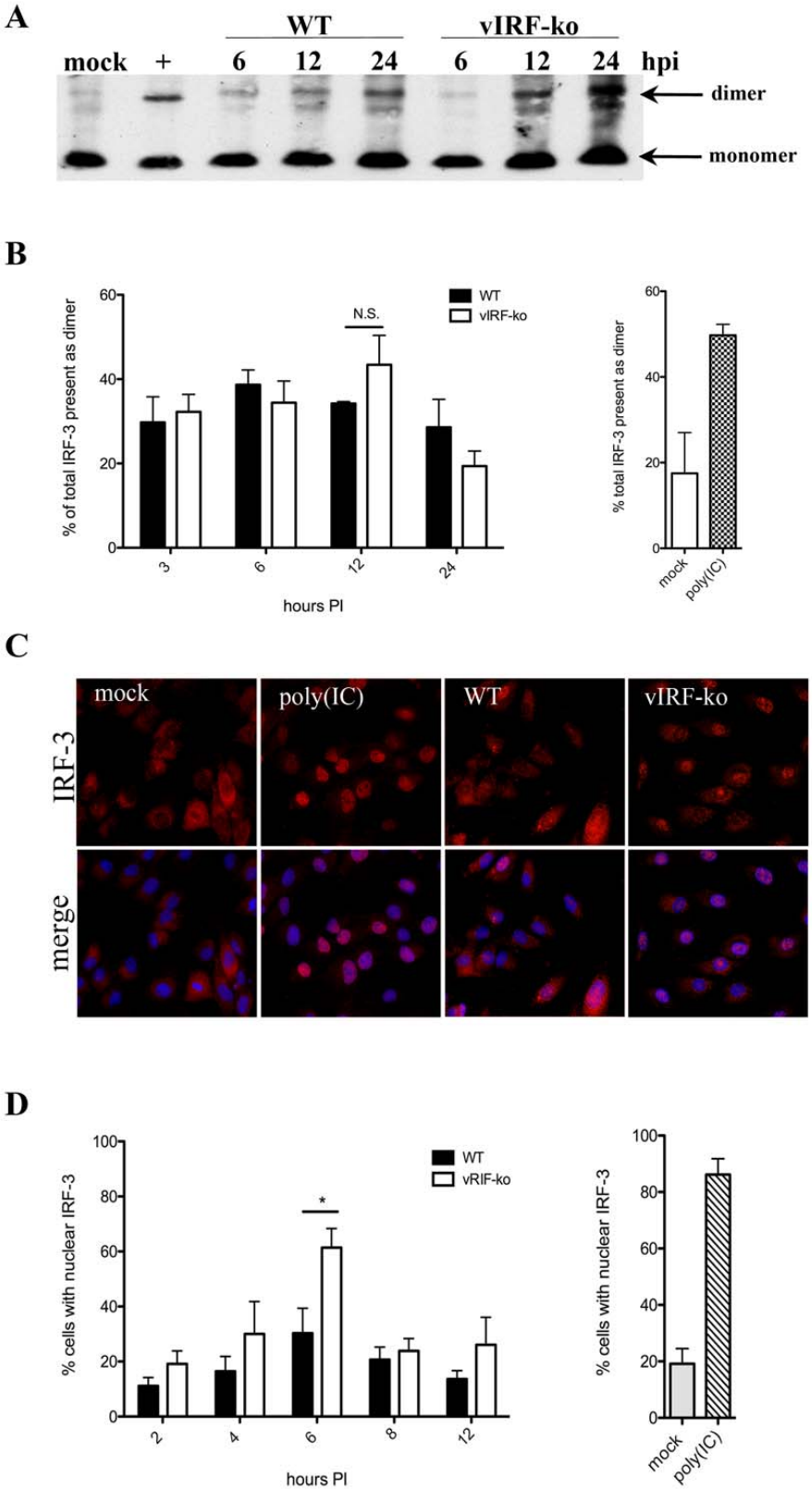
A
WT
vIRF-ko
mock
+
6
12
24
6
12
24
hpi
dimer
monomer
B
% of total IRF-3 present as dimer
WT
vIRF-ko
N.S.
hours PI
% total IRF-3 present as dimer
mock
poly(IC)
C
mock
poly(IC)
WT
vIRF-ko
IRF-3
merge
D
% cells with nuclear IRF-3
WT
vRIF-ko
*
hours PI
% cells with nuclear IRF-3
mock
poly(IC)

Table 2.1. Oligo pairs used for RT-PCR

ORF	oligo	oligo sequence (5'-3')
R6	R6 for	ATC GTT ACT CAC GCA AAT CTT
	R6 rev	TGA AGA CCA CGT TTG CAA ATG
R7	R7 for	TGG AAC AAA GTA ACT GCA GAT
	R7 rev	AAC TCA CTG ATT AAA CCA AGG
R8	R8 for	TGC TGC GAG ACA GGT CGT CAT
	R8 rev	CAG TAG TGC CGG AGG CCT GAT
R9	R9 for	TCC GAC GAG ATC AGC GTA C
	R9 rev	CCC TCG TTA TAC GCG ACC A
R10	R10 for	CGT TTC CCA ATT ATG ATT ATC
	R10 rev	CCG ATA CCG TCT CTC TTG ATC
R11	R11 for	AAC CGG TGC ACC GAC AGT CGC
	R11 rev	CCG TGT CCT CTC GAA AAC ATC
R12	R12 for	ATT GTT GCG ATA ATG ATA AGC
	R12 rev	CCG GTG GCA TCC GCT TCG TTA
R13	R13 for	ATG CAA CCT GTG GTT GCG TAC
	R13 rev	CTG GCG GCC CTG GCA TAT A
R3 (vMIP)	R3 for	CCT ATG GGC TCC ATG AGC
	R3 rev	ATC GTC AAT CAG GCT GCG
IFN-β	IFN-β for	CCT GAA GGC CAA GGA GTA CAG T
	IFN-β rev	GTT CCT GAG GAT TTC CAC TCT G
GAPDH	GAPDH for	GTG GAT ATT GTT GCC ATC AAT
	GAPDH rev	ATA CTT CTC ATG GTT CAC ACC

CHAPTER 3

Viral Interferon Regulatory factors are Critical for Delay of the Host Immune Response Against Rhesus Macaque Rhadinovirus

Bridget A. Robinson[1,2], Megan A. O'Connor[2], He Li[2], Flora Engelmann[2], Britt Poland[3], Richard Grant[3], Victor DeFilippis[2], Ryan D. Estep[2], Ilhem Messaoudi[1,2,3], Scott W. Wong[1,2,3]

1 Department of Molecular Microbiology and Immunology, Oregon Health & Science University, Portland, OR 97239

2 Vaccine and Gene Therapy Institute, Beaverton, OR 97006

3 SNBL USA, Everett, WA, 98203

4 Division of Pathobiology and Immunology, Oregon National Primate Research Center, Beaverton, OR 97006

* This manuscript was submitted to the *Journal of Virology* in July 2011

ABSTRACT

Kaposi's Sarcoma-associated herpesvirus (KSHV), and the closely related γ2-herpesvirus, rhesus macaque rhadinovirus (RRV), are the only known viruses to encode viral homologues of the cellular interferon (IFN) regulatory factors (IRFs). Recent characterization of a vIRF deletion clone of RRV (vIRF-ko RRV) demonstrated that vIRFs inhibit production of type I and type II IFN during RRV infection of peripheral blood mononuclear cells. Because the IFN response is a key component to a host's antiviral defenses, this study has investigated the role of vIRFs in viral replication and the development of the immune response during *in vivo* infection in rhesus macaques (RMs), the natural host of RRV. Experimental infection of RMs with vIRF-ko RRV resulted in decreased viral loads and diminished B cell hyperplasia, a characteristic pathology during acute RRV infection that often develops into more severe lymphoproliferative disorders in immune-compromised animals, similar to pathologies in KSHV-infected individuals. Moreover, *in vivo* infection with vIRF-ko RRV resulted in earlier and sustained production of pro-inflammatory cytokines and earlier induction of an anti-RRV T cell response, when compared to wildtype RRV infection. These findings demonstrate the broad impact vIRFs have on pathogenesis and the immune response *in vivo*, and are the first to validate the importance of vIRFs during *de novo* infection in the host.

INTRODUCTION

Kaposi's Sarcoma-associated Herpesvirus (KSHV) is a γ2-herpesvirus that was identified in 1994 as the cause of AIDS-related Kaposi's Sarcoma (KS) (41), one of the most common malignancies within HIV-infected individuals. KSHV establishes a persistent infection within B cells (8, 55) and is also associated with the malignant B cell disorders, multicentric Castleman's disease (MCD) and primary effusion lymphoma (PEL) (37, 220). Patients who develop MCD and PEL often have a poor outcome, especially if these B cell disorders develop before the introduction of HAART (33). Moreover, recent studies have documented an increase in KS within individuals on long-term HAART therapy, despite maintenance of low HIV viral loads and high CD4 T cell numbers (152). These findings now suggest that the development of KSHV-associated diseases is dependent on other unidentified factors and not simply just immune-suppression.

Studying host-pathogen interactions during *de novo* KSHV infection and disease pathogenesis has been hindered by the scarcity of animal models that recapitulate the human disease (40, 61, 192). Rhesus macaque rhadinovirus (RRV) is a closely related γ-herpesvirus (7, 54, 58, 207) that naturally infects rhesus macaques (RMs) and establishes latency within B cells (16). Moreover, RRV infection of RMs induces an acute hyperproliferation of B cells (69, 256) that often develops into diseases that resemble non-Hodgkin's lymphoma and MCD in immune-compromised animals (172). The striking similarities between KSHV and RRV-associated pathologies (16, 69, 172, 256), along with the nearly co-linear genomic organization (7, 207), make RRV

infection of RMs an ideal model for studying KSHV disease. Moreover, we have recently generated a bacterial artificial chromosome (BAC) clone of RRV_{17577} (WT_{BAC} RRV) (69) which allows us to target specific genes for deletion to effectively address their roles during infection.

KSHV and RRV encode a number of viral homologues of cellular genes involved in immune signaling, apoptosis, and cellular growth and differentiation. Accordingly, these viral homologues play critical roles in subverting the immune response (10). In particular, KSHV and RRV both encode a cluster of viral interferon regulatory factors (vIRFs) (7, 162, 201, 207) which bear significant homology with cellular IRFs, a family of transcription factors that coordinate induction of IFN and other pro-inflammatory cytokines during virus infection (94). RRV encodes eight vIRFs (ORFs R6-R13) within the same genomic region as the 4 vIRFs encoded within KSHV (7, 207). KSHV vIRF-1, -2, and -3 inhibit the induction of interferon (IFN) and subsequent IFN-induced signaling, via direct and indirect interference with cellular IRFs (31, 32, 76, 80, 82, 111, 142, 253, 267). Furthermore, KSHV vIRF-1 demonstrated tumorigenic potential in NIH3T3 cells and nude mice (82), and KSHV vIRF-1, -3, and -4 independently disrupt p53 function, inhibiting p53-induced apoptosis and/or cell cycle control (131, 164, 197, 212). Additional anti-apoptotic functions have also been attributed to KSHV vIRF-1 and vIRF-3. For example, KSHV vIRF-1 binds and sequesters the pro-apoptotic protein, Bim, reducing levels of apoptosis (46), and RNAi knockdown of KSHV vIRF-3 results in increased activity of effector caspases in KSHV-infected PEL cells (254). Collectively, these data demonstrate the functional breadth and diversity of

pathways/cellular functions that are targeted by the vIRFs, but these data do not adequately address the role of vIRFs during *in vivo* infection.

A recombinant clone of RRV lacking all 8 vIRFs (vIRF-ko RRV) was recently generated, and it was demonstrated that RRV vIRFs inhibit the induction of IFN during *de novo* RRV infection in peripheral blood mononuclear cells (PBMCs) and rhesus fibroblasts (Chapter 2). Specifically, infection of PBMCs with vIRF-ko RRV induced significantly more type I (α/β) and type II (γ) IFN compared to WT_{BAC} RRV. Moreover, increased production of IFN-α was most evident within plasmacytoid DCs, which are also important in TLR9-mediated detection of KSHV (250). Therefore, we hypothesized that vIRF-ko RRV infection of RMs would result in increased induction of IFN, promoting a more effective adaptive immune response and potentially limiting viral replication, persistence, and/or acute RRV-associated pathology. This hypothesis was tested by infecting immune-competent RMs with either WT_{BAC} RRV or vIRF-ko RRV, and comparing viral replication and the development of the adaptive immune response. These data show for the first time that vIRFs are critical for efficient viral growth, subversion of early cytokine production and delay of the T cell response, as well as important in development of acute B cell pathologies during RRV infection in RMs.

MATERIALS and METHODS

Cells and Virus. Primary rhesus fibroblasts (RFs) were grown in DMEM (Mediatech, Herndon, VA) supplemented with 10% fetal bovine serum (HyClone, Ogden, UT). Viruses used in these studies include wildtype BAC-derived RRV_{17577} (WT_{BAC} RRV_{17577}) (69), and vIRF-ko BAC-derived RRV_{17577} (vIRF-ko RRV) (Chapter 2). All virus stocks were purified through a 30% sorbitol cushion and re-suspended in PBS, and titers were determined using standard plaque assay in 1^{o} RFs.

Experimental Inoculation of Rhesus Macaques with BAC-generated WT RRV and vIRF-ko RRV. All aspects of the experimental animal studies were performed according to institutional guidelines for animal care and use at the Oregon National Primate Research Center, Beaverton, OR. Expanded specific pathogen-free (ESPF) [sero-negative for RRV, Simian Immunodeficiency Virus (SIV), Type D Simian Retrovirus (SRV), Herpesvirus Simiae (B virus), Simian T-lymphotropic Virus (STLV-1), Rhesus Cytomegalovirus (RCMV) and Simian Foamy Virus (SFV)], were inoculated intravenously with $5x10^6$ plaque-forming units (pfu). Six RMs were infected with BAC-derived WT RRV_{17577} (WT_{BAC} RRV_{17577}) (identification numbers 24807, 24896, 24996, 24916, 21963, and 26473), and 8 RMs were infected with BAC-derived vIRF-ko RRV (identification numbers 24875, 25491, 24799, 25000, 21287, 26448, 26937, and 25241). RM #25241 developed neurological symptoms unrelated to RRV infection at 16 dpi and underwent necropsy 2 days later, so there is no data for this animal after 14 dpi.

Blood was collected on days 1, 3, 5, and 7 post-infection (PI), then weekly for the duration of the experiment, to obtain peripheral blood mononuclear cells (PBMCs). Bronchoalveolar lavage (BAL) was also performed weekly to collect infiltrating immune cells in the lung. Pre-infection samples were collected 4 and 2 weeks prior to RRV infection, as well as on day 0, to establish baseline readings for each animal. PBMCs were isolated from whole blood using Histopaque (Sigma Aldrich, St Louis, MO) per the manufacturer's guidelines.

Viral loads, Persistence, and Detection of WT or vIRF-ko RRV in RMs. To measure viral loads in the infected RMs, total DNA was isolated from whole blood and genome copies were calculated using Taqman primers/probe specific for RRV ORF3 (vMIP): vMIP-1 (5' CCT ATG GGC TCC ATG AGC 3'), vMIP-2 (5' ATC GTC AAT CAG GCT GCG 3'), and vMIP probe (5' TCA TCT GCC GCC ACC CGG TTT A 3') as previously described (69).

The presence of infectious virus was measured via co-culture of PBMCs onto RFs, as described previously (69). Briefly, $2x10^5$ PBMCs were added in duplicate onto confluent monolayers of RFs, serially diluted 1:3 across a 24-well plate, and the presence of cytopathic effect (CPE), and scored accordingly (69). A maximum score of 5 indicates CPE was present at the highest dilution ($2.5x10^3$ PBMCs/well), and half scores represent CPE in only 1 of the replicate wells at that respective dilution. At peak days of viremia, co-culture supernatant/cells were collected and directly used as template to verify the presence of RRV via nested PCR for RRV ORF3 (vMIP). These

analyses utilized the vMIP-1 and vMIP-2 oligos (above) for the initial reaction, and vMIP-3 (5' CCC GAA CTC TGC TGT TTG 3') and vMIP-4 (5' TGG GAC GCT TGT CCA CCG 3') for the nested reaction. We also amplified a fragment within ORF R10 (vIRF) to differentiate WT and vIRF-ko RRV using the following oligos, R10-1 (5' CGT TTC CCA ATT ATG ATT ATC 3') and R10-2 (5' CCG ATA CCG TCT CTC TTG ATC 3').

To check for persistence of the RRV genome, CD20+ B cells were isolated via FACS from 5-10x10^7 PBMCs collected between 3 and 6 months PI. DNA was extracted from CD20+ cells with the PureGene DNA extraction kit, per manufacturer's protocol (Qiagen, Valencia, CA), and analyzed via nested PCR for RRV ORF3 (vMIP), as described above.

Measurement of T and B cell Proliferation. PBMCs and BAL cells were stained for extracellular markers CD8b (Beckman Coulter, Brea, CA) and CD4 (eBioscience, San Diego, CA) to define CD4 and CD8 T cell subsets, as well as CD20 (Biolegend, San Diego, CA), CD27 (eBioscience), and IgD (Southern Biotech, Birmingham, AL) to define naïve, marginal zone (MZ)-like, and memory B cell subsets, as described previously (154). Cells were subsequently fixed and permeabilized per manufacturer's protocol (BioLegend) and then stained for Ki67 (BD Pharmingen, San Jose, CA), a nuclear antigen involved in DNA replication. Samples were acquired on an LSRII instrument (BD), and data were analyzed using FlowJo software (TreeStar, Ashland, OR). Complete blood counts were obtained to determine peripheral lymphocyte

numbers for each RM, and used to convert the percentages of Ki67+ CD4 and CD8 T cells into total cell numbers/μl blood. Total lymphocyte counts in the BAL cannot be accurately determined, so only percentages of Ki67+ CD4 and CD8 T cells are shown. Baseline levels of Ki67+ cells were measured at two time points prior to RRV infection, averaged, and set to 1. Subsequent time points were then calculated and expressed as a fold change in Ki67+ population compared to baseline in each RM.

Intracellular Cytokine Staining. PBMCs and BAL cells were stimulated overnight with RRV at MOI=1, followed by a 6h incubation with Brefeldin A (Sigma, St Louis, MO) to block cytokine secretion. Stimulation with either an anti-CD3 antibody (FN18, Invitrogen Biosource, Carlsbad, CA) or Vaccinia Virus (VV) were used as positive and negative controls, respectively. Cells were then stained to define T cell populations using CD8b and CD4, followed by intracellular staining for IFN-γ and TNF-α. Cells were acquired on an LSR II (BD), and data analysis was carried out using FlowJo software. Final data is represented as the percentage of total CD4 or CD8 T cells that expressed IFN-γ after *ex vivo* stimulation with RRV, and non-specific responses (to VV stimulation) were subtracted for each time point. These non-specific responses never exceeded 0.5% of responding cells.

Measuring Serum RRV Antibodies. Plasma was collected from RMs weekly, and antiviral IgG levels were measured using a standard ELISA assay with plates coated with optimized amounts of RRV-infected cell lysate. Serial three-fold dilutions of RM plasma were incubated in triplicate on ELISA plates for 1 hr, washed, and signal was

detected and quantified using anti-IgG-HRP and chromagen substrate. Log-log transformation of the linear portion of the curve was then performed, and a value of 0.1 OD units was used as the cut-off point to calculate end point titers. Each plate included a positive control sample that allowed normalization of ELISA titers between assays, and a negative control sample to ensure the specificity of the assay conditions.

Luminex Analysis. To measure cytokines in infected RMs, plasma was collected from blood on 0, 1, 3, 5, 7 and 14 days post-infection (dpi). Twenty-three cytokines were simultaneously measured using the MILLIPLEX Non-human primate 23-plex cytokine kit (Millipore, Billerica, MA) in an initial survey. Later analyses focused on 8 cytokines (IFN-γ, IL-12/23 p40, IL-18, sCD40L, IL-1ra, IL-6, and IL-8) found to be differentially upregulated during RRV infection. Analysis was performed on the Luminex 100/200 system. Baseline readings of cytokines (pg/ml) in each macaque were measured on 0 dpi and subtracted from each time point for normalization of the data.

Measuring IFN-α in the Plasma. Plasma was obtained during the first 2 weeks post-RRV infection was stored at -80C until all time points could be assayed simultaneously. To assay for biologically active type I IFN, we generated an IFN-responsive cell line. RFs stably expressing human telomerase (tRFs) (121) were transduced with a replication defective lentivirus encoding firefly luciferase downstream of an IFN-stimulated response element (ISRE) (Qiagen). Transduced tRF-ISRE cell cultures were

then purified by exposure to 3ug/mL puromycin, resistance to which is conferred by the lentivirus.

To normalize luciferase expression, the tRF-ISRE cells were transiently transfected with pRL-SV40 (Promega, Madison, WI) 24h prior to assay using the Amaxa nucleofection system (Kit L, program T-30) (Lonza, Köln, Germany). Plasma was then added to the reporter cells for 6h, and firefly and renilla luciferase expression were individually measured in succession using the Dual-glo Luciferase Assay system, per the manufacturer's protocol (Promega). Data is represented as a ratio of firefly:renilla expression, and any background signal at 0 dpi was subtracted from all subsequent time points.

Statistical Analysis. Data were analyzed using GraphPad Instat (GraphPad Software, La Jolla, CA), and significant differences were determined via unpaired *t-test* for averaged data, and via the Mann-Whitney test for T cell responses and cytokine production, with values of $p \leq 0.05$ considered significant.

RESULTS

Infection of Rhesus Macaques with vIRF-ko RRV results in lower viral loads and earlier detection of lytic virus. Immune-competent, expanded specific pathogen free (ESPF) rhesus macaques (RMs) were infected intravenously with $5x10^6$ plaque forming units (pfu) of either WT_{BAC} RRV (*n* = 6), or vIRF-ko RRV (*n* = 8). The infected RMs were monitored for 10 weeks post-infection to assess viral loads, lymphocyte proliferation, anti-RRV T cell and antibody responses, and changes in plasma cytokine levels. RRV DNA was initially detected 14 days post-infection (dpi) in 3 animals, and viral loads peaked at 28 dpi in all 6 WT_{BAC} RRV-infected RMs (Fig. 3.1A). In contrast, viral loads in 6 of the 8 RMs infected with vIRF-ko RRV remained below the level of detection for this assay during the entire study (Fig. 3.1B). Interestingly, the remaining 2 vIRF-ko RRV-infected animals (RM# 21287 and 25241) presented with quantifiable viral loads at 7 dpi (Fig. 3.1B). Although peak viral loads in the 2 vIRF-ko RRV-infected animals were much lower than WT RRV-infected macaques, quantifiable viral loads were detected 1-2 weeks earlier than the WT_{BAC} RRV-infected RMs (Fig. 3.1A).

Co-culture methods were utilized to measure infectious virus and validate the presence of RRV. Peripheral blood mononuclear cells (PBMCs) from infected RMs were co-cultured with 1^o RFs weekly, monitored for cytopathic effect (CPE) and subsequently given a viremic score (69). Viremia was detected at 21 dpi and peaked at 28 dpi in all WT_{BAC} RRV-infected RMs (Fig. 3.1C), which correlated with viral loads (Fig. 3.1A). Although viral loads were below the limit of detection by qPCR in 6 of the vIRF-ko RRV-infected animals (Fig. 3.1B), we were able to detect the presence of infectious

virus in 7 of the vIRF-ko RRV infected animals, with peak viremic scores between 0.5-2.5 (Fig. 3.1D). Moreover, we were able to detect infectious virus at 7 dpi in 4 vIRF-ko RRV-infected animals, and in 7 animals at 14 dpi, 1-2weeks earlier than in WT_{BAC} RRV-infected animals (Fig. 3.1C). Earlier detection of infectious virus correlated with the earlier detection of viral loads in 2 of the vIRF-ko RRV-infected RMs (Fig. 3.1B). When co-culture wells reached full CPE on 14 and 28 dpi for the vIRF-ko and WT_{BAC} RRV-infected animals, respectively, cells and supernatant were collected and subjected to PCR analyses to verify the presence of RRV and differentiate between WT_{BAC} and vIRF-ko RRV. Nested PCR within RRV ORF3 (vMIP) verified that infectious virus recovered from the infected RMs was RRV (Fig. 3.1E), including the vIRF-ko RRV-infected animals with undetectable viral loads (Fig. 3.1B). Additionally, a second PCR analysis distinguished WT RRV from vIRF-ko RRV via amplification of a region within ORF R10 (vIRF), confirming that the vIRF-ko RRV infected animals only received the recombinant virus (Fig. 3.1E).

The vIRFs are important for the induction of the characteristic B cell hyperplasia during acute RRV infection. Acute B cell hyperplasia is a defining form of pathology observed early during RRV infection (69, 172, 256). In these studies, all 6 WT_{BAC} RRV-infected RMs developed B cell hyperplasia between 28-42 dpi, with peak numbers of $CD20^+$ B cells averaging 6-fold higher than day 0 (Fig. 3.2A). Furthermore, after this initial proliferative burst, WT_{BAC} RRV-infected RMs continued to maintain a higher baseline of total CD20+ cells at 56 and 63 dpi, compared to levels prior to infection ($p \leq 0.002$) (Fig. 3.2A). In contrast, the vIRF-ko-infected RMs experienced

only a modest increase (~ 2 fold) in total CD20+ B cells, with peak numbers significantly lower ($p < 0.05$) than WT_{BAC} RRV-infected RMs (Fig. 3.2A).

To further characterize the CD20+ population during this hyperplastic phase, we assessed the proliferative burst within naïve ($CD27^{neg}$, IgD^{pos}), marginal zone (MZ)-like ($CD27^{pos}$, IgD^{pos}), and memory ($CD27^{pos}$, IgD^{neg}) B cell populations by measuring changes in the expression of the proliferation marker Ki67 (183). Upon antigen encounter, naïve B cells simultaneously acquire memory markers and begin a robust proliferative burst. In WT_{BAC} RRV–infected RMs, the increase in total CD20+ B cell coincided with a distinct increase in Ki67+ memory B cells (Fig. 3.2B), but here were no obvious proliferative bursts within naïve or MZ-like B cell populations (data not shown). Thus, these observations suggest that B cell hyperplasia is driven by naive B cells converting into memory B cells. and potentially bystander proliferation of memory B cells, as well. Not surprisingly, there was a less significant increase in Ki67+ B cells in the vIRF-ko RRV-infected RMs (Fig. 3.2B and data not shown), which is in accordance with the lack of B cell hyperplasia in these animals.

Deletion of the vIRFs does not inhibit persistence of RRV. To examine whether deletion of the vIRFs would inhibit viral persistence of RRV within B cells, the main site of RRV persistence (16), nested PCR analysis was used to look for RRV DNA within a purified B cell population ($CD20^{+}$) at ≥3 months post-infection. These analyses confirmed the presence of RRV genomes within CD20+ B cells in both WT_{BAC}

and vIRF-ko RRV-infected RMs (Fig. 3.2C), indicating that vIRF-ko RRV can infect and persist within B cells, despite lower viral loads initially (Fig. 3.1).

Reduced T cell proliferation after infection with vIRF-ko RRV. T cells typically undergo a burst of proliferation following antigenic stimulation, which can be assessed by measuring changes in the frequency of Ki67+ cells (154). PBMCs were analyzed weekly to measure the kinetics and the magnitude of the CD4 and CD8 T cell proliferative response (Fig. 3.3A-D). T cell proliferation was detected in the blood of both WT_{BAC} and vIRF-ko RRV-infected RMs at 14 dpi, peaked between 28-35 dpi, and contracted by 49 dpi in both CD4 (Fig. 3.3A) and CD8 (Fig. 3.3B) subsets. Overall, however, T cell proliferation within the blood was less robust in the animals infected with vIRF-ko RRV (Fig. 3.3A and B). Simultaneously, proliferative T cell responses were also analyzed in the lung via bronchoalveolar lavage (BAL). Within the BAL, proliferation of CD4 and CD8 T cells was more temporally distinct than in the blood, with a marked increase in Ki67+ cells specifically at 35 dpi in both WT_{BAC} and vIRF-ko RRV-infected animals (Fig. 3.3C and D). Moreover, similar to responses in the blood, the level of T cell proliferation in the BAL of vIRF-ko infected animals was slightly lower than that of WT_{BAC} RRV infected animals (Fig. 3.3C and D).

Frequency of RRV-specific T cells is higher in the absence of vIRFs. To further characterize the T cell response, the frequency of RRV-specific CD4 and CD8 T cells was measured by intracellular cytokine staining following *ex vivo* stimulation with

RRV. Due to blood volume constraints, not every animal could be evaluated at all the time points.

Within the PBMCs, RRV-specific CD4 T cells were detected 7-14 days earlier in vIRF-ko RRV-infected RMs compared to WT_{BAC} RRV-infected animals (Fig. 3.4A and B). Specifically, 5 of the 6 vIRF-ko RRV-infected RMs analyzed had a measurable CD4 response in the blood on 7 dpi (Fig. 3.4B), whereas none of the WT_{BAC} RRV-infected RMs had a measured response (Fig 3.4A). Moreover, the peak median CD4 response occurred 7 dpi in the vIRF-ko RRV infected animals, but not until 21 dpi after WT_{BAC} RRV-infected RMs (Fig. 3.4A). Similarly, the CD8 response in the blood was also initiated at 7 dpi in the vIRF-ko RRV-infected RMs (Fig. 3.4D), while WT_{BAC} RRV-infected animals did not develop a CD8 response in the blood until 21 dpi (Fig. 3.4C).

The RRV-specific CD4 (Fig. 3.4E and F) and CD8 (Fig. 3.4G and H) T cell responses in the lung (BAL cells) were also detected 7 dpi in the vIRF-ko RRV-infected RMs, and the median response peaked at 21 dpi (Fig. 3.4F and H). Moreover, the responding T cell population persisted in BAL cells within the first 63 dpi, with 2-4% of CD4 T cells and 4-7% of CD8 T cells responding to RRV stimulation in the vIRF-ko RRV-infected animals (Fig. 3.4F and H). In WT_{BAC} RRV-infected animals, only 2 animals had measurable T cell responses on 7 dpi in BAL cells and persisted at 1-2% and 3-4% of CD4 (Fig. 3.4E) and CD8 (Fig. 3.4G) T cell populations, respectively. Overall, in comparison to WT_{BAC} RRV infection, there is earlier initiation of the anti-RRV T cell response in vIRF-ko RRV-infected RMs, most significant in the blood on 7 dpi (CD4, p

= 0.03; CD8, p = 0.07) (Fig. 3.4A-D). Likewise, the vIRF-ko RRV-infected RMs maintained higher median responses in the lung during the first 2 months post-RRV infection (Fig. 3.4E-H).

Similar antibody response in WT_{BAC} RRV and vIRF-ko RRV-infected RMs. To determine whether the RRV antibody response was also influenced by the vIRFs, plasma was collected weekly and assayed using an anti-RRV IgG ELISA. Interestingly, despite earlier detection of RRV via real-time PCR and in co-cultures (Fig. 3.1), and earlier T cell responses in the vIRF-ko RRV-infected RMs (Fig. 3.4), the anti-RRV IgG response in these animals displayed similar kinetics and magnitude as the WT_{BAC} RRV-infected RMs (Fig. 3.5). Peak antibody titers were reached at approximately 35 dpi, and maintained throughout 63 dpi in all the RMs in this study.

vIRFs disrupt early cytokine production during *de novo* RRV infection. The adaptive immune response is greatly influenced by the innate immune response. Therefore, innate cytokine production was assayed by measuring plasma levels of several key cytokines using a non-human primate (NHP)-specific luminex kit. To identify cytokines with differential expression patterns between WT and vIRF-ko RRV-infected RMs, plasma was initially analyzed from 4 WT_{BAC} and 4 vIRF-ko RRV-infected animals with the 23-plex NHP cytokine kit. Of the 23 cytokines measured, only 12 were present at quantifiable levels after RRV infection: G-CSF, IL-13, IL-15, IL-17, MCP-1 TGF-α, IL-12/23 p40, IL-18, IFN-γ, IL-1ra, sCD40L, and IL-8 (Fig. 3.6 and Fig. S3.1). The final 6 cytokines in that list demonstrated potential differences

between WT_{BAC} RRV and vIRF-ko RRV infection, and were further analyzed in all the animals in this study (Fig 3.6).

An increase in plasma levels of measured cytokines was detected 1 dpi in most of the RRV-infected animals in this study (Fig. 3.6). However, several cytokines were differentially expressed in WT_{BAC} and vIRF-ko RRV-infected RMs. Specifically, plasma levels of IFN-γ quickly peaked at 1 dpi in both groups, but levels of IFN-γ were maintained through the first 7 days only in the vIRF-ko RRV-infected animals (Fig. 3.6A and B). Peak levels of IL-12p40 were observed at 1 dpi in animals infected with vIRF-ko RRV (Fig 3.6D), whereas there was a delay in IL-12p40 production in the WT_{BAC} RRV-infected RMs, which peaked at 14 dpi (Fig 3.6C). Production of IL-1ra also occurred early (1-3 dpi), but demonstrated a second wave of production between 7-14 dpi only in the vIRF-ko RRV-infected animals (Fig. 3.6G and H). Levels of sCD40L were also quite different between vIRF-ko and WT_{BAC} RRV-infected RMs (Fig. 3.6I and J). Six of the seven vIRF-ko RRV-infected RMs has measureable sCD40L in the plasma at 1 dpi, and all 7 RMs had a measurable sCD40L response at 7 dpi (Fig 3.6J). The WT RRV-infected animals, however, showed minimal sCD40L production, even at 7 dpi (Fig. 3.6I). In total, these data demonstrate the importance of vIRFs in inhibiting early and sustained production of several Th1-specific and pro-inflammatory cytokines after RRV infection.

vIRFs inhibit production of IFN-alpha after RRV infection. In recent comparisons of WT_{BAC} RRV and vIRF-ko RRV, it was demonstrated that vIRFs play a role in

inhibiting production of type I IFN, particularly in plasmacytoid dendritic cells (pDCs) (Chapter 2). Therefore, to determine whether the vIRFs effectively inhibited IFN production during *in vivo* infection in the RM, we developed a type I IFN-responsive cell line to assay for the presence of biologically active IFN in the plasma of the infected RMs. Telomerized rhesus fibroblasts (tRFs) were generated to stably express firefly luciferase under the control of an IFN-stimulated response element (ISRE) in the promoter, tRF-ISRE cells. The tRF-ISRE cell line was demonstrated to be responsive to IFN-α stimulation in a dose-dependent manner (Fig. 3.7C). To standardize luciferase readings, tRF-ISRE cells were also transiently transfected with a plasmid constitutively expressing renilla luciferase 24h prior to addition of RM plasma. To normalize IFN-α responses in each animal, any background response measured at 0 dpi was subtracted from all subsequent time points. Type I IFN production was detected in six of the 8 vIRF-ko RRV-infected RMs at 1 dpi, and was maintained through the first 2 weeks post-infection (Fig. 3.7B). Additionally, there was an increase in the median response at 7 and 14 dpi, with all of the vIRF-ko RRV-infected RMs producing measurable IFN-α at the later time points (Fig. 3.7B). In contrast, IFN production was not detected in WT_{BAC} RRV-infected RMs until 7-14 dpi, and only in 3 of the 6 WT_{BAC} RRV-infected RMs, and at half the magnitude of the vIRF-ko RRV-infected animals (Fig. 3.7A-B).

DISCUSSION

Herpesviruses have evolved a number of strategies to overcome the innate immune response and evade the subsequent adaptive response (10, 237) in order to initiate a productive infection and establish latency. These immune evasion strategies include disruption of the interferon (IFN) response, cytokine/chemokine production and signaling, as well as interference with antigen processing and presentation. KSHV and RRV, in particular, are equipped with a set of unique immune evasion molecules, including viral interferon regulatory factors (vIRFs) (170). The data presented here demonstrate an inhibitory role for vIRFs in development of the immune response during primary RRV infection in the rhesus macaque (RM).

WT_{BAC} and vIRF-ko RRV share similar growth kinetics *in vitro* (Chapter 2); however, the significant reduction in viral loads detected following vIRF-ko infection of RMs clearly establishes a critical role for vIRFs during RRV infection *in vivo*. Despite the overall lower viral loads in the vIRF-ko RRV-infected RMs, we were able to detect RRV viral DNA in 2 RMs at 7 dpi, which was 1-2 weeks earlier than following WT_{BAC} RRV infection (Fig 3.1, (172)). Likewise, detection of infectious virus in the vIRF-ko RRV-infected RMs also peaked 2 weeks earlier. This demonstrates deletion of vIRFs did not completely inhibit viral replication in the RM, but rather that vIRF-ko RRV infection results in earlier lytic replication that is quickly brought under control, never reaching the same magnitude as in WT_{BAC} RRV infection. There are potentially multiple reasons for the differences in viral loads and lytic replication. One likely reason is that early and maintained production of type I IFN in the absence of vIRFs

induces an antiviral state that efficiently inhibits vIRF-ko RRV replication and limits viral spread. In fact, all of the vIRF-ko RRV-infected RMs generated a sustained IFN-α response in the first 14 dpi, whereas only 2 of the WT_{BAC} RRV-infected RMs (RM# 24896 and 26473) demonstrated sustained type I IFN production. Similarly, IFN-α production by pDCs was significantly higher following *in vitro* infection with vIRF-ko RRV compared to WT_{BAC} RRV infection (Chapter 2). Alternatively, earlier detection of lytic replication and decreased viral loads in vIRF-ko RRV-infected RMs could be due to the reduced ability of this virus to inhibit apoptosis. Deletion of the vIRFs may result in a potential increase in apoptotic, infected cells in the animal, which could increase clearance of these cells and effectively limit the detection of viral DNA. This hypothesis is supported by the observations that KSHV vIRF-1 and vIRF-3 have anti-apoptotic functions necessary for lytic viral production (46), and for *in vitro* survival of KSHV-infected PEL cells, respectively (254). A third possibility is the vIRFs are important for driving transcription of viral immune modulation genes needed to promote viral replication, as has been shown by the ability of KSHV vIRF-1 to drive transcription of vIL-6 (177). Therefore, it is likely that, along with inhibition of IFN, the RRV vIRFs are also targeting apoptotic signaling and viral gene transcription, which would collectively disrupt viral replication in the RM. These possibilities will need to be individually addressed in future studies.

An earlier induction of the anti-RRV T cell response was also detected in vIRF-ko RRV-infected RMs, which may also be contributing to decreased viral loads. Additionally, the increased IFN-α levels in the vIRF-ko RRV-infected animals may

serve to directly enhance the development and/or maintenance of memory T cells (100). Moreover, IFN-α can also enhance differentiation and activation of DCs (143), thereby promoting antigen presentation in the vIRF-ko RRV-infected RMs. Alternatively, earlier T cell responses in the vIRF-ko RRV infected animals may be mediated by direct vIRF modulation of antigen presentation. Indeed, previous studies have shown that KSHV vIRF-1 plays a role in inhibiting IFN-γ-induced expression of MHC-I (127). Moreover, data presented here and elsewhere show that RRV vIRFs also act upstream by inhibiting the production of IFN-γ [Fig. 3.6 and (Chapter 2)], a key cytokine in an effective Th1 immune response. Additionally, vIRF-ko RRV infection also resulted in earlier production of IL-12, another pivotal cytokine in the development of an antiviral adaptive immune response. Therefore, deletion of vIRFs results in increased and sustained type I IFN and Th1 cytokine responses, which collectively could orchestrate a more efficient T cell response in the vIRF-ko RRV infected RMs.

Deletion of the vIRFs resulted in significantly decreased B cell hyperplasia, a hallmark of RRV infection (172). One reason for the reduced B cell hyperplasia may be decreased viral loads in the vIRF-ko RRV-infected animals. However, the comparable anti-RRV IgG response in WT_{BAC} and vIRF-ko RRV-infected RMs suggests that hyperplastic B cells are not all RRV-specific. Indeed, B cell hyperplasia is thought to be driven by vIL-6, a functional homologue of its cellular counterpart (113, 171-173). Previous studies showed that KSHV vIRF-1 can bind to the KSHV vIL-6 promoter and drive its transcription in latently-infected PEL cells *in vitro* (177). Therefore, if vIL-6

expression is even partially controlled by any of the vIRF(s) during RRV infection, this may be the basis of the decreased B cell hyperplasia following vIRF-ko RRV infection.

In summary, the findings presented here demonstrate a broad impact of vIRFs on the immune response and pathogenesis during *in vivo* RRV infection. Further characterization of the molecular functions of RRV vIRFs will provide insight into novel antiviral therapies and advance our understanding of host-pathogen interactions during KSHV infection.

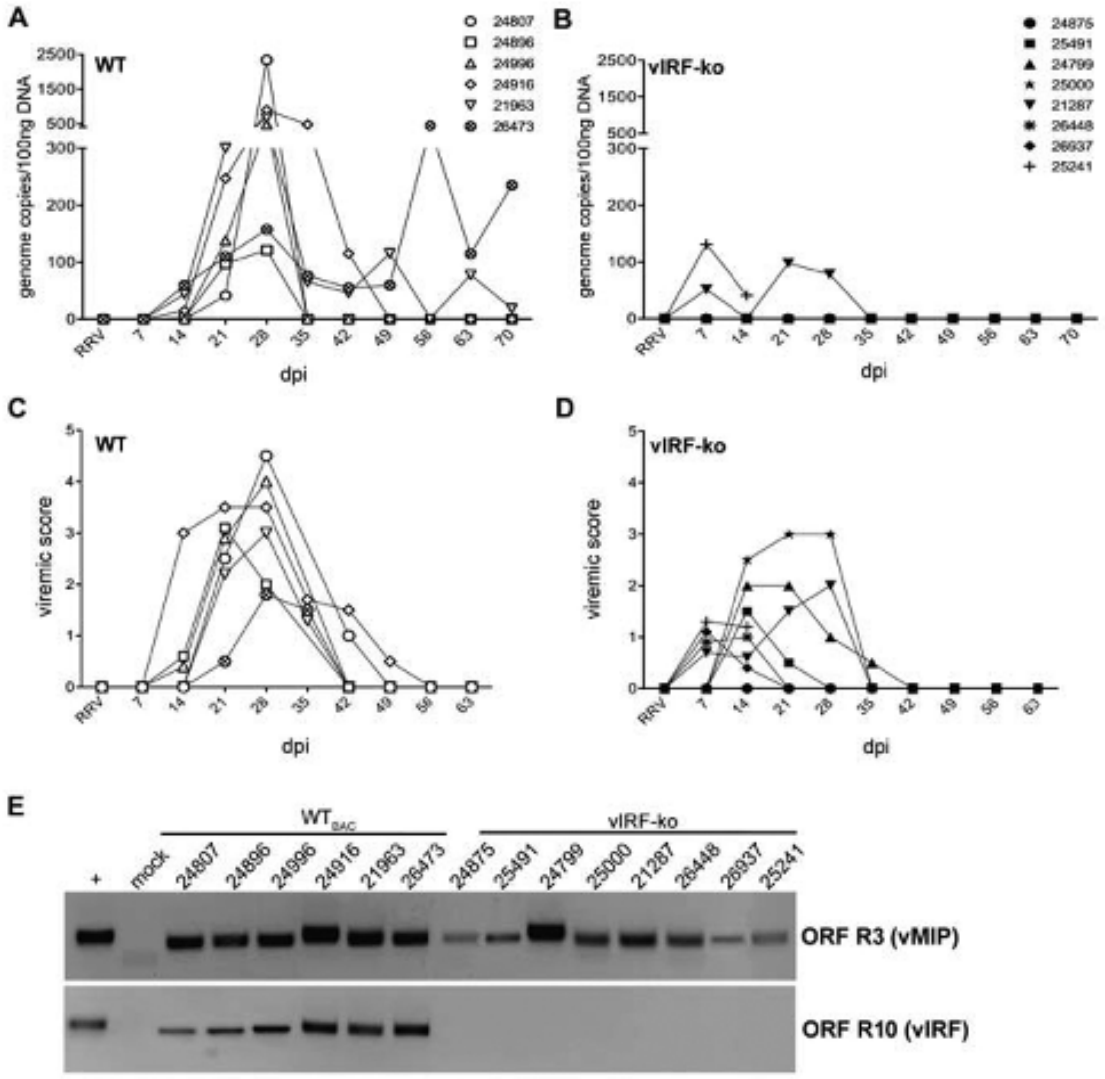

FIGURE 3.1. Detection of RRV DNA and measured lytic replication in RRV-infected RMs. Expanded specific pathogen free rhesus macaques (RM) were infected with $5x10^6$ pfu I.V. with WT_{BAC} RRV (n = 6) or vIRF-ko RRV (n = 8). Each RM is labeled with an ID number and an individual symbol. (A, B) Whole blood was analyzed weekly via qPCR to determine RRV viral loads. Data are represented as number of RRV genome copies/100ng DNA in each of the (A) WT_{BAC} RRV-infected RMs and the (B) vIRF-ko RRV-infected RMs. (C, D) $2x10^5$ PBMCs were co-cultured with confluent RFs, and serially diluted (1:3) across a 24well plate. Viremic score correlates with the highest dilution of PBMCs that resulted in CPE when co-cultured with RFs. A viremic score of 5 indicates the presence of CPE in wells with the highest dilution of PBMCs ($2.5x10^3$ PBMCs), and duplicate wells at each dilution equal 0.5. (E) The presence of RRV DNA in co-cultures was verified via nested PCR using primers for RRV ORF R3 (vMIP), as well as RRV ORF R10 (vIRF) to differentiate WT and vIRF-ko RRV.

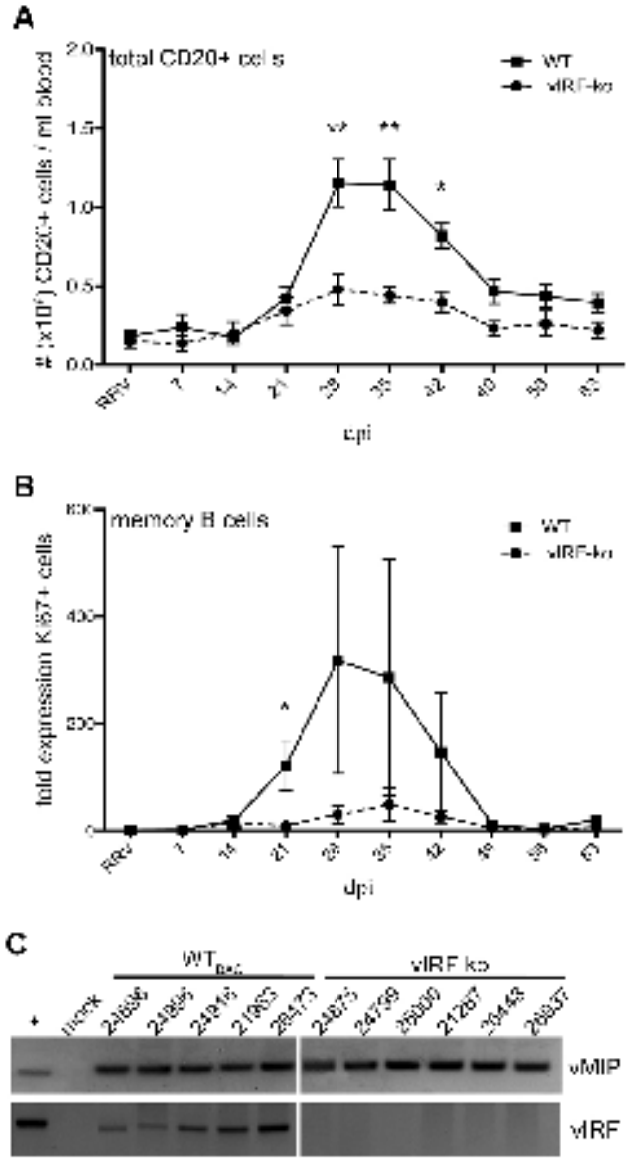

FIGURE 3.2. Decreased B cell hyperplasia in vIRF-ko RRV-infected RMs. (A) Absolute numbers of CD20+ cells were calculated using a complete blood count machine (Hemavet) to get total lymphocytes/ml blood, and this number was multiplied by the percentage of CD20+ lymphocytes. Data are represented as absolute number ($x10^6$) of CD20+ cells/ml peripheral blood, and are averaged (± SEM) among the WT RRV cohort (n = 6) and the vIRF-ko RRV cohort (n = 8). (B) The frequency of Ki67+ memory B cells is represented as an average (± SEM), with the baseline (pre-infection) Ki67+ population set to 1. (C) The presence of RRV DNA was analyzed within CD20+ cells between 3 and 6 months PI. CD20+ B cells were sorted from PBMCs, DNA was extracted, and PCR was performed to detect RRV ORF R3 (vMIP) to demonstrate RRV persistence within B cells in each animal. *, $p \leq .05$; **, $p \leq .01$.

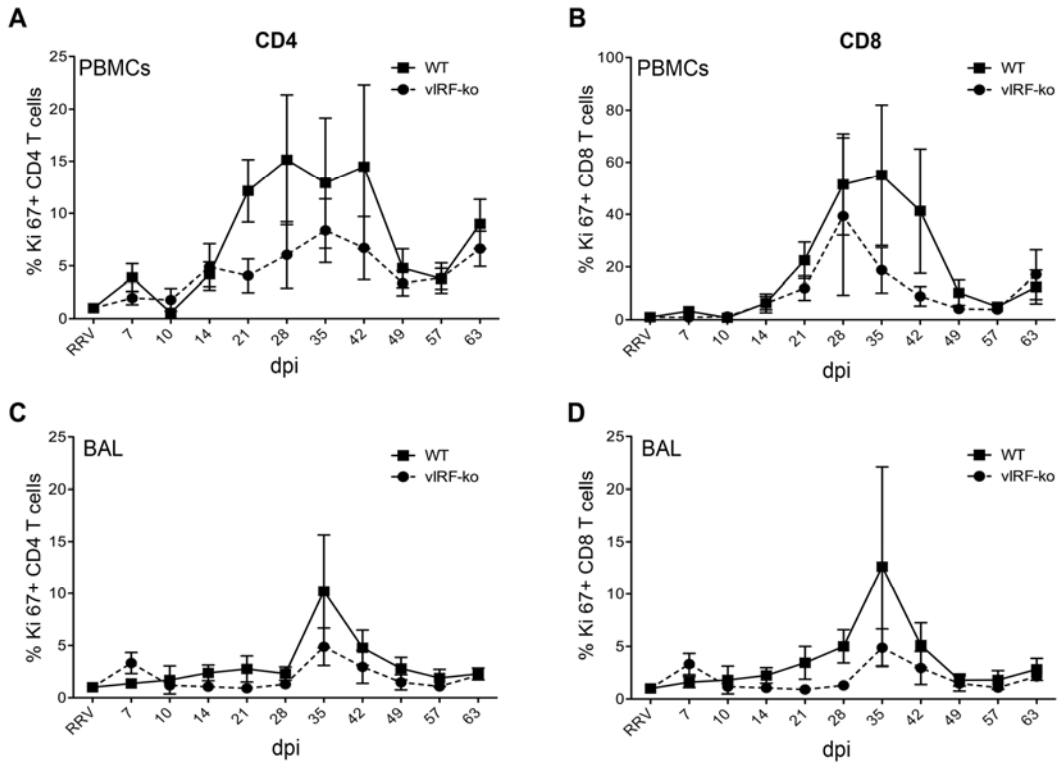

FIGURE 3.3. CD4 and CD8 T cell proliferation in peripheral blood and bronchoalveolar lavage. The frequency of proliferating (Ki67+) CD4 and CD8 T cells within (A,B) PBMCs and (C,D) BAL cells was determined by surface staining for CD4 and CD8, followed by intracellular cytokine staining for Ki67. Cells were then analyzed via flow cytometry. Pre-infection samples were used to establish a baseline of 1, and fold change in Ki67+ populations were calculated for each time point in each animal. Data are presented as an average (± SEM) among the WT_{BAC} RRV-infected RMs and the vIRF-ko RRV-infected RMs.

FIGURE 3.4. Infection of RMs with vIRF-ko RRV initiates an earlier RRV-specific T cell response. The frequency of RRV-specific T cells within (A-D) PBMCs and (E-H) BAL cells was determined after *ex vivo* stimulation with RRV (O/N), followed by surface staining for CD4 and CD8, and intracellular cytokine staining for IFN-γ and TNF-α. WT_{BAC} RRV-infected RMs are represented in graphs on the left, and vIRF-ko RRV-infected RMs are represented in graphs on the right. Baseline (pre-infection) and non-specific responses are subtracted from all time points. Median responses are displayed on the graphs as horizontal lines at each time point. Boxed time points indicate where significantly different responses were calculated between WT_{BAC} and vIRF-ko RRV-infected animals (7 dpi in CD4, $p = 0.03$; 7 dpi in CD8, $p = 0.07$).

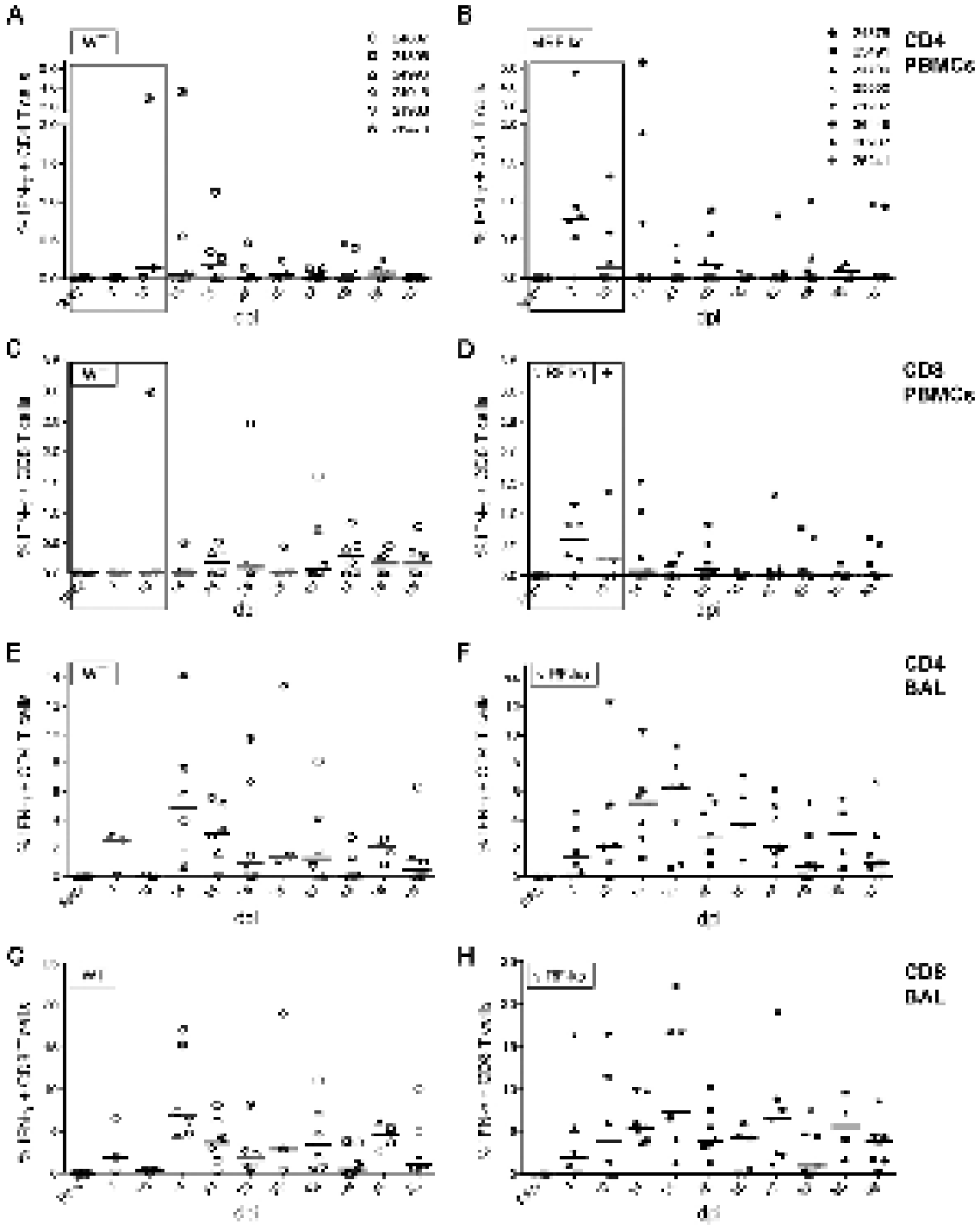
A
B
CD4
PBMCs
C
D
CD8
PBMCs
E
F
CD4
BAL
G
H
CD8
BAL

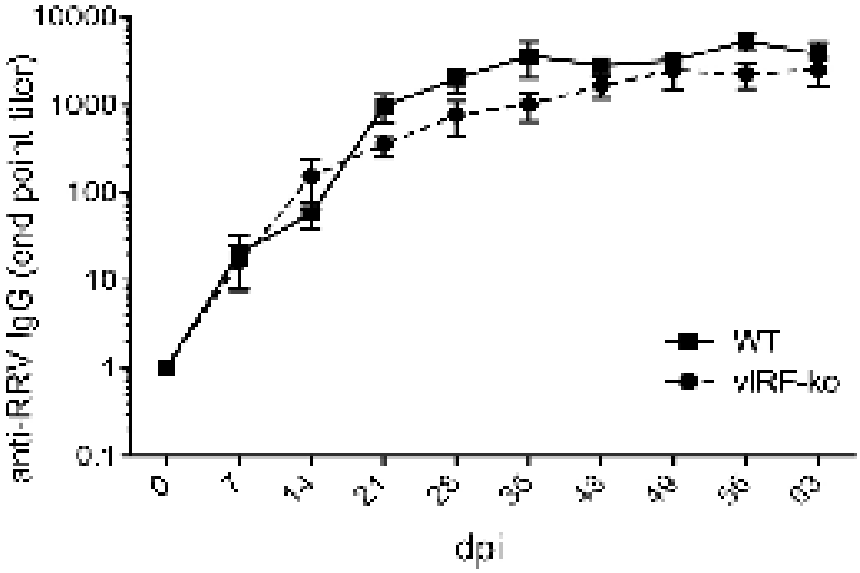

FIGURE 3.5. Anti-RRV IgG responses in RMs infected with WT_{BAC} RRV or vIRF-ko RRV. IgG end point titers were determined using an RRV-specific ELISA. Data are represented as an average (± SEM) of WT_{BAC} RRV-infected RMs (*n* = 6) and vIRF-ko RRV-infected RMs (*n* = 8).

FIGURE 3.6. Cytokine levels in the plasma of RRV-infected RMs. Plasma cytokine levels were measured using the rhesus-specific luminex kit: (A,B) IFN-γ, (C,D) IL-12p40, (E,F) IL-18, (G,H) IL-1ra, (I,J) sCD40L, and (K,L) IL-8. Cytokine responses measured prior to infection were subtracted from subsequent time points, and are graphed as pg/ml, with median responses represented as horizontal bars at each time point. WT_{BAC} RRV-infected RMs are graphed on the left, and vIRF-ko RRV-infected RMs are graphed on the right.

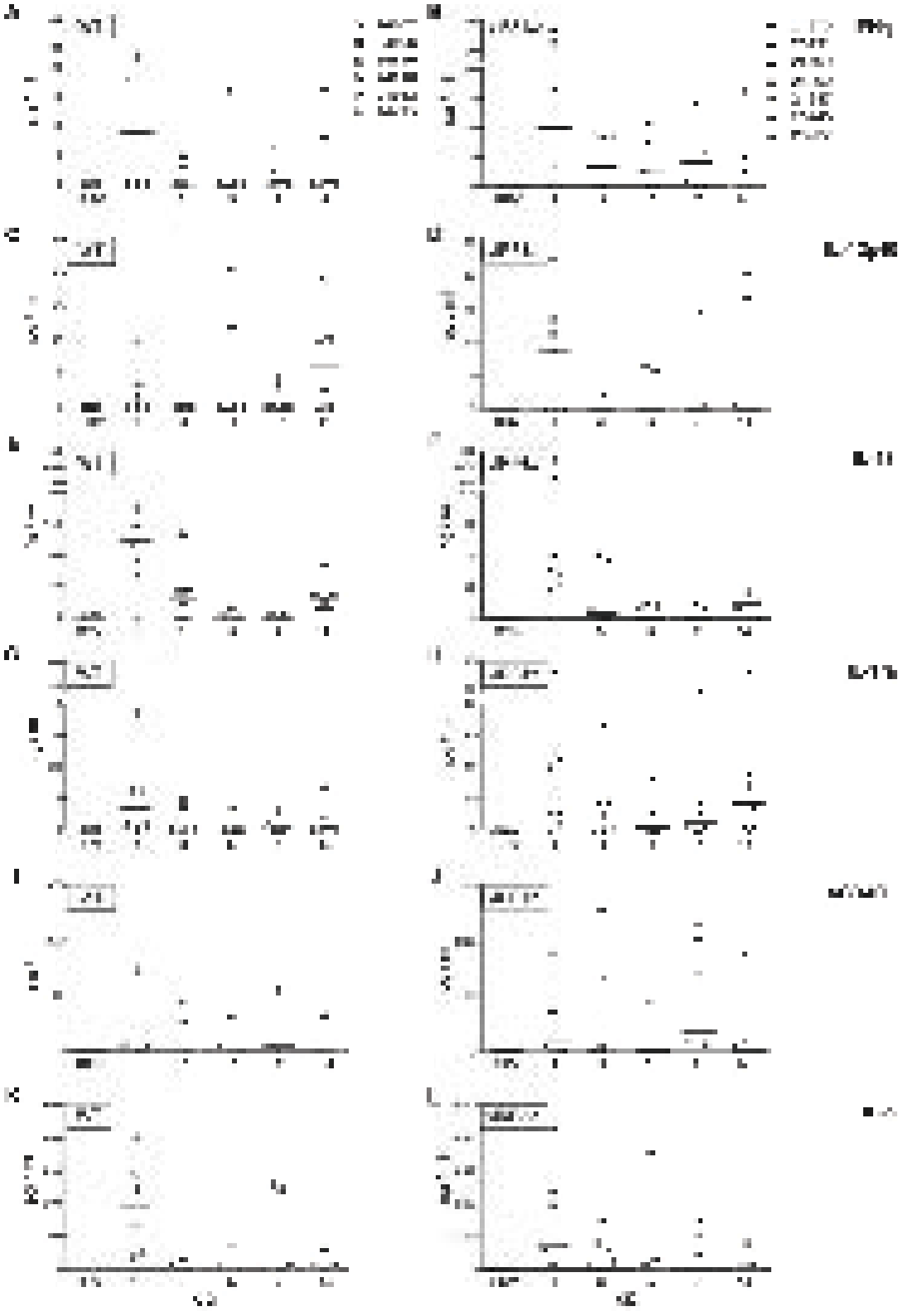

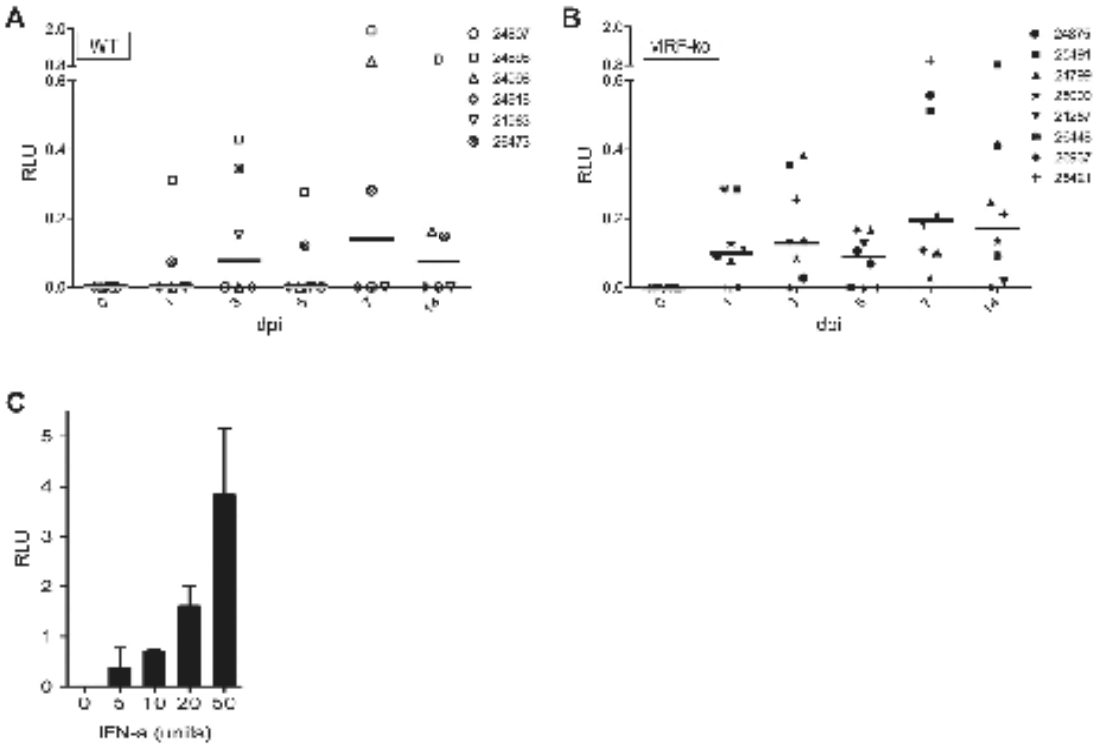

FIGURE 3.7. Measuring biologically active type I IFN in the plasma of RRV-infected RMs. Biologically active IFN-α was measured in plasma from (A) WT_{BAC} RRV-infected RMs or (B) vIRF-ko RRV-infected RMs. Plasma was added to tRF-ISRE for 6h, and firefly luciferase levels were normalized to renilla luciferase (constitutive promoter) for each sample. Baseline readings (pre-infection) were subtracted from all subsequent time points, and data are represented as relative luciferase units (RLU). (C) Recombinant human IFN-α2 (0-50units) was added to the tRF-ISRE cells for 6h, and normalized values are represented as RLU.

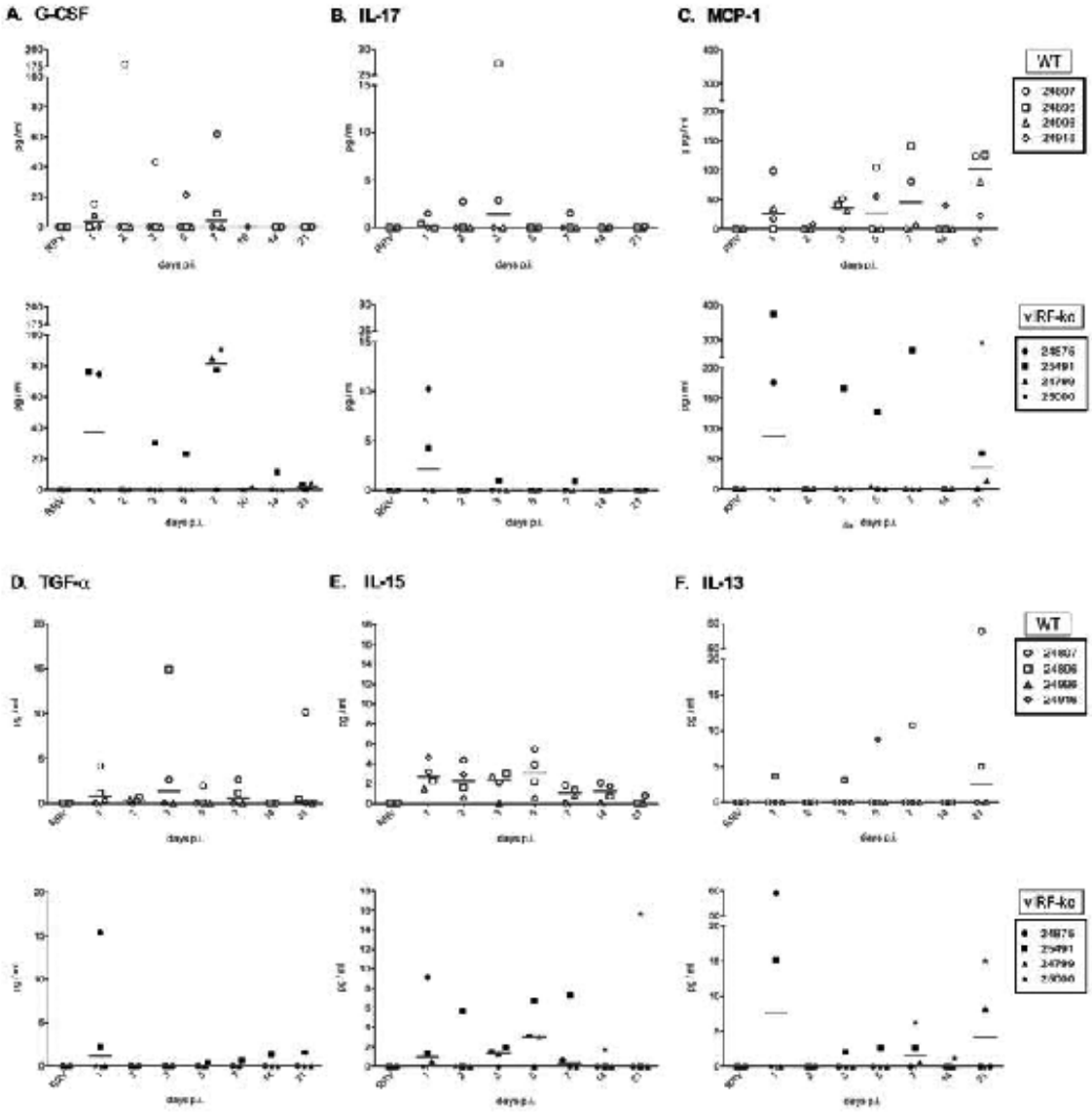

FIGURE S3.1. Cytokine levels in the plasma of RRV-infected RMs. Twenty-three cytokines were measured in the plasma of 4 WTBAC RRV-infected RMs (24807, 24896, 24996, 24916) and 4 vIRF-ko RRV-infected RMs (24875, 25491, 24799, 25000) in an initial screen using the 23-plex rhesus-specific luminex kit. In addition to the 6 cytokines listed in Fig. 3.6, (A) G-CSF, (B) IL-17, (C) MCP-1, (D) TGF-α, (E) IL-15, and (F) IL-13 were also present at measurable levels in these animals. Baseline levels of cytokines, measured prior to infection, were subtracted from each time point to normalize values. Data are graphed as pg/ml and median responses are represented with a horizontal bar.

CHAPTER 4

Individual RRV vIRFs interfere with the induction of IFN and IFN-mediated transcription

Bridget A Robinson[1,2], Scott W Wong* [1,2,3]

[1] Department of Molecular Microbiology and Immunology, Oregon Health & Science University, Portland, OR 97239

[2] Vaccine and Gene Therapy Institute, Beaverton, OR 97006

[3] Division of Pathobiology and Immunology, Oregon National Primate Research Center,
Beaverton, OR 97006

* Corresponding author
Vaccine and Gene Therapy Institute
505 NW 185th Ave
Beaverton, OR 97006
Phone: 503.690.5285
Fax: 503.418.2719
wongs@ohsu.edu

ABSTRACT

The eight viral interferon (IFN) regulatory factors (vIRFs) (ORFs R6-R13) encoded within rhesus macaque rhadinovirus (RRV) share unique similarity with cellular IRFs, key factors in IFN signaling pathways. Collectively, RRV vIRFs serve to inhibit induction of type I and type II IFNs, and dysregulate cellular IRF-3 during *de novo* RRV infection; recently demonstrated through utilization of a vIRF deletion mutant of RRV, vIRF-ko RRV. Moreover, vIRF-ko RRV infection of rhesus macaques further demonstrated the role of vIRFs in inhibiting the host immune response and promoting acute B cell hyperplasia. To characterize the eight RRV vIRFs, this study undertook a functional evaluation of each vIRF to assess their role in inhibiting induction of IFN and IFN-stimulated genes, as well as their transforming potential in NIH3T3 cells. Reporter assays revealed that R6 vIRF can independently inhibit transcription mediated by IRF-3 and by type I IFN. Additionally, stable expression of R7, R8, and R9 vIRFs resulted in increased growth potential and anchorage-independent growth in NIH3T3 cells, suggesting these viral proteins have oncogenic potential. This data supports the role of vIRFs in evasion of the IFN response and promoting tumorigenesis. Furthermore, our findings establish the 8 vIRFs have unique functions, and thus, will need to be individually analzyed during *de novo* RRV infection.

INTRODUCTION

The interferon (IFN) response is a key element in a host's innate immune defenses, and is coordinated by IFN regulatory factors (IRFs), a family of 9 transcription factors that orchestrate transcription of IFN and IFN-induced genes (94). Cellular IRF-3 is constitutively expressed in virtually all cell types and is crucial for potentiating the type I IFN (IFN-α/β) response during virus infection. Viruses are quickly detected by a number of pathogen recognition receptors (PRRs) present on the plasma membrane, the endosomal membrane and within the cytosol (125, 176). PRRs induce a signaling cascade that converges on C-terminal phosphorylation of IRF-3, which is normally maintained in the cytoplasm in a hypophosphorylated, inactive state (94). Phosphorylated IRF-3 homodimerizes and translocates into the nucleus, and through cooperation with other factors, including the transcription cofactor p300/CBP, it orchestrates transcription of type I IFNs, IFN-β (112, 138, 260) and IFNα_1 (84, 136). Type I IFNs are then charged with inducing transcription of 100s of genes that facilitate the antiviral response (101, 244).

Rhesus macaque rhadinovirus (RRV) and Kaposi's sarcoma-associated herpesvirus (KSHV) are two closely related γ-herpesviruses that infect rhesus macaques (RMs) and humans, respectively (7, 207). Immune-compromised persons infected with KSHV can develop distinct B cell malignancies, multicentric Castleman's disease (MCD) and primary effusion lymphoma (PEL) (89, 223). Similarly, RRV infection of immune-compromised RMs can also result in an MCD-like disease (172). Because RRV and KSHV establish life-long infections in their respective hosts and can cause a variety of

malignancies, these viruses encode a number of genes that both induce transformation and evade the host immune response (10). Of particular interest are the viral interferon regulatory factors (vIRFs), unique to KSHV and RRV (170). The vIRFs are so named because of their homology to cellular IRFs (162, 207).

RRV encodes 8 vIRFs (ORFs R6-R13) that share ~12-18% identity with human and rhesus cellular IRF-8, also known as IFN consensus sequence binding protein (ICSBP), and cellular IRF-9, also known as IFN-stimulated gene factor 3γ (ISGF3γ) (7, 207). IRF-9 is a necessary component of ISGF3, which drives transcription induced by type I IFN (239), and IRF-8 is important for transcription of IL-12 and IL-18, which promote an effective Th1 immune response (86, 205). Additionally, IRF-8 is also required for development of plasmacytoid dendritic cells (pDCs) (204), potent IFN-α producing cells in the blood. The eight RRV vIRFs also share ~25% AA identity with KSHV vIRF-1 (ORF K9), which functions to inhibit transcription mediated by IRF-1 and IRF-3, as well as type I and type II IFN (31, 76, 82, 127, 134, 162, 267). And in addition to directly disrupting IRF functions, KSHV vIRF-1 also inhibits apoptosis by disrupting TGF-β signaling (211), and through binding and inhibiting p53 (164), as well as another pro-apoptotic protein, Bim (46). In fact, vIRF-1 was the first KSHV protein that demonstrated transforming activity *in vivo* (82). However, it has been difficult to evaluate the function of vIRFs during *de novo* KSHV infection due to poor lytic replication, and inadequate *in vivo* models (169).

Recent characterization of a vIRF deletion mutant of RRV (vIRF-ko RRV) has provided evidence that vIRFs function to inhibit induction of type I and type II IFN during *de novo* infection (Chapter 2). Moreover, vIRF-ko RRV infection resulted in a significant increase in nuclear IRF-3 at early times post-infection, suggesting one or more vIRFs inhibits IRF-3 activation or nuclear translocation during WT RRV infection. Our current study focused on the functions of individual RRV vIRFs with regards to their ability to disrupt IRF-3 function and subsequent transcription, as well as IFN-mediated transcription. And because each vIRF likely has multiple functions, we also did an initial survey of their transforming potential *in vitro*. We've found that R7, R8 and R9 vIRFs demonstrate increased proliferative capacity and anchorage-independent growth in NIH3T3 cells, suggesting each has potential oncogenic capacity. Additionally, R6 vIRF significantly inhibited IFN-induced transcription and IRF-3-mediated transcription of genes driven by an IFN-stimulated response element (ISRE) in the promoter. Moreover, we also demonstrate that R6 vIRF can bind to cellular IRF-3, and this interaction increases following IRF-3 activation in the cell, providing a potential mechanism for the vIRF-mediated inhibition of transcription.

MATERIALS and METHODS

Cell culture, nucleofection, transfection and other reagents. Telomerized rhesus fibroblasts (tRFs) (121), and HEK293 endothelial cells were maintained in DMEM (Mediatech, Herndon, VA) supplemented with 10% FBS (HyClone, Ogden, UT). NIH 3T3 mouse fibroblasts were maintained in DMEM with 5% bovine calf serum (HyClone). For transient expression, vIRF expression plasmids was electroporated into tRFs with the AMAXA Nucleofector II (AMAXA Biosystems, Gaithersburg, MD) using cell line Kit L and the T-030 program. Two million cells were resuspended in 100 µl AMAXA solution with 1-2 µg of DNA. After electroporation, cells were recovered in 500 µl pre-warmed RPMI for 30min at 37°C and plated in complete DMEM. For luciferase assays and to generate stable vIRF clones, DNA was transfected into 293 or 3T3 cells using TransIT LT1 reagent per manufacturer's protocol (Mirus, Madison, WI).

Poly(I:C) (Sigma, St. Louis, MO) was resuspended in PBS and used to stimulate cells via transfection using TransIT LT1 (Mirus). Recombinant human IFN-α2 (PBL, Piscataway, NJ) was resuspended in PBS with 0.1% BSA, and stored at -70C. The Cantell strain of Sendai Virus (SeV) was purchased from Charles River (Wilmington, MA).

Cloning the 8 vIRFs for transient expression assays. Each of the 8 vIRFs (ORF R6-R13) were amplified from purified WT_{BAC} RRV_{17577} DNA, and engineered with a C-terminal hemagglutinin (HA) tag just upstream of the stop codon. Oligos used for

amplification are listed in Table 4.1. Each vIRF was cloned into pcDNA3.1(-), and each clone was subsequently sequenced to verify the HA epitope was in-frame and the vIRF sequence was correct. For transient expression of the HA-tagged vIRF constructs, 2ug plasmid DNA was nucleofected into $2x10^6$ tRFs.

Luciferase assays. To measure IRF-mediated transcription, we used a reporter plasmid encoding firefly luciferase driven by 5 ISRE in the promoter (pISRE-LUC) (Promega, Madison, WI). We normalized luciferase readings with dual, constitutive expression of renilla luciferase (pRL-SV40) (Promega). HEK293 cells were seeded into 24well plates and transfected overnight with 500ng DNA total [250ng pISRE-LUC/ 10ng pRL-SV40/ 50ng vIRF-HA-pcDNA3.1/ 190ng empty pcDNA3.1(-)]. Negative controls did not include any vIRF-HA-pcDNA3.1(-), but 240ng empty plasmid instead. Cells were then stimulated with IFN-α (50U) or transfected with poly(IC) (10ug) for 6h, and cells were transferred to 96well, white luminometer plates and reporter assays were conducted using the Dual-Glo Luciferase assay per protocol guidelines (Promega). Data was made relative to luciferase units recorded for empty vector plus stimulus [IFN or poly(IC)].

Immunofluorescene and microscopy. Telomerized RFs were grown on glass coverslips in 12-well plates, and fixed with 4% paraformaldehyde in PBS (20min, R.T.). Cells were then permeabilized and blocked in 5% normal goat serum (ngs)/0.1% Triton X in PBS (PBST) (1h, R.T.) prior to staining, and all subsequent steps were performed in 1% ngs/PBST. Cells on coverslips were stained with anti-human IRF-3 mAb (clone SL012.1) (BD Pharmingen, San Diego, CA) and then stained with anti-

mouse IgG-Texas Red (Vector Labs, Burlingame, CA). Subsequently, cells were also stained with anti-HA-FITC (Sigma), and nuclei/DNA were detected using Hoechst 33258 dye. Cells on coverslips were mounted onto slides using Vectashield (Vector Labs) and examined on a Zeiss Axio Imager.M1 microscope (Zeiss Imaging Solutions, Thornwood, NY). Images were acquired using a Zeiss Axiocam camera (MRm) with Axiovision software (version 4.6), and subsequently processed using Adobe Photoshop (Adobe Systems, San Jose, CA).

Co-Immunoprecipitation and immunoblotting. 1.5-2x10^6 tRFs were collected for co-immunoprecipitation (co-IP) in native lysis buffer (50mM Tris-Cl (pH 8), 150mM NaCl, 1% NP40) with freshly added protease inhibitors and phosphatase inhibitors (Sigma), and immunoprecipitated with IRF-3 pAb (FL-423) (Santa Cruz, Santa Cruz, CA) or HA mAb (Sigma) O/N at 4C. Subsequently, 20ul Protein A/G beads (Sigma) were incubated with IP lysates for 4h at 4C. Beads and lysate were then washed 4x with 1X PBS at 4C, and beads were then resuspended in 100ul RIPA buffer (1X PBS, 1% NP-40, 0.1% sodium dodecyl sulfate, 0.5% sodium deoxycholate) with freshly added protease and phosphatase inhibitors (Sigma).

Nuclear and cytoplasmic fractions were collected per kit protocol (NE-PER, ThermoScientific, Pittsburgh, PA). Protein concentrations for all lysates were measured by Bradford analysis, and equivalent amounts of protein samples were loaded and run on a 10% SDS-polyacrylamide gel and protein was transferred to nitrocellulose membrane via semi-dry transfer. Membranes were blocked with 5% BSA/TBST and

probed with anti-human IRF-3 pAb (FL-423) (Santa Cruz) or anti-HA mAb (Sigma). Secondary, anti-mouse or anti-rabbit, IgG-HRP antibody (Sigma) was subsequently added, and signal was detected via chemiluminescence.

Stable vIRF clones, proliferation and soft agarose assays. Transfected NIH 3T3 cells expressing each vIRF clone were selected for neomycin resistance using G418 (1 mg/ml), and individual cell clones were isolated using cylinders and maintained under G418 selection (0.75 mg/ml). To monitor proliferation and development of foci, $2.5x10^5$ NIH 3T3 cells, stably-expressing a single vIRF clone, were plated into each well of a 6-well dish and monitored for 6 days. Each day, one well was trypsinized and total live cells were counted. Development of foci was monitored and photographed at 7 days post-infection.

For soft agar assays, $5x10^3$ NIH 3T3 cells, stably transfected with a single RRV vIRF clone, were mixed in 1.5ml DMEM with 5% BCS and 0.3% melted agarose, then plated on top of a 1.5ml bottom layer of DMEM with 0.6% agarose in a 35mm dish. Each clone was plated in triplicate wells. Cells were fed with ~300μl medium every 3 days, and foci in soft agar were photographed after 3-4 weeks.

RNA extraction and RT-PCR. Stable NIH 3T3 clones of each RRV vIRF were harvested for RNA using an RNA extraction kit, per manufacturers protocol (Qiagen, Valencia, CA). RNA was treated with DNase (Promega), and expression of each

transcript was verified via RT-PCR using vIRF specific oligos, as previously published (Chapter 2, Table 2.1).

Statistical analyses. Data were analyzed using GraphPad Instat (GraphPad Software, La Jolla, CA), and significant differences were determined via unpaired *t-test*, with values of $p \leq 0.05$ considered significant.

RESULTS

Differential spatial expression of RRV vIRFs. To individually analyze each of the eight RRV vIRFs (ORF R6-R13), we generated vIRF clones within pcDNA3.1(-) with a C-terminal HA tag for ectopic expression in cell culture. Oligos used to make these constructs are listed in Table 4.1. Telomerized rhesus fibroblasts (tRFs) were nucleofected with individual vIRF constructs, and expression was examined 24h later. Expression of each vIRF was detected using an antibody against the HA epitope at the C terminus of the protein, and indirect immunofluorscence analysis (IFA) demonstrated that each vIRF displayed unique spatial expression within tRFs (Fig. 4.1). RRV vIRFs encoded by ORFs R9 and R13 did not demonstrate efficient expression in tRFs, but we were able to verify expression via IFA in HEK 293 cells (data not shown). R6 vIRF demonstrated cytoplasmic and nuclear expression, but was also expressed in a distinct punctate, perinuclear pattern in most cells (Fig. 4.1). R7 vIRF was expressed with a more diffuse pattern throughout the nucleus and cytoplasm, but also demonstrated unique, localized nuclear expression within about half of the cells (Fig. 4.1). R8, R10, and R11 vIRFs were expressed in the nucleus, as well as diffusely in the cytoplasm. The most unique expression pattern was demonstrated by R12 vIRF, which was expressed as small rings within the nucleus (Fig. 4.1, and inset). The disparate spatial expression patterns of the RRV vIRFs suggest each may be unique in its function. Simply stated, each vIRF may impact different cellular proteins/functions based upon the specific intracellular compartment in which each vIRF is expressed.

R6 vIRF inhibits IRF-3 mediated transcription. Through utilization of a recombinant clone of RRV with all 8 vIRFs deleted (vIRF-ko RRV), we've recently demonstrated that the vIRFs inhibit induction of IFN during RRV infection (Chapter 2). To further characterize which vIRFs mediate inhibition of IFN, we analyzed each vIRF clone for its ability to inhibit induction of IRF-3 mediated transcription. Using poly(I:C) as a stimulus for IRF-3 activation (87), we analyzed whether expression of individual vIRFs would inhibit IRF-3-mediated transcription in a reporter assay. HEK293 cells were transiently transfected with a firefly luciferase plasmid under the control of an IFN-stimulated response element (ISRE)-containing promoter, along with a single C-terminally HA-tagged vIRF clone. Overnight expression resulted in approximately 40% of the cells expressing each vIRF construct, as determined via immunofluorescence (data not shown). Cells were then transfected with poly(I:C) to induce activation of IRF-3, and firefly luciferase levels were normalized by dual expression of a constitutively expressed renilla luciferase. As a positive control for this assay, we included KSHV vIRF-1 (ORF K9), which inhibited IRF-3 mediated transcription by approximately 80% (Fig. 4.2). These analyses demonstrated each of the 8 RRV vIRFs has a distinct effect on IRF-3 mediated transcription. R6 vIRF expression resulted in the most significant inhibitory effect in this assay with 60% inhibition of poly(IC)-induced transcription (Fig. 4.2A). R9-R13 vIRFs each demonstrated moderate inhibition (20-40%), and R8 vIRF seemed to have no effect on IRF-3 mediated transcription in this assay. Interestingly, expression of R7 vIRF further enhanced IRF-3-induced transcription by 3-fold over poly(IC) stimulation alone (Fig. 4.2A).

To further analyze the inhibitory effect of R6 vIRF, we performed a dose-response curve and demonstrated increasing amounts of R6 vIRF correlated with increased inhibition of IRF-3-mediated transcription, upwards of 80% inhibition at the highest concentration (Fig. 4.2B). Furthermore, co-transfection of R6 and R7 vIRFs established the inhibitory effect mediated by R6 is dominant to the transcriptional enhancement mediated by R7 vIRF expression (Fig. 4.2C). These findings suggest that individual RRV vIRFs are sufficient for inhibiting or enhancing IRF-3 mediated transcription.

R6 vIRF inhibits IFN-induced transcription. Whether individual RRV vIRFs also impact the induction of IFN-mediated transcription was addressed in a similar reporter assay using pISRE-LUC to measure transcription, and pRL-SV40 for normalization. Cells were transfected with reporter plasmids and a single vIRF-HA construct overnight, then stimulated with recombinant IFN-α2 for 6h prior to analysis. KSHV vIRF-1 (ORF K9) was used as a positive control for inhibition of IFN-stimulated transcription (31, 82, 134) (Fig. 4.3A). Similar to KSHV vIRF-1, R6 vIRF expression resulted in 50% inhibition of IFN-mediated transcription (Fig. 4.3A). The inhibition mediated by R6 was shown to be dose-dependent, but increasing the amount of R6 expression vector did not increase inhibition more than 50% (Fig. 4.3B). Overall, the remaining RRV vIRFs demonstrated a less dramatic effect (0-25% inhibition) on IFN-stimulated transcription (Fig. 4.3A). R7 vIRF expression showed no inhibition, but rather a slight increase in IFN-mediated transcription in these assays (Fig. 4.3A).

Moreover, even in the absence of a stimulus (IFN or poly(IC)), expression of R7 vIRF still enhanced transcription of ISRE-driven genes over the control (data not shown).

R6 vIRF interacts with cellular IRF-3. Pathogen recognition results in a signaling cascade that converges on the activation of IRF-3 and induction of type I IFN (125). Since R6 vIRF can independently inhibit this pathway (Fig. 4.2), the question remained as to whether R6 vIRF may be imparting this inhibitory effect through interactions with cellular IRF-3. tRFs were transfected with HA-tagged R6 or R7 vIRF clones and native cellular lysates were collected 48h later, immunoprecipitated (IP'd) with an IRF-3 or HA antibody, and analyzed via SDS-PAGE and western. These analyses demonstrated that R6-HA co-immunoprecipitates with cellular IRF-3 when expressed in tRFs. This interaction appears to be specific for R6 vIRF, as R7-HA was not pulled down with IRF-3 in this same assay (Fig. 4.4A).

To further analyze the interaction between R6 vIRF and IRF-3, immunofluorescence microscopy was used to examine their co-localization in tRFs transiently transfected with R6-HA vIRF. In unstimulated cells, IRF-3 is mainly expressed within the cytoplasm, as demonstrated by tRFs expressed with pEGFP (Fig. 4.4B). Likewise, transfection of R6 vIRF or R7 vIRF does not remarkably alter expression of cellular IRF-3, and R6 vIRF is expressed with some co-localization with cellular IRF-3 in tRFs (Fig. 4.4B). When cells are stimulated with poly(IC), IRF-3 becomes activated and is more readily detected in the nucleus (Fig. 4.4B). Moreover, there is increased co-localization of R6 vIRF and cellular IRF-3 within the nucleus and cytoplasm following

poly(IC) stimulation (Fig. 4.4B). Conversely, co-localization is not apparent between R7 vIRF and cellular IRF-3, regardless of poly(IC) stimulation (Fig. 4.4B). Also of note, vIRF expression did not ablate nuclear localization of IRF-3 following poly(IC) stimulation, nor did the stimulation result in a dramatic change in vIRF expression, as both R6 and R7 vIRFs were still detected within both the cytoplasm and nucleus. These results demonstrate that R6 vIRF, but not R7 vIRF, interacts and co-localizes with cellular IRF-3, and this interaction seems to be enhanced following an IRF-3-activating stimulus [poly(IC)].

Although there was an apparent increase in interaction between R6 vIRF and IRF-3 following poly(IC) stimulation, it was difficult to determine if there was any change in localized expression of the R6 vIRF. Therefore, we analyzed expression of R6 vIRF and cellular IRF-3 in nuclear and cytoplasmic lysates for a more quantified analysis of spatial expression (Fig. 4.4C). In unstimulated tRFs, cellular IRF-3 is expressed mainly in the cytoplasm (Fig. 4.4C), as we have shown via immunofluorescence, as well (Fig. 4.4B). Following infection with Sendai Virus (SeV), IRF-3 becomes activated and moves into the nucleus (Fig. 4.4C), similar to what is seen after poly(IC) stimulation (Fig. 4.4B). In In unstimulated tRFs, the majority of R6 vIRF is expressed in the nucleus, but following IRF-3 activation via SeV infection, an increased portion of R6 vIRF was expressed within the cytosol (Fig. 4.4C). The whole of these data demonstrate that R6 vIRF binds to cellular IRF-3, and their co-localization is enhanced following IRF-3 stimulation. Moreover, cytoplasmic expression of R6 vIRF is also increased following IRF-3-activating stimulus [poly(IC) or SeV infection], suggesting

the interaction between R6 vIRF and IRF-3 may be enhanced within the cytosol (Fig. 4.2).

Individual vIRFs have transforming potential. To further examine the function(s) of the RRV vIRFs, we generated stable clones within NIH 3T3 cells to assess transforming potential of individual vIRFs within these cells. We also generated a stable clone of KSHV vIRF-1 (ORF K9) as a positive control, because its transforming potential has already been established within this system (82, 134). Expression of each stable 3T3 vIRF clone was verified via RT-PCR (data not shown). Transformative properties include uncontrolled proliferation, loss of contact inhibition, and anchorage-independent growth. So, to initially assess these properties, we monitored proliferation of each of the stable vIRF clones over a 6d period. Stably expressing 3T3 clones were plated at equal densities on day 0, and counted on each day thereafter. This analysis demonstrated a significant increase in cellular proliferation in R8 vIRF stably expressing cells (>2-fold higher than empty pcDNA3.1), most evident between 3-6d after cells were seeded (Fig. 4.5A). Additionally, vIRFs encoded by R7, R9, and R12, as well as KSHV vIRF-1 (K9), also demonstrated an increase in growth kinetics between 3-6d, but proliferation was not significantly higher than cells expressing empty vector (Fig. 4.5A). Differentially, R0 and R12 vIRFs demonstrated proliferation kinetics similar to that of control cells, and expression of R11 vIRF induced an increase in cell growth at day 4, but this proliferation was quickly attenuated at day 5 (Fig. 4.5A). Proliferation was sustained throughout the 6d time course in cells expressing R6, R7, R8, and R9 vIRFs. Additionally, after a week in culture, cells stably expressing R7

vIRF clones developed foci in the 3T3 monolayer (Fig. 4.5B). However, further analysis of the other 7 vIRF clones demonstrated that increased proliferative capacity did not always correlate with foci formation, as demonstrated by the lack of foci formation in the cells expressing R8 and R9 vIRF (data not shown). RRV vIRF clones that did not enhance proliferative capacity also did not promote foci formation, as demonstrated by R12 vIRF (Fig. 4.5B). The increased growth potential of 3T3 clones expressing R6, R7, R8, and R9 vIRFs, as well as the development of foci in R7 vIRF-expressing cells, demonstrate that expression of specific vIRFs results in a loss of contact inhibition.

Anchorage-independent growth, another common characteristic in transformed cells, was assayed by plating single cell suspensions within soft agarose and monitoring development of foci. Cells from each stable vIRF expression clone were mixed with soft agarose medium and complete medium, and monitored over the course of 4 weeks. For positive controls, we included a constitutively active Ras (V12Ras), a known oncogenic protein, as well as KSHV vIRF-1 (ORF K9), both of which demonstrate tumorigenic properties (82, 186) (Fig. 4.5C). We noted the formation of foci within clones expressing R7, R8, and R9 vIRFs after 4 weeks in soft agar medium (Fig. 4.5C). Examination of ~100 individual cells in each vIRF expressing 3T3 clone, we noted expression of R7, R8, and R9 vIRFs resulted in anchorage-independent growth 33-44% of the time, versus ~1% in cells expressing empty vector (Table 4.2). Likewise, the remaining 5 vIRFs did not display any anchorage independent growth, and behaved similarly to cells expressing empty vector (Fig. 4.5C, Table 4.2). These data

demonstrate that R7, R8, and R9 vIRFs have varying degrees of transforming potential in NIH 3T3 cells *in vitro.*

DISCUSSION

KSHV and RRV have pirated a number of cellular genes, including the viral IRFs (vIRFs), that functionally disrupt innate and adaptive immune responses (10, 170). Due to their sequence similarity with cellular IRFs, it was hypothesized that vIRFs inhibit the functions of IRFs, including IFN signaling. Indeed, 3 of the 4 KSHV vIRFs disrupt IRF functions *in vitro*, and thus, inhibit the induction of IFN and IFN-induced transcription (170). Moreover, initial studies of a vIRF deletion mutant of RRV (vIRF-ko RRV) demonstrated the vIRFs collectively inhibit induction of type I and type II IFN during *de novo* infection (Chapter 2). Therefore, to understand the function of each of the eight RRV vIRFs, we utilized reporter assays to induce ISRE-driven gene expression via IRF-3 activation [poly(IC) or SeV infection] or IFN-induced signaling. We have demonstrated that expression of individual RRV vIRFs inhibited IRF-3 mediated transcription between 20-60% in our reporter assays, with R6 vIRF demonstrating the most significant inhibition. Moreover, we've also demonstrated R6 vIRF binds to cellular IRF-3, suggesting this interaction could potentially serve to disrupt nuclear accumulation of IRF-3 and inhibit subsequent transcription. Additionally, expression of R6 vIRF also inhibited IFN-α-induced transcription, suggesting R6 vIRF functions to inhibit this pathway in a capacity independent of IRF-3 inhibition, or potentially disrupts another cellular function common to both pathways. The inhibitory nature of the RRV vIRFs is similar to that of KSHV vIRF-1, which can independently inhibit induction of IFN-β, as well as transcription of genes induced by type I and type II IFN signaling (76, 82, 127, 134, 267). KSHV vIRF-1 functions via binding and sequestering the transcriptional cofactor, p300/CBP, which is necessary for

IRF-3 mediated transcription (31, 133, 137, 210). Likewise, KSHV vIRF-1 may function in a similar manner to inhibit IFN-induced transcription, as deletion of the p300-binding region on vIRF-1 eliminated its inhibitory effect on IFN signaling (127). Whether R6 vIRF functionally inhibits transcription via binding to IRF-3, or whether R6 vIRF employs disparate functions to inhibit IRF-3 and IFN-mediated transcription will need to be explored further.

Of interest, R7 vIRF expression consistently increased poly(IC)-induced transcription in our reporter assay by 2.5 fold over poly(IC) stimulation alone (Fig. 4.2). Likewise, in the absence of a stimulus, R7 vIRF expression also stimulated the ISRE promoter approximately 3-fold over unstimulated, mock cells (data not shown), suggesting R7 vIRF enhances transcription independent of activated IRF-3. There is evidence that KSHV vIRF-3 can enhance IRF-3 and IRF-7 mediated transcription when it's binding to these IRFs at the promoter (140). More recently, KSHV vIRF-3 has been shown to bind to Myc modulator 1 (MM1-α), a c-Myc suppressor, resulting in uncontrolled growth and differentiation mediated by unchecked transcription of c-Myc regulated genes (141). KSHV vIRF-1 is also able to stimulate transcription, but does so more directly, via binding to a viral promoter driving transcription of modulator of immune recognition 1 (MIR1/ORF K3), viral dihydrofolate reductase (vDHFR/ORF 2) and viral IL-6 (vIL-6/ORF K2) (177). RRV and KSHV vIL-6 similarly function to induce proliferation of B cells *in vitro* (99, 113), and vIL-6 is hypothesized to be a key component in the development of B cell malignances in KSHV-infected persons (11, 179) and RRV-infected RMs (171). There are two ISRE-like elements within the vIL-6

promoter that confer responsiveness to type I IFN (42). Therefore, R7 vIRF may be enhancing cellular IRF functions to drive transcription of IFN to indirectly increase transcription of vIL-6, effectively promoting cellular proliferation during infection. Interestingly, R7 vIRF expression also resulted in increased growth potential and anchorage independent growth when stably expressed in NIH3T3 cells. Although the mechanism of transformation in these analyses is independent of other viral genes, our data suggest R7 vIRF possesses pro-oncogenic properties that may be related to its enhancement of transcription of target genes, which could potentially also include other RRV genes.

We've demonstrated that individual vIRFs can inhibit or enhance induction of IFN and IFN-induced transcription, and these roles may be linked to transforming potential of specific vIRFs. These data correlate with recent findings demonstrating that deletion of the eight vIRFs results in an increase in IFN production and initiation of an earlier adaptive immune response during *de novo* RRV infection (Chapters 2 and 3). Additionally, the distinct spatial expression of each of the vIRFs could also be an indication to their function(s) during infection. Future analyses will focus on individual vIRFs to precisely define their roles in the context of RRV infection and in the development of RRV-associated malignancies.

FUTURE DIRECTIONS

To complete these studies, further characterization of the interaction between R6 vIRF and cellular IRF-3 will need to be carried out. We've demonstrated that R6 expression inhibits IRF-3 mediated transcription, and R6 vIRF can bind to IRF-3. However, because we looked at total IRF-3, we do not know if R6 vIRF binds to activated, phosphorylated IRF-3. This could be addressed via co-IP using a phospho-specific IRF-3 antibody. Moreover, we can also assess differences in levels of phospho-IRF-3 following a stimulus (poly(IC)) to determine if expression of R6 vIRF-1 inhibits activation/phosphorylation of IRF-3.

The overall spatial expression of R6 vIRF changes from mostly nuclear, to nuclear and cytoplasmic after an IRF-3 stimulus (poly(IC)). However, we still don't know the exact mechanism by which R6 vIRF inhibits IRF-3-mediated transcription. It's possible that phosphorylated IRF-3 is shuttled out of the nucleus via its binding to R6 vIRF, or that the R6 vIRF:IRF-3 interaction blocks IRF-3 from binding with some other protein or to the DNA. These possibilities could be addressed by examining co-IPs of R6 vIRF and phosphorylated IRF-3 following an IRF-3 activating stimulus, such as polyIC treatment, and comparing nuclear and cytoplasmic lysates. If R6 vIRF is shuttling phospho-IRF-3 out of the nucleus, one would expect an increase in the R6 vIRF:phospho-IRF-3 interaction within the cytoplasm following an IRF-3 stimulus. Furthermore, if R6 vIRF is blocking IRF-3 from binding DNA, this question could be addressed using electrophoretic mobility shift assay (EMSA) with IFN-β promoter elements (PRD I/III) or ISRE as target DNA. If R6 vIRF does play a role in blocking cellular IRF-3 from

binding DNA, we should see a decrease in cellular IRF-3 binding to and ISRE probe as increased amounts of R6 vIRF are added.

We also cannot assume R6 vIRF binding to IRF-3 mediates transcriptional inhibition, as it's been demonstrated KSHV vIRF-1 can bind to several IRFs, but it's the interaction with p300/CBP that is responsible for transcriptional inhibition (31, 133, 137, 210). Therefore, by disrupting the binding of R6 vIRF and cellular IRF-3 via mutation of the binding region, we could determine whether R6 expression inhibits IRF-3 mediated transcription without directly binding IRF-3.

As an additional point of interest, the spatial expression of R12 vIRF was specifically unique; distinct rings within the nucleus. This organization is similar to the organization of PML bodies, which are organizational and regulatory centers for a number of cellular processes, including DNA repair, transcription, IFN responses, and apoptosis (190). Moreover, several herpesviruses specifically target and disrupt PML bodies during infection (70), suggesting the potential antiviral nature of these structures, and the likelihood of being a target during RRV infection, as well. The potential interaction between vIRF R12 and PML bodies, and the function of such an interaction, is also currently being investigated.

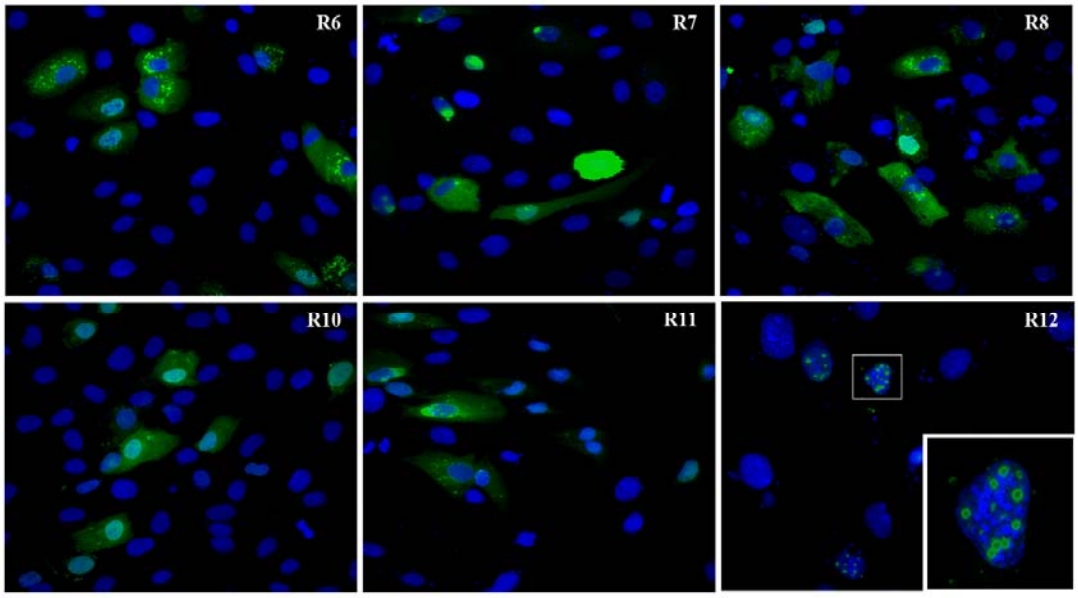

FIGURE 4.1. Expression of RRV vIRFs. The RRV vIRFs were cloned into pcDNA3.1(-) with an HA tag at the C-terminus. Six of the vIRF constructs (ORFs R6, R7, R8, R10, R11, R12) were each ectopically expressed in tRFs via nucleofection. Nucleofected cells were plated onto coverslips and fixed 48h later. Expression of each vIRF was visualized using an anti-HA-FITC mAb (green), and nuclei were stained with Hoechst 33258 (blue). The inset in the R12 field is a magnified version of the boxed region. Magnification, 200x and 400x (R12).

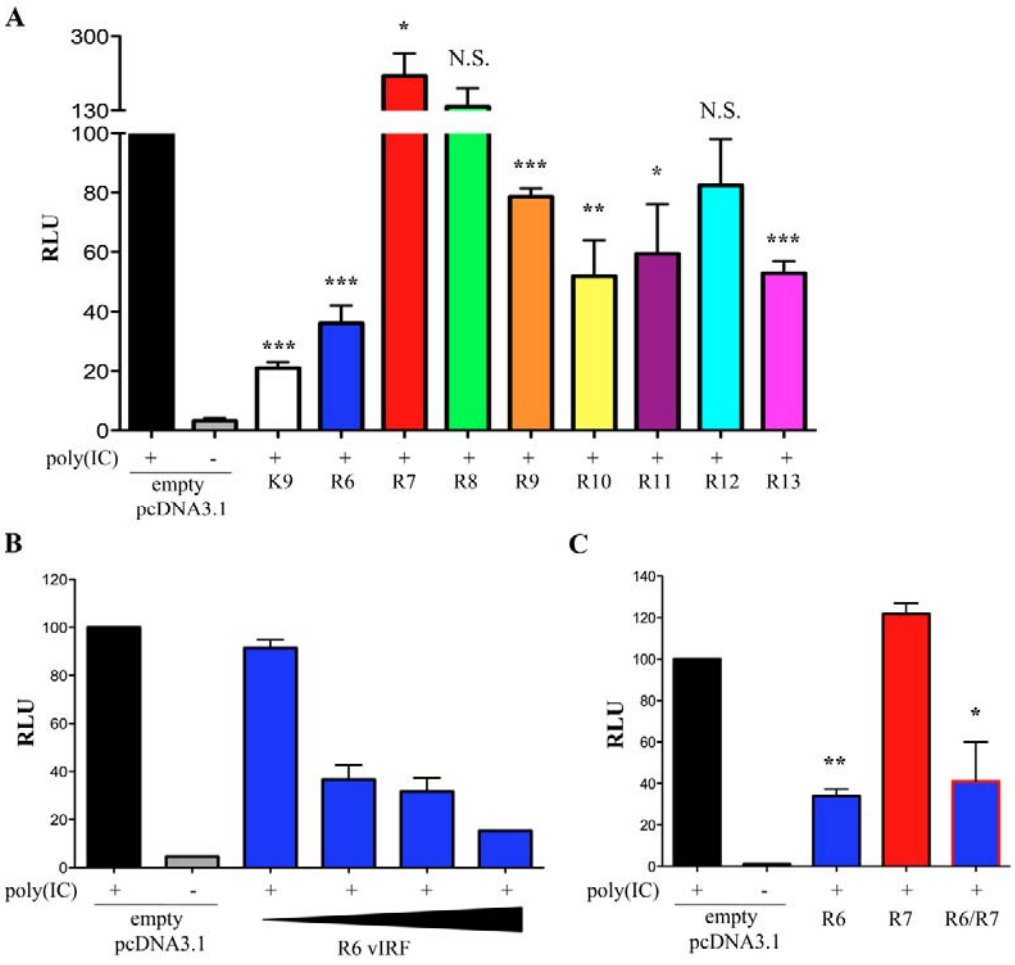

FIGURE 4.2. Individual vIRFs inhibit poly(IC)-induced transcription. HEK293 cells were transfected overnight with an individual vIRF-HA construct (50ng or 0ng), pISRE-luc (250ng), pRL_SV40 (10ng), and empty pcDNA3.1 (190ng or 240ng). Cells were then transfected with poly(IC), and assayed 6h later. Firefly luciferase levels were normalized to renilla luciferase in each well, and all conditions were made relative to the positive control [empty vector + poly(IC)]. **(A)** Each RRV vIRF was analyzed independently, and KSHV vIRF-1 (K9) was included as a control. **(B)** Cells were transfected with increasing amounts of R6-HA-pcDNA3.1 (5ng, 25ng, 50ng, 100ng) and a corresponding decrease in empty pcDNA3.1 to equal 500ng total DNA per well. **(C)** Total amount of DNA transfected per well was 500ng including 50ng vIRF-HA construct; either 50ng of R6-HA or R7-HA or and co-transfection of 25ng of each construct. Data are averaged (±SEM) from 4 (A) and 2 (B,C) independent experiments. N.S, not significant; ***, $p \leq .001$; **, $p \leq 0.01$; *, $p \leq 0.05$.

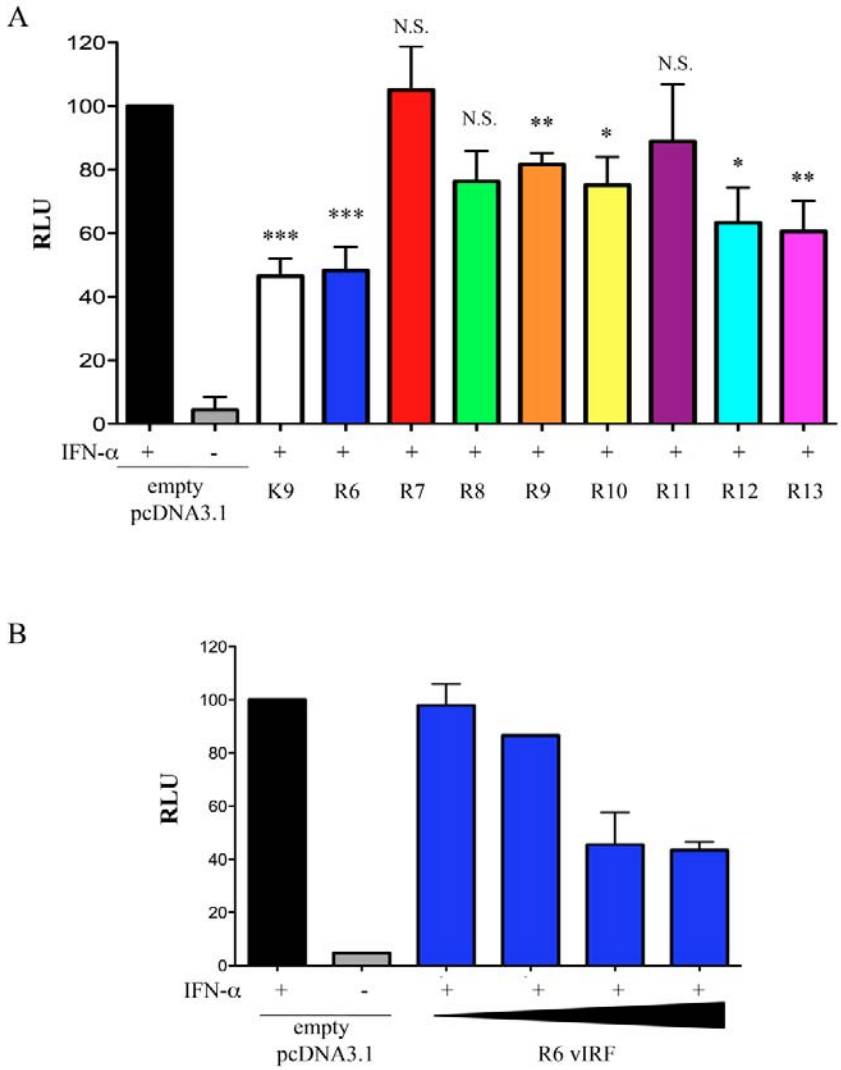

FIGURE 4.3. Individual vIRFs inhibit IFN-α induced transcription. HEK293 cells were transfected overnight with individual vIRF-HA constructs (50ng or 0ng), pISRE-luc (250ng), pRL_SV40 (10ng), and empty pcDNA3.1 (190ng or 240ng). Cells were then stimulated with rhIFN-α2 (100Units/well) and assayed for firefly and renilla luciferase 6h later using the Dual-glo luciferase assay kit (Promega). **(A)** As a control, KSHV vIRF-1 (K9) was also included. **(B)** Cells were transfected with increasing amounts of R6-HA-pcDNA3.1 (5ng, 25ng, 50ng, 100ng) and a corresponding decrease in empty pcDNA3.1 to equal 500ng total DNA per well. N.S, not significant; ***, $p \leq 0.001$; ** $p \leq 0.01$; *, $p \leq 0.05$.

FIGURE 4.4. R6 vIRF interacts with cellular IRF-3. tRFs were nucleofected with R6-HA-pcDNA3.1, R7-HA-pcDNA3.1, pEGFP or nothing (mock). **(A)** Native lysates were collected 48h later and divided in half to IP with either α-IRF3 pAb or α-HA mAb O/N at 4C. IP lysates were then incubated for 4h with Protein A/G beads, washed and analyzed via western blot for IRF-3 and HA. **(B)** Cells transiently expressing R6-HA or R7-HA constructs were grown on coverslips O/N. Subsequently, these cells were transfected with 0 or 10ug poly(IC) for 6h, then fixed and permeabilized. Cells were stained for α-IRF3 pAb (red), followed by α-HA mAb (green), and Hoechst 33258 (blue) for nuclei detection. **(C)** Cells transiently expressing R6-HA pcDNA3.1 for 36h, were subsequently stimulated with SeV (0 or 100 HA units/1x10^6 cells) for 6h and then nuclear and cytoplasmic lysates were collected and analyzed via western for total IRF-3 and HA expression, to detect R6 vIRF. O/N, overnight; α, anti; IP, immunoprecipitate; WB, western blot; SeV, Sendai Virus.

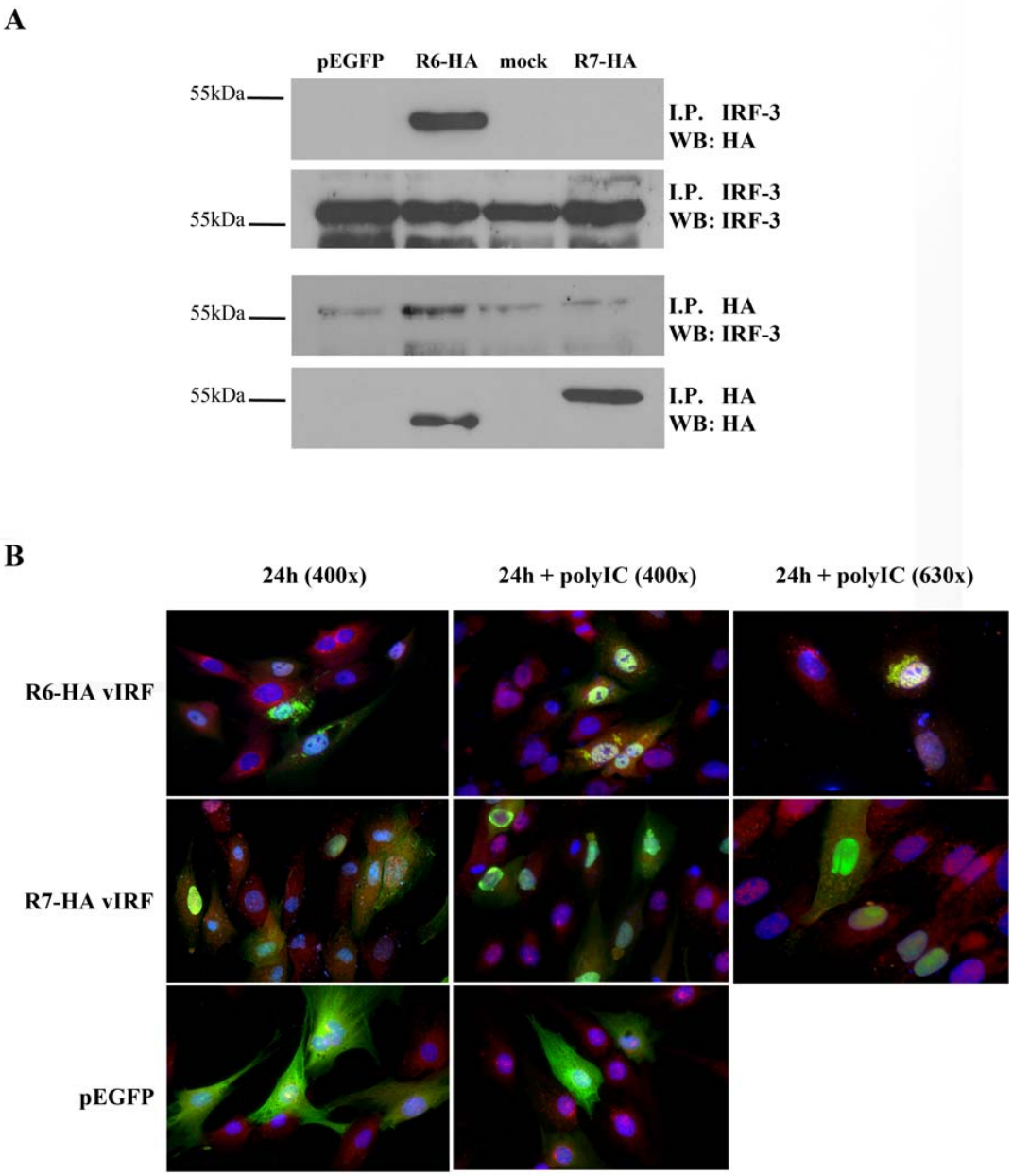
A
pEGFP
R6-HA
mock
R7-HA
55kDa
I.P. IRF-3
WB: HA
55kDa
I.P. IRF-3
WB: IRF-3
55kDa
I.P. HA
WB: IRF-3
55kDa
I.P. HA
WB: HA
B
24h (400x)
24h + polyIC (400x)
24h + polyIC (630x)
R6-HA vIRF
R7-HA vIRF
pEGFP
C
cytosol
nuclear
SeV
-
+
-
+
WB: IRF-3
WB: HA (R6 vIRF)

Fig. 4.5. R7, R8, and R9 vIRFs have oncogenic potential *in vitro*. NIH3T3 cells were stably transfected with each vIRF construct, and individual clones were monitored for increased growth potential and foci formation. A stable clone of empty pcDNA3.1 was included as a negative control and used to determine statistical significance, and a clone of K9-HA (KSHV vIRF-1) was included as a positive control. **(A, B)** NIH3T3 cells stably transfected with a vIRF-HA clone were plated into each well of a 6-well plate at a density of $2x10^5$ cells/well. **(A)** One well was harvested and counted each day for 6 days, and **(B)** wells were monitored for the development of foci formation after a week in culture. Magnification, 50x. **(C)** Cells ($5x10^3$) from each stable vIRF-HA clone were individually mixed with 0.3% agarose as a single-cell suspension and plated into one well of a 6-well plate. Single cell suspensions were monitored for anchorage-independent growth via development of foci within 3-4 weeks. A clone of a constitutively active Ras (V12Ras) was included as a second positive control. Magnification, 320x. *** $p \leq 0.001$; **, $p \leq 0.01$; *, $p \leq 0.05$.

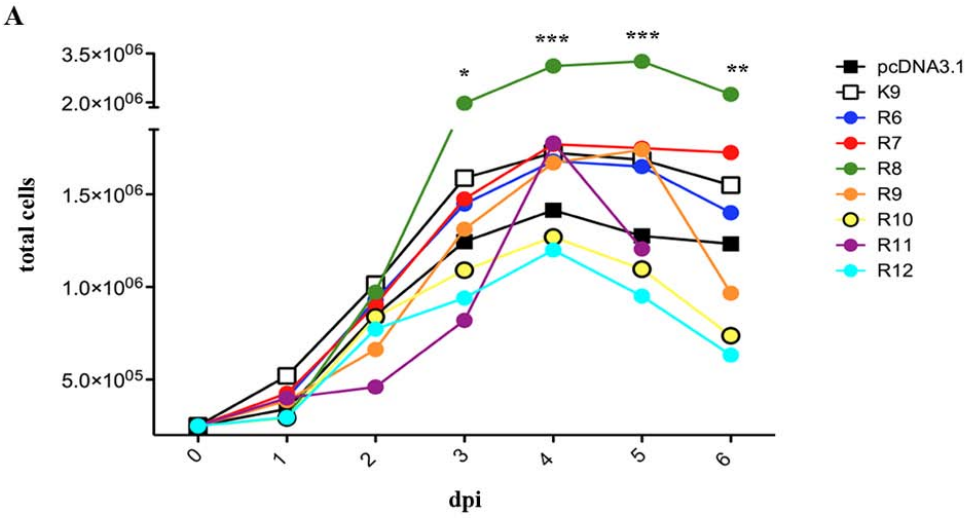
A
3.5×10^06
2.0×10^06
1.5×10^06
1.0×10^06
5.0×10^05
total cells
0
1
2
3
4
5
6
dpi
*
***
***
**
pcDNA3.1
K9
R6
R7
R8
R9
R10
R11
R12

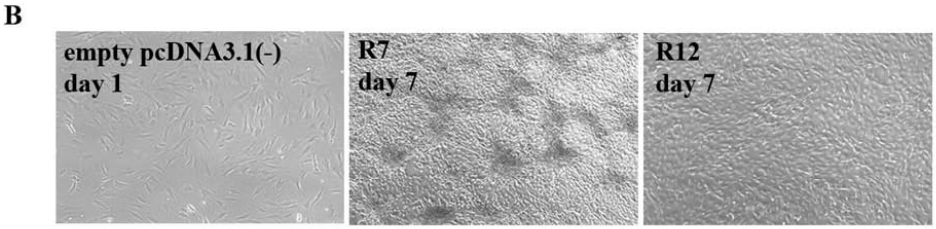
B
empty pcDNA3.1(-)
day 1
R7
day 7
R12
day 7

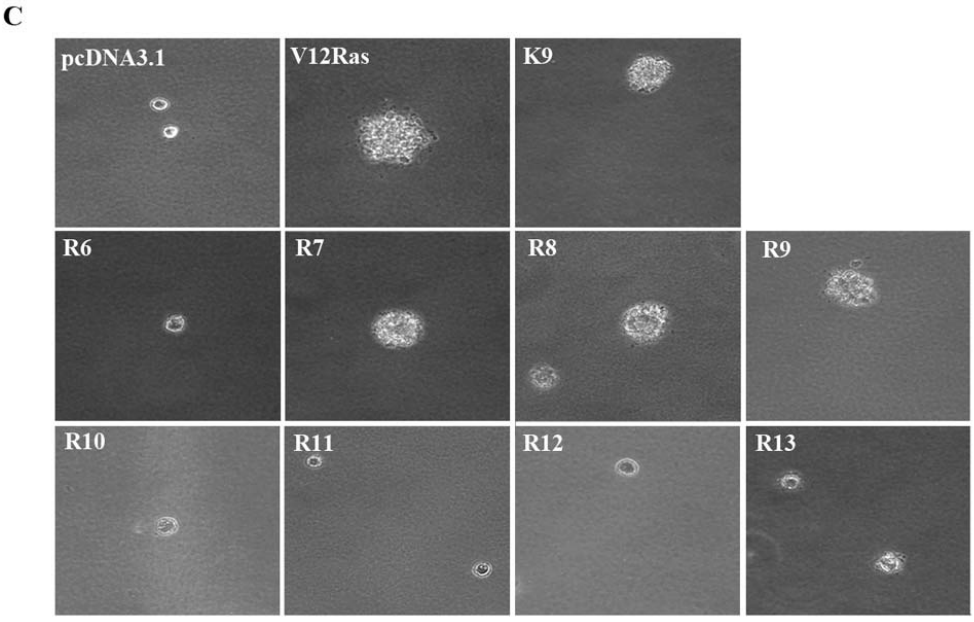
C
pcDNA3.1
V12Ras
K9
R6
R7
R8
R9
R10
R11
R12
R13

TABLE 4.1: Oligos for cloning vIRFs into pcDNA3.1(-)

vIRF	oligos	oligo sequence (5'-3')*#
R6	R6 for	ctt ggc agt **gcggccgc** ATG GCT ACC TGG CGC CCA CCT
	R6 rev-HA	cgt **gaattc** tca agc gta gtc tgg gac gtc gta tgg gta TTC AAA GTG CCG ATA TAT TTC
R7	R7 for	ctt ggc agt GCGGCCGC atg gcg ggc cgt gga gtc gat
	R7 rev-HA	cgt **gaattc** tga agc gta gtc tgg gac gtc gta tgg gta CGA GCA GGC CAC CCC ATC ATC
R8	R8 for	ctt ggc agt **gcggccgc** ATG GAG CGG CCG GTC CGA GTG
	R8 rev-HA	cgt **gaattc** tta agc gta gtc tgg gac gtc gta tgg gta AAC ATT AGC GGC GGA CAA CGC
R9	R9 for	ctt ggc agt **gcggccgc** ATG GAT TCT GGA TGC TAT GCC
	R9 rev-HA	agc **ggatcc** tta agc gta gtc tgg gac gtc gta tgg gta TGA GCA CCA CG GGA AGG ATT
R10	R10 for	ctt ggc agt **gcggccgc** ATG GCC GCT GGG GAA TCG AGA
	R10 rev-HA	agc **ggatcc** tta agc gta gtc tgg gac gtc gta tgg gta TTC AAA GTG CCT ATA GAT TTC
R11	R11 for	ctt ggc agt **gcggccgc** ATG GCG GAA CGC GAT ATG GAT
	R11 rev-HA	cgt **gaattc** tta agc gta gtc tgg gac gtc gta tgg gta CTT CCT CCC ATA CGG TGC GAG
R12	R12 for	ctt ggc agt **gcggccgc** ATG GCG GAA GGA CGG GCA GGG
	R12 rev-HA	cgt **gaattc** tca agc gta gtc tgg gac gtc gta tgg gta CTG GGC CGC ATC CCC GCA CGC
R13	R13 5' for	ctt ggc agt **gcggccgc** ATG ACC GAG ATA GAA ATC ACT
	R13 3' rev-HA	cgt **gaattc** cta agc gta gtc tgg gac gtc gta tgg gta CAA AAT CCA CCG AGC CGC CCG

* restriction enzyme sites are in bold
\# gene-specific sequence is in upper case

TABLE 4.2:
Transforming properties of vIRF clones in NIH 3T3 cells

vIRF	colony formation in soft agar (%)*
empty pcDNA3.1	1.4
R6	1.0
R7	41.2
R8	33.0
R9	44.0
R10	2.3
R11	0.5
R12	1.9
R13	4.6

*** % cells forming colonies at 3-4weeks**

CHAPTER 5

SUMMARY and CONCLUSIONS

I. The role of vIRFs during RRV Infection

A. Generation and characterization of vIRF-ko RRV

In Chapter 2 of this thesis, we characterized a vIRF deletion mutant of RRV, vIRF-ko RRV. Using the RRV_{17577} BAC (69), we deleted all 8 vIRFs from the genome to assess their overall role during *de novo* RRV infection. Our initial analysis demonstrated that deletion of the vIRFs did not alter the growth properties of RRV in fibroblasts, nor inhibit RRV infection of rhesus PBMCs, which include critical cell populations during *in vivo* infection, such as B cells (16). Additionally, we analyzed the sequence of the entire genome by directly comparing it to WT_{BAC} RRV DNA using complete genome hybridization. Our findings confirmed that deletion of the vIRFs did not result in any unintended nucleotide changes outside of the deleted region. Therefore, we determined we could effectively utilize the vIRF-ko recombinant clone to further study the impact of vIRFs during RRV infection.

The significance of generating such a recombinant virus is noteworthy, because it has been difficult to study the role of any particular viral gene during *de novo* KSHV infection (169). Also, because KSHV and RRV are the only viruses known to encode proteins with homology to cellular IRFs, studying the vIRFs during RRV infection offers the opportunity to study their impact on immune responses and pathogenesis during *in vivo* infection, as well. Moreover, given that KSHV vIRF-1 and vIRF-3 are

two of the few viral proteins detected in KSHV-associated malignancies (89, 179), and that there is overwhelming *in vitro* evidence demonstrating vIRFs function in tumorigenesis and immune evasion, the potentially critical role of these proteins in KSHV pathogenesis is undeniable. Thus, if we can better understand their impact during infection, the vIRFs could be prospective targets of future antiviral therapies.

B. Functional characterization of vIRFs

1. vIRFs modulate the IFN response during de novo RRV infection

In vitro comparison of WT RRV and vIRF-ko RRV infection demonstrated the presence of vIRFs significantly inhibits induction of type I and type II IFN. Because RRV encodes other viral proteins that potentially inhibit the IFN response as well (10), the fact that we observed such a significant difference demonstrates the considerable impact vIRFs have on the innate immune response during *de novo* infection. Specifically, we noted that vIRF-ko RRV infection resulted in increased type I IFN production within pDCs within the first 48 hpi. pDCs are the most potent IFN-α producing cells in the body (75), and the impact of these findings is important when considering what's happening during *in vivo* RRV infection. In general, DCs are one of the first cell types to encounter and take up antigen following virus infection, and coupled with the ability of pDCs to recognize and respond to KSHV *in vitro* (250), these findings could account for the sustained IFN-α production detected in the plasma of the RMs infected with vIRF-ko RRV (Chapter 3). If the vIRFs can inhibit IFN production by this critical cell population within the infected animal, then this would offer a lengthened window of time for the virus to establish infection and delay the initiation of an effective immune

response. This could explain what we observed in the RRV-infected RMs, and the impact of vIRFs on the adaptive immune response will be discussed further in a later section.

We did not look for RRV within pDCs in our experimentally infected animals, as this population is so small (<1% of the total PBMC population) (48) it would be difficult to get an adequate number of pDCs from our routine tissue and blood collections. However, a preliminary *in vitro* experiment, utilizing GFP expressing clones of WT RRV and vIRF-ko RRV, has demonstrated both viruses can infect pDCs, as measured via flow cytometry (data not shown). Collectively, the *in vitro* and *in vivo* analysis of type I IFN production within pDCs and RM plasma samples, suggest that one or more vIRFs are inhibiting production of type I IFN within RRV-infected pDCs.

Transcription of type I IFN relies heavily on cellular IRF-3, as it is expressed in most cell types and is activated upon viral infection (94, 112, 138). Therefore, it wasn't surprising that the inhibition of type I IFN was preceded by a spatial dysregulation of IRF-3 during WT RRV infection, as described in Chapter 2. We also analyzed IFN-induced signaling, the Jak/STAT pathway (Fig 1.3), via analysis of phosphorylation and nuclear localization of STAT1 and STAT2 (data not shown), but did not observe obvious differences between WT RRV and vIRF-ko RRV infection. However, the temporal role vIRFs play in inhibiting this pathway is difficult to assess, and the overall lower levels of type I IFN induction in fibroblasts (Chapter 2) may indicate IFN signaling is limited in these cells, and should be examined in a different cell type.

Differentially, the effect of vIRFs on the activation of proteins within the Jak/STAT pathway may be better understood by examining IFN-induced signaling in the context of individually expressed vIRFs.

Infection with vIRF-ko RRV also resulted in increased induction of type II IFN, IFN-γ. The production of IFN-γ is restricted mostly to NK cells and activated T cells, as part of the innate and adaptive immune responses, respectively. Because the induction of IFN-γ was observed so early after vIRF-ko RRV infection (6 hpi *in vitro*, and by 1 dpi *in vivo*), it's likely the source is from NK cells, which may be activated via the early production of type I IFN (165) (Fig. 1.4). We have not examined whether NK cells are specifically infected *in vitro*, but the possibility that vIRFs are playing a direct role in inhibiting IFN-γ within infected NK cells cannot be excluded.

2. Modulation of the IFN response by individual RRV vIRFs

In Chapter 4, we characterized individual vIRFs as to their function in transcription of ISRE-driven genes following IRF-3 activation and IFN stimulation. We demonstrated that the eight vIRFs had varying ranges of inhibition and enhancement of transcription in these reporter assays. Of significant note is that R6 vIRF specifically demonstrated marked inhibition of transcription mediated by both IRF-3 and type I IFN, functioning similarly to KSHV vIRF-1 (Chapter 4) (76, 82, 127, 134, 267). Moreover, R6 vIRF is also able to bind cellular IRF-3, and this interaction is enhanced following IRF-3 stimulation. Therefore, this interaction could be responsible for the decreased nuclear

accumulation of IRF-3 following WT RRV infection, but this hypothesis has yet to be tested directly.

Another interesting finding was that expression of R7 vIRF actually enhanced transcription in response to IRF-3 activation and IFN stimulation. Similar characteristics have been assigned to KSHV vIRF-3, which can enhance IRF-3 and IRF-7 mediated transcription, as well as promote c-Myc mediated transcription. The latter has a distinct role in aiding transformation, which could be the intended effect of R7 vIRF mediated transcription. Indeed, stable expression of R7 vIRF resulted in increased growth potential and anchorage-independent growth in NIH3T3 cells (Chapter 4). If not induction of a cellular oncogene, R7 vIRF may be driving transcription of viral genes, as demonstrated by the ability of KSHV vIRF-1 to drive transcription of vIL-6 (177). vIL-6 is thought to be a key component of KSHV and RRV-associated B cell malignancies (11, 99, 113, 171). Another possibility is that the intended target of R7 vIRF is enhancement of transcription of type I IFNs, which in turn drives transcription of vIL-6 (42), and thus, R7 vIRF may indirectly promote cellular proliferation and tumorigenesis. Whether the RRV vIL-6 gene is also responsive to IFN, and whether RRV vIRFs are able to promote its transcription have not yet been examined.

As mentioned previously, sequence analyses suggested RRV initially acquired 4 vIRFs (ORFs R6-R9), and these four genes later underwent a duplication to result in a total of 8 vIRFs (207). The data presented within suggest the duplicated vIRFs (ORFs R10-

R13) do not possess completely redundant functions with R6-R9 vIRFs. A prime example of this is the functional disparities between R7 and R11 vIRFs. Although they share >50% sequence similarity, R7 vIRF enhances IRF-3-mediated transcription, but R11 vIRF appeared to have little affect on IRF-3 mediated transcription (Chapter 4). Additionally, R7 vIRF demonstrated tumorigenic potential in NIH3T3 cells, and R11 vIRF did not (Chapter 4). This example demonstrates the disparity of function between the RRV vIRFs, and suggests that the sequence similarities in the 4 duplicated vIRFs does not equate to redundancy in function. Therefore, future analyses will need to address the roles of all 8 vIRFs as distinct genes with unique properties.

C. The role of RRV vIRFs on the Host Immune Response and Pathogenesis

1. Impact on viral replication and latency

In Chapter 3 of this thesis, we utilized the vIRF-ko RRV recombinant clone to assess the impact of vIRFs on RRV infection of rhesus macaques, the natural host. In acute WT RRV infection, viral loads were measured by 2 weeks PI, and peaked at 4 weeks PI. Infection of RMs with vIRF-ko RRV resulted in undetectable viral loads in all but 2 RMs, in which very low levels were detected as early as 1 week PI. Again, this supports the hypothesis that deletion of the vIRFs results in lower levels of antigen due to earlier detection and immunological control of the virus.

Deletion of the vIRFs does not appear to impact persistence of RRV within the CD20+ population. However, because there was a more robust immune response during acute infection, it's plausible that vIRF-ko RRV will be easily controlled during the future if

the animal becomes immune-compromised. These studies are currently ongoing, as the vIRF-ko RRV-infected animals have subsequently been infected with SIVmac239 and are being monitored for changes in RRV-specific T cell responses and for the development of lymphoproliferative disorders. Additional analysis of persistence within the RMs has demonstrated RRV can also be detected within T cells and antigen presenting cells (HLA-DR+) (data not shown). This is the first demonstration that RRV is persistent within cell types other than B cells; however, these preliminary analyses do not suggest the vIRFs alter or change persistence within specific cellular populations (data not shown).

2. Impact on cytokine production

The induction of most cytokines is controlled at the level of transcription. Thus, vIRFs could potentially interfere with the production of any number of pro-inflammatory cytokines to control the immune response during RRV infection. Indeed, the vIRF-ko RRV-infected animals demonstrated prolonged production of both IFN-γ and IL-12, an important mediator of an effective Th1 response during viral infections. IL-12 is regulated by IRF-1 and IRF-8, as well as NFκB, all of which could be direct targets of the vIRFs. Preliminary analysis of IL-12 and IL-18 transcripts in RRV infected PBMCs *in vitro* did not demonstrate a difference between WT and vIRF-ko RRV infected cultures (data not shown). However, vIRF-ko RRV infection did result in an increase in cellular IRF-8 transcript, which is upregulated by IFN-γ signaling (data not shown). Therefore, an increase in IRF-8 could translate to an increase in IL-12 production at later time points. It's difficult to recapitulate development of an immune response in

cell culture, so if vIRFs are indirectly inhibiting levels of certain cytokines, this may be difficult to measure during an *in vitro* infection.

3. Impact on T cell response

By measuring the non-specific proliferation of T cells in the RMs, we can assess their overall activation, which is assumed to be due to RRV infection in the ESPF animals. Although the kinetics of T cell proliferation are similar in all the animals, these responses demonstrate a trend towards lessened proliferation within the vIRF-ko RRV-infected RMs. This may be due to the lower viral loads in these animals (i.e., earlier detection and control of vIRF-ko RRV means less available antigen, which results in a lessened response). It is also likely that the lower antigen stimulus in the vIRF-ko RRV-infected RMs also results in lessened bystander proliferation. Interestingly, however, even if there is less antigen and decreased proliferation of T cells, the vIRF-ko RRV-infected animals develop an RRV-specific T cell response at 7 dpi, 2 weeks earlier than WT RRV-infected animals. As mentioned earlier, this indicates the vIRFs are functioning to inhibit early immune responses to avoid detection, thus, allowing RRV more time to replicate to higher levels and delay the onset of the specific T cell response.

We measured T cell responses based on IFN-γ production following RRV stimulation. Additionally, there is prolonged detection of IFN-γ within the plasma of vIRF-ko RRV infected RMs, lasting from 1 dpi to 7 dpi. The early production of IFN-γ is likely from NK cells, but we cannot exclude the possibility that the sustained production (> 7dpi)

may also be attributed to activated T cells, as these animals did have specific CD4 and CD8 responses at 7 dpi. The extent of IFN-γ production from either NK cells or T cells, and the role vIRFs play in inhibiting the induction of IFN-γ, will need to be further evaluated in RRV-infected PBMC cultures *in vitro*.

4. Impact on RRV-associated pathologies

In Chapter 4, our *in vitro* analysis of individual vIRFs demonstrated that R7, R8, and R9 vIRFs all possess oncogenic potential in NIH3T3 cells, suggesting these vIRFs could play a role in development of RRV-associated B cell malignancies. Indeed, vIRF-ko RRV infection of RMs resulted in a significant decrease in acute B cell hyperplasia (Chapter 3). Whether this is a direct result of the vIRF functions, or a byproduct of decreased viral replication will need to be further examined. Determining whether any of the vIRFs are still expressed after acute viral replication would potentially highlight their role in pathogenesis, as KSHV and RRV infection result in pathologies while in a latent state (81). It has been demonstrated that KSHV vIRF-1 and vIRF-3 are present within infected cells in KSHV-associated tumors, but only within a subset of the infected cells (89, 179). Likewise, expression of specific vIRFs may only be evident during development of disease, and the RMs used in these studies were not immune-compromised, and therefore, were not likely to develop RRV-associated B cell disorders. Nonetheless, the significant decrease in acute B cell hyperplasia is a likely indication that vIRF-ko RRV lacks something necessary for development of RRV-associated malignancies.

II. Future Directions

The findings communicated in this thesis clearly demonstrate the collectively crucial impact vIRFs have during RRV infection; with effects ranging from inhibition of the IFN response to diminishing acute pathologies during RRV infection of RMs. These data offer important strides in understanding the roles of vIRFs during infection and disease, but also present new questions to investigate. Some of the unknowns have been mentioned above, but I'll expand on a couple key questions.

First, I'll mention again that it will be necessary to delineate the specific functions of each of the RRV vIRFs to completely understand our findings. The data presented here demonstrates that each vIRF appears to have unique properties, and these proteins should therefore, be assessed individually.

The ability of vIRFs to inhibit the IFN response can have an immediate impact on development of the antiviral state, and we've shown that deletion of the vIRFs also initiates an earlier adaptive immune response in the RM, as well. What this data does not differentiate is whether the vIRFs have a direct or indirect impact on the adaptive immune response (Fig 1.4). Most likely, the answer is both. We can start by positing that the roles of vIRFs are likely restricted to inhibiting signaling and transcription, as has been shown for the KSHV vIRFs (170). Specific RRV vIRFs have direct roles in IFN inhibition, as we've demonstrated in Chapter 4, which then shapes the adaptive response accordingly. Additionally, specific vIRFs may also directly affect the adaptive response by inhibiting expression of proteins involved in antigen

processing/presentation or by disrupting the production or signaling of Th1 cytokines. KSHV vIRF-1 has been shown to specifically inhibit transcription of MHC-I (127), which would impede antigen presentation during the course of infection. The fact that we see earlier T cell responses in the vIRF-ko RRV animals suggests the vIRFs may not only be inhibiting the induction of type I IFN, but could be directly inhibiting antigen presentation, as well. The role of RRV vIRFs in directly inhibiting the adaptive immune response will need to be addressed by initially characterizing individual vIRFs *in vitro* with specific analyses designed to look at the adaptive response independent of IFN signaling. Also, utilizing the RRV BAC, systematic characterization of viruses deleted for each vIRF will need to be carried out to determine the different roles of each vIRF during RRV infection, as well.

Another fundamental question is whether the vIRFs are important for promoting tumorigenesis during *in vivo* RRV infection. We have yet to directly address whether RMs infected with vIRF-ko RRV still develop B cell malignancies. Due to the significantly diminished B cell hyperplasia during acute vIRF-ko RRV infection, it's rational to hypothesize that these animals may lack some component necessary for development of lymphoproliferative disorders. Indeed, if deletion of the vIRFs results in an infection that never develops into the characteristic B cell malignancies, this would be an incredible advancement in understanding and targeting KSHV-associated diseases. However, since vIRF-ko RRV can still persist within these RMs, the potential for this virus to cause disease still exists. We are currently conducting studies in

immune-compromised RMs to examine whether deletion of the vIRFs inhibits the development of disease, or reduces the incidence B cell malignancies.

MATERIALS and METHODS

This section is meant to augment the materials and methods sections within chapters 2-4. These detailed methods include additional information for new protocols, protocols in which I've made specific changes, or those that are not routinely performed within Dr. Scott Wong's laboratory.

Co-cultures and viremic score for RRV-infected rhesus macaques

A 24-well plate of 1° rhesus fibroblasts (RFs) was seeded ($5x10^4$ cells/well) the day before collection of blood from rhesus macaques (RMs). Blood was collected weekly from infected RMs, and PBMCs were isolated using Histopaque, per manufacturer's protocol. Serial dilutions of PBMCs are then added to the RFs in duplicate, as follows. In the first 2 rows of the plate, add $2x10^5$ PBMCs (suspended in 100ul complete RPMI) to the first wells. Subsequently, 1:3 dilutions of PBMCs are made across 5 wells (i.e., $6x10^4$ PBMCs in the second well, $2x10^4$ PBMCs in the third well, $6x10^3$ PBMCs in the fourth well, and $2x10^3$ PBMCs in the fifth well). Leave the 6^{th} well as mock-treated RFs. Monitor the plate every few days for the development of RRV-specific cytopathic effect (CPE), and mark which wells are positive for CPE. Development of CPE should be complete within 4-6weeks after plating; I found that PBMC co-cultures from vIRF-ko RRV-infected RMs resulted in CPE much later than WT RRV, and needed to monitor these plates until 6 weeks post-plating.

To generate a viremic score (0-5), CPE is monitored within individual wells. A score of 1 indicates CPE in the wells with $2x10^5$ PBMCs (the lowest dilution), and a score of 5 indicates CPE in wells with $2x10^3$ PBMCs (the highest dilution). Since PBMCs were co-cultured in duplicate, each well of the duplicate dilution is scored 0.5.

When RFs in the co-culture plates reached complete CPE, cells and supernatants from individual wells were collected and stored at -80C. The collected cells/supernatant was then used directly as template for PCR reactions to validate the presence of RRV DNA. Alternatively, if the level of viremia is low, as in the case of the vIRF-ko RRV-infected animals, DNA can be purified from the cells/supernatant and used as template.

PCR and RT-PCR analyses

1. **nested vMIP in co-cultures.** Use 10ul of the cells/supernatant from co-culture plates, or purified DNA from the cells/supernatant, as template for PCR reactions to screen for vMIP (ORF R3) to verify the presence of RRV lytic replication in PBMCs from infected RMs. Initial vMIP reactions are performed in a 50ul reaction with the following settings: 1 cycle of 95C for 3min; 40 cycles of 95C for 20sec, 58C for 30sec, 68C for 30sec; 1 cycle of 68C for 7min; and leave at 4C. Oligos used are vMIP-1 (#171) (5' CCT ATG GGC TCC ATG AGC 3') and vMIP-2 (#172) (5' ATC GTC AAT CAG GCT GCG 3') and this reaction produces a 255bp product. To perform the nested reaction, use 10ul of reaction 1 as template in a 50ul reaction with the following settings: 1 cycle at 95C for 3min; 40 cycles of 95C for 30sec, 56C for 30sec, 68C for 1min; 1 cycle of 68C for 7min; and leave at 4C until

you can run your product out on a 1% agarose gel. Oligos used for the nested reaction are vMIP-3 (#169) (5'CCC GAA CTC TGC TGT TTG 3') and vMIP-4 (#170) (5' TGG GAC GCT TGT CCA CCG 3') and this reaction produces a 190bp product.

2. **Real-time PCR (type I and type II IFNs).** RNA was extracted from infected cells using a Qiagen RNA extraction kit, resuspended in 40ul RNase-free H20, and treated with RQ1 DNase (5ul DNase + 5ul buffer) for 1.5h at 37C. The DNase reaction was terminated via incubation at 68C, 10min. First strand cDNA synthesis was carried out with 1ug RNA and using the High-Capacity cDNA reverse transcription kit (ABI). cDNA was then amplified using the Taqman PreAmp master mix kit (ABI) with TaqMan Gene Expression assays (ABI) specific for rhesus IFN-β (Rh_03648734), IFN-$\alpha_{1/13}$ (Rh_03456606), IFN-γ (Rh_02621721), IL-12 (Rh_02621748), IL-18 (Rh_02787951), IRF-1 (Rh_00971962), IRF-3 (Rh_02839170), IRF-7 (Rh_02839175), IRF-8 (Rh_02841197), IRF-9 (Hs_00196051), ISG15 (Rh_02879913), IFNaR2 (Rh-02829927), and IFNgR1 (Rh_02787824). Amplification was performed in a 50ul reaction with 14 amplification cycles, per kit protocol (ABI), and subsequently resuspended 1:10 in TE, pH 8, and stored at -20C. (Do not include the GAPDH expression assay kit when performing the cDNA amplification as it is already present in high enough levels which negates the need for amplification).

To perform real-time PCR analysis to quantify individual transcripts, 20ul reactions were performed in duplicate wells on the same plate. The TaqMan Gene Expression Assays were used for the primer/probes, as listed above, and rhesus GAPDH (Rh_02621745) was used as a normalization control, and was also performed in duplicate on each sample and included on the same plate. For experimental samples, 10ul of the amplified cDNA were used per well, and reactions were run with 2 initial steps (50C for 2min, and 95C for 10min) followed by 40 amplification cycles (95C for 15sec, 60C for 1min), then held at 4C.

Standard curves (5, 3-fold dilutions: the quantity (ng RNA) and range of the standard curve, and the source material, need to be determined empirically for each transcript) were included on each plate for each transcript being analyzed, and GAPDH was always included for normalization. To normalize between plates, you need to generate one stock for each standard curve; either use a cDNA clone of the transcript and calculate exact copies of the transcript/ng nucleic acid, or have one consistently used sample of cells. These studies utilized the latter. Mock tRFs were used to make standard curves for GAPDH, IRF-1, IRF-3, IRF-9, IL-12, and IL-18. Poly(IC)-treated tRFs were used for standard curves for IFN-$\alpha_{1/13,}$ and IFN-β. PBMCs treated with IFN-α2 were used to make standard curves for IRF-7, IRF-8, and IFN-γ.

Using the C_T values generated following the real-time PCR reaction, along with the calculated ng RNA used to make the standard curve, an equation is formulated for

each transcript. The C_T values from each experimental sample can then be put into the calculation to determine the amount of transcript. (The computer software does this for you now). The ng of target RNA are calculated for each sample are then you need to divide that by the ng GAPDH RNA in that same sample to normalize the data [(target ng RNA/GAPDH ng RNA) = normalized amount of target]. Using this system, you cannot quantify the exact amounts of RNA and everything needs to be made relative to another control included on the plate. Also, some experimental systems or cell types may require a different normalization gene; the normalization transcript should be abundant and should not be altered in your experimental system.

3. **Expression of each RRV vIRF (RNA and DNA).** Unique oligo pairs were designed to amplify a ~300bp fragment within each RRV vIRF to identify mRNA transcripts in infected cells, as well as for differentiation of WT RRV genomic DNA compare to vIRF-ko RRV genomic DNA from infected RMs.

***In vitro* RRV infections (tRFs and 1^o rhesus PBMCs)**

Cells were infected with WT_{BAC} RRV (clone 13) or vIRF-ko RRV (clone 11) at MOI=1 in complete DMEM (tRFs) or serum-free RPMI (PBMCs). Infection of tRFs was carried out in 200ul/well in a 12well plate with coverslips, with continuous rocking for 2h at 37C, and 1.5ml complete DMEM was added back, and cells were kept at 37C for the remainder of the experiment. If multiple time points are being analyzed, plate them

in separate plates so the plate can be removed and fixed individually (4% paraformaldehyde, 20min, r.t.). PBMCs were cultured in serum-free RPMI and all time points were infected simultaneously in serum-free RPMI (total of 200ul media/well) in a flat-bottom 96well plate at 37C. Specific wells of PBMCs were transferred to a round-bottom 96well plate at designated time points post-infection for staining.

Immunofluorescence analysis

Untreated cells are seeded onto glass coverslips in 12 well plates at a density of $0.5x10^5$ cells/well. Cells transfected via nucleofection are seeded at $0.8x10^5$ due to some expected cell death following nucleofection. After treatment/infection cells are fixed in freshly made 3% paraformaldehyde/PBS for 20min at room temperature, washed twice with 1X PBS, and can be stored at 4C in PBS. Cells are blocked in 5% normal goat serum (ngs)/1X PBS with 0.1% tween20 for at least 1h at room temperature. Immunofluorescence staining is performed in a humidity chamber protected from the light, i.e., wet paper towels are lined in an opaque container with a sealed lid or covered with foil. Parafilm is placed in the humidity chamber, and all staining will take place on the parafilm. Antibody is diluted in 1% ngs/PBS with 0.1% tween20 and ~10-15ul is pipetted onto the parafilm for each coverslip. Coverslips are then placed cell-side down onto the 15ul antibody and stained with primary antibody O/N at 4C. Coverslips are returned to the 12well plate and washed 3X in 1X PBS/0.1% tween20. Cells are then stained with fluorescently labeled secondary for at least 1h at room temperature, followed by Hoechst (1:500) for 1min at room temperature. Coverslips are finally washed 3X in 1X PBS/0.1% tween20, and mounted cell-side down onto glass slides

using Vectashield (Vector Labs), and then sealed with nail polish. Dilutions and antibodies used for these studies are as follows, α-IRF-3 mAb (clone SL012.1, BD Pharmingen) (1:50); α-Rabbit-IgG-Texas Red (1:100); α-HA-FITC mAb (clone HA-7, Sigma) (1:250). To look specifically at cell surface expression, exclude the use of tween20 when blocking and washing.

ICCS for IFN-α

Fresh PBMCs were isolated from whole blood (max bleed to get ~$30x10^6$ cells for one experiment) from an ESPF RM, and plated at $1x10^6$ cells/well in a 96well flat-bottom plate. Three or four wells (3-4 million) were used for each condition. Cells were infected at MOI=1 in a total of 200ul serum-free RPMI for 12, 24, and 48 hpi. Uninfected PBMCs were included as a negative control, and HSV-1 infection (MOI=1) was included as a positive control for IFN-α production. At each time point, cells were transferred to a 96well round-bottom plate for staining. Cells were washed once in PBS, and surface stained in 50ul PBS with the following antibodies CD3-pacific blue (SP34), CD20-ECD (B9E9), CD14-A700 (M5E2), HLA DR-APC Cy7 (L243), CD11c-APC (3.9), and CD123-PerCp Cy5.5 (6H6) for 1h at 4C. Cells were washed 2 times in PBS and subsequently fixed in fixation buffer (BioLegend) for 20min at 4C, permeabilized and stained for intracellular IFN-α (MMHA-2) (PBL). IFN-α was labeled using Zenon labeling technology (FITC), per kit protocol (Molecular Probes, Eugene, OR). INF-α was labeled [1ug Ab:5ul labeling reagent (3:1 molar ratio of labeled Fab: antibody)] for 5min at r.t., followed by incubation with 5ul blocking reagent for an additional 5min at r.t., just prior to use. Zenon labeling with PE and

pacific blue were also successful when using this Ab to detect IFN-α via ICCS. Cells were washed 2 times with wash buffer, followed by once in PBS, and resuspended in 100ul PBS. Samples were acquired on an LSRII instrument (BD, San Jose, CA), and data were analyzed using FlowJo software (TreeStar, Ashland, OR).

Native Western for IRF-3

Collect cells in native lysis buffer (50mM Tris-Cl, pH 8, 150mM NaCl, 1% NP40) plus freshly added inhibitors (protease and phosphatase); approximately 100ul buffer for $2x10^6$ cells, but should be determined empirically. Resuspend via vortexing and pipetting up and down, and always keep at 4C or on ice.

For native IRF-3 western analysis, prepare separate running buffers for the lower chamber (25mM Tris-Cl pH 6.8, 192mM glycine) and the upper chamber [25mM Tris-Cl pH 8.4, 192mM glycine, 1% deoxycholate (DOC) (Sigma, D 6750)]. The upper chamber buffer should be pH'd after addition of DOC. Use pre-cast 7.5% READY GELS (BioRad) (7.5% Acrylamide/bis=29/1; .375 M Tris-Cl, pH 8,8, NO SDS). Pre-run the gel at a constant current (40mA) for 30min at 4C. Make sure the buffers aren't leaking; to ensure a proper seal and that the upper and lower buffers don't mix, use KY lubricant along the gel bottom and sides before clamping it into the BioRad running box. Keep buffers and pre-cast gels at 4C and always use buffers that are < 3months old.

Mix native lysate with n equal amount of 2x native loading buffer (125mM Tris-Cl pH 6.8, 30% glycerol, BPB), and load into gel (maximum of ~30ul per well in 10well-do

not overload). Run gel at 4C using a constant current (40mA) for 50minutes, or until the dye reaches the bottom of the gel.

Soak the gel in SDS electrophoresis buffer for 30minutes at r.t. prior to transfer. This removes the DOC that may inhibit protein transfer (particularly the monomeric form of IRF-3). Transfer gel to PVDF membrane (remember to equilibrate the membrane in methanol first) that has been equilibrated in semi-dry transfer buffer (18.6mM Tris, 143 mM glycine, 20% methanol) for 15min at r.t. Perform a semi-dry transfer for 60min at 100mA. Proceed with blocking (5% milk/TBS) for 1h at r.t. and incubation with anti-IRF-3 pAb (FL-423, Santa Cruz) (1:750) O/N at 4C. Wash membrane in TBST (3x5min) and incubate with secondary anti-rabbit IgG-HRP (1:2000) (1h, r.t.) wash in TBST (5x5min), and detect via chemiluminescence. There should be 2 bands in each lane, the lower band is the monomeric form of IRF-3 and the upper band is dimerized IRF-3.

Luminex Analysis

Plasma samples (~1ml) were saved and aliquoted (50ul or 100ul per tube) during the collection of PBMCs, and stored at -80C. For luminex analysis, follow kit protocol (milliplex NHP-plex) using 25ul plasma per well, and perform in duplicate. Make sure the bottom of the luminex plate does not touch anything during the staining and washing of the procedure (tape another 96well lid on the bottom of the plate to assure the liquid does not get wicked out of the wells).

REFERENCES

1. **Ablasser, A., F. Bauernfeind, G. Hartmann, E. Latz, K. A. Fitzgerald, and V. Hornung.** 2009. RIG-I-dependent sensing of poly(dA:dT) through the induction of an RNA polymerase III-transcribed RNA intermediate. Nat Immunol **10:**1065-72.
2. **Agalioti, T., S. Lomvardas, B. Parekh, J. Yie, T. Maniatis, and D. Thanos.** 2000. Ordered recruitment of chromatin modifying and general transcription factors to the IFN-beta promoter. Cell **103:**667-78.
3. **Ahmad, R., S. El Bassam, P. Cordeiro, and J. Menezes.** 2008. Requirement of TLR2-mediated signaling for the induction of IL-15 gene expression in human monocytic cells by HSV-1. Blood **112:**2360-8.
4. **Akula, S. M., P. P. Naranatt, N. S. Walia, F. Z. Wang, B. Fegley, and B. Chandran.** 2003. Kaposi's sarcoma-associated herpesvirus (human herpesvirus 8) infection of human fibroblast cells occurs through endocytosis. J Virol **77:**7978-90.
5. **Akula, S. M., N. P. Pramod, F. Z. Wang, and B. Chandran.** 2001. Human herpesvirus 8 envelope-associated glycoprotein B interacts with heparan sulfate-like moieties. Virology **284:**235-49.
6. **Akula, S. M., N. P. Pramod, F. Z. Wang, and B. Chandran.** 2002. Integrin alpha3beta1 (CD 49c/29) is a cellular receptor for Kaposi's sarcoma-associated herpesvirus (KSHV/HHV-8) entry into the target cells. Cell **108:**407-19.
7. **Alexander, L., L. Denekamp, A. Knapp, M. R. Auerbach, B. Damania, and R. C. Desrosiers.** 2000. The primary sequence of rhesus monkey rhadinovirus isolate 26-95: sequence similarities to Kaposi's sarcoma-associated herpesvirus and rhesus monkey rhadinovirus isolate 17577. J Virol **74:**3388-98.
8. **Ambroziak, J. A., D. J. Blackbourn, B. G. Herndier, R. G. Glogau, J. H. Gullett, A. R. McDonald, E. T. Lennette, and J. A. Levy.** 1995. Herpes-like sequences in HIV-infected and uninfected Kaposi's sarcoma patients. Science **268:**582-3.
9. **Aoki, Y., E. S. Jaffe, Y. Chang, K. Jones, J. Teruya-Feldstein, P. S. Moore, and G. Tosato.** 1999. Angiogenesis and hematopoiesis induced by Kaposi's sarcoma-associated herpesvirus-encoded interleukin-6. Blood **93:**4034-43.
10. **Areste, C., and D. J. Blackbourn.** 2009. Modulation of the immune system by Kaposi's sarcoma-associated herpesvirus. Trends Microbiol **17:**119-29.
11. **Arora, A., E. Chiao, and S. K. Tyring.** 2007. AIDS malignancies. Cancer Treat Res **133:**21-67.
12. **AuCoin, D. P., K. S. Colletti, Y. Xu, S. A. Cei, and G. S. Pari.** 2002. Kaposi's sarcoma-associated herpesvirus (human herpesvirus 8) contains two functional lytic origins of DNA replication. J Virol **76:**7890-6.
13. **Ballestas, M. E., and K. M. Kaye.** 2001. Kaposi's sarcoma-associated herpesvirus latency-associated nuclear antigen 1 mediates episome persistence through cis-acting terminal repeat (TR) sequence and specifically binds TR DNA. J Virol **75:**3250-8.
14. **Bechtel, J., A. Grundhoff, and D. Ganem.** 2005. RNAs in the virion of Kaposi's sarcoma-associated herpesvirus. J Virol **79:**10138-46.
15. **Beral, V., T. A. Peterman, R. L. Berkelman, and H. W. Jaffe.** 1990. Kaposi's sarcoma among persons with AIDS: a sexually transmitted infection? Lancet **335:**123-8.
16. **Bergquam, E. P., N. Avery, S. M. Shiigi, M. K. Axthelm, and S. W. Wong.** 1999. Rhesus rhadinovirus establishes a latent infection in B lymphocytes in vivo. J Virol **73:**7874-6.

17. **Bhattacharya, S., R. Eckner, S. Grossman, E. Oldread, Z. Arany, A. D'Andrea, and D. M. Livingston.** 1996. Cooperation of Stat2 and p300/CBP in signalling induced by interferon-alpha. Nature **383:**344-7.
18. **Bilello, J. P., S. M. Lang, F. Wang, J. C. Aster, and R. C. Desrosiers.** 2006. Infection and persistence of rhesus monkey rhadinovirus in immortalized B-cell lines. J Virol **80:**3644-9.
19. **Birkmann, A., K. Mahr, A. Ensser, S. Yaguboglu, F. Titgemeyer, B. Fleckenstein, and F. Neipel.** 2001. Cell surface heparan sulfate is a receptor for human herpesvirus 8 and interacts with envelope glycoprotein K8.1. J Virol **75:**11583-93.
20. **Biron, C. A., K. B. Nguyen, G. C. Pien, L. P. Cousens, and T. P. Salazar-Mather.** 1999. Natural killer cells in antiviral defense: function and regulation by innate cytokines. Annu Rev Immunol **17:**189-220.
21. **Bisson, S. A., A. L. Page, and D. Ganem.** 2009. A Kaposi's sarcoma-associated herpesvirus protein that forms inhibitory complexes with type I interferon receptor subunits, Jak and STAT proteins, and blocks interferon-mediated signal transduction. J Virol **83:**5056-66.
22. **Blasig, C., C. Zietz, B. Haar, F. Neipel, S. Esser, N. H. Brockmeyer, E. Tschachler, S. Colombini, B. Ensoli, and M. Sturzl.** 1997. Monocytes in Kaposi's sarcoma lesions are productively infected by human herpesvirus 8. J Virol **71:**7963-8.
23. **Boehme, K. W., M. Guerrero, and T. Compton.** 2006. Human cytomegalovirus envelope glycoproteins B and H are necessary for TLR2 activation in permissive cells. J Immunol **177:**7094-102.
24. **Boehmer, P. E., and I. R. Lehman.** 1997. Herpes simplex virus DNA replication. Annu Rev Biochem **66:**347-84.
25. **Boshoff, C., T. F. Schulz, M. M. Kennedy, A. K. Graham, C. Fisher, A. Thomas, J. O. McGee, R. A. Weiss, and J. J. O'Leary.** 1995. Kaposi's sarcoma-associated herpesvirus infects endothelial and spindle cells. Nat Med **1:**1274-8.
26. **Bowie, A. G., and L. Unterholzner.** 2008. Viral evasion and subversion of pattern-recognition receptor signalling. Nat Rev Immunol **8:**911-22.
27. **Boyne, J. R., and A. Whitehouse.** 2006. gamma-2 Herpes virus post-transcriptional gene regulation. Clin Microbiol Infect **12:**110-7.
28. **Brown, K. N., and S. M. Barratt-Boyes.** 2009. Surface phenotype and rapid quantification of blood dendritic cell subsets in the rhesus macaque. J Med Primatol **38:**272-8.
29. **Bryant, M. L., P. A. Marx, S. M. Shiigi, B. J. Wilson, W. P. McNulty, and M. B. Gardner.** 1986. Distribution of type D retrovirus sequences in tissues of macaques with simian acquired immune deficiency and retroperitoneal fibromatosis. Virology **150:**149-60.
30. **Burysek, L., and P. M. Pitha.** 2001. Latently expressed human herpesvirus 8-encoded interferon regulatory factor 2 inhibits double-stranded RNA-activated protein kinase. J Virol **75:**2345-52.
31. **Burysek, L., W. S. Yeow, B. Lubyova, M. Kellum, S. L. Schafer, Y. Q. Huang, and P. M. Pitha.** 1999. Functional analysis of human herpesvirus 8-encoded viral interferon regulatory factor 1 and its association with cellular interferon regulatory factors and p300. J Virol **73:**7334-42.
32. **Burysek, L., W. S. Yeow, and P. M. Pitha.** 1999. Unique properties of a second human herpesvirus 8-encoded interferon regulatory factor (vIRF-2). J Hum Virol **2:**19-32.
33. **Carbone, A., E. Cesarman, M. Spina, A. Gloghini, and T. F. Schulz.** 2009. HIV-associated lymphomas and gamma-herpesviruses. Blood **113:**1213-24.

34. **Casper, C., E. Krantz, S. Selke, S. R. Kuntz, J. Wang, M. L. Huang, J. S. Pauk, L. Corey, and A. Wald.** 2007. Frequent and asymptomatic oropharyngeal shedding of human herpesvirus 8 among immunocompetent men. J Infect Dis **195:**30-6.
35. **Casper, C., and A. Wald.** 2007. The use of antiviral drugs in the prevention and treatment of Kaposi sarcoma, multicentric Castleman disease and primary effusion lymphoma. Curr Top Microbiol Immunol **312:**289-307.
36. **Cesarman, E.** 2002. The role of Kaposi's sarcoma-associated herpesvirus (KSHV/HHV-8) in lymphoproliferative diseases. Recent Results Cancer Res **159:**27-37.
37. **Cesarman, E., Y. Chang, P. S. Moore, J. W. Said, and D. M. Knowles.** 1995. Kaposi's sarcoma-associated herpesvirus-like DNA sequences in AIDS-related body-cavity-based lymphomas. N Engl J Med **332:**1186-91.
38. **Chadburn, A., E. M. Hyjek, W. Tam, Y. Liu, T. Rengifo, E. Cesarman, and D. M. Knowles.** 2008. Immunophenotypic analysis of the Kaposi sarcoma herpesvirus (KSHV; HHV-8)-infected B cells in HIV+ multicentric Castleman disease (MCD). Histopathology **53:**513-24.
39. **Chan, S. R., C. Bloomer, and B. Chandran.** 1998. Identification and characterization of human herpesvirus-8 lytic cycle-associated ORF 59 protein and the encoding cDNA by monoclonal antibody. Virology **240:**118-26.
40. **Chang, H., L. M. Wachtman, C. B. Pearson, J. S. Lee, H. R. Lee, S. H. Lee, J. Vieira, K. G. Mansfield, and J. U. Jung.** 2009. Non-human primate model of Kaposi's sarcoma-associated herpesvirus infection. PLoS Pathog **5:**e1000606.
41. **Chang, Y., E. Cesarman, M. S. Pessin, F. Lee, J. Culpepper, D. M. Knowles, and P. S. Moore.** 1994. Identification of herpesvirus-like DNA sequences in AIDS-associated Kaposi's sarcoma. Science **266:**1865-9.
42. **Chatterjee, M., J. Osborne, G. Bestetti, Y. Chang, and P. S. Moore.** 2002. Viral IL-6-induced cell proliferation and immune evasion of interferon activity. Science **298:**1432-5.
43. **Chen, J., K. Ueda, S. Sakakibara, T. Okuno, and K. Yamanishi.** 2000. Transcriptional regulation of the Kaposi's sarcoma-associated herpesvirus viral interferon regulatory factor gene. J Virol **74:**8623-34.
44. **Chiu, Y. H., J. B. Macmillan, and Z. J. Chen.** 2009. RNA polymerase III detects cytosolic DNA and induces type I interferons through the RIG-I pathway. Cell **138:**576-91.
45. **Choi, Y. B., and J. Nicholas.** 2008. Autocrine and paracrine promotion of cell survival and virus replication by human herpesvirus 8 chemokines. J Virol **82:**6501-13.
46. **Choi, Y. B., and J. Nicholas.** 2010. Bim nuclear translocation and inactivation by viral interferon regulatory factor. PLoS Pathog **6**.
47. **Chung, E., S. B. Amrute, K. Abel, G. Gupta, Y. Wang, C. J. Miller, and P. Fitzgerald-Bocarsly.** 2005. Characterization of virus-responsive plasmacytoid dendritic cells in the rhesus macaque. Clin Diagn Lab Immunol **12:**426-35.
48. **Coates, P. T., S. M. Barratt-Boyes, L. Zhang, V. S. Donnenberg, P. J. O'Connell, A. J. Logar, F. J. Duncan, M. Murphey-Corb, A. D. Donnenberg, A. E. Morelli, C. R. Maliszewski, and A. W. Thomson.** 2003. Dendritic cell subsets in blood and lymphoid tissue of rhesus monkeys and their mobilization with Flt3 ligand. Blood **102:**2513-21.
49. **Cohen, J. I., S. E. Straus, and A. M. Arvin.** 2007. Varicella-Zoster Virus Replication, Pathogenesisi, and Management, 5th ed. Wolters Kluwer Health/Lippincott Williams & Wilkins, Philadelphia.

50. **Compton, T., E. A. Kurt-Jones, K. W. Boehme, J. Belko, E. Latz, D. T. Golenbock, and R. W. Finberg.** 2003. Human cytomegalovirus activates inflammatory cytokine responses via CD14 and Toll-like receptor 2. J Virol **77:**4588-96.
51. **Coscoy, L.** 2007. Immune evasion by Kaposi's sarcoma-associated herpesvirus. Nat Rev Immunol **7:**391-401.
52. **Cunningham, C., S. Barnard, D. J. Blackbourn, and A. J. Davison.** 2003. Transcription mapping of human herpesvirus 8 genes encoding viral interferon regulatory factors. J Gen Virol **84:**1471-83.
53. **Dai, J., N. J. Megjugorac, S. B. Amrute, and P. Fitzgerald-Bocarsly.** 2004. Regulation of IFN regulatory factor-7 and IFN-alpha production by enveloped virus and lipopolysaccharide in human plasmacytoid dendritic cells. J Immunol **173:**1535-48.
54. **Damania, B., and R. C. Desrosiers.** 2001. Simian homologues of human herpesvirus 8. Philos Trans R Soc Lond B Biol Sci **356:**535-43.
55. **Decker, L. L., P. Shankar, G. Khan, R. B. Freeman, B. J. Dezube, J. Lieberman, and D. A. Thorley-Lawson.** 1996. The Kaposi sarcoma-associated herpesvirus (KSHV) is present as an intact latent genome in KS tissue but replicates in the peripheral blood mononuclear cells of KS patients. J Exp Med **184:**283-8.
56. **DeFilippis, V. R., D. Alvarado, T. Sali, S. Rothenburg, and K. Fruh.** 2010. Human cytomegalovirus induces the interferon response via the DNA sensor ZBP1. J Virol **84:**585-98.
57. **Der, S. D., A. Zhou, B. R. Williams, and R. H. Silverman.** 1998. Identification of genes differentially regulated by interferon alpha, beta, or gamma using oligonucleotide arrays. Proc Natl Acad Sci U S A **95:**15623-8.
58. **Desrosiers, R. C., V. G. Sasseville, S. C. Czajak, X. Zhang, K. G. Mansfield, A. Kaur, R. P. Johnson, A. A. Lackner, and J. U. Jung.** 1997. A herpesvirus of rhesus monkeys related to the human Kaposi's sarcoma-associated herpesvirus. J Virol **71:**9764-9.
59. **DeWire, S. M., E. S. Money, S. P. Krall, and B. Damania.** 2003. Rhesus monkey rhadinovirus (RRV): construction of a RRV-GFP recombinant virus and development of assays to assess viral replication. Virology **312:**122-34.
60. **Di Lorenzo, G., P. A. Konstantinopoulos, L. Pantanowitz, R. Di Trolio, S. De Placido, and B. J. Dezube.** 2007. Management of AIDS-related Kaposi's sarcoma. Lancet Oncol **8:**167-76.
61. **Dittmer, D., C. Stoddart, R. Renne, V. Linquist-Stepps, M. E. Moreno, C. Bare, J. M. McCune, and D. Ganem.** 1999. Experimental transmission of Kaposi's sarcoma-associated herpesvirus (KSHV/HHV-8) to SCID-hu Thy/Liv mice. J Exp Med **190:**1857-68.
62. **Dittmer, D. P.** 2003. Transcription profile of Kaposi's sarcoma-associated herpesvirus in primary Kaposi's sarcoma lesions as determined by real-time PCR arrays. Cancer Res **63:**2010-5.
63. **Dittmer, D. P., C. M. Gonzalez, W. Vahrson, S. M. DeWire, R. Hines-Boykin, and B. Damania.** 2005. Whole-genome transcription profiling of rhesus monkey rhadinovirus. J Virol **79:**8637-50.
64. **Donnelly, R. P., and S. V. Kotenko.** 2010. Interferon-lambda: a new addition to an old family. J Interferon Cytokine Res **30:**555-64.
65. **Edelman, D. C.** 2005. Human herpesvirus 8--a novel human pathogen. Virol J **2:**78.
66. **Eroshkin, A., and A. Mushegian.** 1999. Conserved transactivation domain shared by interferon regulatory factors and Smad morphogens. J Mol Med **77:**403-5.
67. **Esteban, M., M. A. Garcia, E. Domingo-Gil, J. Arroyo, C. Nombela, and C. Rivas.** 2003. The latency protein LANA2 from Kaposi's sarcoma-associated herpesvirus inhibits

apoptosis induced by dsRNA-activated protein kinase but not RNase L activation. J Gen Virol **84:**1463-70.

68. **Estep, R. D., M. K. Axthelm, and S. W. Wong.** 2003. A G protein-coupled receptor encoded by rhesus rhadinovirus is similar to ORF74 of Kaposi's sarcoma-associated herpesvirus. J Virol **77:**1738-46.
69. **Estep, R. D., M. F. Powers, B. K. Yen, H. Li, and S. W. Wong.** 2007. Construction of an infectious rhesus rhadinovirus bacterial artificial chromosome for the analysis of Kaposi's sarcoma-associated herpesvirus-related disease development. J Virol **81:**2957-69.
70. **Everett, R. D.** 2001. DNA viruses and viral proteins that interact with PML nuclear bodies. Oncogene **20:**7266-73.
71. **Fang, S., J. P. Jensen, R. L. Ludwig, K. H. Vousden, and A. M. Weissman.** 2000. Mdm2 is a RING finger-dependent ubiquitin protein ligase for itself and p53. J Biol Chem **275:**8945-51.
72. **Feldman, S. B., M. Ferraro, H. M. Zheng, N. Patel, S. Gould-Fogerite, and P. Fitzgerald-Bocarsly.** 1994. Viral induction of low frequency interferon-alpha producing cells. Virology **204:**1-7.
73. **Fensterl, V., and G. C. Sen.** 2009. Interferons and viral infections. Biofactors **35:**14-20.
74. **Fiola, S., D. Gosselin, K. Takada, and J. Gosselin.** 2010. TLR9 contributes to the recognition of EBV by primary monocytes and plasmacytoid dendritic cells. J Immunol **185:**3620-31.
75. **Fitzgerald-Bocarsly, P., J. Dai, and S. Singh.** 2008. Plasmacytoid dendritic cells and type I IFN: 50 years of convergent history. Cytokine Growth Factor Rev **19:**3-19.
76. **Flowers, C. C., S. P. Flowers, and G. J. Nabel.** 1998. Kaposi's sarcoma-associated herpesvirus viral interferon regulatory factor confers resistance to the antiproliferative effect of interferon-alpha. Mol Med **4:**402-12.
77. **Foreman, K. E., J. Friborg, B. Chandran, H. Katano, T. Sata, M. Mercader, G. J. Nabel, and B. J. Nickoloff.** 2001. Injection of human herpesvirus-8 in human skin engrafted on SCID mice induces Kaposi's sarcoma-like lesions. J Dermatol Sci **26:**182-93.
78. **Foster-Cuevas, M., G. J. Wright, M. J. Puklavec, M. H. Brown, and A. N. Barclay.** 2004. Human herpesvirus 8 K14 protein mimics CD200 in down-regulating macrophage activation through CD200 receptor. J Virol **78:**7667-76.
79. **Friedman-Kien, A. E.** 1981. Disseminated Kaposi's sarcoma syndrome in young homosexual men. J Am Acad Dermatol **5:**468-71.
80. **Fuld, S., C. Cunningham, K. Klucher, A. J. Davison, and D. J. Blackbourn.** 2006. Inhibition of interferon signaling by the Kaposi's sarcoma-associated herpesvirus full-length viral interferon regulatory factor 2 protein. J Virol **80:**3092-7.
81. **Ganem, D.** 2007. Kaposi's Sarcoma-associated Herpesvirus, 5th ed. Wolters Kluwer Health/Lippincott Williams & Wilkins, Philadelphia.
82. **Gao, S. J., C. Boshoff, S. Jayachandra, R. A. Weiss, Y. Chang, and P. S. Moore.** 1997. KSHV ORF K9 (vIRF) is an oncogene which inhibits the interferon signaling pathway. Oncogene **15:**1979-85.
83. **Gao, S. J., L. Kingsley, M. Li, W. Zheng, C. Parravicini, J. Ziegler, R. Newton, C. R. Rinaldo, A. Saah, J. Phair, R. Detels, Y. Chang, and P. S. Moore.** 1996. KSHV antibodies among Americans, Italians and Ugandans with and without Kaposi's sarcoma. Nat Med **2:**925-8.

84. **Genin, P., R. Lin, J. Hiscott, and A. Civas.** 2009. Differential regulation of human interferon A gene expression by interferon regulatory factors 3 and 7. Mol Cell Biol **29:**3435-50.
85. **Giddens, W. E., Jr., C. C. Tsai, W. R. Morton, H. D. Ochs, G. H. Knitter, and G. A. Blakley.** 1985. Retroperitoneal fibromatosis and acquired immunodeficiency syndrome in macaques. Pathologic observations and transmission studies. Am J Pathol **119:**253-63.
86. **Giese, N. A., L. Gabriele, T. M. Doherty, D. M. Klinman, L. Tadesse-Heath, C. Contursi, S. L. Epstein, and H. C. Morse, 3rd.** 1997. Interferon (IFN) consensus sequence-binding protein, a transcription factor of the IFN regulatory factor family, regulates immune responses in vivo through control of interleukin 12 expression. J Exp Med **186:**1535-46.
87. **Gitlin, L., W. Barchet, S. Gilfillan, M. Cella, B. Beutler, R. A. Flavell, M. S. Diamond, and M. Colonna.** 2006. Essential role of mda-5 in type I IFN responses to polyriboinosinic:polyribocytidylic acid and encephalomyocarditis picornavirus. Proc Natl Acad Sci U S A **103:**8459-64.
88. **Greene, W., and S. J. Gao.** 2009. Actin dynamics regulate multiple endosomal steps during Kaposi's sarcoma-associated herpesvirus entry and trafficking in endothelial cells. PLoS Pathog **5:**e1000512.
89. **Greene, W., K. Kuhne, F. Ye, J. Chen, F. Zhou, X. Lei, and S. J. Gao.** 2007. Molecular biology of KSHV in relation to AIDS-associated oncogenesis. Cancer Treat Res **133:**69-127.
90. **Grossman, Z., J. Iscovich, F. Schwartz, E. Azizi, A. Klepfish, A. Schattner, and R. Sarid.** 2002. Absence of Kaposi sarcoma among Ethiopian immigrants to Israel despite high seroprevalence of human herpesvirus 8. Mayo Clin Proc **77:**905-9.
91. **Guggemoos, S., D. Hangel, S. Hamm, A. Heit, S. Bauer, and H. Adler.** 2008. TLR9 contributes to antiviral immunity during gammaherpesvirus infection. J Immunol **180:**438-43.
92. **Hahn, A. M., L. E. Huye, S. Ning, J. Webster-Cyriaque, and J. S. Pagano.** 2005. Interferon regulatory factor 7 is negatively regulated by the Epstein-Barr virus immediate-early gene, BZLF-1. J Virol **79:**10040-52.
93. **Hervas-Stubbs, S., J. L. Perez-Gracia, A. Rouzaut, M. F. Sanmamed, A. Le Bon, and I. Melero.** 2011. Direct effects of type I interferons on cells of the immune system. Clin Cancer Res **17:**2619-27.
94. **Honda, K., and T. Taniguchi.** 2006. IRFs: master regulators of signalling by Toll-like receptors and cytosolic pattern-recognition receptors. Nat Rev Immunol **6:**644-58.
95. **Honda, K., H. Yanai, H. Negishi, M. Asagiri, M. Sato, T. Mizutani, N. Shimada, Y. Ohba, A. Takaoka, N. Yoshida, and T. Taniguchi.** 2005. IRF-7 is the master regulator of type-I interferon-dependent immune responses. Nature **434:**772-7.
96. **Honda, R., and H. Yasuda.** 2000. Activity of MDM2, a ubiquitin ligase, toward p53 or itself is dependent on the RING finger domain of the ligase. Oncogene **19:**1473-6.
97. **Honess, R. W., and B. Roizman.** 1974. Regulation of herpesvirus macromolecular synthesis. I. Cascade regulation of the synthesis of three groups of viral proteins. J Virol **14:**8-19.
98. **Horvai, A. E., L. Xu, E. Korzus, G. Brard, D. Kalafus, T. M. Mullen, D. W. Rose, M. G. Rosenfeld, and C. K. Glass.** 1997. Nuclear integration of JAK/STAT and Ras/AP-1 signaling by CBP and p300. Proc Natl Acad Sci U S A **94:**1074-9.

99. **Hu, F., and J. Nicholas.** 2006. Signal transduction by human herpesvirus 8 viral interleukin-6 (vIL-6) is modulated by the nonsignaling gp80 subunit of the IL-6 receptor complex and is distinct from signaling induced by human IL-6. J Virol **80:**10874-8.
100. **Huber, J. P., and J. D. Farrar.** 2011. Regulation of effector and memory T-cell functions by type I interferon. Immunology **132:**466-74.
101. **Isaacs, A., and J. Lindenmann.** 1957. Virus interference. I. The interferon. Proc R Soc Lond B Biol Sci **147:**258-67.
102. **Ito, T., R. Amakawa, M. Inaba, S. Ikehara, K. Inaba, and S. Fukuhara.** 2001. Differential regulation of human blood dendritic cell subsets by IFNs. J Immunol **166:**2961-9.
103. **Iwamura, T., M. Yoneyama, K. Yamaguchi, W. Suhara, W. Mori, K. Shiota, Y. Okabe, H. Namiki, and T. Fujita.** 2001. Induction of IRF-3/-7 kinase and NF-kappaB in response to double-stranded RNA and virus infection: common and unique pathways. Genes Cells **6:**375-88.
104. **Jacobson, L. P., T. E. Yamashita, R. Detels, J. B. Margolick, J. S. Chmiel, L. A. Kingsley, S. Melnick, and A. Munoz.** 1999. Impact of potent antiretroviral therapy on the incidence of Kaposi's sarcoma and non-Hodgkin's lymphomas among HIV-1-infected individuals. Multicenter AIDS Cohort Study. J Acquir Immune Defic Syndr **21 Suppl 1:**S34-41.
105. **Janeway, C. A., Jr., P. Travers, M. Walport, and S. M.J.** 2004. Immunobiology: The Immune System in Health and Disease. Garland Publishing.
106. **Jayachandra, S., K. G. Low, A. E. Thlick, J. Yu, P. D. Ling, Y. Chang, and P. S. Moore.** 1999. Three unrelated viral transforming proteins (vIRF, EBNA2, and E1A) induce the MYC oncogene through the interferon-responsive PRF element by using different transcription coadaptors. Proc Natl Acad Sci U S A **96:**11566-71.
107. **Jenner, R. G., M. M. Alba, C. Boshoff, and P. Kellam.** 2001. Kaposi's sarcoma-associated herpesvirus latent and lytic gene expression as revealed by DNA arrays. J Virol **75:**891-902.
108. **Johnson, K. E., and D. M. Knipe.** 2010. Herpes simplex virus-1 infection causes the secretion of a type I interferon-antagonizing protein and inhibits signaling at or before Jak-1 activation. Virology **396:**21-9.
109. **Johnson, K. E., B. Song, and D. M. Knipe.** 2008. Role for herpes simplex virus 1 ICP27 in the inhibition of type I interferon signaling. Virology **374:**487-94.
110. **Jones, K. D., Y. Aoki, Y. Chang, P. S. Moore, R. Yarchoan, and G. Tosato.** 1999. Involvement of interleukin-10 (IL-10) and viral IL-6 in the spontaneous growth of Kaposi's sarcoma herpesvirus-associated infected primary effusion lymphoma cells. Blood **94:**2871-9.
111. **Joo, C. H., Y. C. Shin, M. Gack, L. Wu, D. Levy, and J. U. Jung.** 2007. Inhibition of interferon regulatory factor 7 (IRF7)-mediated interferon signal transduction by the Kaposi's sarcoma-associated herpesvirus viral IRF homolog vIRF3. J Virol **81:**8282-92.
112. **Juang, Y. T., W. Lowther, M. Kellum, W. C. Au, R. Lin, J. Hiscott, and P. M. Pitha.** 1998. Primary activation of interferon A and interferon B gene transcription by interferon regulatory factor 3. Proc Natl Acad Sci U S A **95:**9837-42.
113. **Kaleeba, J. A., E. P. Bergquam, and S. W. Wong.** 1999. A rhesus macaque rhadinovirus related to Kaposi's sarcoma-associated herpesvirus/human herpesvirus 8 encodes a functional homologue of interleukin-6. J Virol **73:**6177-81.
114. **Kaposi, M.** 1872. Idiopathisches multiples pigmentsarkom her haut. Arch Dermat Schypilol**:**265-273.

115. **Kawai, T., and S. Akira.** 2010. The role of pattern-recognition receptors in innate immunity: update on Toll-like receptors. Nat Immunol **11:**373-84.
116. **Kennedy, P. G., and R. J. Cohrs.** 2010. Varicella-zoster virus human ganglionic latency: a current summary. J Neurovirol **16:**411-8.
117. **Kerur, N., M. V. Veettil, N. Sharma-Walia, V. Bottero, S. Sadagopan, P. Otageri, and B. Chandran.** 2011. IFI16 Acts as a Nuclear Pathogen Sensor to Induce the Inflammasome in Response to Kaposi Sarcoma-Associated Herpesvirus Infection. Cell Host Microbe **9:**363-75.
118. **Ketloy, C., A. Engering, U. Srichairatanakul, A. Limsalakpetch, K. Yongvanitchit, S. Pichyangkul, and K. Ruxrungtham.** 2008. Expression and function of Toll-like receptors on dendritic cells and other antigen presenting cells from non-human primates. Vet Immunol Immunopathol **125:**18-30.
119. **Kim, T., S. Pazhoor, M. Bao, Z. Zhang, S. Hanabuchi, V. Facchinetti, L. Bover, J. Plumas, L. Chaperot, J. Qin, and Y. J. Liu.** 2010. Aspartate-glutamate-alanine-histidine box motif (DEAH)/RNA helicase A helicases sense microbial DNA in human plasmacytoid dendritic cells. Proc Natl Acad Sci U S A **107:**15181-6.
120. **Kirchhoff, S., T. Sebens, S. Baumann, A. Krueger, R. Zawatzky, M. Li-Weber, E. Meinl, F. Neipel, B. Fleckenstein, and P. H. Krammer.** 2002. Viral IFN-regulatory factors inhibit activation-induced cell death via two positive regulatory IFN-regulatory factor 1-dependent domains in the CD95 ligand promoter. J Immunol **168:**1226-34.
121. **Kirchoff, V., S. Wong, J. S. St, and G. S. Pari.** 2002. Generation of a life-expanded rhesus monkey fibroblast cell line for the growth of rhesus rhadinovirus (RRV). Arch Virol **147:**321-33.
122. **Koyama, S., K. J. Ishii, C. Coban, and S. Akira.** 2008. Innate immune response to viral infection. Cytokine **43:**336-41.
123. **Krausgruber, T., D. Saliba, G. Ryzhakov, A. Lanfrancotti, K. Blazek, and I. A. Udalova.** 2010. IRF5 is required for late-phase TNF secretion by human dendritic cells. Blood **115:**4421-30.
124. **Krug, A., G. D. Luker, W. Barchet, D. A. Leib, S. Akira, and M. Colonna.** 2004. Herpes simplex virus type 1 activates murine natural interferon-producing cells through toll-like receptor 9. Blood **103:**1433-7.
125. **Kumar, H., T. Kawai, and S. Akira.** 2011. Pathogen recognition by the innate immune system. Int Rev Immunol **30:**16-34.
126. **Kurt-Jones, E. A., M. Chan, S. Zhou, J. Wang, G. Reed, R. Bronson, M. M. Arnold, D. M. Knipe, and R. W. Finberg.** 2004. Herpes simplex virus 1 interaction with Toll-like receptor 2 contributes to lethal encephalitis. Proc Natl Acad Sci U S A **101:**1315-20.
127. **Lagos, D., M. W. Trotter, R. J. Vart, H. W. Wang, N. C. Matthews, A. Hansen, O. Flore, F. Gotch, and C. Boshoff.** 2007. Kaposi sarcoma herpesvirus-encoded vFLIP and vIRF1 regulate antigen presentation in lymphatic endothelial cells. Blood **109:**1550-8.
128. **Lagos, D., R. J. Vart, F. Gratrix, S. J. Westrop, V. Emuss, P. P. Wong, R. Robey, N. Imami, M. Bower, F. Gotch, and C. Boshoff.** 2008. Toll-like receptor 4 mediates innate immunity to Kaposi sarcoma herpesvirus. Cell Host Microbe **4:**470-83.
129. **Langlais, C. L., J. M. Jones, R. D. Estep, and S. W. Wong.** 2006. Rhesus rhadinovirus R15 encodes a functional homologue of human CD200. J Virol **80:**3098-103.
130. **Lee, E. C., D. Yu, J. Martinez de Velasco, L. Tessarollo, D. A. Swing, D. L. Court, N. A. Jenkins, and N. G. Copeland.** 2001. A highly efficient Escherichia coli-based chromosome engineering system adapted for recombinogenic targeting and subcloning of BAC DNA. Genomics **73:**56-65.

131. **Lee, H. R., Z. Toth, Y. C. Shin, J. S. Lee, H. Chang, W. Gu, T. K. Oh, M. H. Kim, and J. U. Jung.** 2009. Kaposi's sarcoma-associated herpesvirus viral interferon regulatory factor 4 targets MDM2 to deregulate the p53 tumor suppressor pathway. J Virol **83:**6739-47.
132. **Lefort, S., A. Soucy-Faulkner, N. Grandvaux, and L. Flamand.** 2007. Binding of Kaposi's sarcoma-associated herpesvirus K-bZIP to interferon-responsive factor 3 elements modulates antiviral gene expression. J Virol **81:**10950-60.
133. **Li, M., B. Damania, X. Alvarez, V. Ogryzko, K. Ozato, and J. U. Jung.** 2000. Inhibition of p300 histone acetyltransferase by viral interferon regulatory factor. Mol Cell Biol **20:**8254-63.
134. **Li, M., H. Lee, J. Guo, F. Neipel, B. Fleckenstein, K. Ozato, and J. U. Jung.** 1998. Kaposi's sarcoma-associated herpesvirus viral interferon regulatory factor. J Virol **72:**5433-40.
135. **Li, Q., R. Means, S. Lang, and J. U. Jung.** 2007. Downregulation of gamma interferon receptor 1 by Kaposi's sarcoma-associated herpesvirus K3 and K5. J Virol **81:**2117-27.
136. **Lin, R., P. Genin, Y. Mamane, and J. Hiscott.** 2000. Selective DNA binding and association with the CREB binding protein coactivator contribute to differential activation of alpha/beta interferon genes by interferon regulatory factors 3 and 7. Mol Cell Biol **20:**6342-53.
137. **Lin, R., P. Genin, Y. Mamane, M. Sgarbanti, A. Battistini, W. J. Harrington, Jr., G. N. Barber, and J. Hiscott.** 2001. HHV-8 encoded vIRF-1 represses the interferon antiviral response by blocking IRF-3 recruitment of the CBP/p300 coactivators. Oncogene **20:**800-11.
138. **Lin, R., C. Heylbroeck, P. M. Pitha, and J. Hiscott.** 1998. Virus-dependent phosphorylation of the IRF-3 transcription factor regulates nuclear translocation, transactivation potential, and proteasome-mediated degradation. Mol Cell Biol **18:**2986-96.
139. **Little, R. F., and R. Yarchoan.** 2003. Treatment of gammaherpesvirus-related neoplastic disorders in the immunosuppressed host. Semin Hematol **40:**163-71.
140. **Lubyova, B., M. J. Kellum, A. J. Frisancho, and P. M. Pitha.** 2004. Kaposi's sarcoma-associated herpesvirus-encoded vIRF-3 stimulates the transcriptional activity of cellular IRF-3 and IRF-7. J Biol Chem **279:**7643-54.
141. **Lubyova, B., M. J. Kellum, J. A. Frisancho, and P. M. Pitha.** 2007. Stimulation of c-Myc transcriptional activity by vIRF-3 of Kaposi sarcoma-associated herpesvirus. J Biol Chem **282:**31944-53.
142. **Lubyova, B., and P. M. Pitha.** 2000. Characterization of a novel human herpesvirus 8-encoded protein, vIRF-3, that shows homology to viral and cellular interferon regulatory factors. J Virol **74:**8194-201.
143. **Luft, T., K. C. Pang, E. Thomas, P. Hertzog, D. N. Hart, J. Trapani, and J. Cebon.** 1998. Type I IFNs enhance the terminal differentiation of dendritic cells. J Immunol **161:**1947-53.
144. **Lund, J., A. Sato, S. Akira, R. Medzhitov, and A. Iwasaki.** 2003. Toll-like receptor 9-mediated recognition of Herpes simplex virus-2 by plasmacytoid dendritic cells. J Exp Med **198:**513-20.
145. **Lund, J. M., M. M. Linehan, N. Iijima, and A. Iwasaki.** 2006. Cutting Edge: Plasmacytoid dendritic cells provide innate immune protection against mucosal viral infection in situ. J Immunol **177:**7510-4.
146. **Malmgaard, L.** 2004. Induction and regulation of IFNs during viral infections. J Interferon Cytokine Res **24:**439-54.

147. **Mansfield, K. G., S. V. Westmoreland, C. D. DeBakker, S. Czajak, A. A. Lackner, and R. C. Desrosiers.** 1999. Experimental infection of rhesus and pig-tailed macaques with macaque rhadinoviruses. J Virol **73:**10320-8.
148. **Marie, I., J. E. Durbin, and D. E. Levy.** 1998. Differential viral induction of distinct interferon-alpha genes by positive feedback through interferon regulatory factor-7. EMBO J **17:**6660-9.
149. **Mark, L., O. B. Spiller, M. Okroj, S. Chanas, J. A. Aitken, S. W. Wong, B. Damania, A. M. Blom, and D. J. Blackbourn.** 2007. Molecular characterization of the rhesus rhadinovirus (RRV) ORF4 gene and the RRV complement control protein it encodes. J Virol **81:**4166-76.
150. **Marrack, P., J. Kappler, and T. Mitchell.** 1999. Type I interferons keep activated T cells alive. J Exp Med **189:**521-30.
151. **Martin, J. N.** 2007. The epidemiology of KSHV and its association with malignant disease. Cambridge University Press.
152. **Maurer, T., M. Ponte, and K. Leslie.** 2007. HIV-associated Kaposi's sarcoma with a high CD4 count and a low viral load. N Engl J Med **357:**1352-3.
153. **Melchjorsen, J., J. Rintahaka, S. Soby, K. A. Horan, A. Poltajainen, L. Ostergaard, S. R. Paludan, and S. Matikainen.** 2010. Early innate recognition of herpes simplex virus in human primary macrophages is mediated via the MDA5/MAVS-dependent and MDA5/MAVS/RNA polymerase III-independent pathways. J Virol **84:**11350-8.
154. **Messaoudi, I., A. Barron, M. Wellish, F. Engelmann, A. Legasse, S. Planer, D. Gilden, J. Nikolich-Zugich, and R. Mahalingam.** 2009. Simian varicella virus infection of rhesus macaques recapitulates essential features of varicella zoster virus infection in humans. PLoS Pathog **5:**e1000657.
155. **Mettenleiter, T. C., B. G. Klupp, and H. Granzow.** 2009. Herpesvirus assembly: an update. Virus Res **143:**222-34.
156. **Miller, D. M., Y. Zhang, B. M. Rahill, W. J. Waldman, and D. D. Sedmak.** 1999. Human cytomegalovirus inhibits IFN-alpha-stimulated antiviral and immunoregulatory responses by blocking multiple levels of IFN-alpha signal transduction. J Immunol **162:**6107-13.
157. **Miyamoto, M., T. Fujita, Y. Kimura, M. Maruyama, H. Harada, Y. Sudo, T. Miyata, and T. Taniguchi.** 1988. Regulated expression of a gene encoding a nuclear factor, IRF-1, that specifically binds to IFN-beta gene regulatory elements. Cell **54:**903-13.
158. **Mocarski, E. S., T. Shenk, and R. F. Pass.** 2007. Cytomegaloviruses, 5th ed. Wolters Kluwer Health/Lippincott Williams & Wilkins, Philadelphia.
159. **Monini, P., S. Colombini, M. Sturzl, D. Goletti, A. Cafaro, C. Sgadari, S. Butto, M. Franco, P. Leone, S. Fais, G. Melucci-Vigo, C. Chiozzini, F. Carlini, G. Ascherl, E. Cornali, C. Zietz, E. Ramazzotti, F. Ensoli, M. Andreoni, P. Pezzotti, G. Rezza, R. Yarchoan, R. C. Gallo, and B. Ensoli.** 1999. Reactivation and persistence of human herpesvirus-8 infection in B cells and monocytes by Th-1 cytokines increased in Kaposi's sarcoma. Blood **93:**4044-58.
160. **Montaner, S., A. Sodhi, A. Molinolo, T. H. Bugge, E. T. Sawai, Y. He, Y. Li, P. E. Ray, and J. S. Gutkind.** 2003. Endothelial infection with KSHV genes in vivo reveals that vGPCR initiates Kaposi's sarcomagenesis and can promote the tumorigenic potential of viral latent genes. Cancer Cell **3:**23-36.
161. **Montoya, M., G. Schiavoni, F. Mattei, I. Gresser, F. Belardelli, P. Borrow, and D. F. Tough.** 2002. Type I interferons produced by dendritic cells promote their phenotypic and functional activation. Blood **99:**3263-71.

162. **Moore, P. S., C. Boshoff, R. A. Weiss, and Y. Chang.** 1996. Molecular mimicry of human cytokine and cytokine response pathway genes by KSHV. Science **274:**1739-44.
163. **Moore, P. S., S. J. Gao, G. Dominguez, E. Cesarman, O. Lungu, D. M. Knowles, R. Garber, P. E. Pellett, D. J. McGeoch, and Y. Chang.** 1996. Primary characterization of a herpesvirus agent associated with Kaposi's sarcomae. J Virol **70:**549-58.
164. **Nakamura, H., M. Li, J. Zarycki, and J. U. Jung.** 2001. Inhibition of p53 tumor suppressor by viral interferon regulatory factor. J Virol **75:**7572-82.
165. **Nguyen, K. B., T. P. Salazar-Mather, M. Y. Dalod, J. B. Van Deusen, X. Q. Wei, F. Y. Liew, M. A. Caligiuri, J. E. Durbin, and C. A. Biron.** 2002. Coordinated and distinct roles for IFN-alpha beta, IL-12, and IL-15 regulation of NK cell responses to viral infection. J Immunol **169:**4279-87.
166. **Nicholas, J., V. R. Ruvolo, W. H. Burns, G. Sandford, X. Wan, D. Ciufo, S. B. Hendrickson, H. G. Guo, G. S. Hayward, and M. S. Reitz.** 1997. Kaposi's sarcoma-associated human herpesvirus-8 encodes homologues of macrophage inflammatory protein-1 and interleukin-6. Nat Med **3:**287-92.
167. **Nishiyama, Y.** 2004. Herpes simplex virus gene products: the accessories reflect her lifestyle well. Rev Med Virol **14:**33-46.
168. **O'Connor, C. M., and D. H. Kedes.** 2006. Mass spectrometric analyses of purified rhesus monkey rhadinovirus reveal 33 virion-associated proteins. J Virol **80:**1574-83.
169. **O'Connor, C. M., and D. H. Kedes.** 2007. Rhesus monkey rhadinovirus: a model for the study of KSHV. Curr Top Microbiol Immunol **312:**43-69.
170. **Offermann, M. K.** 2007. Kaposi sarcoma herpesvirus-encoded interferon regulator factors. Curr Top Microbiol Immunol **312:**185-209.
171. **Orzechowska, B. U., M. Manoharan, J. Sprague, R. D. Estep, M. K. Axthelm, and S. W. Wong.** 2009. Viral interleukin-6 encoded by rhesus macaque rhadinovirus is associated with lymphoproliferative disorder (LPD). J Med Primatol **38 Suppl 1:**2-7.
172. **Orzechowska, B. U., M. F. Powers, J. Sprague, H. Li, B. Yen, R. P. Searles, M. K. Axthelm, and S. W. Wong.** 2008. Rhesus macaque rhadinovirus-associated non-Hodgkin lymphoma: animal model for KSHV-associated malignancies. Blood **112:**4227-34.
173. **Osborne, J., P. S. Moore, and Y. Chang.** 1999. KSHV-encoded viral IL-6 activates multiple human IL-6 signaling pathways. Hum Immunol **60:**921-7.
174. **Oxman, M. N.** 2010. Zoster vaccine: current status and future prospects. Clin Infect Dis **51:**197-213.
175. **Pahl, H. L.** 1999. Activators and target genes of Rel/NF-kappaB transcription factors. Oncogene **18:**6853-66.
176. **Paludan, S. R., A. G. Bowie, K. A. Horan, and K. A. Fitzgerald.** 2011. Recognition of herpesviruses by the innate immune system. Nat Rev Immunol **11:**143-54.
177. **Park, J., M. S. Lee, S. M. Yoo, K. W. Jeong, D. Lee, J. Choe, and T. Seo.** 2007. Identification of the DNA sequence interacting with Kaposi's sarcoma-associated herpesvirus viral interferon regulatory factor 1. J Virol **81:**12680-4.
178. **Park, J., T. Seo, S. Hwang, D. Lee, Y. Gwack, and J. Choe.** 2000. The K-bZIP protein from Kaposi's sarcoma-associated herpesvirus interacts with p53 and represses its transcriptional activity. J Virol **74:**11977-82.
179. **Parravicini, C., B. Chandran, M. Corbellino, E. Berti, M. Paulli, P. S. Moore, and Y. Chang.** 2000. Differential viral protein expression in Kaposi's sarcoma-associated herpesvirus-infected diseases: Kaposi's sarcoma, primary effusion lymphoma, and multicentric Castleman's disease. Am J Pathol **156:**743-9.

180. **Parsons, C. H., L. A. Adang, J. Overdevest, C. M. O'Connor, J. R. Taylor, Jr., D. Camerini, and D. H. Kedes.** 2006. KSHV targets multiple leukocyte lineages during long-term productive infection in NOD/SCID mice. J Clin Invest **116:**1963-73.
181. **Pica, F., and A. Volpi.** 2007. Transmission of human herpesvirus 8: an update. Curr Opin Infect Dis **20:**152-6.
182. **Picchio, G. R., R. E. Sabbe, R. J. Gulizia, M. McGrath, B. G. Herndier, and D. E. Mosier.** 1997. The KSHV/HHV8-infected BCBL-1 lymphoma line causes tumors in SCID mice but fails to transmit virus to a human peripheral blood mononuclear cell graft. Virology **238:**22-9.
183. **Pitcher, C. J., S. I. Hagen, J. M. Walker, R. Lum, B. L. Mitchell, V. C. Maino, M. K. Axthelm, and L. J. Picker.** 2002. Development and homeostasis of T cell memory in rhesus macaque. J Immunol **168:**29-43.
184. **Platanias, L. C.** 2005. Mechanisms of type-I- and type-II-interferon-mediated signalling. Nat Rev Immunol **5:**375-86.
185. **Pozharskaya, V. P., L. L. Weakland, J. C. Zimring, L. T. Krug, E. R. Unger, A. Neisch, H. Joshi, N. Inoue, and M. K. Offermann.** 2004. Short duration of elevated vIRF-1 expression during lytic replication of human herpesvirus 8 limits its ability to block antiviral responses induced by alpha interferon in BCBL-1 cells. J Virol **78:**6621-35.
186. **Pruitt, K., and C. J. Der.** 2001. Ras and Rho regulation of the cell cycle and oncogenesis. Cancer Lett **171:**1-10.
187. **Raghu, H., N. Sharma-Walia, M. V. Veettil, S. Sadagopan, and B. Chandran.** 2009. Kaposi's sarcoma-associated herpesvirus utilizes an actin polymerization-dependent macropinocytic pathway to enter human dermal microvascular endothelial and human umbilical vein endothelial cells. J Virol **83:**4895-911.
188. **Rappocciolo, G., H. R. Hensler, M. Jais, T. A. Reinhart, A. Pegu, F. J. Jenkins, and C. R. Rinaldo.** 2008. Human herpesvirus 8 infects and replicates in primary cultures of activated B lymphocytes through DC-SIGN. J Virol **82:**4793-806.
189. **Rappocciolo, G., F. J. Jenkins, H. R. Hensler, P. Piazza, M. Jais, L. Borowski, S. C. Watkins, and C. R. Rinaldo, Jr.** 2006. DC-SIGN is a receptor for human herpesvirus 8 on dendritic cells and macrophages. J Immunol **176:**1741-9.
190. **Reineke, E. L., and H. Y. Kao.** 2009. Targeting promyelocytic leukemia protein: a means to regulating PML nuclear bodies. Int J Biol Sci **5:**366-76.
191. **Renne, R., D. Blackbourn, D. Whitby, J. Levy, and D. Ganem.** 1998. Limited transmission of Kaposi's sarcoma-associated herpesvirus in cultured cells. J Virol **72:**5182-8.
192. **Renne, R., D. Dittmer, D. Kedes, K. Schmidt, R. C. Desrosiers, P. A. Luciw, and D. Ganem.** 2004. Experimental transmission of Kaposi's sarcoma-associated herpesvirus (KSHV/HHV-8) to SIV-positive and SIV-negative rhesus macaques. J Med Primatol **33:**1-9.
193. **Renne, R., W. Zhong, B. Herndier, M. McGrath, N. Abbey, D. Kedes, and D. Ganem.** 1996. Lytic growth of Kaposi's sarcoma-associated herpesvirus (human herpesvirus 8) in culture. Nat Med **2:**342-6.
194. **Rezaee, S. A., C. Cunningham, A. J. Davison, and D. J. Blackbourn.** 2006. Kaposi's sarcoma-associated herpesvirus immune modulation: an overview. J Gen Virol **87:**1781-804.
195. **Rezaee, S. A., J. A. Gracie, I. B. McInnes, and D. J. Blackbourn.** 2005. Inhibition of neutrophil function by the Kaposi's sarcoma-associated herpesvirus vOX2 protein. AIDS **19:**1907-10.

196. **Rickinson, A. B., E. Kieff, and .** 2007. Epstein-Barr Virus, 5th ed. Wolters Kluwer Health/Lippincott Williams & Wilkins, Philadelphia.
197. **Rivas, C., A. E. Thlick, C. Parravicini, P. S. Moore, and Y. Chang.** 2001. Kaposi's sarcoma-associated herpesvirus LANA2 is a B-cell-specific latent viral protein that inhibits p53. J Virol **75:**429-38.
198. **Roan, F., J. C. Zimring, S. Goodbourn, and M. K. Offermann.** 1999. Transcriptional activation by the human herpesvirus-8-encoded interferon regulatory factor. J Gen Virol **80 (Pt 8):**2205-9.
199. **Roizman, B., L. E. Carmichael, F. Deinhardt, G. de-The, A. J. Nahmias, W. Plowright, F. Rapp, P. Sheldrick, M. Takahashi, and K. Wolf.** 1981. Herpesviridae. Definition, provisional nomenclature, and taxonomy. The Herpesvirus Study Group, the International Committee on Taxonomy of Viruses. Intervirology **16:**201-17.
200. **Roizman, B., D. M. Knipe, and R. J. Whitley.** 2007. Herpes Simplex Viruses, 5th ed. Wolters Kluwer Health/Lippincott Williams & Wilkins, Philadelphia.
201. **Russo, J. J., R. A. Bohenzky, M. C. Chien, J. Chen, M. Yan, D. Maddalena, J. P. Parry, D. Peruzzi, I. S. Edelman, Y. Chang, and P. S. Moore.** 1996. Nucleotide sequence of the Kaposi sarcoma-associated herpesvirus (HHV8). Proc Natl Acad Sci U S A **93:**14862-7.
202. **Sato, M., N. Hata, M. Asagiri, T. Nakaya, T. Taniguchi, and N. Tanaka.** 1998. Positive feedback regulation of type I IFN genes by the IFN-inducible transcription factor IRF-7. FEBS Lett **441:**106-10.
203. **Sato, M., H. Suemori, N. Hata, M. Asagiri, K. Ogasawara, K. Nakao, T. Nakaya, M. Katsuki, S. Noguchi, N. Tanaka, and T. Taniguchi.** 2000. Distinct and essential roles of transcription factors IRF-3 and IRF-7 in response to viruses for IFN-alpha/beta gene induction. Immunity **13:**539-48.
204. **Savitsky, D., T. Tamura, H. Yanai, and T. Taniguchi.** 2010. Regulation of immunity and oncogenesis by the IRF transcription factor family. Cancer Immunol Immunother **59:**489-510.
205. **Scharton-Kersten, T., C. Contursi, A. Masumi, A. Sher, and K. Ozato.** 1997. Interferon consensus sequence binding protein-deficient mice display impaired resistance to intracellular infection due to a primary defect in interleukin 12 p40 induction. J Exp Med **186:**1523-34.
206. **Schmidt, K., E. Wies, and F. Neipel.** 2011. Kaposi's Sarcoma-Associated Herpesvirus Viral Interferon Regulatory Factor 3 Inhibits Gamma Interferon and Major Histocompatibility Complex Class II Expression. J Virol **85:**4530-7.
207. **Searles, R. P., E. P. Bergquam, M. K. Axthelm, and S. W. Wong.** 1999. Sequence and genomic analysis of a Rhesus macaque rhadinovirus with similarity to Kaposi's sarcoma-associated herpesvirus/human herpesvirus 8. J Virol **73:**3040-53.
208. **Seifi, A., E. M. Weaver, M. E. Whipple, M. Ikoma, J. Farrenberg, M. L. Huang, and J. Vieira.** 2011. The lytic activation of KSHV during keratinocyte differentiation is dependent upon a suprabasal position, the loss of integrin engagement, and calcium, but not the interaction of cadherins. Virology **410:**17-29.
209. **Sen, N., M. Sommer, X. Che, K. White, W. T. Ruyechan, and A. M. Arvin.** 2010. Varicella-zoster virus immediate-early protein 62 blocks interferon regulatory factor 3 (IRF3) phosphorylation at key serine residues: a novel mechanism of IRF3 inhibition among herpesviruses. J Virol **84:**9240-53.
210. **Seo, T., D. Lee, B. Lee, J. H. Chung, and J. Choe.** 2000. Viral interferon regulatory factor 1 of Kaposi's sarcoma-associated herpesvirus (human herpesvirus 8) binds to, and

inhibits transactivation of, CREB-binding protein. Biochem Biophys Res Commun **270:**23-7.

211. **Seo, T., J. Park, and J. Choe.** 2005. Kaposi's sarcoma-associated herpesvirus viral IFN regulatory factor 1 inhibits transforming growth factor-beta signaling. Cancer Res **65:**1738-47.
212. **Seo, T., J. Park, D. Lee, S. G. Hwang, and J. Choe.** 2001. Viral interferon regulatory factor 1 of Kaposi's sarcoma-associated herpesvirus binds to p53 and represses p53-dependent transcription and apoptosis. J Virol **75:**6193-8.
213. **Seo, T., J. Park, C. Lim, and J. Choe.** 2004. Inhibition of nuclear factor kappaB activity by viral interferon regulatory factor 3 of Kaposi's sarcoma-associated herpesvirus. Oncogene **23:**6146-55.
214. **Shah, K. M., S. E. Stewart, W. Wei, C. B. Woodman, J. D. O'Neil, C. W. Dawson, and L. S. Young.** 2009. The EBV-encoded latent membrane proteins, LMP2A and LMP2B, limit the actions of interferon by targeting interferon receptors for degradation. Oncogene **28:**3903-14.
215. **Siegal, F. P., N. Kadowaki, M. Shodell, P. A. Fitzgerald-Bocarsly, K. Shah, S. Ho, S. Antonenko, and Y. J. Liu.** 1999. The nature of the principal type 1 interferon-producing cells in human blood. Science **284:**1835-7.
216. **Sin, S. H., D. Roy, L. Wang, M. R. Staudt, F. D. Fakhari, D. D. Patel, D. Henry, W. J. Harrington, Jr., B. A. Damania, and D. P. Dittmer.** 2007. Rapamycin is efficacious against primary effusion lymphoma (PEL) cell lines in vivo by inhibiting autocrine signaling. Blood **109:**2165-73.
217. **Skepper, J. N., A. Whiteley, H. Browne, and A. Minson.** 2001. Herpes simplex virus nucleocapsids mature to progeny virions by an envelopment --> deenvelopment --> reenvelopment pathway. J Virol **75:**5697-702.
218. **Sodhi, A., S. Montaner, and J. S. Gutkind.** 2004. Viral hijacking of G-protein-coupled-receptor signalling networks. Nat Rev Mol Cell Biol **5:**998-1012.
219. **Sorensen, L. N., L. S. Reinert, L. Malmgaard, C. Bartholdy, A. R. Thomsen, and S. R. Paludan.** 2008. TLR2 and TLR9 synergistically control herpes simplex virus infection in the brain. J Immunol **181:**8604-12.
220. **Soulier, J., L. Grollet, E. Oksenhendler, P. Cacoub, D. Cazals-Hatem, P. Babinet, M. F. d'Agay, J. P. Clauvel, M. Raphael, L. Degos, and et al.** 1995. Kaposi's sarcoma-associated herpesvirus-like DNA sequences in multicentric Castleman's disease. Blood **86:**1276-80.
221. **Spiller, O. B., D. J. Blackbourn, L. Mark, D. G. Proctor, and A. M. Blom.** 2003. Functional activity of the complement regulator encoded by Kaposi's sarcoma-associated herpesvirus. J Biol Chem **278:**9283-9.
222. **Sullivan, R., B. J. Dezube, and H. B. Koon.** 2006. Signal transduction targets in Kaposi's sarcoma. Curr Opin Oncol **18:**456-62.
223. **Sullivan, R. J., L. Pantanowitz, C. Casper, J. Stebbing, and B. J. Dezube.** 2008. HIV/AIDS: epidemiology, pathophysiology, and treatment of Kaposi sarcoma-associated herpesvirus disease: Kaposi sarcoma, primary effusion lymphoma, and multicentric Castleman disease. Clin Infect Dis **47:**1209-15.
224. **Sunil-Chandra, N. P., J. Arno, J. Fazakerley, and A. A. Nash.** 1994. Lymphoproliferative disease in mice infected with murine gammaherpesvirus 68. Am J Pathol **145:**818-26.
225. **Swaminathan, S.** 2005. Post-transcriptional gene regulation by gamma herpesviruses. J Cell Biochem **95:**698-711.

226. **Tabeta, K., P. Georgel, E. Janssen, X. Du, K. Hoebe, K. Crozat, S. Mudd, L. Shamel, S. Sovath, J. Goode, L. Alexopoulou, R. A. Flavell, and B. Beutler.** 2004. Toll-like receptors 9 and 3 as essential components of innate immune defense against mouse cytomegalovirus infection. Proc Natl Acad Sci U S A **101:**3516-21.
227. **Takaoka, A., Z. Wang, M. K. Choi, H. Yanai, H. Negishi, T. Ban, Y. Lu, M. Miyagishi, T. Kodama, K. Honda, Y. Ohba, and T. Taniguchi.** 2007. DAI (DLM-1/ZBP1) is a cytosolic DNA sensor and an activator of innate immune response. Nature **448:**501-5.
228. **Takaoka, A., H. Yanai, S. Kondo, G. Duncan, H. Negishi, T. Mizutani, S. Kano, K. Honda, Y. Ohba, T. W. Mak, and T. Taniguchi.** 2005. Integral role of IRF-5 in the gene induction programme activated by Toll-like receptors. Nature **434:**243-9.
229. **Taylor, R. T., and W. A. Bresnahan.** 2006. Human cytomegalovirus IE86 attenuates virus- and tumor necrosis factor alpha-induced NFkappaB-dependent gene expression. J Virol **80:**10763-71.
230. **Taylor, R. T., and W. A. Bresnahan.** 2006. Human cytomegalovirus immediate-early 2 protein IE86 blocks virus-induced chemokine expression. J Virol **80:**920-8.
231. **Thanos, D., and T. Maniatis.** 1995. Virus induction of human IFN beta gene expression requires the assembly of an enhanceosome. Cell **83:**1091-100.
232. **Tough, D. F., P. Borrow, and J. Sprent.** 1996. Induction of bystander T cell proliferation by viruses and type I interferon in vivo. Science **272:**1947-50.
233. **Trinchieri, G.** 1989. Biology of natural killer cells. Adv Immunol **47:**187-376.
234. **Tugizov, S. M., J. W. Berline, and J. M. Palefsky.** 2003. Epstein-Barr virus infection of polarized tongue and nasopharyngeal epithelial cells. Nat Med **9:**307-14.
235. **Unterholzner, L., S. E. Keating, M. Baran, K. A. Horan, S. B. Jensen, S. Sharma, C. M. Sirois, T. Jin, E. Latz, T. S. Xiao, K. A. Fitzgerald, S. R. Paludan, and A. G. Bowie.** 2010. IFI16 is an innate immune sensor for intracellular DNA. Nat Immunol **11:**997-1004.
236. **van Lint, A. L., M. R. Murawski, R. E. Goodbody, M. Severa, K. A. Fitzgerald, R. W. Finberg, D. M. Knipe, and E. A. Kurt-Jones.** 2010. Herpes simplex virus immediate-early ICP0 protein inhibits Toll-like receptor 2-dependent inflammatory responses and NF-kappaB signaling. J Virol **84:**10802-11.
237. **Vandevenne, P., C. Sadzot-Delvaux, and J. Piette.** 2010. Innate immune response and viral interference strategies developed by human herpesviruses. Biochem Pharmacol **80:**1955-72.
238. **Varani, S., M. Cederarv, S. Feld, C. Tammik, G. Frascaroli, M. P. Landini, and C. Soderberg-Naucler.** 2007. Human cytomegalovirus differentially controls B cell and T cell responses through effects on plasmacytoid dendritic cells. J Immunol **179:**7767-76.
239. **Veals, S. A., C. Schindler, D. Leonard, X. Y. Fu, R. Aebersold, J. E. Darnell, Jr., and D. E. Levy.** 1992. Subunit of an alpha-interferon-responsive transcription factor is related to interferon regulatory factor and Myb families of DNA-binding proteins. Mol Cell Biol **12:**3315-24.
240. **Verpooten, D., Y. Ma, S. Hou, Z. Yan, and B. He.** 2009. Control of TANK-binding kinase 1-mediated signaling by the gamma(1)34.5 protein of herpes simplex virus 1. J Biol Chem **284:**1097-105.
241. **Vieira, J., and P. M. O'Hearn.** 2004. Use of the red fluorescent protein as a marker of Kaposi's sarcoma-associated herpesvirus lytic gene expression. Virology **325:**225-40.
242. **Virgin, H. W. t., P. Latreille, P. Wamsley, K. Hallsworth, K. E. Weck, A. J. Dal Canto, and S. H. Speck.** 1997. Complete sequence and genomic analysis of murine gammaherpesvirus 68. J Virol **71:**5894-904.

243. **Voumvourakis, K. I., D. K. Kitsos, S. Tsiodras, G. Petrikkos, and E. Stamboulis.** 2010. Human herpesvirus 6 infection as a trigger of multiple sclerosis. Mayo Clin Proc **85:**1023-30.
244. **Waddell, S. J., S. J. Popper, K. H. Rubins, M. J. Griffiths, P. O. Brown, M. Levin, and D. A. Relman.** 2010. Dissecting interferon-induced transcriptional programs in human peripheral blood cells. PLoS One **5:**e9753.
245. **Wang, F. Z., S. M. Akula, N. P. Pramod, L. Zeng, and B. Chandran.** 2001. Human herpesvirus 8 envelope glycoprotein K8.1A interaction with the target cells involves heparan sulfate. J Virol **75:**7517-27.
246. **Wang, J. P., E. A. Kurt-Jones, O. S. Shin, M. D. Manchak, M. J. Levin, and R. W. Finberg.** 2005. Varicella-zoster virus activates inflammatory cytokines in human monocytes and macrophages via Toll-like receptor 2. J Virol **79:**12658-66.
247. **Wang, J. T., S. L. Doong, S. C. Teng, C. P. Lee, C. H. Tsai, and M. R. Chen.** 2009. Epstein-Barr virus BGLF4 kinase suppresses the interferon regulatory factor 3 signaling pathway. J Virol **83:**1856-69.
248. **Weaver, B. K., K. P. Kumar, and N. C. Reich.** 1998. Interferon regulatory factor 3 and CREB-binding protein/p300 are subunits of double-stranded RNA-activated transcription factor DRAF1. Mol Cell Biol **18:**1359-68.
249. **Wen, K. W., and B. Damania.** 2010. Kaposi sarcoma-associated herpesvirus (KSHV): molecular biology and oncogenesis. Cancer Lett **289:**140-50.
250. **West, J. A., S. M. Gregory, V. Sivaraman, L. Su, and B. Damania.** 2011. Activation of plasmacytoid dendritic cells by Kaposi's sarcoma-associated herpesvirus. J Virol **85:**895-904.
251. **White, J. A., P. A. Todd, J. L. Yee, A. Kalman-Bowlus, K. S. Rodgers, X. Yang, S. W. Wong, P. Barry, and N. W. Lerche.** 2009. Prevalence of viremia and oral shedding of rhesus rhadinovirus and retroperitoneal fibromatosis herpesvirus in large age-structured breeding groups of rhesus macaques (Macaca mulatta). Comp Med **59:**383-90.
252. **Whitley, R. J., and B. Roizman.** 2001. Herpes simplex virus infections. Lancet **357:**1513-8.
253. **Wies, E., A. S. Hahn, K. Schmidt, C. Viebahn, N. Rohland, A. Lux, T. Schellhorn, A. Holzer, J. U. Jung, and F. Neipel.** 2009. The Kaposi's Sarcoma-associated Herpesvirus-encoded vIRF-3 Inhibits Cellular IRF-5. J Biol Chem **284:**8525-38.
254. **Wies, E., Y. Mori, A. Hahn, E. Kremmer, M. Sturzl, B. Fleckenstein, and F. Neipel.** 2008. The viral interferon-regulatory factor-3 is required for the survival of KSHV-infected primary effusion lymphoma cells. Blood **111:**320-7.
255. **Wilkins, C., and M. Gale, Jr.** 2010. Recognition of viruses by cytoplasmic sensors. Curr Opin Immunol **22:**41-7.
256. **Wong, S. W., E. P. Bergquam, R. M. Swanson, F. W. Lee, S. M. Shiigi, N. A. Avery, J. W. Fanton, and M. K. Axthelm.** 1999. Induction of B cell hyperplasia in simian immunodeficiency virus-infected rhesus macaques with the simian homologue of Kaposi's sarcoma-associated herpesvirus. J Exp Med **190:**827-40.
257. **Wu, L., E. Fossum, C. H. Joo, K. S. Inn, Y. C. Shin, E. Johannsen, L. M. Hutt-Fletcher, J. Hass, and J. U. Jung.** 2009. Epstein-Barr virus LF2: an antagonist to type I interferon. J Virol **83:**1140-6.
258. **Yamanishi, K., Y. Mori, and P. E. Pellett.** 2007. Human Herpesviruses 6 and 7, 5th ed. Wolters Kluwer Health/Lippincott Williams & Wilkins, Philadelphia.

259. **Yoneyama, M., and T. Fujita.** 2010. Recognition of viral nucleic acids in innate immunity. Rev Med Virol **20:**4-22.
260. **Yoneyama, M., W. Suhara, Y. Fukuhara, M. Fukuda, E. Nishida, and T. Fujita.** 1998. Direct triggering of the type I interferon system by virus infection: activation of a transcription factor complex containing IRF-3 and CBP/p300. EMBO J **17:**1087-95.
261. **Yu, Y., S. E. Wang, and G. S. Hayward.** 2005. The KSHV immediate-early transcription factor RTA encodes ubiquitin E3 ligase activity that targets IRF7 for proteosome-mediated degradation. Immunity **22:**59-70.
262. **Zhang, J. J., U. Vinkemeier, W. Gu, D. Chakravarti, C. M. Horvath, and J. E. Darnell, Jr.** 1996. Two contact regions between Stat1 and CBP/p300 in interferon gamma signaling. Proc Natl Acad Sci U S A **93:**15092-6.
263. **Zhou, F. C., Y. J. Zhang, J. H. Deng, X. P. Wang, H. Y. Pan, E. Hettler, and S. J. Gao.** 2002. Efficient infection by a recombinant Kaposi's sarcoma-associated herpesvirus cloned in a bacterial artificial chromosome: application for genetic analysis. J Virol **76:**6185-96.
264. **Zhu, F. X., J. M. Chong, L. Wu, and Y. Yuan.** 2005. Virion proteins of Kaposi's sarcoma-associated herpesvirus. J Virol **79:**800-11.
265. **Zhu, F. X., S. M. King, E. J. Smith, D. E. Levy, and Y. Yuan.** 2002. A Kaposi's sarcoma-associated herpesviral protein inhibits virus-mediated induction of type I interferon by blocking IRF-7 phosphorylation and nuclear accumulation. Proc Natl Acad Sci U S A **99:**5573-8.
266. **Zhu, Y., L. Huang, and D. G. Anders.** 1998. Human cytomegalovirus oriLyt sequence requirements. J Virol **72:**4989-96.
267. **Zimring, J. C., S. Goodbourn, and M. K. Offermann.** 1998. Human herpesvirus 8 encodes an interferon regulatory factor (IRF) homolog that represses IRF-1-mediated transcription. J Virol **72:**701-7.